

**UNIVERSITY OF SÃO PAULO  
INSTITUTE OF CHEMISTRY  
Postgraduate Program in Chemistry**

HAQ NAWAZ

**Derivatização de celulose sob condições homogêneas: cinética e mecanismo de acilação do biopolímero em LiCl/DMAC e líquidos iônicos/solventes apróticos dipolares**

**Versão corrigida da tese defendida**

São Paulo

Date of submission in SPG:

20/01/2014

**HAQ NAWAZ**

**Cellulose derivatization under homogeneous conditions: Kinetics and mechanism of biopolymer acylation in LiCl/DMAC and ionic liquids-dipolar aprotic solvents**

*Thesis submitted to the Institute of Chemistry,  
The University of São Paulo for Ph.D. Degree  
in Chemistry (Physical Organic Chemistry)*

*Supervisor: Prof. Dr. Omar A. El Seoud*

São Paulo

2014

Haq Nawaz

Cellulose derivatization under homogeneous conditions: Kinetics and mechanism of biopolymer acylation in LiCl/DMAC and ionic liquids-dipolar aprotic solvents

*Thesis submitted to the Institute of Chemistry,  
The University of São Paulo for Ph.D. Degree  
in Chemistry (Physical Organic Chemistry)*

Approved by:

**Examination Board**

**Prof. Dr.**

Institution:

Signature:

**Prof. Dr.**

Institution:

Signature:

**Prof. Dr.**

Institution:

Signature:

*A famous proverb: "Hard work is key to success"*

*This research is dedicated to my parents, brothers and sister,  
especially elder brother Ghulam Shabbir and my beloved mother  
whose financial and moral support leads me to success.*

## **ACKNOWLEDGEMENT**

All praises for God, the Almighty, Who gave me the opportunity to accomplish this job. For Almighty Allah's unlimited guidance and blessings upon me to accomplish this Ph.D. dissertation in a better way. All respect for his Holy Prophet (Peace Be upon Him) who enabled us to recognize our creator.

It is difficult to acknowledge everybody who supported me during any stage of my studies and research career; especially to cover the efforts of everybody who assisted me.

First and foremost are my beloved parents who provided me good nurture and nature, gave me courage to face problems all the time by saying "no pain no gain" mainly my elder brother Ghulam Shabbir who planted the root of interest towards education as he knew the importance and awareness of education. I can never forget my mother's prayers, care and sacrifices, which are still with me from the first day. My deep appreciation, regards and heartiest thanks are for my brothers, the only sister and uncle for their cooperative attitude and continuous struggle throughout my life.

I feel great honor and unlimited pleasures to express my sincere thanks to my research supervisor Prof. Dr. Omar A. El Seoud, Institute of Chemistry, University of Sao Paulo, because the work presented in this dissertation would never have been accomplished without his keen interest, attention and continuous encouragement. I am grateful for his continuous guidance, encouragement and particularly for his kind behavior. I am lucky to have such a nice professor and find no suitable words to thank him.

I also feel great honor to express my special thanks to my Co-supervisor Prof. Dr. Herbert Sixta and Dr. Michael Hummel, Department of Forest Products Technology, School of Chemical Technology, Aalto University, Espoo, Finland and Dr. Alistair King from Department of Chemistry, University of Helsinki, Finland. I am mainly grateful for his very kind behavior.

I would like to express my special thanks to Prof. Dr. Josef Wilhelm Baader and Prof. Elizabeth Areas whose skillful discussion, fruitful suggestions and friendly attitude throughout my stay in this Institute, gave me enough encouragement to do this job.

My deep appreciation and heartfelt thanks are for my lab colleagues, specifically, Paula Galgano, Romeu Casarano, Paulo A. Pires, Shirley Possidonio, Carina Loffredo, Priscilla, Ludmila,

Luis, Valdeneia, Ana Luiza and Cezar for their nice cooperation and continuous encouragement during my research career. I can never forget the efforts and continuous guideline of Paula Galgano in all my administrative process here in Institute of Chemistry. Special thanks to Carina and Shirley in helping to write my annual reports in Portuguese. My deep appreciations are for Paulo A. Pires and Romeu Casarano for their continuous guideline and valuable suggestions during my research work.

Thanks to all the graduate and undergraduate students, Daniela, Jamillee, Paulinho, Mariana, Carine, Nanci, Michelle, Thais-1, Thais-2 and Fernanda for their nice time and help.

I would like to thank to all the IQ-USP postgraduate, central analytical and chemical store staff for their continuous favor and kind behavior.

I would like to pay my special thanks to all my friends Bakhat Ali, Riaz Hussain, Muhammad Imran, Shahzad Ahmed, Muhammad Ibrahim, Muhammad Khalid, Rashid Nazir, Ajaz Hussain, Umar Nishan and Anees Ahmed.

Special thanks to my family particularly my mother and brothers; Ghulam Shabbir, Rab Nawaz, Muhammad Nawaz, and the only sister for their continuous courage and care.

Finally, I am most grateful to TWAS (The academy of sciences for the developing world) and CNPq (The Brazilian National Council for scientific & Technological development) for providing me the funds for my Ph.D. studies.

Haq Nawaz

January 20, 2014

São Paulo

## **ABSTRACT**

Nawaz, H. **Cellulose derivatization under homogeneous conditions: Kinetics and mechanism of biopolymer acylation in LiCl/DMAC and ionic liquids-dipolar aprotic solvents** 2014. 188p. Ph.D. Thesis – Graduate Program in Chemistry. The Institute of Chemistry, The University of São Paulo, São Paulo.

The objective of this work is to study the reactivity in cellulose acylation by carboxylic acid anhydrides under homogeneous conditions in dipolar aprotic solvents (DAS), including LiCl/*N,N*-dimethylacetamide (DMAC) and ionic liquids (ILs)/DAS. Factors that contribute to reactivity were quantified by studying the dependence of reaction rates on temperature and solvent composition. After establishing that conductivity is an appropriate experimental technique to calculate the rate constants, we studied the kinetics of the homogeneous uncatalyzed and catalyzed acylation of microcrystalline cellulose, MCC, with carboxylic acid anhydrides with different acyl chain-length (*N<sub>c</sub>*; ethanoic to hexanoic) in the following solvent systems: LiCl/DMAC; mixtures of the IL, 1-allyl-3-methylimidazolium chloride, (AlMeImCl) and acetonitrile (MeCN), DMAC, dimethyl sulfoxide (DMSO) and sulfolane. The anhydroglucose unit of cellulose carries one primary- and two secondary hydroxyl groups. We used cyclohexylmethanol, CHM, and *trans*-1,2-cyclohexanediol, CHD, as model compounds for the hydroxyl groups of the anhydroglucose unit of cellulose. The ratios of rate constants of acylation of primary (CHM; Prim-OH) and secondary (CHD; Sec-OH) groups were employed, after correction, in order to split the overall rate constants of the reaction of MCC into contributions from the discrete OH groups. For the model compounds, we have found that  $k_3(\text{Prim-OH})/k_3(\text{Sec-OH}) > 1$ , akin to reactions of cellulose under heterogeneous conditions; this ratio increases as a function of increasing *N<sub>c</sub>*. The overall and partial rate constants of the acylation of MCC decrease from ethanoic- to butanoic anhydride and then increase for pentanoic- and hexanoic anhydride, due to subtle changes in- and compensations of the enthalpy and entropy of activation.

Rate constants for the acetylation of MCC, by ethanoic anhydride in the presence of increasing concentrations of the ionic liquid, IL, 1-allyl-3-methylimidazolium chloride in dipolar aprotic solvents, DAS, *N,N*-dimethylacetamide, DMAC, acetonitrile, MeCN, dimethylsulfoxide,

DMSO and sulfolane, have been calculated from conductivity data. The third order rate constants showed a linear dependence on [IL]. These results have been explained by assuming that the reactant is cellulose hydrogen-bonded to the IL. This is corroborated by kinetic data of the acetylation of cyclohexyl methanol, FTIR spectroscopy of the latter compound, and cellobiose in mixtures of IL/DAS, and conductivity of the binary solvent mixtures in absence, and presence of MCC. Cellulose acetylation is faster in IL/DMAC and IL/DMSO than in IL/MeCN and IL/Sulfolane. This difference is explained, in part, based the high viscosity of the biopolymer solutions in IL-Sulfolane. Additional explanation came from microscopic solvents properties and molecular dynamics, MD simulations. The solvatochromic data (empirical polarity and basicity) have shown the importance of solvent basicity; basic solvents hydrogen-bond to the hydroxyl groups of cellulose increasing its accessibility, hence its reactivity. This is the case of DMAC and DMSO. Results of MD simulations indicated hydrogen-bond formation between the hydroxyl groups of the anhydroglucose unit of MCC, (Cl<sup>-</sup>) of the IL, and the dipole of the DMAC and DMSO.

It has been observed that cellulose acylation in LiCl/DMAC is efficiently catalyzed by imidazole, but not by p-tosyl chloride. FTIR and <sup>1</sup>H NMR have indicated the formation of *N*-acylimidazole which is the acylating agent. The overall and partial rate constants of the acylation of MCC decreased from ethanoic- to butanoic-anhydride and then increased for pentanoic- and hexanoic anhydride, due to subtle changes in- and compensations of the enthalpy and entropy of activation.

**Keywords:** Cellulose acylation; cellulose carboxylic esters; chemical kinetics; ionic liquids/dipolar aprotic solvents.



## RESUMO

Nawaz , H. **Derivatização de celulose sob condições homogêneas: cinética e mecanismo de acilação do biopolímero em LiCl/DMAC e líquidos iônicos/solventes apróticos dipolares** 2014 . 188p. Tese de Ph.D.; Programa de Pós-Graduação em Química; Instituto de Química , Universidade de São Paulo, São Paulo.

O objetivo deste trabalho é estudar a reatividade de acilação de celulose por anidridos de ácidos carboxílicos sob condições homogêneas em solventes apróticos dipolares (SAD), incluindo LiCl/*N,N*-dimetilacetamida (DMAC) e líquidos iônicos (LIs)/SAD. Os factores que contribuem para a reatividade foram quantificados através do estudo da dependência das constantes de velocidade e parâmetros de ativação sobre a composição do solvente. Após estabelecer que a condutividade é uma técnica experimental adequada para calcular as constantes de velocidade, foi estudada a acilação não catalisada e catalisada de celulose microcristalina, MCC. Foram empregados anidridos de ácidos carboxílicos com diferentes grupos acila (acetil a hexanoil;  $N_c = 2$  a 6) nos seguintes sistemas de solventes: LiCl/DMAC, misturas de LI cloreto de 1-alil-3-metilimidazólio ( AIMeImCl ) e acetonitrila (MeCN), DMAC , dimetilsulfóxido (DMSO ) e sulfolano. Na celulose, a unidade anidra de glucose possui um grupo hidroxila primário e dois hidroxilas secundários. Usamos ciclohexilmetanol, CHM, e *trans*-1 ,2-ciclo-hexanodiol, CHD , como compostos modelo para os grupos (OH) primário e secundários, respectivamente. As razões das constantes de velocidade de acilação dos compostos modelo (CHM; Prim-OH) e (CHD; SEC-OH) foram empregados, após correção, a fim de dividir as constantes de velocidade global da reação de MCC em contribuições dos grupos (OH) presentes. Para os compostos modelo, verificou-se que  $k_3$  (Prim-OH) /  $k_3$  (Sec-OH) > 1, semelhante as reações de celulose sob condições heterogêneas; esta relação aumenta como uma função do aumento da  $N_c$ . As constantes de velocidade globais e parciais de acilação de MCC diminuíam de anidrido etanóico a butanóico e, em seguida, aumentam para anidrido pentanóico e hexanóico, devido a mudanças sutis em  $\Delta H^\ddagger$  e compensações da entalpia e entropia de ativação.

As constantes de velocidade para a acetilação de MCC, por anidrido etanóico na presença de concentrações crescentes do LI em DMAC, MeCN, DMSO e sulfolano foram calculados a partir de dados de condutividade. As constantes de velocidade de terceira ordem mostraram dependência linear sobre [LI]. Estes resultados foram explicados assumindo que o reagente é celulose ligado ao LI por ligação de hidrogénio. Isto foi confirmado pelos dados cinéticos da acetilação de CHM, espectroscopia de IV do último composto, e de celobiose nas misturas de LI/SAD e condutividade das misturas de solventes binários, na ausência e presença de MCC. A acetilação de celulose é mais rápida nas misturas de em LI com DMAC e DMSO do que com MeCN e sulfolano. Esta diferença é explicada, em parte, com base na alta viscosidade das soluções de biopolímeros em LI/sulfolano. Obteve-se mais informações sobre os efeitos do solvente molecular a partir das propriedades microscópicas dos solventes e simulações por dinâmica molecular, DM. Os dados solvatocrômicos (polaridade empírica e basicidade) têm mostrado a importância da basicidade do solvente; solventes mais básicos formam ligações de hidrogénio mais fortes com os grupos (OH) da celulose, aumentando sua acessibilidade e, conseqüentemente sua reatividade. Este é o caso de DMAC e DMSO. Os resultados das simulações por DM indicaram a formação de ligações de hidrogénio, entre os grupos (OH) da unidade de glucose anidra do MCC, ( $\text{Cl}^-$ ) de LI, e o dipolo do DMAC e DMSO .

Observamos que a acilação de celulose em LiCl/DMAC é eficientemente catalisada por imidazol, mas não pelo cloreto de tosila. Resultados de IV de FT e RMN de  $^1\text{H}$  indicaram a formação de *N*-acilimidazol que é o agente de acilação. As constantes globais e parciais de velocidade de acilação do MCC diminuíram de anidrido etanóico a butanóico e depois aumentou para anidrido pentanóico e hexanóico, devido a mudanças sutis em- e compensações da entalpia e entropia de ativação.

**Palavras-chave:** Celulose, acilação de; ésteres carboxílicos de celulose; cinética química ; líquidos iônicos; solventes apróticos dipolares .

## LIST OF ABBREVIATIONS AND ACRONYMS

Ac-Im: *N*-Acylimidazole

AFM: Atomic force microscopy

AKD: Alkyl ketene dimer

AlMeImCl: 1-allyl-3-methylimidazolium chloride

AlMeImF: 1-allyl-3-methylimidazolium fluoride

AUG: Anhydroglucose unit

BC: Bacterial cellulose

BCTMP: Bleached chemithermomechanical pulps

BnMeImCl: 1-benzyl-3-methylimidazolium chloride

BuMeImBr: 1-(1-butyl)-3-methylimidazolium bromide

CA: Cellulose acetate,

CDI: *N,N*-carbonyldiimidazole

CHD: *Trans*-1,2-cyclohexanediol

CHM: Cyclohexylmethanol

COSY: Correlation spectroscopy

CUEN: Cupric ethylenediamine

DCC: Dicyclohexyl carbodiimide

DAS: Dipolar aprotic solvent

DMAC: *N,N*-dimethylacetamide

DMAP: 4-(*N,N*-dimethylamino)pyridine

DMF: Dimethylformamide

DMI: 1,3-dimethyl-2-imidazolidinone

DMSO: Dimethyl sulfoxide

DP: Average degree of polymerization

DS: Degree of substitution

DSC: Differential scanning calorimetry

EtMeImCl: 1-ethyl-3-methylimidazolium chloride

FTIR: Fourier transform infrared spectroscopy  
GPC: Gel permeation chromatography  
HMQC: Heteronuclear multiple quantum coherence  
HPLC: High-performance liquid chromatography  
HRS: Homogeneous reaction scheme  
Ic: Index of crystallinity of the biopolymer  
IL: Ionic liquid  
Im: Imidazole  
MCC: Microcrystalline cellulose  
MeCN: Acetonitrile  
Melm: Methylimidazole  
MW: Microwave radiation  
MPa: Millipascal  
NMR: Nuclear magnetic resonance  
NSSC: Neutral sulfite semichemical  
RCOF: Acyl fluoride  
SAXS: Small-angle X-ray scattering  
SEM: Scanning electron microscopy  
SE: Strong electrolyte  
SLS: Static light scattering  
 $S_N$ : Nucleophilic substitution  
STM: Scanning tunnelling microscopy  
TAAF: Tetraallylammonium fluoride  
TBAF: Tetra (1-butyl) ammonium fluoride  
TDMSCl: Hexyldimethylchlorosilane  
TEA: Triethylamine, TsCl: Tosyl chloride  
TEM: Transmission electron microscopy  
TGA: Thermogravimetric analysis  
TMS: Tetramethylsilane, WAXS: Wide-angle X-ray scattering

## SUMMARY

<b>1. INTRODUCTION</b>	<b>21</b>
1.1. Principles and relevance of biomass to green chemistry	21
1.1.1. Position of cellulose within the biomass	23
1.1.2. Sources of cellulose	24
1.1.2.1. Conventional sources	25
1.1.2.2. Other sources of cellulose	26
1.2. Industrial production of cellulose	27
1.2.1. Pulping process	27
1.2.1.1. Mechanical pulping	28
1.2.1.2. Chemical pulping	29
1.2.1.2.1. kraft pulping	29
1.2.1.2.2. Acid sulfite pulping	30
1.2.1.2.3. Neutral sulfite semichemical pulping (NSSC)	30
1.3. Structure of cellulose	31
1.3.1. Supramolecular structure of cellulose	31
1.3.2. Molecular structure of cellulose	33
1.3.3. Morphological structure of cellulose	35
1.3.4. X-ray crystallography of cellulose I	36
1.3.5. Some relevant characteristic of cellulose	38
1.3.5.1. Degree of polymerization of cellulose	38
1.3.5.2. Index of crystallinity (I <sub>c</sub> ) of cellulose	39
1.3.5.3. $\alpha$ -Cellulose content	40
1.4. Derivatization of cellulose	40
1.4.1. Strategies for derivatization of cellulose	40
1.4.2. Derivatization under heterogeneous reaction conditions	40
1.4.3. The homogeneous reaction scheme	41
1.4.4. Derivatization of cellulose under homogeneous reaction conditions	42

1.5. Steps for cellulose derivatization under homogenous conditions	44
1.5.1. Cellulose activation	44
1.5.2. Strategies for cellulose activation	44
1.5.2.1. Activation by solvent exchange	45
1.5.2.2. Water entrainment by partial solvent distillation	45
1.5.2.3. Thermal activation	46
1.6. Cellulose dissolution	46
1.6.1. Mechanism of cellulose dissolution	47
1.6.2. Dissolution scheme	49
1.7. Cellulose derivatization under homogeneous reaction conditions	52
1.7.1. Derivatization scheme under HRS	52
1.7.2. Derivatization in strong electrolytes /dipolar aprotic solvents	53
1.7.3. Representative examples for cellulose derivatization in SE/DAS	53
1.8. Ionic Liquids	66
1.8.1. Some physical properties of ionic liquids	69
1.8.1.1. Thermal stability	69
1.8.1.2. Polarity	70
1.8.1.3. Viscosity	71
1.8.1.4. Hydrogen bonding	71
1.8.2. Cellulose dissolution and dissolution mechanism in ILs	71
1.8.3. Cellulose derivatization in ionic liquids with mixtures of DAS	74
1.9. Solvatochromism	77
1.9.1. Understanding solvation process	77
<b>2. OBJECTIVES</b>	<b>79</b>
<b>3. EXPERIMENTAL PART</b>	<b>80</b>
3.1. Materials	80
3.1.1. Cellulose	80
3.1.2. Solvents and reagents	80
3.2. Material characterization: cellulose; cellulose derivatives; derivatives	

of model compounds for cellulose	81
3.2.1. Determination of index of crystallinity by X-ray diffraction	81
3.2.2. Degree of polymerization of cellulose by viscosity	81
3.2.3. Ester characterization of model compounds by FTIR and <sup>1</sup> H NMR	82
3.2.4. Determination of the degree of substitution of cellulose esters	83
3.3. Syntheses	84
3.3.1. Syntheses of CHM and CHD acetates	84
3.3.2. Syntheses of cellulose esters in LiCl/DMAC	85
3.3.3. Syntheses of cellulose acetate in IL/DAS	85
3.3.4. Microwave-assisted synthesis of 1-allyl-3-methylimidazolium chloride (AlMelmCl)	86
3.4. Kinetic studies	86
3.4.1. Equipment	86
3.4.2. Preparation of solutions for kinetic studies: cellulose solutions in LiCl/DMAC and in IL/DAS	87
3.4.3. Kinetics of acylation of model compounds of cellulose in LiCl/DMAC and IL/DAS	89
3.4.4. Kinetics of acylation of cellulose in LiCl/DMAC, and IL/DAS	91
3.5. Mechanistic studies	93
3.5.1. Detection of the intermediate in imidazole-catalyzed acylation, by <sup>1</sup> H NMR and FTIR	93
3.6. Theoretical calculations	94
3.6.1. Molecular dynamics, MD, simulations in LiCl/DMAC	94
3.6.2. MD, simulations in IL-DAS	95
3.7- Additional experiments	96
3.7.1. Probing hydrogen bonding of ILs with CHM or cellobiose by FTIR	96
3.7.2. Determination of the microscopic properties of reaction media by solvatochromic dyes	96
3.7.3. Rheology of mixtures of IL and DAS	97

<b>4. RESULTS AND DISCUSSIONS</b>	<b>98</b>
4.1. Relevance of kinetic data to cellulose chemistry	98
4.2. Uncatalyzed acylation of cellulose in LiCl/DMAC	99
4.2.1. Setup of the kinetic experiment and calculation of the individual rate constants	99
4.3. Cellulose acetylation in IL-DAS	109
4.3.1: Reaction order and product isolation	109
4.3.2. Dependence of the kinetic data on the nature of the molecular solvent	114
4.4. MD, simulations in IL-DAS	125
4.5. Imidazole-catalyzed acylation of cellulose in LiCl/DMAC	132
4.5.1. Acylation by acid anhydrides in the presence of tosylchloride or Imidazole	132
4.5.2. Detection of the intermediate in imidazole-catalyzed acylation, by <sup>1</sup> H NMR and FTIR	135
4.5.3. Proof that acylimidazole is the actual acylating agent	137
4.5.4. Reaction order and activation parameters	139
<b>5. CONCLUSION</b>	<b>146</b>
<b>6. REFERENCES</b>	<b>148</b>
<b>7. APPENDIX</b>	<b>177</b>



## FIGURES INDEX

<b>Figure 1.1:</b>	Estimated oil production and consumption capacity in the world up to 2030.	23
<b>Figure 1.2:</b>	Schematic representation of wood pulping process.	28
<b>Figure 1.3:</b>	From cellulose sources to cellulose molecules.	33
<b>Figure 1.4:</b>	Open chain and closed ring form of glucose unit.	33
<b>Figure 1.5:</b>	Molecular structure of single strands of cellulose fiber.	34
<b>Figure 1.6:</b>	Intra- and intermolecular hydrogen bonds in cellulose.	35
<b>Figure 1.7:</b>	Isolated microfibrils of cellulose of different origin.	36
<b>Figure 1.8:</b>	Projections of a two-chain model of cellulose I.	38
<b>Figure 1.9:</b>	X-ray diffraction pattern of: crude pine wood.	40
<b>Figure 1.10:</b>	Thermal activation procedure for cellulose.	47
<b>Figure 1.11:</b>	Proposed mechanisms of cellulose-LiCl/DMAC complexation.	48
<b>Figure 1.12:</b>	Proposed model for cellulose/LiCl/DMAC interaction for dissolution.	49
<b>Figure 1.13:</b>	Simplified structures for the interaction of TBAF and DMSO, and for cellulose solution in TBAF/DMSO.	50
<b>Figure 1.14:</b>	Schematic representation of the effect of water on solution of cellulose in TBAF/DMSO.	51
<b>Figure 1.15:</b>	A schematic representation of derivatization by the HRS.	53
<b>Figure 1.16:</b>	Homogeneous acylation of MCC in LiCl/DMAC using acid anhydrides.	54
<b>Figure 1.17:</b>	Possible side reactions of tetraalkylammonium fluoride-hydrates.	56
<b>Figure 1.18:</b>	Schemes for the <i>in situ</i> activation of carboxylic acids.	57
<b>Figure 1.19:</b>	Formation of mixed anhydride of acetic- and fatty carboxylic acid.	58
<b>Figure 1.20:</b>	Dependence of $DS_{\text{Reduced}}$ on $N_c$ in different solvent systems.	60
<b>Figure 1.21:</b>	Schematic representation of acylation by carboxylic acid chloride/tertiary amine as a derivatizing agent.	60
<b>Figure 1.22:</b>	Representative scheme for the reaction of cellulose with alkylketene dimmers.	61
<b>Figure 1.23:</b>	Schematic representation of the conversion of cellulose (ROH) into cationic	

	ester by the reaction with <i>N</i> -methyl-2-pyrrolidinone.	62
<b>Figure 1.24:</b>	Use of tosylate moiety as a bulky group for C6-OH position of cellulose.	63
<b>Figure 1.25:</b>	Synthesis of cellulose tosylate and further derivatives by $S_N$ reactions.	64
<b>Figure 1.26:</b>	Allylation of cellulose dissolved in TBAF/DMSO.	66
<b>Figure 1.27:</b>	Using hexyldimethylsilyl moieties as protecting groups in the regioselective synthesis of cellulose ethers.	66
<b>Figure 1.28:</b>	Publications between 2000 to 2013, found in the SciFinder database for the term “cellulose and ionic liquid”	69
<b>Figure 1.29:</b>	Common structures of cations and anions of ILs.	70
<b>Figure 1.30:</b>	Normalized solvent polarity scale.	72
<b>Figure 1.31:</b>	Hydrogen bonding interaction between imidazolium cation and chloride anion.	75
<b>Figure 1.32:</b>	Hydrogen bonding interaction between 1-ethyl-3-methylimidazolium acetate and cellobiose.	76
<b>Figure 1.33:</b>	Different routes for cellulose modification in ILs.	77
<b>Figure 1.34:</b>	Suggested mechanism for the fluoride ion-mediated cellulose ethanoate hydrolysis and. IL-F/aldehyde mixture.	78
<b>Figure 1.35:</b>	Molecular structures of selected solvatochromic probes.	80
<b>Figure 3.1:</b>	Chemical structures of CHM and CHD acetates.	85
<b>Figure 3.2:</b>	Schematic representation of the apparatus used in kinetic study.	89
<b>Figure 3.3:</b>	Variation of solution conductivity for.uncatalyzed acylation of CHM.	92
<b>Figure 3.4:</b>	Variation of solution conductivity for.uncatalyzed acylation of MCC.	94
<b>Figure 3.5:</b>	Molecular structures of the probes used in solvatochromism.	98
<b>Figure 4.1:</b>	Typical plots showing the variation of solution conductivity for CHM, CHD and MCC.	102
<b>Figure 4.2:</b>	Model compounds for cellulose.	102
<b>Figure 4.3:</b>	Dependence of $k_3$ and DS on the number of carbon atoms of the acyl group	108
<b>Figure 4.4:</b>	Dependence of the activation parameters on the number of carbon atoms of the acyl group.	109

<b>Figure 4.5:</b>	Dependence of the enthalpy and entropy on the number of carbon atoms of the acyl group.	110
<b>Figure 4.6:</b>	Plots for calculation of the pseudo first-order rate constant ( $k_{obs}$ ).	111
<b>Figure 4.7:</b>	Dependence of overall $k_3$ on [IL].	112
<b>Figure 4.8:</b>	Relationship between $k_3$ and molar concentration of ionic liquid.	112
<b>Figure 4.9:</b>	The “dimer nucleophilic mechanism” for dependence of $k_3$ on [amine].	113
<b>Figure 4.10:</b>	Graph between [IL] and wave number of Cellobiose ( $\text{cm}^{-1}$ ).	114
<b>Figure 4.11:</b>	Dependence of solution conductivity on [IL] in DMAC.	115
<b>Figure 4.12:</b>	Dependence of solution conductivity on [IL] in Sulfolane.	116
<b>Figure 4.13:</b>	Dependence of the difference in activation parameters on [IL].	121
<b>Figure 4.14:</b>	Representative rheology plot (shear stress as a function of shear rate).	123
<b>Figure 4.15:</b>	Typical Arrhenius plot ( $\ln \eta$ versus $1/T$ at $40 \text{ s}^{-1}$ ).	124
<b>Figure 4.16:</b>	Dependence of solvent properties on [IL] in MCC-IL-DMAC.	125
<b>Figure 4.17:</b>	Dependence of solvent properties on [IL] in MCC-IL-DMSO/Sulfolane.	126
<b>Figure 4.18:</b>	Snapshot of an MD simulation frame showing the oligomer and its first solvation shell.	128
<b>Figure 4.19:</b>	The radial distribution function, RDF ( $g(r)$ ) of ( $\text{Cl}^-$ ) around the oligomer, in DMAC, and MeCN.	132
<b>Figure 4.20:</b>	The radial distribution function, RDF ( $g(r)$ ) of ( $\text{Cl}^-$ ) of the oligomer, in DMSO and Sulfolane.	132
<b>Figure 4.21:</b>	Suggested mechanism for the catalytic effect of TsCl on the acylation by acid anhydrides.	134
<b>Figure 4.22:</b>	Superimposed $^1\text{H}$ NMR spectra of authentic samples of acetic anhydride and tosyl chloride.	135
<b>Figure 4.23:</b>	A complete reaction mechanism for the imidazole-catalyzed acylation of cellulose.	136
<b>Figure 4.24:</b>	$^1\text{H}$ NMR spectra in $\text{CDCl}_3$ of imidazole acetic anhydride and an equimolar mixture of both reactants.	137
<b>Figure 4.25:</b>	The IR $1850\text{-}1650 \text{ cm}^{-1}$ spectral region for the reaction of acetic anhydride	

	and Imidazole.	138
<b>Figure 4.26:</b>	Number of molecules that remain in contact after collisions as function of time (in ps).	140
<b>Figure 4.27:</b>	Typical plots showing the variation of solution conductivity in function of time obtained for MCC with different anhydrides.	141
<b>Figure 4.28:</b>	Dependence of the degree of substitution of cellulose esters, DS, on the number of carbon atoms of the acyl group of RCOIm or (RCO) <sub>2</sub> O.	144
<b>Figure 4.29:</b>	Dependence of $k_3$ or DS on the number of carbon atoms of the acyl group in Im-catalyzed acylation of MCC.	145

## TABLES INDEX

<b>Table 1.1:</b>	Partial chemical composition of some lignocellulosic materials.	24
<b>Table 1.2:</b>	World largest producers of paper and cellulose.	26
<b>Table 1.3:</b>	DP range of various cellulose materials.	39
<b>Table 1.4:</b>	Dissolution of cellulose from different sources in strong electrolytes/dipolar aprotic solvents.	52
<b>Table 1.5:</b>	Agents and conditions for cellulose derivatization.	67
<b>Table 3.1:</b>	Experimental details of the kinetics of acylation of CHM and CHD by carboxylic acid anhydrides.	92
<b>Table 3.2:</b>	Experimental conditions for the imidazole-catalyzed acylation of model compounds with acid anhydrides.	93
<b>Table 3.3:</b>	Concentration of IL/DAS used for the acetylation of MCC in IL/DAS.	95
<b>Table 4.1:</b>	Ratio of the acid anhydrides employed for the hydroxyl groups of model compounds and cellulose.	101
<b>Table 4.2:</b>	Third order rate constants and activation parameters for the acylation of CHM, CHD, and MCC, in 4.28% LiCl/DMAC.	103
<b>Table 4.3:</b>	IR and $^1\text{H}$ NMR data of the reaction products of CHM and CHD under the conditions of the kinetic experiments.	105
<b>Table 4.4:</b>	Overall and partial third order rate constants $k_3$ , and activation parameters for the acetylation of MCC in IL/DAS mixtures.	117
<b>Table 4.5:</b>	Rate Constants (overall $k_3$ ) and activation parameters for the acetylation of MCC in LiCl-DMAC; IL-DMAC, IL-MeCN, IL-DMSO and IL-Sulfolane.	120
<b>Table 4.6:</b>	Physical properties of various solvent mixtures: IL/DMSO; IL/sulfolane; IL/DMAC; LiCl/DMAC and pure IL samples.	122
<b>Table 4.7:</b>	Energies of flow of pure IL and its solution with MCC and various DAS.	124
<b>Table 4.8:</b>	Results of molecular dynamics simulations of the system oligomer/IL-DAS	129
<b>Table 4.9:</b>	Mulliken atomic charges of ethanoic anhydride and <i>N</i> -acetylimidazole.	139
<b>Table 4.10:</b>	Third order rate constants and activation parameters for the imidazole-catalyzed acylation of MCC in 4% LiCl/DMAC.	142

## 1. INTRODUCTION

### 1.1. Principles and relevance of biomass to green chemistry

The development of polymer technology and consequent increase in world production of petroleum-based polymers has unquestionably resulted in important benefits for diverse industrial sectors. At present, fossil resources, such as petroleum and coal, account for *ca.* 86% of energy and 96% of organic chemicals (Diamantoglou et al., 1996).

The major change seen in recent years is the introduction of green chemistry whose aim is to reduce chemistry-related impact on our lives. Green chemistry searches for alternative, environmentally friendly chemical processes and, at the same, time strive to decrease cost. The 12 basic principles of green chemistry are: (Anastas et al., 1998; Anastas et al., 2002; Anastas et al., 2007; Anastas et al., 2009; Anastas, 2011).

**1-Prevention:** It is better to prevent waste than to treat or clean up waste after it has been created.

**2- Atom economy:** Synthetic methods should be designed to maximize the incorporation of all materials used in the process into the final product.

**3- Less hazardous chemical syntheses:** Wherever practicable, synthetic methods should be designed to use and generate substances that possess little or no toxicity to human health and the environment.

**4- Designing safer chemicals:** Chemical products should be designed to affect their desired function while minimizing their toxicity.

**5- Safer solvents and auxiliaries:** The use of auxiliary substances (e.g; solvents, separation agents etc.) should be made unnecessary wherever possible and innocuous when used.

**6- Design for energy efficiency:** Energy requirements of chemical processes should be recognized for their environmental and economic impact and should be minimized. If possible, synthetic methods should be conducted at ambient temperature and pressure.

**7- Use of renewable feedstock:** A raw material or feedstock should be renewable rather than depleting whenever technically and economically practicable.

**8- Reduce derivatives:** Unnecessary derivatization (use of blocking groups, protection /deprotection, and temporary modification of physical/chemical processes) should be minimized or avoided if possible because such steps require additional reagents and can generate waste.

**9- Catalysis:** Catalytic reagents (as selective as possible) are superior to stoichiometric reagents.

**10- Design for degradation:** Chemical products should be designed so that at the end of their function, they breakdown into innocuous products and do not persist in the environment.

**11- Real-time analysis for pollution prevention:** Analytical methodologies need to be further developed to allow for real-time, in-process monitoring and control prior to the formation of hazardous chemicals.

**12- Inherently safer chemistry for accident prevention:** Substances and the form of a substance used in a chemical process should be chosen to minimize the potential for chemical accidents, including releases, explosions and fires.

The environmental problems associated with petroleum-based products, coupled with ever-increased demand on crude oil have led to the perception that renewable alternatives should be seriously considered and developed. For example, it is estimated that within two decades fossil-based resources will not be enough to meet world demand. In this regard, biomass-based raw materials have attracted much interest and proved to be a feasible alternative (BeMiller et al., 2009; Van Zyl et al., 2011; Steinbach et al., 2011).

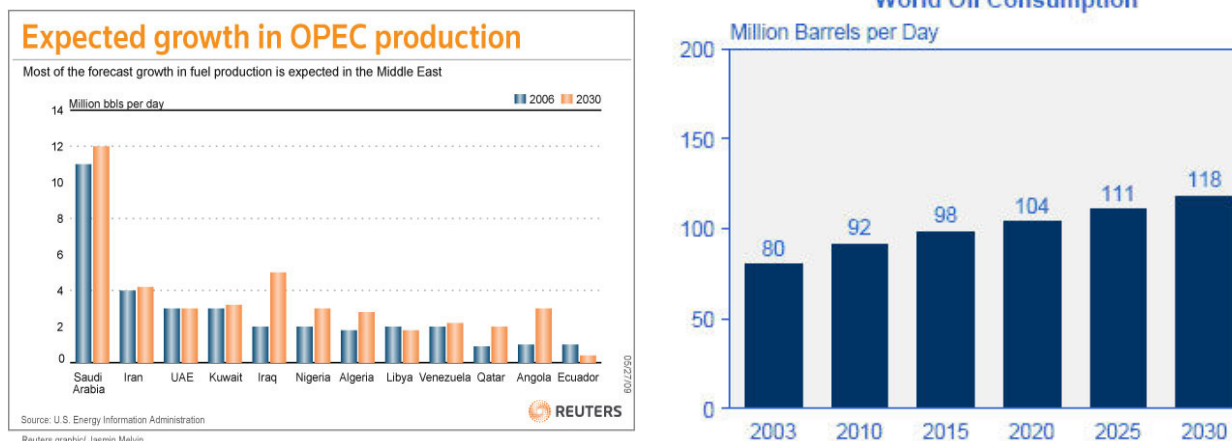


**Figure 1.1:** Estimated oil production and consumption capacity in the world up to 2030.

<https://www.google.com.br/search?q=petroleum+production+demand+projection&tbm=isch&tbo=u&source=univ&sa=X&ei=Bl3JUtgHHeiysQTP2oCQDw&ved=0CIYBELAE&biw=1600&bih=728> (Accessed on 06-01-2014).

Additionally, synthetic polymers are resistant to chemical, photochemical, and enzymatic degradation. This has led, *inter alia*, to an increasingly serious waste disposal problems resulting, e.g., in discouraging/banning the use of polyethylene bags in the supermarkets of several countries, including some parts of Brazil.

Polymers are currently employed in diverse sectors, including paint, food, cosmetic, car, and building industries. In most of these applications, biopolymers, particularly those from renewable sources such as cellulose, chitin/chitosan, and starch represent interesting alternatives, due to their structural versatility, ready biodegradability, and relatively low cost (Cao et al., 2000; Srinivasa et al., 2007). Undoubtedly, these eco-friendly polymers are an important contribution in the search for solutions for the waste-disposal problem; the reduction of CO<sub>2</sub> emission; the development of biocompatible devices, and edible packing films (BeMiller et al., 2009; Van Zyl et al., 2011; Steinbach et al., 2011). In summary, derivatives of biopolymers are here to stay because of their compliance to the principles of green chemistry, in addition to their favorable properties and competitive cost.



### 1.1.1. Position of cellulose within the biomass

Biomass is biological material derived from living, or recently living organisms. This term most often refers to plants or plant-derived materials that are specifically called lignocellulosic biomass (Biomass Energy Center United Kingdom). As an energy source, biomass can either be used directly via combustion to produce heat, or indirectly after converting it to biofuel. Polymeric materials, especially having renewable raw material, has been the subject of research since they retain the sustainable development of economy, technology and environmentally friendly. These polymers (cellulose, hemicellulose and lignin) comply with green chemistry.

The main sources of cellulose are plants; however it can also be isolated by some algae, fungi, and bacteria (French & Bertoniere, 1993). Wood, however, is still the main source of cellulose. This biopolymer is synthesized in plants by photosynthesis in the presence of sunlight using CO<sub>2</sub> from the atmosphere, producing glucose (C<sub>6</sub>H<sub>12</sub>O<sub>6</sub>) with the release of oxygen. Cellulose structure is the output of cellulose chains which are the result of thousands of repeating units of anhydroglucose units (Klock et al., 2005). There are two well-known classes of wood species, hardwood (deciduous) and softwood (coniferous). The fibers are a distinguishing feature for these two classes. Hardwoods, such as eucalyptus have short fibers and conifers have longer fibers such as pine. The composition of wood has much influence on the efficiency of the process for producing the cellulose. Consequently, the pulping and bleaching hardwood is easier than the conifer because the former is stronger, and has less lignin (17 to 26% compared to 20 to 32%) (Tessier & Savoie, 2000).

Representative compositions of lignocellulosic materials are shown below in Table 1.1.

**Table 1.1:** Partial chemical composition of some lignocellulosic materials. (Nevell & Zeronian, 1985; Tammanini & Hauly, 2004; Canettieri et al., 2001; Mussato & Roberto, 2002; Bobleter, 1998; Heinze, 1998).

Lignocellulosic material	% Cellulose	% Hmeicellulose	% Lignin
cotton	95	2	1
jute	60	15	16
sisal	73	14	11
Pinus	49.5	11.0	27.2

<b>Lignocellulosic material</b>	<b>% Cellulose</b>	<b>% Hmeicellulose</b>	<b>% Lignin</b>
Barley bran	23.0	32.7	24.4
Corn cobs	31.7	34.7	20.3
Corn leaves	37.6	34.5	12.6
Bagasse	40.2	26.4	25.2
Rice straw	43.5	22.0	17.2
Wheat straw	33.8	31.8	20.1
Sorghum straw	34.0	44.0	20.0
Oat hulls	30.5	28.6	23.1
eucalyptus Grand	40.2	15.7	26.9
eucalyptus globules	46.3	17.1	22.9

### **1.1.2. Sources of cellulose**

Cellulose is the most common organic polymer in nature, constituting ca. 40% to 50% of most plants. Its natural sources can be considered from two classes; it can be conventional, or extensively employed (e.g., cotton and wood) or non-conventional or less developed (e.g., sisal).

#### **1.1.2.1. Conventional sources**

Brazil is one of the largest world producers of pulp and paper. The main competitive advantage is that 100% of the production of pulp and paper in Brazil comes from planted forests, which are renewable resources. Pulp-producing Brazilian forests are among the most productive in the world. Currently, eucalyptus plants produce an annual average 41m<sup>3</sup> of wood per hectare as compared to pine plants, which has the mean annual productivity 35m<sup>3</sup> of wood per hectare. Currently there are about 5.5 million hectares of planted forest in Brazil, of which 1.7 million hectares are intended for the production of pulp and paper. This area equals only 0.2% of the arable land of the country; as the world leader in the production of eucalyptus pulp, Brazil produced in 2008, 12.85 million tons of pulp and 9.85 million tons of paper. (BRACELPA, 2009)

Leading countries in the manufacture of paper and cellulose are shown below in Table 1.2.

**Table 1.2:** World largest producers of paper and cellulose (BRACELPA 2011)

<b>Paper</b>		<b>Cellulose</b>	
<b>Countries</b>	<b>Tons (mil)</b>	<b>Countries</b>	<b>Tons (mil)</b>
China	86391	United States	48329
United States	71613	China	20813
Japan	26279	Canada	17079
Germany	20902	Brazil	13315
Canada	12857	Sweden	11463
Sweden	10933	Finland	9003
Finland	10602	Japan	8506
South Korea	10481	Russia	7235
Brazil	9428	Indonesia	5971
Indonesia	9363	Chile	5000
India	8693	India	3803
Italy	8449	Germany	2542
Others	84696	Others	24898
<b>Total</b>	<b>370687</b>	<b>Total</b>	<b>177957</b>

### 1.1.2.2. Other sources of cellulose

The first example is sisal-based cellulose. Currently, Brazil is the largest producer and exporter of sisal fiber and about 70 % of Brazilian sisal is exported to European and Asian markets. The cultivation of sisal is concentrated in the Northeast areas such as; the states of Bahia, Paraiba and Rio Grande do Norte that are the major producers of the national production with 93.5, 3.5 and 3 %, respectively. The main applications of the sisal fiber are: making ropes, twine, marine cables, carpets, bags, brooms, and upholstery. It has also been used for the manufacture of pulp for the production of high strength kraft paper, and other types of fine paper, and for cigarette filter, sanitary napkin, diaper, etc. (Martin et al., 2009)

Bacterial cellulose (BC) is also an important raw material for pulp and paper industry. It can be synthesized by the genera *Acetobacter*, *Rhizobium*, *Agrobacterium*, and *Sarcina*. The

most efficient production has been from the bacterium *Acetobacter xylinum*, which has been used in several studies as a template for the production of pulp. Research shows that the bacterial cellulose is chemically identical to plant cellulose; it differs in crystallinity (high) and degrees of polymerization (DP) which is between 2000 and 6000, in few cases range between 16,000 and 20,000. The morphology of bacterial cellulose is strictly dependent on the culture conditions (Bielecki et al., 2005). BC has gained much attention in various field of life. It has diverse applications such as making tires, used in textiles and in high quality speaker diaphragms (Nishi et al., 1990). BC is also used in biomedical field because of its good biocompatibility. It is used for manufacturing of the artificial blood vessels for microsurgery (Klemm et al. 2001) scaffolds for tissue engineering (Bäckdahl et al., 2006) and wound dressings for burn or wound repair (Alvarez et al., 2004; Legeza et al., 2004). It shows low toxicity and non-allergenicity. Recent efforts have been made to improve the antibacterial properties of BC membranes. (Maneerung et al., 2008; Phisalaphong & Jatupaiboon, 2008; Cai et al., 2011). BC composites (polyhydroxyalkanoates) are suitable particularly for soft tissue engineering applications such as cardiac tissue engineering, heart valve reconstruction, and drug delivery studies (Basnett et al. 2012).

## **1.2. Industrial production of cellulose**

### **1.2.1. Pulping process**

Modern cellulose pulp and paper industry has evolved from an ancient time when Chinese developed the paper in ca. 105 A.D. The following discussion is focused on wood, as it is the main source of cellulose. Other material is processed by processes similar to wood, except for the operational conditions. Cellulose fibers in wood are bound to each other by complex organic "glue" called lignin. The lignin produced from the pulping process is separated and burnt to produce energy, or used to make useful chemical products, e.g., sulfonate.

The main purpose of pulping process is to extract cellulose from other components in the wood (or other source), including lignin, waxes and resins as much as possible without destroying the fiber strength (Wangaard, F. F. 1981). Before wood can be pulped, it must undergo debarking. Bark contains little or no fibrous material, and is removed either

mechanically or hydraulically. Debarked logs are then sent to a chipper where they are chopped into small pieces ready for pulping. (Sun & Cheng, 2005). At the end of pulping process, 90-95% of bleached pulped cellulose is achieved as seen in Figure 1.2.

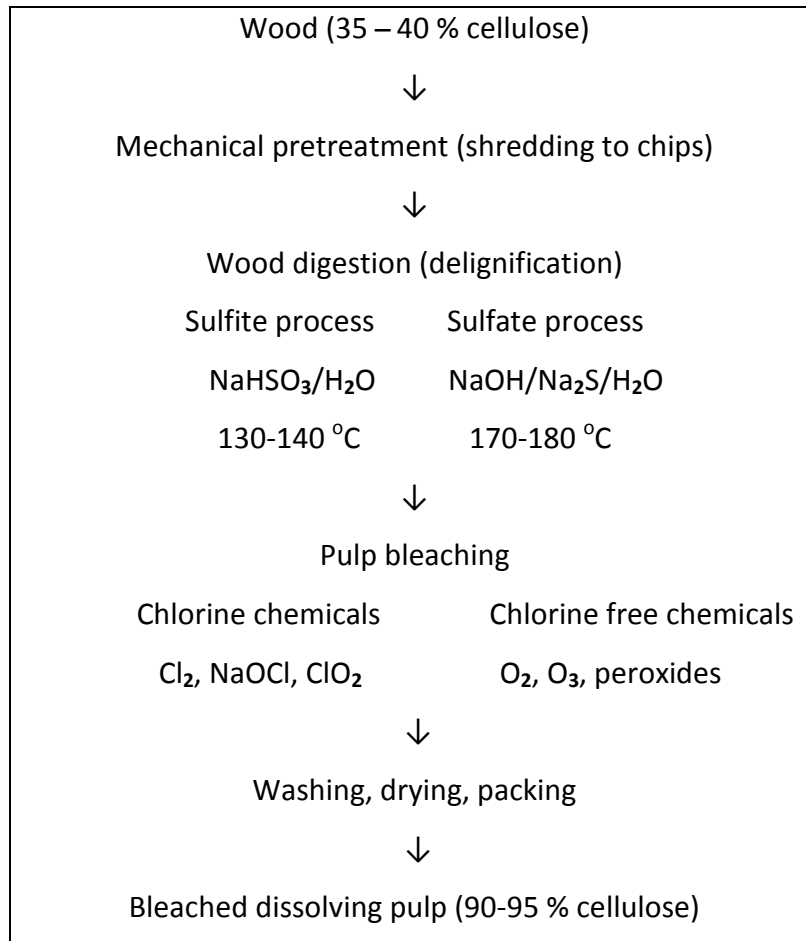


**Figure 1.2:** Schematic representation of wood pulping process (Klemm et al. 1998).

Pulping can be done either by mechanical, chemical, or semi mechanical (a combination of mechanical and chemical) methods, depending upon the type of product to be obtained. These methods are briefly explained below.

### **1.2.1.1. Mechanical pulping**

Mechanical pulping is more important than all other processes in a sense that it converts almost all of the wood used in this process into paper. Lignin is not removed during mechanical pulping. The presence of lignin is responsible for low durability and yellowing with age. This process is further divided into several processes on the basis of conditions applied. Thermomechanical pulping process is a kind of mechanical pulping in which wood chips are exposed to steam at higher temperature and pressure before the separation of fibers. Higher temperature soften the lignin contents and make the fiber separation much easier. Pulp made in this process is stronger and need less electrical energy. This pulp can be bleached further to produce bleached chemithermomechanical pulps (BCTMP) with yields of 87-90% (Sharman et al. 1994).

Another process is called stone groundwood process. Revolving disks are used to grind wood chips into pulp. There can be a problem of wood damage due to friction and heat. So water is added to overcome this problem. Mechanical (or groundwood) pulping method produces the highest yield of pulp. Groundwood pulp has many qualities that make it satisfactory for printing, but also has disadvantages, such as low strength, low brightness, and the tendency to become yellow with time. Paper made from mechanical pulp, also has a high quantity of imperfections or unfibered bundles of fiber that were torn from the wood during grinding. Groundwood pulp is used for low-quality papers used for newspapers, telephone directories, catalogs, and "pulp" magazines, as well as household items such as paper towels and tissues.

### **1.2.1.2. Chemical pulping**

Chemical method is the most important as it results in the removal of almost all the lignin and other non-fibrous material of the wood. This method produces the highest-quality papers such as printing and writing papers. The only disadvantage of this process is its low fibrous yield which is generally 50-55%, lower than the other pulping methods. There are several chemical pulping methods some of which are discussed in the following section.

#### **1.2.1.2.1. kraft pulping**

In this method digestion of wood chips is done at high temperature and pressure in the presence of white liquor (aqueous solution of sodium sulfide and sodium hydroxide). This white liquor dissolves the lignin and separates the cellulose fibers. There are two types of digester systems; batch and continuous. Batch digester system is used in most of the kraft pulp processes. In this process, after completion of cooking step, all the contents of digester are sent to blow tank from where they are sent to pulp washer. In this washer, spent cooking liquor is separated from the pulp. Then pulp is subjected to different washing and possibly bleaching steps. After washing pulp is pressed and dried into finished products (U.S. Environmental Protection Agency 1983). The waste products such as spent cooking liquor and pulp wash are combined to form black liquor which is concentrated to strong black liquor and then fired in a recovery furnace. Inorganic chemicals such as sodium salts with some calcium salts are collected at the bottom of the furnace as a molten smelt. In almost all the pulp and paper industries, heat generated in the process is not sufficient to run the plant so conventional industrial boilers are used that burn coal, natural gas, oil or wood (Source Category Report 1983).

#### **1.2.1.2.2. Acid sulfite pulping**

Over the years, pollution laws have resulted in the use of different chemicals. The sulfite process was for a long time the most important chemical pulping process, but has been largely replaced by alkaline pulping. This sulfite pulping method is similar to kraft method except for the difference of some chemicals used in the cooking liquor. Sulfurous acid is used instead of caustic solution for the dissolution of lignin. Sodium, magnesium, ammonium, or calcium bisulfites are used to buffer the cooking solution. Digestion is carried out in the presence of sulfurous acid/bisulfites at elevated temperature and pressure in the digester. After the completion of cooking step, the material is pumped into dump tank at low pressure. The red liquor (spent sulfite liquor) is treated and discarded. The pulp is washed, processed and knots and bundles of fibers are removed through centrifugation. At the end, it is bleached, pressed and dried (U.S. Environmental Protection Agency 1977). Sulfur dioxide (SO<sub>2</sub>) is generated in this

process which is considered the major pollution causing agents in the industry. The recovery systems such as acid fortification tower and multiple effect evaporators are used to collect  $\text{SO}_2$  so that it can be reused.

### **1.2.1.2.3. Neutral sulfite semichemical pulping**

As the name indicates, neutral solution of sodium sulfite and sodium carbonate are used in this process. Sulfite ions remove the lignin from the wood by reacting with it and sodium bicarbonate act as buffer solution (Benjamin, M. et al 1969). In this process small portion of lignin is removed during cooking and achieves high yield upto 60-80 % as compared to 50-55% in other chemical processes which is the major difference when compared to all other pulping processes (Hendrickson, et al. 1970). Some mills operate inconjunction with kraft mills mix their spent liquor with kraft liquor. The recovery processes are very similar to that of sulfite process. Sulfur dioxide is the major pollutant in this process which can be recovered using absorbing towers, blower tanks, digesters and recovery furnaces (Caleano et al. 1972).

## **1.3. Structure of cellulose**

Cellulose structure is one of the most unique in carbohydrate chemistry but it has an intense effect on the type of chemical reaction which takes place during this biopolymer modification. Although sufficient research has been done on the morphology of cellulose but new information is constantly being discovered by employing new technological advances along with conventional analytical tools.

Instrumental methods have been advanced in cellulose research such as crystallography and microscopy to understand the complexity of cellulose; amorphous and crystalline part of cellulose and direction of cellulose chains in unit cells (Antoinette c. O'sullivan. 1997). Computational chemistry has played an important role to understand the complex structure of cellulose and its interaction and reaction in different solvent systems. Cellulose has three major structural levels that will be briefly discussed below: 1) supramolecular level; 2) molecular level and 3) morphological level (Klemm et al. 1998).



### 1.3.1. Supramolecular structure of cellulose

As the name indicates, cellulose is a type of sugar ("ose"). It consists of a long chain of monomer repeating units, glucose. The structure of cellulose is formed by repeating D-glucose units which are condensed together through  $\beta$ -1,4-glycosidic linkage. Elemental analysis showed that cellulose contains carbon, hydrogen and oxygen in 44.4%, 6.2 % and 49.3 % respectively, which is equivalent to an empirical formula of  $(C_6H_{10}O_5)_n$  (AGU) whose molar mass is 162.14 g/mol (Eastmound et al., 1989).

Wood is composed of outer thick layer of cell wall and inner thin layer contains cellulosic material. Cellulose is composed of large number of macro fibers which are further divided into smaller microfibrils. These microfibrils are formed by the combination of 36 individual cellulose molecules (Habibi et al. 2010) which are packed into a larger unit called microfibrillated cellulose that constitutes the cellulose fibres. The diameter of elementary fibrils is 5nm and that of microfibrillated cellulose has the diameter ranging from 20nm to 50 nm. The microfibrils are formed in the process of biosynthesis and have length in several micrometers. Each microfibril is considered as small hair like strand within the cellulose crystal, which is linked along the microfibril axis by disordered amorphous area (Azizi et al. 2005). These smaller microfibrils constitute the cellulose chains consisting of repeating unit of glucose as depicted in Figure 1.3 (Lavoine et al., 2012).

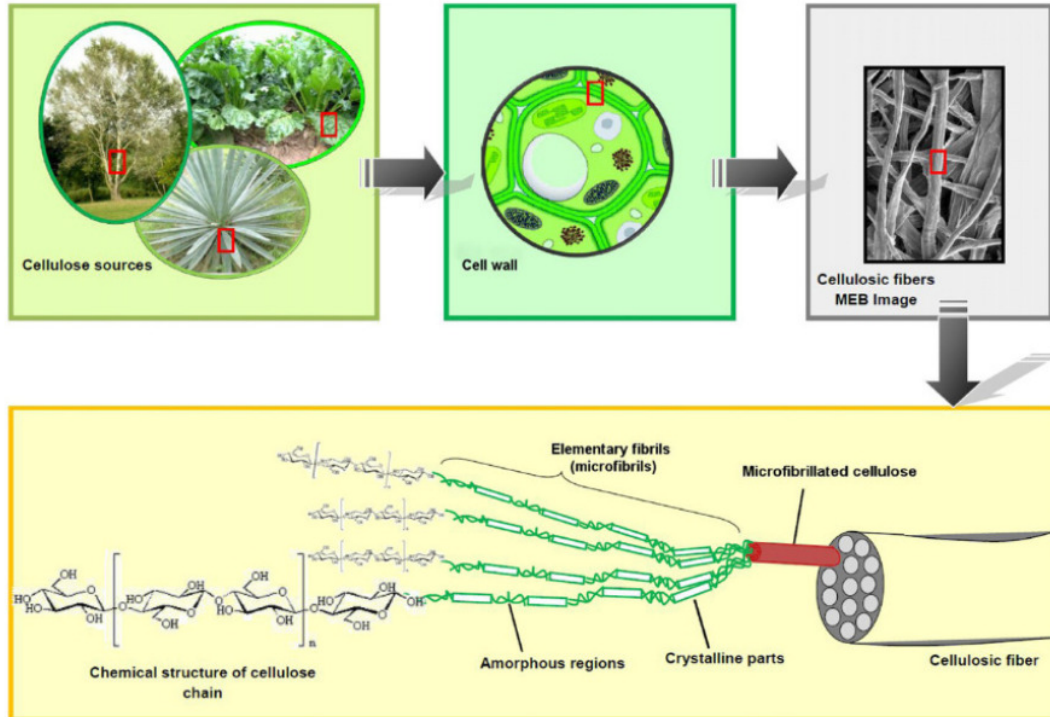


**Figure 1.3:** From cellulose sources to cellulose molecules. Details of the cellulosic fiber structure with emphasis on the cellulose micro fibrils (colored). [Reproduced from Lavoine et al., 2012 with permission]

### 1.3.2. Molecular structure of cellulose

Cellulose is a biopolymer composed of D-glucose units which condense through  $\beta$  (1 $\rightarrow$ 4)-glycosidic bonds and differ from starch, glycogen and other carbohydrates because of  $\alpha$  (1 $\rightarrow$ 4)-glycosidic bonds in them. It is a straight chain biopolymer composed of repeating units called anhydroglucos unit as shown in Figure 1.4.

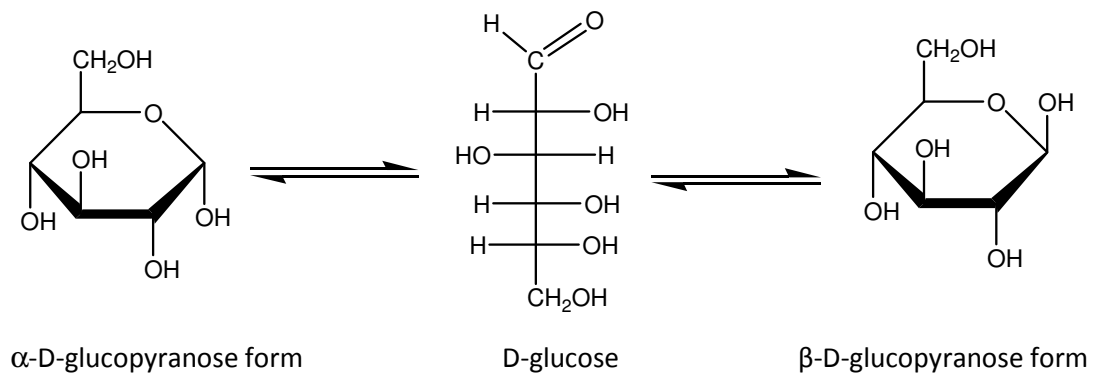


**Figure 1.4:** Open chain and closed ring form of glucose unit

When hydroxyl group at C-1 and  $-\text{CH}_2\text{OH}$  group at C-5 are on opposite sides of the ring's plane (a *trans* arrangement), this arrangement is designated as " $\alpha$ -" and it is called " $\beta$ -" when they are on the same side of the plane. Two units of glucose linked with each other through  $\beta$  (1 $\rightarrow$ 4)-glycosidic bonds to form cellobiose and these repeating units of cellobiose constitute the cellulose chains as shown in Figure 1.5.

Cellulose is a straight chain polymer with multiple hydroxyl groups on the glucose ring. Considering the dimerized cellobiose as the basic unit, the cellulose can be considered as an isotactic polymer of cellobiose. When cellulose is hydrolyzed with an aqueous acid, D-Glucose is produced in a quantitative yield as a result of hydrolysis (Klemm et al 1998). Anhydroglucose unit consists of two secondary hydroxyl groups at C-2, C-3, and one primary hydroxyl group at C-6 positions, which are responsible for the cellulose modification. The vicinal secondary hydroxy groups represent a typical glycol structure. The ring oxygen atom and bridging one are responsible for the intra- and intermolecular interactions (hydrogen bonding) and in degradation reactions.

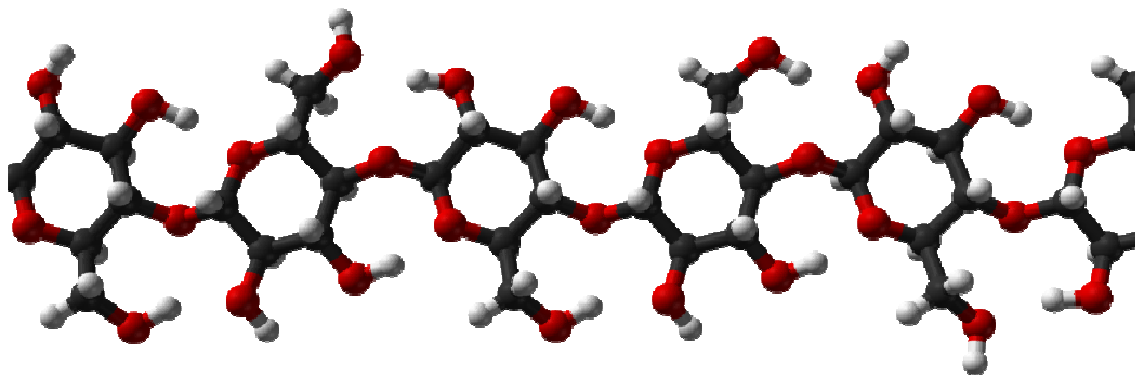


**Figure 1.5:** Molecular structure of single strands of cellulose fiber. The colors employed for atom designation are: white, hydrogen; black, carbon; red, oxygen (<http://en.wikipedia.org/wiki/Cellulose> (Accessed on 01-10-2013)).

The molecular structure of cellulose leads to extensive inter- and intra-molecular hydrogen bonding as shown below in Figure 1.6 (El Seoud et al. 2013). The consequence of this bonding, and van der Waals interactions, (Medronho et al. 2012) is that cellulose chains align in

an ordered state to form crystalline regions, whereas the less ordered segments constitute the amorphous part as shown in Figure 1.3. The ratio of ordered to disordered regions (index of crystallinity,  $I_c$ ) of cellulose varies considerably with its origin and the extent of treatment, both physical and chemical, to which the raw material was submitted.

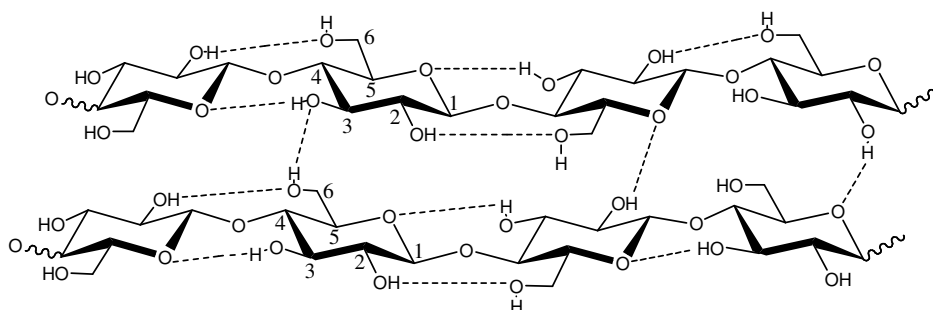


**Figure 1.6:** Intra- and intermolecular hydrogen bonds in cellulose. The anhydroglucose units, AGUs, are linked by 1,4- $\beta$ -glycosidic bonds ( El Seoud et al., 2013)

This structural feature bears on several aspects of chemistry and applications of cellulose; we dwell here on cellulose processing and reactivity. For example, cellulose cannot be processed by the techniques most frequently employed for synthetic polymers, namely, injection molding and extrusion from the melt. The reason is that its temperature of melting presumably lies above the temperature of its thermal decomposition. Several commercial cellulose derivatives, in particular cellulose acetate, CA, and nitrate, are soluble, however, in common organic solvents, e.g., acetone, alcohol and chloroform, and can be extruded as fibers, films, rods and sheets. Since the AGU has three free OH groups (at C2, C3 and C6) it is possible, in principle, to obtain derivatives of any degree of substitution, DS, *directly* by adjusting the molar ratio (derivatizing agent)/AGU. In practice, however, this is not feasible, because: (i) the three hydroxyls have different reactivities both under heterogeneous (Malm et al. 1953) and homogeneous reaction conditions (Nawaz et al. 2012) (ii) The accessibilities of the *same* hydroxyl group in the amorphous and crystalline regions are different (Klemm et al. 1998). Consequently, it is not feasible to obtain *uniformly substituted* cellulose derivative with DS, say of 1 to 2.5 *directly*, *i.e.*, by the (heterogeneous) reaction of a slurry of cellulose in the derivatizing reagent. The reason is that the products obtained will be heterogeneous, even if the (average) DS is achieved. The AGU's of the amorphous regions will be more substituted

than their counterparts in the crystalline regions. This heterogeneity may lead, for example, to serious solubility problems in solvents that are usually industrially employed, e.g., acetone (Law R. C. 2004).

### 1.3.3. Morphological structure of cellulose

Morphology of cellulose plays an important role in its dissolution, regeneration and further modification process. The most used techniques employed today for determination of cellulose morphology are electron microscopic techniques (scanning and transmission electron microscopy). Elementary fibril has been considered as the smallest morphological unit by various authors (Muhlethaler, 1965; Heyn; 1966). A uniform fibril was considered of about 3.5nm in diameter (Fengel and Wegener 1989). SEM investigations and WAXS (Wide-angle X-ray scattering) data (Fink et al. 1990) shows that the size of fibril is debatable and considered in the range of 3-20nm in diameter depending upon the cellulose sources. The larger morphological units are formed with diameters between 10-50nm by the aggregation of microfibril units as shown below in Figure 1.7.

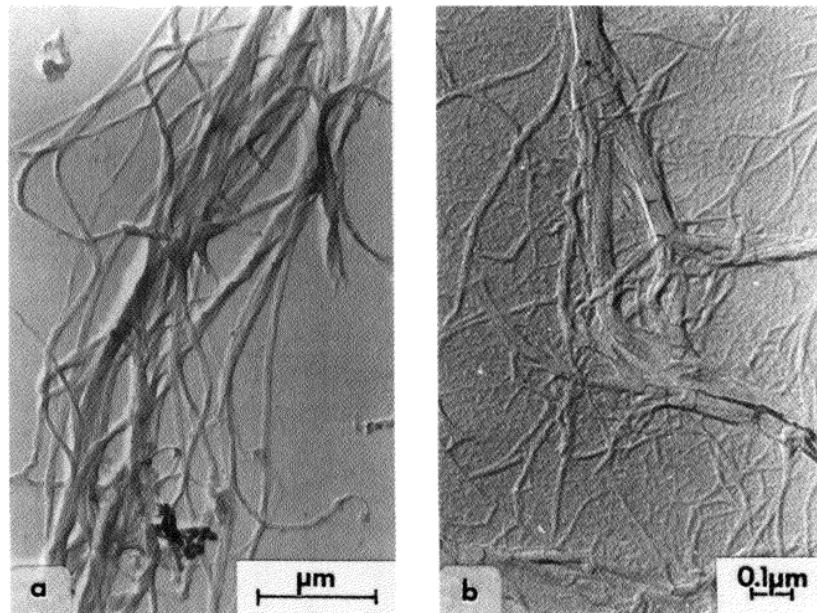


**Figure 1.7:** Isolated microfibrils of cellulose of different origin (a) cotton linters, (b) spruce sulfite pulp (Klemm et al. 1998).

### 1.3.4. X-ray crystallography of cellulose I

Various techniques have been used for its structure determination including Raman spectroscopy (Atalla and VanderHart, 1989), scanning electron microscopy (SEM), (Fengel and Stoll, 1989) atomic force microscopy (AFM), (Hanley et al., 1992; Kuutti et al., 1995) transmission electron microscopy (TEM), (Purz et al. 1995) and scanning tunnelling microscopy (STM), (Frommer, 1992).

Crystalline nature of cellulose was first discovered by Von Naegeli in 1858 using polarizing microscope (von Nageli, 1858). Elucidation of the crystal structure of cellulose began with (Sponser and Dore., 1926) who suggested a single chain unit cell with dimensions:  $a = 0.61$ ;  $b$  (fiber axis  $= 1.034$ ;  $c = 0.54$  nm; and  $\beta = 88^\circ$ . Eleven years later, (Meyer and Misch 1937) explained that the unit cell parameters along the fiber axis direction is shorter than the fully extended length of a cellobiose residue by proposing a model with a curve, resulting from the formation of a hydrogen bond between the C(3) of one glucose residue and the ring oxygen of the next (Preston, 1986).

Highly crystalline celluloses (e.g. *Valonia ventricosa*) were studied and gave sufficient resolved spectrum which showed slightly different diffraction pattern with indication of an eight-chain unit cell (Honjo and Watanabe, 1958). Wood, cotton, ramie and other fibrous celluloses, of medium crystallinity, were found to be consistent with a two-chain monoclinic unit cell as shown in Figure 1.8.

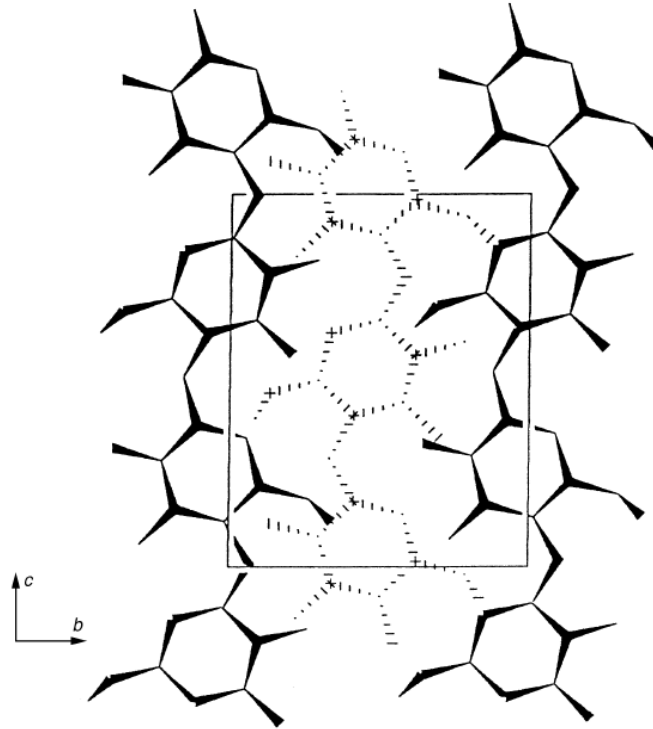


**Figure 1.8:** Projections of a two-chain model of cellulose I (*Valonia ventricosa*) perpendicular to  $bc$  plane (Woodcock and Sarko, 1980).

A unit cell with one non- $90^\circ$  angle ( $a \neq b \neq c$  and  $\gamma \neq \alpha = \beta = 90^\circ$ ), with dimensions:  $a = 0.778$ ;  $b = 0.820$ ;  $c$  (fiber axis)  $1.034$  nm; and angle  $\gamma = 96.5^\circ$  (Woodcock and Sarko, 1980). It was accepted that the two-chain unit cells of other native celluloses could very nearly be considered as sub-cells of the eight-chain *Valonia* unit cell. The unit cell contains a two-ring portion of the cellulose chain which is  $1.034$  nm in length, called the fiber repeat.

### 1.3.5. Some relevant characteristic of cellulose

Cellulose is a tasteless, odorless and is hydrophilic biopolymer with contact angle of  $20$ - $30^\circ$  (Bishop et al. 2007). It is insoluble in water and most of the organic solvents. Cellulose is a chiral and biodegradable material. It can be broken down into glucose units when treated with concentrated acids at higher temperature, or with enzymes (cellulases). Cellulose is present more in crystalline form which can be converted into amorphous form at high temperature

(320 °C) and pressure (25 MPa), or by extensive grinding (Deguchi et al. 2006). Some relevant characteristics of cellulose are discussed below.

### 1.3.5.1. Degree of polymerization of cellulose

The molecular size of cellulose can be defined in terms of its average degree of polymerization (*DP*). The average molar mass results from the product of the *DP* and the molar mass of the repeating AGU. The *DP* values of cellulose samples differ widely, depending on origin and pretreatment. Table 1.3 presented *DP* values of several types of native and regenerated cellulose as shown below (Klemm et al. 1998).

**Table 1.3:** DP range of various cellulose materials

Material	Range of DP
Native cotton	up to 12000
Scoured and bleached cotton linters	800-1800
Wood pulp (dissolving pulp)	600-1200
Man-made cellulose filaments and fibers	250-500
Cellulose powders (prepared by partial hydrolysis and mechanical disintegration)	100-200

### 1.3.5.2. Index of crystallinity (*I<sub>c</sub>*) of cellulose

Crystallinity index of cellulose can be determined using X-ray diffraction method. The crystallinity index of cellulose, *I<sub>c</sub>*, is calculated from the formula

$$I_c = 1 - (I_{\min} / I_{\max})$$

where *I<sub>min</sub>* is the intensity minimum of amorphous portion of cellulose between  $2\theta = 18$  and  $19^\circ$ , and *I<sub>max</sub>* is the intensity of the crystalline peak at the maximum between  $2\theta = 22$  and  $23^\circ$ .



(Possidonio et al. 2009). A more refined method for the determination of Ic is based on peak area, obtained by deconvolution of the X-ray diffraction curve, as shown in Figure 1.9.

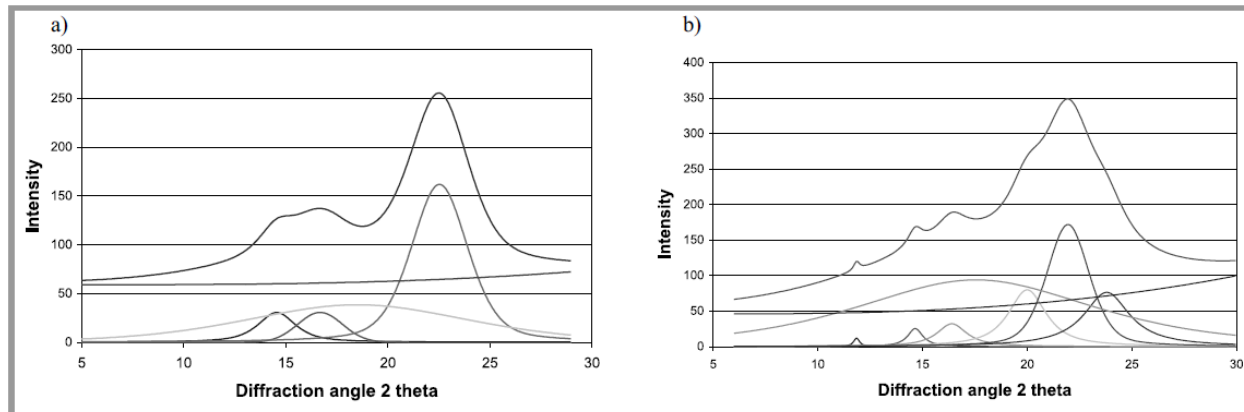


**Figure 1.9:** X-ray diffraction pattern of: a); crude pine wood, b); pinewood mercerised by 25% alkali solution for 45 minutes.

It can be seen from Figure 1.9 (a) that only three peaks are obtained in the X-ray diffraction pattern of unmodified pine wood at  $2\theta = 15^\circ$ ,  $17^\circ$  and  $22.7^\circ$ ; these are derived from cellulose I. The latter is the form of cellulose found in nature. When the sample was examined after mercerization (i.e., after treatment with alkali solution), three additional peaks appeared at  $2\theta = 12.5^\circ$ ,  $20^\circ$  and  $22^\circ$ . These are due to cellulose II which can be obtained from cellulose I by either of two processes: (a) regeneration, which is the solubilization of cellulose I in a solvent followed by reprecipitation by dilution in water to give cellulose II, or (b) mercerization, which is the process of swelling native fibers in concentrated alkali, to yield cellulose II on removal of the swelling agent (Osullivan, C. A., 1997).

These results show that there is a polymorphic transformation of cellulose I into cellulose II that depends upon the chemical pretreatment conditions, e.g; treatment time and concentration of alkaline solution (Borysiak, S. & Doczekalska, B. 2005). The greatest efficiency of polymorphic transition was found at the highest concentration (20-25%) of NaOH used and with increase of mercerization time.

### 1.3.5.3. $\alpha$ -Cellulose content

When cellulose sample is treated with 17.5 % NaOH solution, the part of cellulose sample which is insoluble in this solution, is called  $\alpha$ -cellulose (Dalmeida 1988; Sjostrom 1993).  $\alpha$ -cellulose contents of the sample can be calculated by mass difference of the sample before and after the treatment of this sample with 17.5% NaOH solution using the following equation 1.1.

$$\% \alpha\text{-cellulose} = \frac{\text{mass}_{\alpha\text{-cellulose}} \times 100}{\text{mass}_{\text{cellulose}}} \quad (1.1)$$

The alkali treatment decreased the degree of polymerization (DP) and crystallinity index of the sample. This could be due to alkali induced partial oxidative degradation and swelling of the polymer, leading to a rearrangement of the cellulose chains. Moreover, the  $\alpha$ -cellulose content of the treated sample is increased due to the partial extraction of low molecular fractions of cellulose and hemicelluloses.

## 1.4. Derivatization of cellulose

### 1.4.1. Strategies for derivatization of cellulose

Cellulose derivatization has been carried out using different derivatizing agents (e.g., carboxylic acids activated with catalysts, acid anhydrides acyl chlorides, alkyl halides). This process uses two different reactions conditions, heterogeneous (industrial) and homogeneous reaction conditions which are discussed in detail in the following section. More emphasis is put on carboxylic acid esters because these have been studied in more details than ethers.

### 1.4.2. Derivatization under heterogeneous reaction conditions

The production of cellulose esters by industrial processes, *i.e.*, under heterogeneous reaction conditions is well-established processes. Thanks to relatively recent developments (e.g., fast acetylation/fast hydrolysis process for CAs) these processes are cost-effective; there is no immediate need for major changes in industrial plants. For commodity products, e.g., CA the properties are “adjusted” by blending several batches. Due to these aspects, derivatization

under heterogeneous conditions faces limitations whenever a more rigid control of product characteristics, hence applications, e.g., in filters for hemodialysis where blood compatibility is an essential requirement (Diamantoglou and Vienken, 1996). The (unavoidable) decrease of DP during cellulose derivatization under heterogeneous conditions (e.g., due to acid- or base-catalyzed degradation) is, sometimes intentional, e.g., in order to decrease the viscosity of cellulose xanthate in the rayon production process. Blending of the products of several batches leads to products with acceptably reproducible characteristics/performance. A noticeable limitation is that the heterogeneous reaction is not employed commercially for the production of relatively hydrophobic esters. These compounds are important because of their lower melting temperature (leading to less drastic extrusion conditions); higher solubility in common organic solvents, and compatibility in blends with relatively hydrophobic polymers. In fact, the commercially available ester with the longest acyl group chain is cellulose butyrate. Another problem is connected with obtaining “one-pot” products with mixed substituents, e.g., acetate/butyrate derivatives. This is due to the intrinsic difficulty of controlling the reactivity of two competing reagents (e.g., acetic- and butyric anhydride) under heterogeneous conditions. In summary, the heterogeneous reaction scheme works fine for commodity products; alternative schemes are required for speciality products, one of these is discussed in the next part.

### **1.4.3. The homogeneous reaction scheme**

Some cellulose solvents, the so called derivatizing solvents, dissolve the biopolymer because they transform it into a derivative, hence disrupt the existing hydrogen bonding network. Examples are (solvent system, cellulose derivative formed):  $\text{N}_2\text{O}_4/\text{DMF}$ , nitrite;  $\text{HCO}_2\text{H}/\text{H}_2\text{SO}_4$ , formate;  $\text{F}_3\text{CCO}_2\text{H}$ , trifluoroacetate;  $\text{Cl}_2\text{CHCO}_2\text{H}$ , dichloroacetate; paraformaldehyde/DMSO, hydroxymethyl;  $\text{ClSi}(\text{CH}_3)_3$ , trimethylsilyl. If these solvent systems are employed for cellulose dissolution and derivatization, then functional groups introduced should be easily removable by simple hydrolysis after further derivatization. (El Seoud et al. 2005). One possible problem of this system is the poor reproducibility because of side reactions and formation of some undefined moieties.

On the other hand, there are non-derivatizing solvents that cause dissolution without forming covalent bonds. This is followed by reaction with a derivatizing agent (acid anhydride; acyl chloride/base; alkyl halide/solid NaOH) to give the desired product. We will concentrate on non-derivatizing solvents onwards.

The latest advances in cellulose chemistry are the homogeneous reaction scheme, HRS, where cellulose is dissolved in non-derivatizing solvents. A recent interesting extension of HRS is that employed for obtaining ethers, by using ILs with basic counter-ion, because the reaction does not require an inorganic base in order to activate cellulose, hence is carried out under completely homogeneous conditions (Moellmann et al. 2009). In principle, HRS is free of the consequences of the semi-crystalline structure of cellulose on reactivity because biopolymer chain is decrystallized upon solubilization (Ramos et al. 2005). This does not mean, however, that the cellulose chains are mono-disperse in these solvents, as shown by light scattering of solutions of cellulose in LiCl/DMAC, (Trulove, et al. 2009; Muthukumar et al. 2010; Ramos et al. 2011). Nevertheless, the products are expected to be largely regularly substituted, both within AGU and along the biopolymer backbone. Additional advantages of HRS include: little degradation of the starting polymer; high reproducibility; better control of reactions leading to the introduction of two functional groups (as in mixed esters). (El Seoud and Heinze, 2005). Whereas the relevance to industrial application of negligible cellulose degradation maybe open to question, HRS is definitely superior in terms of much better control of the product characteristics, hence performance. The latter fact is the impetus of continued intense interest in pursuing different aspects of this scheme.

#### **1.4.4. Derivatization of cellulose under homogeneous reaction conditions**

There are only a few solvents that dissolve cellulose physically, *i.e.*, without forming a covalent bond. These include in *N*-methylmorpholine *N*-oxide (Chaudemanche and Navard, 2011), alkaline solutions (Cuissinat and Navard, 2006), and ionic liquids (El Seoud et al. 2007; Pinkert et al. 2010). Most other molecular solvents cause swelling of cellulose to varying extents, but not complete dissolution. Nevertheless, disruption of these interactions can be readily achieved by using strong electrolytes, SEs, in dipolar aprotic solvents, DAS. Examples of SEs

include LiCl and tetraalkylammonium fluoride hydrates ( $R_4NF \cdot xH_2O$ ). Examples of the DAS are *N,N*-dimethylacetamide, DMAC, *N*-methylpyrrolidin-2-one, DMSO and sulfolane. Briefly, these electrolytes dissociate in the DAS employed, due to their high polarity and relative permittivity. A combination of biopolymer-solvent system interactions, including those with the unsolvated ions, and/or their complexes with DAS disrupt the hydrogen-bond network present, leading to biopolymer dissolution. The importance of components of solvent system and the structural characteristics of cellulose can be shown by the following results: (i) tetra (1-butyl) ammonium chloride and bromide are soluble in DMSO but do not dissolve cellulose (Heinze et al 2000). (ii) in the same DAS, LiCl is more effective than LiBr; (iii) TBAF-3H<sub>2</sub>O/DMSO dissolves cellulose at room temperature; the corresponding tetramethylammonium fluoride is ineffective; benzyltrimethylammonium fluoride hydrate is only partially satisfactory (Köhler and Heinze, 2007), whereas dibenzyltrimethylammonium fluoride-0.1 H<sub>2</sub>O is as efficient as TBAF-3H<sub>2</sub>O (Casarano, et al. 2014), (iv) MCC dissolves in LiCl/DMAC more readily than fibrous celluloses; dissolution of the latter depend on their DP and Ic; cotton is frequently mercerized in order to facilitate its dissolution (Marson and El Seoud, 1999; El Seoud et al. 2000; Ass et al. 2006).

In recent years, LiCl/DMAC and tetraalkylfluoride hydrates ( $R_4NF \cdot x H_2O$ ) have become popular solvent systems for dissolution of cellulose, chitin/chitosan and starch. The former system was first employed in order to dissolve polyamides and chitin (Huglin, M. 1972; Kwolek et al. 1977; Austin 1977; McCormick et al. 1979; Gagnaire et al. 1983). Its use quickly spread, and the application to dissolve cellulose was reported for the first time almost concomitantly by McCormick (McCormick 1981) and Turbak (Turbak et al.1981); the (TBAF) system has been developed; thanks to the work of Heinze et al, and the groups at USP, *vide infra* (I did not find the reference). The mechanisms involved in biopolymer dissolution by these solvent systems will be discussed below in more detail.

Despite the advantages of HRS in terms of better product control, there is an obvious need to evaluate the environmental and economic aspects of this approach. We note that published toxicological data show that DMAC (Kennedy 1986) and DMSO (Willhite and Katz, 1984) are much safer solvents for derivatization than, e.g., dichloromethane (Manno et al. 1992) that is employed in industrial, *i.e.*, heterogeneous preparation of cellulose acetate (Bogan and

Brewer, 1985). Due to relatively high cost of the SE/DAS system, it is imperative that HRS is optimized in order to be competitive. For example, DMAC, unreacted acetic anhydride, and the produced acetic acid have been recovered, essentially pure, from the reaction mixture by fractional distillation under reduced pressure (Marson and El Seoud, 1999). Although no attempt has been made to recover LiCl or R<sub>4</sub>NF, they can be precipitated by addition of a suitable, less polar solvent. In principle, heating solutions of quaternary ammonium fluorides may lead to side reactions, e.g., Hofmann elimination (Sharma and Fry, 1983), and other reactions that will be discussed below.

### **1.5. Steps for cellulose derivatization under homogenous conditions**

There are three major steps for cellulose derivatization (activation, dissolution and derivatization) which are discussed in detail below.

#### **1.5.1. Cellulose activation**

Cellulose activation is the first step in the production of cellulose esters and ethers under homogeneous reaction conditions. Different strategies have been used to activate the cellulose prior to dissolution as discussed below.

#### **1.5.2. Strategies for cellulose activation**

Depending on the solvent system employed in order to dissolve cellulose, it is necessary to submit the biopolymer to an “activation” pretreatment step, before its dissolution is attempted; this is the case for LiCl/DMAC. On the other hand, R<sub>4</sub>NF-hydrate/DMSO and ionic liquids dissolve MCC and fibrous celluloses directly, *i.e.*, without prior activation. The objective of activation is to increase the diffusion of reagents into cellulose supra-molecular structure, by making the crystallite surfaces and the crystalline regions more accessible. This is achieved by inter- and intra-crystalline penetration of activating agent into cellulose, which disrupts strong, water-mediated hydrogen bonding between biopolymer chains (Callais et al. 1986; Klemm et al. 1998). The relevance of this step to the success of reaction is demonstrated by erratic results that are obtained if it is not carried out properly. The following results of cellulose acetylation

with 50 wt% acetic anhydride in pyridine, at 30 °C, drive home the point (the Figures refer to acetyl content): no activation, 8.8%; pre-treatment with chloroform/pyridine, 26.4%; same pre-treatment with ethanol/chloroform, 27.6% (Krässig 1986). In case of ILs, cellulose activation step has been employed (Barthel et al. 2006; Heinze et al. 2005), or disregarded, (Wu et al. 2004). Our results showed that this step may not require as there is no change in DS for the outcome of the reaction in acetylation of MCC (Fidale et al. 2009).

### **1.5.2.1. Activation by solvent exchange**

Native or mercerized cellulose can be activated by a solvent exchange scheme, in which the biopolymer is first swollen with water; the latter is displaced by methanol, and then finally by the derivatizing DAS, e.g., DMAC. (McCormick et al. 1985, Pionteck et al. 1996, Dawsey and McCormick, 1990). This method is universal, applicable to all types of cellulose, including bacterial cellulose. It is, however, both laborious and expensive. For example, one day is needed for the activation of MCC, by using 25 mL of water; 64 mL of methanol, and 80 mL of DMAC/g cellulose. Its use is recommended where cellulose dissolution with almost no degradation is required.

### **1.5.2.2. Water entrainment by partial solvent distillation**

Activation by distillation of a part of reaction solvent (*ca.* 25%) is based on the fact that at its boiling point, DAS has sufficiently high vapor pressure to cause extensive fiber swelling. (Ekmanis and Turbak, 1986, Ekmanis 1987, Striegel and Timpa, 1996, Silva and Laver, 1997). This single-step method is simpler, faster than solvent exchange, and consumes less LiCl for biopolymer dissolution (Timpa 1991). Two problems, however, are associated with this method: (i) It does not eliminate water completely, which leads to consumption of a part of acylating agent (Marson 1999); (ii) its use may lead to biopolymer degradation by two routes: The first involves the formation of furan structures by reaction of biopolymer with, *N,N*-dimethylacetamide,  $\text{CH}_3\text{CO}-\text{CH}_2\text{CON}(\text{CH}_3)_2$ , a primary auto-condensation product of DMAC. Reaction of cellulose with this condensation product is slow, and is catalyzed, e.g., by carboxylic acid that is liberated during acylation by a carboxylic anhydride. A faster biopolymer

degradation reaction involves *N,N*-dimethylketeniminium ion  $[\text{CH}_2=\text{C}=\text{N}^+(\text{Me})_2]$  that is formed by dehydration of enol tautomer of DMAC  $[\text{CH}_2=\text{C}(\text{OH})\text{N}(\text{Me})_2]$ . This extremely reactive electrophile causes random chain cleavage, resulting in pronounced and rather fast changes in the molar mass distribution of cellulose (Rosenau et al. 2006).

### 1.5.2.3. Thermal activation

Cellulose activation can be carried out by heating the sample. Because this treatment may lead to biopolymer “hornification” (stiffening of the polymer structure that takes place in lignocellulosic materials upon drying or water removal (Fernandes et al. 2004)), it is usually carried out under reduced pressure. In one procedure, a mixture of cellulose and LiCl is heated under reduced pressure until the water in cellulose is removed, followed by introduction of DMAC (Nawaz et al. 2012). It is important that DAS is also introduced under reduced pressure; establishing atmospheric pressure before the heat-activated polymer is embedded by the solvent leads to erratic results, probably due to pressure-drop induced hornification. This method is simple, less time consuming, and does not cause biopolymer degradation (Marson 1999). Thermal activation process is shown below in Figure 1.10.

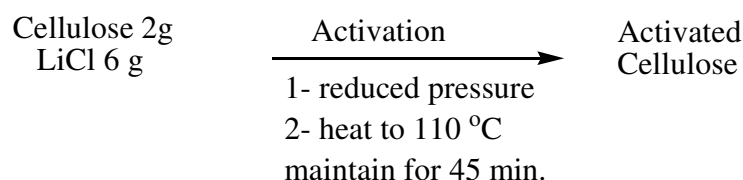


**Figure 1.10:** Thermal activation procedure for cellulose

## 1.6. Cellulose dissolution

After successful activation of cellulose using different activation methods mentioned above, it can be dissolved in different electrolytes/dipolar aprotic solvents for further modification as discussed below.



### 1.6.1. Mechanism of cellulose dissolution

Alternative models have been advanced in order to explain the mechanism of solubilization, some of which are summarized below, Figure 1.11 (McCormick et al. 1985, Berger et al. 1985, El-Kafrawy 1982, Herlinger and Hengstberger, 1985 Vincendon 1985). Most of these are based on the interactions between SE/DAS complex, its component simple- or complex ions (e.g.,  $\text{Li}(\text{DMAC})^+$  macro-cation) and the hydroxyl groups of cellulose (Striegel 1997, Heinze 1998, Striegel 2003, Lindman 2010).

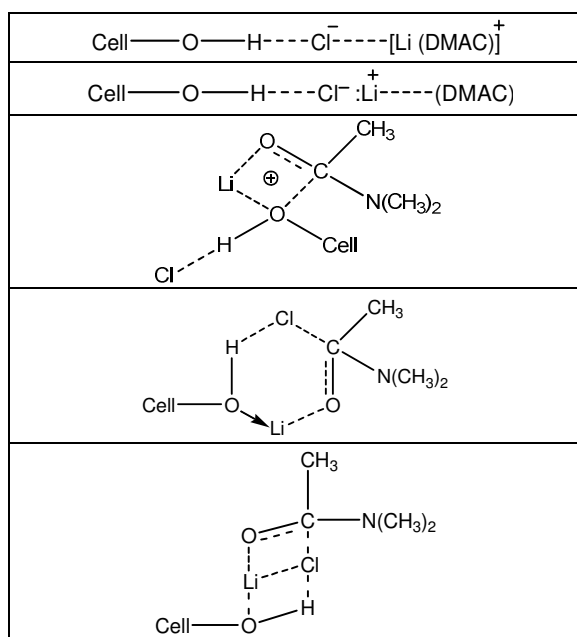


**Figure 1.11:** Proposed mechanisms of cellulose-LiCl/DMAC complexation (El Seoud et al. 2013)

The formation of these structures has been probed by NMR spectroscopy. For LiCl/DMAC (Morgenstern 1992), a decrease in  $^7\text{Li}$  chemical shifts and increase in its peak width at half-height was observed as a function of increasing cellulose concentration. In contrast, no variation in these NMR parameters was observed for LiCl/DMAC solutions in the absence of cellulose, as a function of increasing  $[\text{LiCl}]$ . Therefore, molecular environment of  $\text{Li}^+$  progressively changes as cellulose is added to the solution. The interaction presumably involves an exchange between one DMAC molecules in the inner coordination shell of  $\text{Li}^+$  with a cellulosic hydroxyl group, in a cooperative manner. In addition, the bulky LiCl/DMAC complex would penetrate into the cellulose chains, creating more inner space within 3D biopolymeric structure, thus

contributing further to dissolution. This exchange model is shown in Figure 1.12 (Morgenstern 1992).

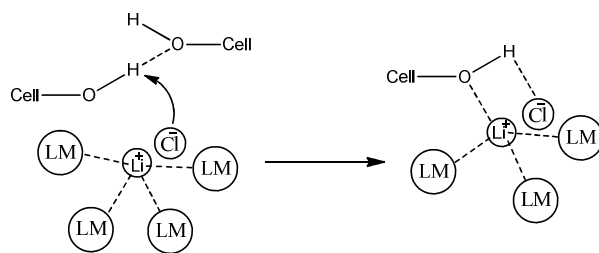


**Figure 1.12:** Proposed model for cellulose/LiCl/DMAC interaction leading to dissolution; LM refers to DMAC molecules solvating the  $\text{Li}^+$  ion.

The importance of  $\text{Cl}^- \cdots \text{H-O-Cell}$ , interactions for cellulose dissolution in LiCl/DMAC has been corroborated by the study of solvatochromism in these solutions. The latter term refers to the effect of medium on the spectra, absorption or emission, of certain compounds (solvatochromic substances or probes) whose spectra are especially sensitive to the properties of the medium. These properties include “acidity”, “basicity”, dipolarity, and polarizability. The information on the properties of the medium is usually obtained from the dependence of solvatochromism (*i.e.*, the value of  $\lambda_{\text{max}}$  of the probe intra-molecular charge-transfer complex) on some experimental variable, e.g., concentration or solution temperature. These probes have been employed in order to investigate the properties of cellulose proper; DMAC, LiCl-DMAC; and cellulose/LiCl-DMAC solutions (Spange et al. 1998, Fidale and Heinze, 2013). Thus high “acidity” of unsolvated  $\text{Li}^+$  was reduced in LiCl/DMAC solution indicating the formation of  $\text{Li}^+$  (DMAC)<sub>n</sub> macro-cation.

Whereas dissolution of cellulose in LiCl/DMAC has little effect on the overall polarity of DAS, the basicity of the medium was affected drastically, indicating strong  $\text{Cl}^- \cdots \text{H-O-Cell}$  interactions. It was concluded that the basicity of the medium (due to both  $\text{Cl}^-$  and the C=O dipole of DMAC) contributes much more than the corresponding acidity (due to essentially free- and complexed  $\text{Li}^+$  ion) to cellulose solubilization. These results agree with previous conclusions on the mechanism of cellulose dissolution in LiCl/DMAC (Lindman et al. 2010). It is interesting to mention that cellulose dissolution in LiCl/DMSO requires decrystallization pretreatment e.g., by ball-milling or extensive swelling by a base (Wang 2012).

The similarity between dissolution by LiCl/DMAC and TBAF-3H<sub>2</sub>O/DMSO has been suggested, as shown in Figure 1.13. The six-membered “ring” that involves two TBAF molecules and one DMSO (Pinkert 2010), or the structure in the presence of cellulose, where the biopolymer is shown to substitute one TBAF molecule (our representation) are clearly oversimplifications due to relatively large distance between (C<sub>4</sub>H<sub>9</sub>N<sup>+</sup>) and nucleophilic species in solution, including (F<sup>-</sup>) counter-ion, and oxygen atoms of the solvent (DMSO; distance R<sub>4</sub>N<sup>+</sup>·····O-solvent > 0.35 nm) (Pinkert et al. 2010, Pliego and Pilo 2008).

Phase diagrams, rheology, and NMR (<sup>19</sup>F and <sup>1</sup>H-NMR, chemical shifts and line widths) have been employed in order to investigate the effect of presence of water on MCC/LiCl-DMAC, and the interactions of cellulose with TBAF/DMSO.

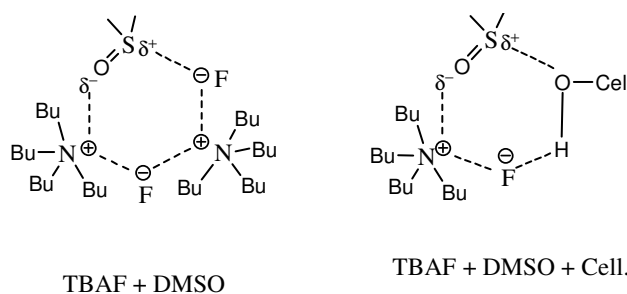


**Figure 1.13:** Simplified structures for the interaction of TBAF and DMSO, (Pinkert 2010) and for cellulose solution in TBAF/DMSO.

### 1.6.2. Dissolution scheme

The former study has indicated that the maximum water content that can be present in the samples so that no cellulose precipitation- or liquid crystal formation occurs is always <3 wt%, even in the most concentrated DMAC/LiCl solutions. The amount of water still tolerable in the mixture is strongly dependent on the concentrations of cellulose and LiCl, being inversely proportional to biopolymer (Chrapava et al. 2003). For solutions of cellulose in TBAF/DMSO, NMR results have indicated that the highly electronegative F<sup>-</sup> ions act as hydrogen-bond acceptors of Cell-OH groups; this breaks the intermolecular hydrogen bonds between cellulosic chains, leading to dissolution of the biopolymer. Solubilization is enhanced by electrostatic repulsion between the negatively-charged cellulose chains, due to proton accepting ability of

$F^-$ . Addition of water solvates the fluoride ion, this leads to a decrease of cellulose solubility and, eventually, to solution gelation. This sequence of events is shown in Figure 1.14 (Ostlund et al. 2009).

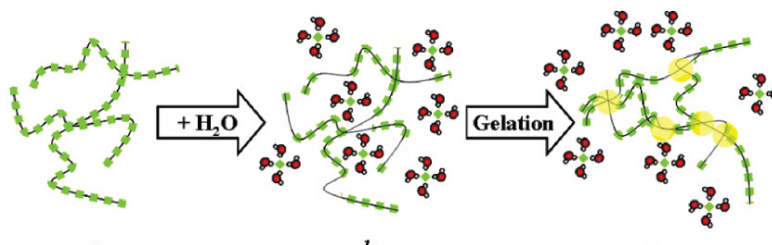


**Figure 1.14:** Schematic representation of the effect of water on solution of cellulose in TBAF/DMSO (reproduced from [Ostlund et al. 2009] with permission).

The cellulose chains are covered with associated fluoride ions (depicted in green). Added water (depicted in red) solvates a fraction of the  $F^-$  ions that are associated with cellulose. The resulting desolvated biopolymer chains (depicted in yellow) associate, by combination of hydrogen-bonding and hydrophobic interactions (Medronho et al. 2012), leading to subsequent precipitation of the biopolymer.

It is important to emphasize that the formation of clear, macroscopically homogeneous cellulose solutions in SEs/DAS does not necessarily mean that chains are molecularly dispersed. Rather they are present as aggregates- designated as “fringed micelles (Ramos et al. 2011), whose aggregation numbers (e.g., 11 for MCC; 21 of mercerized-sisal; 40 for mercerized-cotton) depend on the structural properties of cellulose, its concentration, and the method of solution preparation. This aggregation decreases the accessibility of biopolymer, hence the efficiency of its derivatization. (Ramos et al. 2011). The consequence of this aggregation is that the efficiency of the reaction, in terms of the ratio (derivatizing agent/AGU) that is required in order to achieve a targeted DS is rarely stoichiometric; employing excess reagent is the role. We have summarized the results on cellulose dissolution and study techniques in SEs/DAS as shown in Table 1.4.

**Table 1.4:** Dissolution of cellulose from different sources in strong electrolytes/dipolar aprotic solvents.

Entry	Polysaccharide; DP; Ic	Dissolution solvent system	Dissolution conditions (temperature, heating time)	Techniques employed to study dissolution	Reference
1	MCC	5–8% LiCl/DMAC	150 °C, 2 h	GPC	[Striegel et al. 1995]
2	MCC; 155; 0.81 Bagasse; 780; 0.82	8.3% LiCl/DMAC	155 °C; 1 h	FTIR, X-Ray, SEM	[Marson et al. 1999]
3	Sulfite pulp	8% LiCl/DMAC	RT	WAXD, SAXS	[Ishii et al. 2003]
4	MCC; 126; 0.83 Cotton linter; 400; 0.80 Sisal; 642; 0.67	7.4% LiCl/DMAC	150 °C; 1.5 h	X-Ray Diffraction, SEM,	[Ramos et al. 2005]
5	Fibrous cellulose 390	7% LiCl/DMAC	80 °C; 0.75 h	WAXD, FTIR	[Marsano et al. 2007]
6	MCC; 332	7.5% LiCl/DMAC; 3.5% TBAF/DMSO	130 °C; 2 h 80 °C; 2 h	FTIR, <sup>1</sup> H, <sup>13</sup> C-NMR	[Köhler et al. 2007]
7	MCC; 163	8% LiCl/DMAC	RT; 3 min	WAXS, Density measurement	[Ducheman et al. 2010]
8	MCC; 210–270	1% TBAF/DMSO	60 °C; 20 min,	<sup>19</sup> F, <sup>1</sup> H-NMR	[Ostlund et al. 2009]
9	MCC; 332	10% TBAF/DMSO	60 °C; 1h	<sup>19</sup> F, <sup>1</sup> H-NMR	[Heinze et al. 2010]
10	Sisal; 642; 0.67 Cotton linters, 400; 0.80	8.3% LiCl/DMAC	150 °C; 1.5 h	X-Ray, Viscometry	[Ramos et al. 2011]
11	Canola straw	8% LiCl/DMAC	RT; 5–120 min	X-Ray	[Yousefi et al. 2011]
12	Kraft pulp	8%LiCl/DMAC; 16.25% TBAF/DMSO	4 °C; 5 d	SEC, <sup>13</sup> C-NMR	[Li et al. 2011]
13	Cellulose membrane	8.1% LiCl/DMAC	100 °C; 6 h	HPLC	[Ma et al. 2011]
14	Cotton linters Softwood kraft pulp	9% LiCl/DMAC	40 °C; 0.5–120	GPC, SEM	[Henniges et

15	Cellulose powder	10% LiCl/DMAC	h 100 °C; 7.5 h	SAXS, SEM	al. 2011] [Opdenbosch et al. 2012]
16	MCC; M-cotton; M-sisal	6% LiCl/DMAC	110 °C; 4 h	Viscometry, SLS, <sup>1</sup> H-NMR	[Wang et al. 2012]

More references regarding the dissolution of cellulose and the study techniques employed are recently published elsewhere (El Seoud et al. 2013).

## 1.7. Cellulose derivatization under homogeneous reaction conditions

In principle, derivatization of cellulose can be carried out by using either carboxylic acids proper, or their functional derivatives. The latter include: symmetric and asymmetric acid anhydrides and acyl chlorides in the absence, or presence of catalysts; diketenes; vinyl esters; lactones and lactams (El Seoud et al. 2013).

### 1.7.1. Derivatization scheme under HRS.

A schematic representation of cellulose derivatization by the HRS is shown in Figure 1.15.

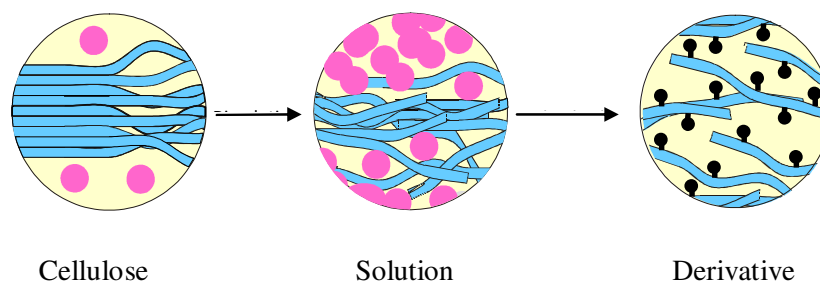


**Figure 1.15:** A schematic representation of derivatization by the HRS.

Activation and dissolution lead to the formation of solvated cellulose chains; these react with the derivatizing agent to produce a cellulose derivative.

### 1.7.2. Derivatization in strong electrolytes / dipolar aprotic solvents

Cellulose derivatization has been reported using quaternary ammonium fluorides, TBAF-3H<sub>2</sub>O in DMSO first reported by (Heinze et al. 2000). Solution of TBAF-3H<sub>2</sub>O in DMSO is capable of dissolving celluloses, including those of very high degree of polymerization (DP) (Ass et al. 2004; Ciacco et al. 2003). This solvent system has been successfully employed for the derivatization of celluloses by employing variable reaction times, temperatures, and derivatizing agent/cellulose molar ratios (Ass et al. 2004; Heinze et al. 2000). Depending on the experimental conditions TBAF-3H<sub>2</sub>O, like the corresponding hydroxide (the F<sup>-</sup> and OH<sup>-</sup> ions are isoelectronic; Kluge & Weston, 2005), may be susceptible to Hofmann elimination (Sharma & Fry, 1983; Albanese, Landini, & Penso, 1998).

### 1.7.3. Representative examples for cellulose derivatization in SE/DAS

Here are some more examples for the cellulose derivatization in SEs/DAS and IL/DAS solvent system. Three different cellulose samples, MCC, cotton linters and mercerized sisal has been acylated by acetic anhydride, Ac<sub>2</sub>O, in the solvent system LiCl/*N,N*-dimethylacetamide, DMAC (4 h, 110 °C), (Ramos et al. 2011). The reaction efficiency has been determined by the relationship between the degree of substitution, DS, of the ester obtained, and the molar ratio Ac<sub>2</sub>O/AGU (anhydroglucose unit of the biopolymer). Recently cellulose has been derivatized in 6% LiCl/DMAC (Nawaz et al. 2012) using appropriate volumes of ethanoic-, butanoic-, or hexanoic anhydride, so that the molar ratio of the corresponding anhydride/AGU was 4.5. The ester DS was determined by titration (ASTM 2002); DS = 2.1, 1.7, 2.5, for cellulose ethanoate, butanoate, and hexanoate, respectively. This process is depicted in Figure 1.16.

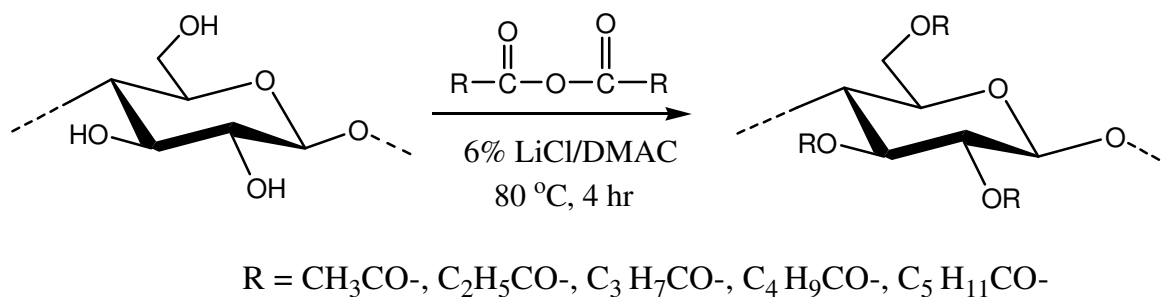


**Figure 1.16:** Homogeneous acylation of MCC in 6% LiCl/DMAC using acid anhydrides (acetic to hexanoic anhydrides).

The potential problems associated with the use of  $R_4NF \cdot xH_2O/DMSO$  include (Casarano et al. 2014, Figure 1.17). The presence of water causes the hydrolysis of acylation agents, and the produced ester via general base catalyzed reaction, thus decreasing the degree of ester substitution (DS) of ester produced (scheme-1 A) or through ketene intermediate (scheme-1 B) (Casarano et al. 2011; Zheng et al. 2013). The electrolyte itself may undergo elimination reaction including Hoffmann elimination (scheme-1 C) or it is subjected to another degradation mechanism, via ylide intermediate pathway (scheme-1 D) (Chempath et al., 2010). The ylide mechanism is akin to the E1cB counterpart, except that the species produced by proton elimination is a zwitterion (Casarano et al. 2011). Lastly, tetraallylammonium fluoride-mono hydrate (TAAF- $H_2O$ ) undergoes polymerization to form linear as well as cross-linked cyclopolymers that do not dissolve cellulose (Scheme-1, E) (Casarano et al. 2011).



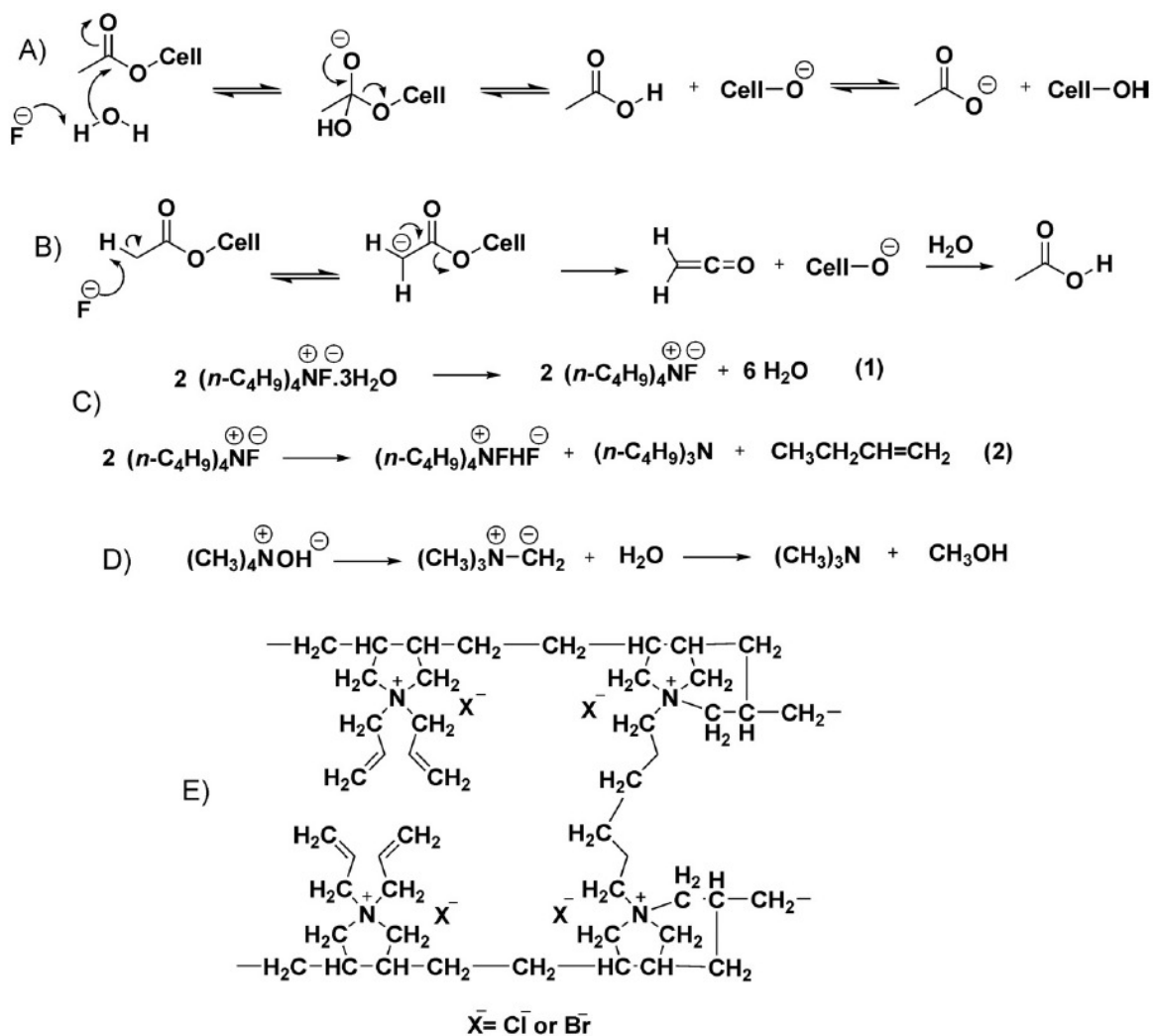


**Figure 1.17:** Possible side reactions of tetraalkylammonium fluoride-hydrates. The schemes are for ester deacylation by the water of hydration, where the (F<sup>-</sup>) is acting as a general-base (A): ester deacylation via ketene intermediate (B): electrolyte degradation by Hofmann elimination (C): electrolyte degradation via ylide mechanism (D): electrolyte polymerization/crosslinking (E).

Due to relatively low pK<sub>a</sub> of the hydroxyl groups of sugars ( $12.3 \pm 0.3$ ) (Izatt et al. 1966) direct esterification with carboxylic acids is inefficient; these have to be activated *in situ* before use, as shown in Figure 1.18 (a–c) below (El Seoud et al. 2005). One such acid-activating reagent is dicyclohexyl carbodiimide, DCC, either alone, or in combination with a powerful nucleophile, e.g., 4-pyrrolidinopyridine, Part A.

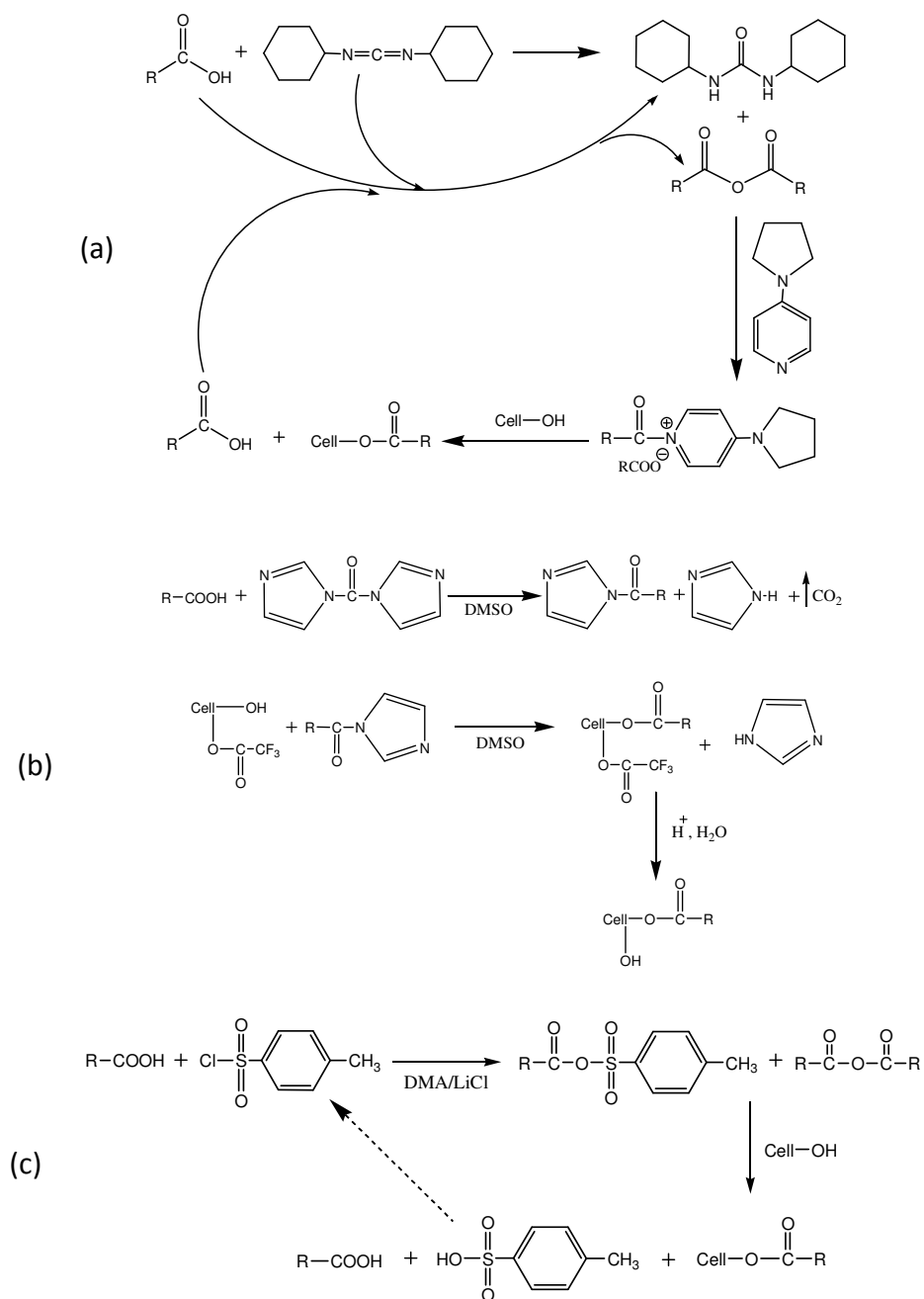


**Figure 1.18:** Schemes for the *in situ* activation of carboxylic acids. (a) shows activation by DCC; (b) shows activation by CDI, resulting in the formation of reactive *N*-acyl imidazole; (c) shows the formation of mixed anhydride between carboxylic- and toluene sulfonic acid.

First, acid anhydride is produced by the reaction of free acid with DCC. Nucleophilic attack by 4-pyrrolidinonepyridine on the anhydride results in the corresponding, highly reactive, acylpyridinium carboxylate; this leads to formation of cellulose ester, plus a carboxylate anion. The latter undergoes a DCC-mediated condensation with a fresh molecule of acid to produce another molecule of anhydride. *N,N*-Carbonyldiimidazole (CDI), may substitute DCC for acid activation, the acylating agent is *N*-acyl imidazole that readily reacts with cellulose to give ester and regenerate imidazole, part B. In another variant, activation is carried out by TsCl/pyridine. As shown, an asymmetric carboxylic-sulfonic acid anhydride is formed, but cellulose attack occurs on the C=O group, since nucleophilic attack on sulfur is slow, and the tosylate moiety is a much better leaving group than the carboxylate group. When the leaving abilities of both groups of the asymmetric anhydride are comparable, mixed esters are obtained. For example, cellulose esters of long-chain fatty acids, e.g., dodecanoate to eicosanoate have been prepared in LiCl/DMAC with this activation method, with almost complete functionalization, DS 2.8–2.9 (Sealey et al. 1996). The (mineral) acid-catalyzed formation of mixed acetic-carboxylic anhydride has been employed in order to synthesize mixed esters of acetic and fatty acids, according to scheme shown in Figure 1.19 (Vaca-Garcia et al. 1998; Peydecastaing et al. 2009).

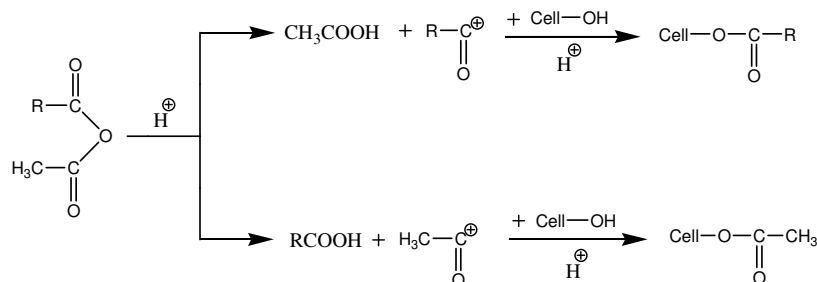


**Figure 1.19:** Formation of mixed anhydride of acetic- and fatty carboxylic acid.

The same approach has been employed for obtaining carboxylate-phosphonate mixed esters by the reaction of cellulose with carboxylic-phosphonic mixed anhydride (Heinze et al. 2012). Similar to other esterification reactions, there is large preference for tosylation at C6 position of AGU, and all accessible tosyl celluloses (up to DS = 2.3) are soluble in DMSO (Siegmond et al. 2002).

In the simultaneous reaction of cellulose with mixtures of acetic-, propionic-, and butyric anhydride, the  $DS_{\text{Acetate}}$  is usually larger than  $DS_{\text{Propionate}}$  or  $DS_{\text{Butyrate}}$  because of the higher electrophilicity of the acyl group-, and smaller volume of the first anhydride (Ramos et al. 2005). The efficiency of acetylation of MCC; mercerized cotton linters; mercerized sisal, as expressed by the dependence of DS on  $(\text{RCO})_2\text{O}/\text{AGU}$  is described by the following exponential decay equation 1.2:

$$[DS = DS_0 + Ae^{-[(\text{RCO})_2\text{O}/\text{AGU}]/B}] \quad (1.2)$$

where (A) and (B) are regression coefficients. Values of (B) were found to correlate linearly with the aggregation number,  $N_{\text{agg}}$ , of dissolved cellulose chains,  $(B) = 1.709 + 0.034 N_{\text{agg}}$ . This result quantifies the dependence of cellulose accessibility, hence reactivity on its state of aggregation (Ramos et al. 2011). For the same cellulose, under distinct reaction conditions, the dependence of DS on the number of carbon atoms of the acyl group of anhydride,  $N_c$ , is not linear; it decreases on going from acetic to butyric anhydride, then increases for pentanoic- and hexanoic anhydride, as shown in Figure 1.20. In the latter we have employed, for convenience, the following reduced degree of substitution shown in equation 1.3:

$$[DS_{\text{Reduced}} = (DS_{\text{Carboxyate}} - DS_{\text{Butyrate}})/(DS_{\text{Hexanoate}} - DS_{\text{Butyrate}})] \quad (1.3)$$

This dependence, is not related to the solvent employed (SE/DAS or ionic liquid) or the method of heating, conventional (*i.e.*, by convection) or microwave. This is due to a complex dependence of the  $\Delta H^\ddagger$  and  $T\Delta S^\ddagger$  terms on  $N_c$  (Nawaz et al, 2012).

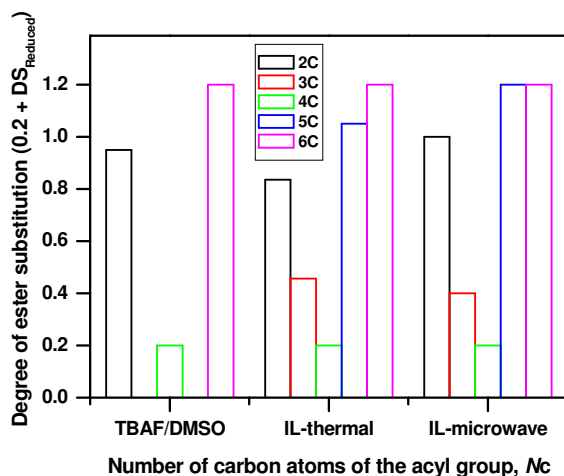


**Figure 1.20:** Dependence of  $DS_{\text{Reduced}}$  on  $N_c$  in different solvents, under convection- and microwave heating. The DS are: 0.79, 0.38, and 2.40 (butyrate) 1.07, 2.72 and 2.90 (hexanoate), respectively.

Cellulose esterification with anhydrides is catalyzed by nucleophiles, in particular imidazole, pyridine, and 4-(*N,N*-dimethylamino) pyridine, with a large decrease in reaction time. The reactive species is the *N*-acyl derivative of the tertiary amine. A recent kinetic study on acylation in LiCl/DMAC has indicated that this rate enhancement, relative to the uncatalyzed reaction, is due to smaller enthalpy, and larger (*i.e.*, less negative) entropy of activation (Nawaz et al. 2013).

Derivatization by acyl chloride/tertiary amine is shown in Figure 1.21; base is employed in order to scavenge the liberated HCl, the results are similar to the reaction with acid anhydrides (Guo et al. 2012).

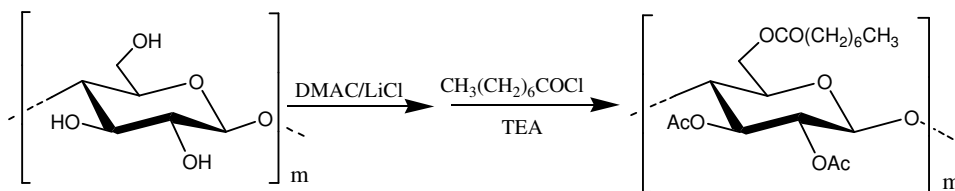


**Figure 1.21:** Schematic representation of acylation by carboxylic acid chloride/tertiary amine as a derivatizing agent.

The reaction scheme with alkyl ketene dimers is shown in Figure 1.22. Mixed acetoacetic/carboxylic esters have also been synthesized. Having a relatively acidic -methylene group, these  $\beta$ -ketoesters can be cross-linked to produce coatings with excellent solvent resistance (Edgar et al. 1995; Yoshida et al. 2007; Yoshida et al. 2006; Song et al. 2012).

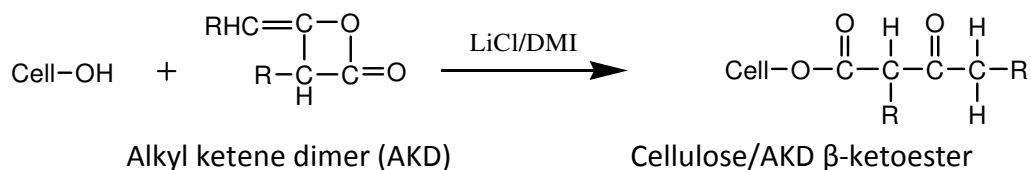


**Figure 1.22:** Representative scheme for the reaction of cellulose with alkylketene dimers. The produced  $\beta$ -ketoesters form enolates that can be employed in cross-linking of cellulose chain.

Vinyl esters: e.g., vinyl acetate, benzoate and laurate have been employed in order to obtain cellulose esters in TBAF-3H<sub>2</sub>O/DMSO. This is a (reversible) trans- esterification reaction. Its efficiency is based on the fact that one of the products, vinyl alcohol readily tautomerize to (volatile) acetaldehyde, thus driving the equilibrium to products (Heinze et al. 2003).

Esters with a cationic charge have been synthesized by the reaction of a lactam (*N*-methyl-2-pyrrolidinone;  $\epsilon$ -caprolactam; *N*-methyl-2-piperidone) with cellulose in the presence of TsCl, according to Figure 1.23, where R-OH refers to cellulose (Zarth et al. 2011). Similar strategies have been employed for the synthesis of cellulose esters in R<sub>4</sub>NF·xH<sub>2</sub>O/DMSO solutions. This includes the reaction of cellulose with activated carboxylic acids (Heinze et al, 2007) acid anhydrides and vinyl esters, (Beatriz et al. 2004; Casarano et al. 2011), carboxylic acid anhydride catalyzed by a diazole or triazole (Hussain et al. 2004; Nagel et al. 2010).

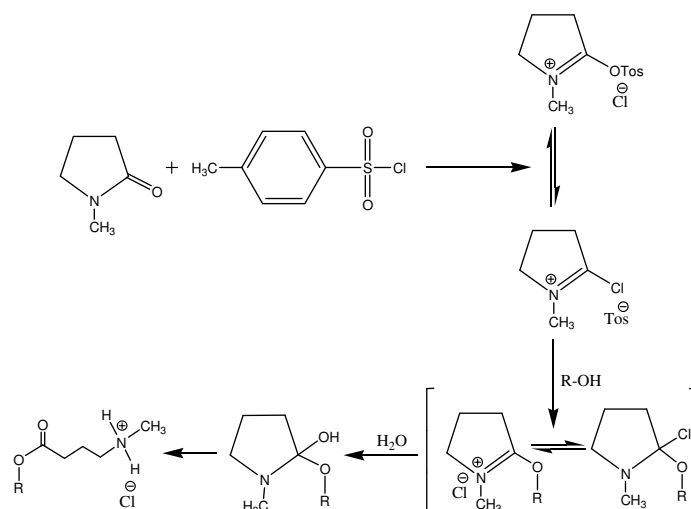


**Figure 1.23:** Schematic representation of the conversion of cellulose (ROH) into cationic ester by the reaction with *N*-methyl-2-pyrrolidinone.

Obtaining cellulose esters of other acids, e.g., tosylate; brosylate; mesylate; triflate is important *per se*, and because these moieties are employed for synthesis of cellulose derivatives with some control over regioselectivity. One such application involves their use as bulky groups, in particular at C6-OH position; this permits derivatization at C2-OH and C3-OH positions, see Figure 1.24.

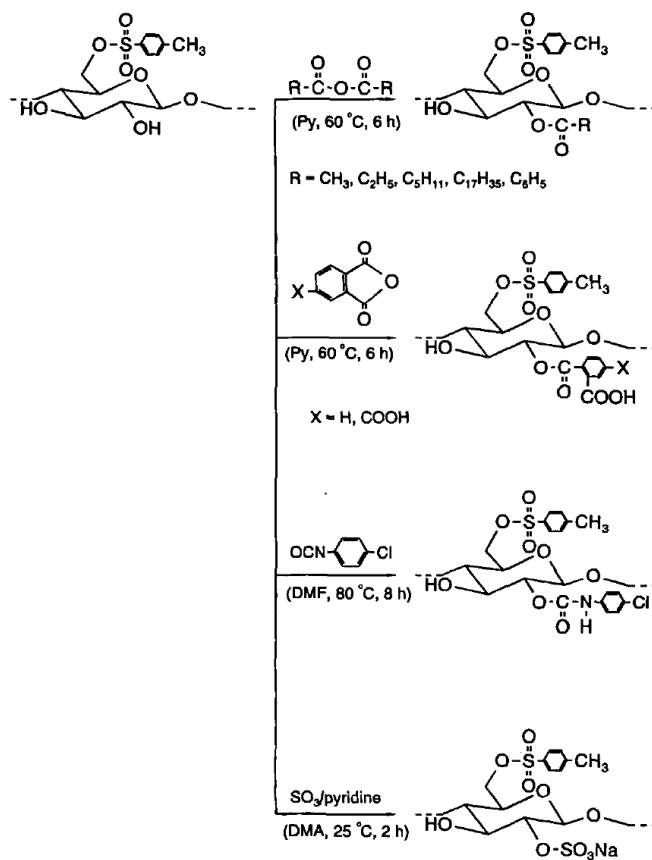


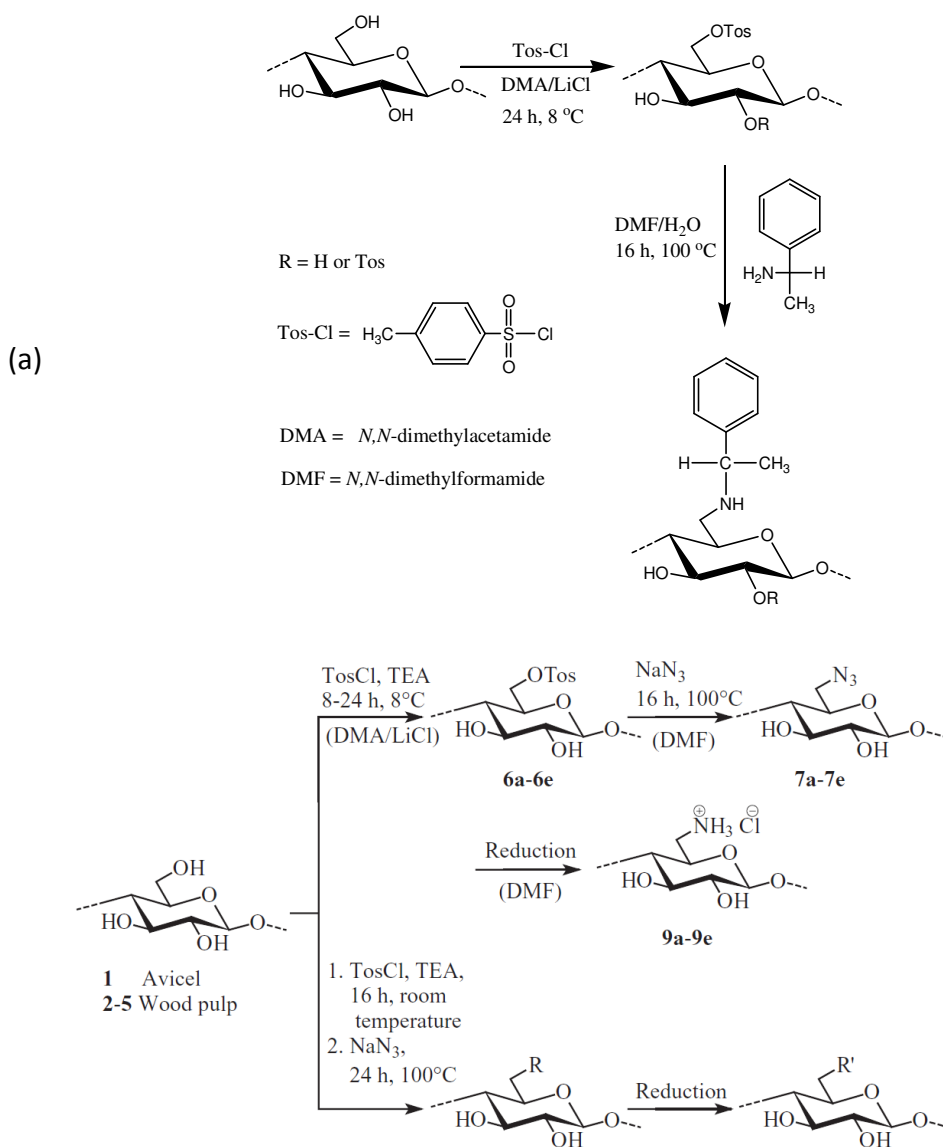
**Figure 1.24:** Use of tosylate moiety as a bulky group for C6-OH position of cellulose, leading to regioselective reaction at secondary hydroxyl groups (reproduced from [Heinze et al. 1997] with permission).

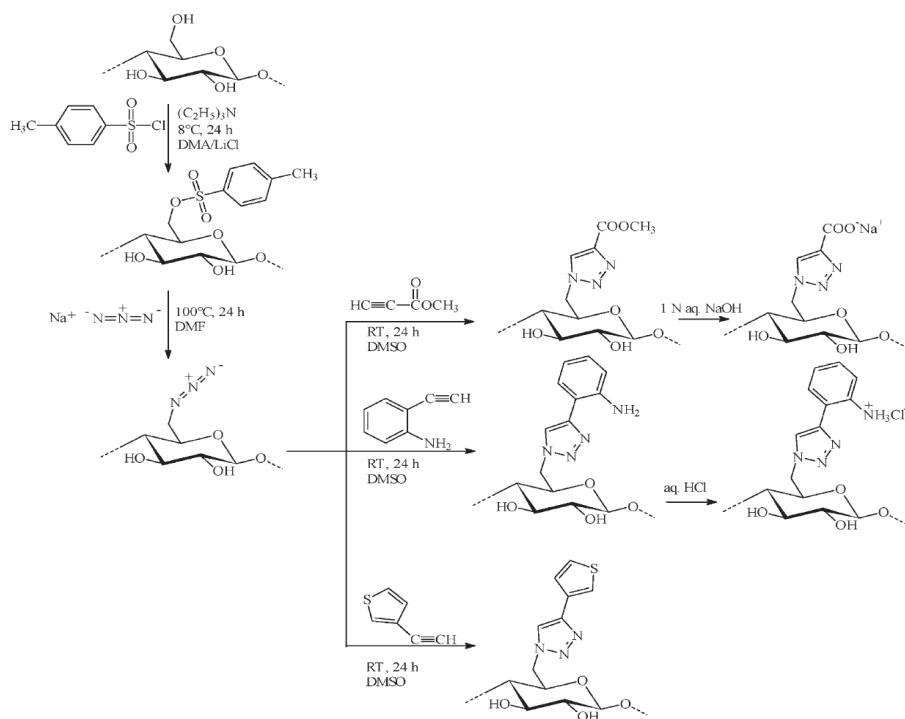
They are also good leaving groups, so that they can be substituted by  $\text{S}_{\text{N}}$  reactions to produce cellulose deoxy derivatives (Heinze et al. 2012; Heinze et al. 2009). In fact, this reaction usually occurs during tosylation by TsCl, the ratio of cellulose tosylate/deoxychlorocellulose is calculated from (Cl and S) elemental analysis (McCormick et al. 1990). The most extensively studied derivative of this series is the tosylate. It is carried out by reacting dissolved cellulose with tosyl chloride in the presence of TEA at low temperature (5–10 °C) for several hours, followed by ester precipitation and purification. Figure 1.25 shows some examples of further  $\text{S}_{\text{N}}$  reactions of cellulose tosylates.

The etherification of cellulose in LiCl/DMAC and TBAF/DMSO, even with reactive halides, e.g., allyl- and benzyl bromide is slow and requires long reaction time (Isogai et al. 1986; Isogai et al. 1987; Ramos et al. 2005). Therefore, an alkali is employed in order to activate cellulose,



Figure 1.25. An interesting procedure, employed for both cellulose and starch, is so called “induced phase separation”. This involves addition of finely divided, dry NaOH or KOH (usually obtained by employing with ultra Turrax mixers) to the cellulose/SE-DAS solution, leading to the formation of cellulose II or starch reactive gels on the solid particle/solution interface; this enhanced reactivity leads to products with relatively high DS (e.g., 2.2 for CMC) (Pezold-Welcke et al. 2009; Nishimura et al. 1997; Heinze et al. 2008).





(c) (reproduced from [Pezold-Welcke et al. 2009; Liebert et al. 2006] with permission)

**Figure 1.25:** Synthesis of cellulose tosylate and its transformation into further products by  $S_N$  reactions. (a) Transformation into cellulose deoxyamine. If required, the latter group can be quaternized to give cationic cellulose derivative (Heinze et al. 2001). The cellulose deoxy azide can be converted into amines by reduction, part (b), (Heinze et al. 2006), or into heterocyclic rings by click chemistry, part (c) (Liebert et al. 2006). Click chemistry is a term used to generate substances quickly and reliably by joining small units' together (Kolb et al. 2001)

Allyl cellulose has been successfully synthesized in dimethyl sulfoxide (DMSO)/tetrabutylammonium fluoride trihydrate (TBAF) solvent system in the presence of NaOH (Heinze et al. 2008). The degree of substitution was from 0.50 to 2.98 depending upon the molar ratio of allyl chloride/AGU, NaOH and reaction time. The allylation scheme has been shown in Figure 1.26.

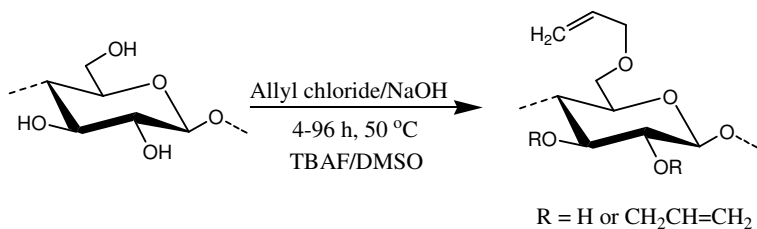


**Figure 1.26:** Allylation of cellulose dissolved in TBAF/DMSO.

Another activation procedure involves imidazole, as shown in the synthesis of 3-*O*-propargyl cellulose by using hexyldimethylsilyl moieties as protecting groups, Figure 1.27 (Fenn et al. 2009; Schumann et al. 2009). It is worth mentioning that products with “mixed” functional groups have been synthesized in these solvents, e.g., ethers; (Zabivalova et al. 2007; Zabivalova et al. 2008).

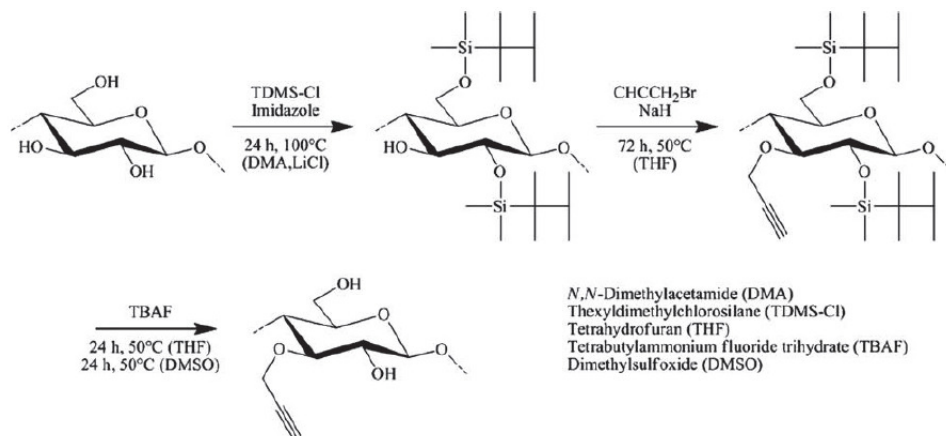


**Figure 1.27:** Using hexyldimethylsilyl moieties as protecting groups in the regioselective synthesis of cellulose ethers (reproduced from [Fenn et al. 2009] with permission).

Cellulose derivatizing agents and conditions most usually employed, as well as main techniques used, are summarized in Table 1.5. For convenience, we have organized the derivative in the order: Esters of carboxylic- and sulfonic acids; nonionic and ionic ethers, and miscellaneous derivatives.

**Table 1.5:** Agents and conditions for cellulose derivatization and main study techniques.

Entry	Cellulose type; DP; lc	Derivatizing agent	Reaction conditions: Ratio derivatizing agent/AGU; Temp. °C; Reaction time, h	DS range	Solvent used	Study Techniques	References
<i>esters of carboxylic- and sulfonic acids</i>							
1	MCC; hard wood pulp	Butyric anhydride; diketene	3:1; 30–40 min; 110 °C	0.3–2.9	7% LiCl/DMAC	GPC, <sup>1</sup> H, <sup>13</sup> C-NMR	[Edgar et al. 1995]
2	MCC	Acid anhydrides; diketene	1–3:1; 18 h; RT	1 - 2.8	8% LiCl/DMAC	X-Ray diffraction, <sup>13</sup> C-NMR	[Marson et al. 1999]
3	MCC; 0.79	Ac <sub>2</sub> O	1–9:1; 110 °C; 4 h	0.9–2.8	6% LiCl/DMAC	X-Ray, <sup>13</sup> C-NMR	[Regiani 1999]
4	MCC	Acid anhydrides	1–4.5:1; 18 h; 60 °C	1–2.8	8% LiCl/DMAC	Viscometry, X-Ray Diffraction	[El Seoud et al. 2000]
5	Whatman CF-11; 190	Chloroacetic acid; TsCl	1:1; 24 h; 40–50 °C	1.5–2.6	9% LiCl/DMAC	<sup>1</sup> H, <sup>19</sup> F-NMR	[Glasser et al. 2000]
6	MCC; 260	Acyl chlorides, TsCl	5:1; 80 °C; 2 h	2.96	7.5% LiCl/DMAC	<sup>1</sup> H-NMR, FTIR	[Heinze et al. 2003]
7	MCC, hardwood pulp	Diketene; Butyric anhydride	3:1; 110 °C; 40 min.	0.90, 0.30	5% LiCl/DMAC, DMSO, NMP	GPC, DSC, <sup>1</sup> H-NMR, <sup>13</sup> C-NMR	[Yoshida et al. 2006]
8	MCC; 300; Spruce sulfite pulp; 650	Acetic anhydride; vinyl carboxylates	2.3–10:1; 70 h; 40 °C	0.8–2.7	5% TBAF/DMSO	<sup>1</sup> H, <sup>13</sup> C-NMR FTIR	[Kohler et al. 2007]
9	MCC; 175; Sisal; 800	acid anhydride	4:1; 18 h; 60 °C	2.0	8% LiCl/DMAC	UV-Vis, FTIR	[Casarano et al. 2011]
10	MCC; 175; eucalyptus; 1049	Acid anhydrides	6–13:1; 3 h; 60–100 °C	1.6–2.4	9% TBAF/DMSO	Viscometry, <sup>1</sup> H-NMR	[Casarano et al. 2011]
11	MCC	Adipic anhydride	1–3:1; 2–20 h; 60–90 °C	2.1–2.6	5% LiCl/DMAC; 5% LiCl/DMI	<sup>1</sup> H-NMR, FTIR, SEC	[Liu et al. 2012]
<i>Nonionic and ionic ethers</i>							
12	MCC	TDMSCl, Imidazole	4:1; 100 °C; 24 h	2.0	5% LiCl/DMAC	<sup>1</sup> H, <sup>13</sup> C, COSY, HMQC, NMR	[Koschella et al. 2001]

Entry	Cellulose type; DP; Ic	Derivatizing agent	Reaction conditions: Ratio derivatizing agent/AGU; Temp. °C; Reaction time, h	DS range	Solvent used	Study Techniques	References
14	Sisal; 640; 0.64; Linter; 400; 0.73	ClCH <sub>2</sub> CO <sub>2</sub> Na/Na OH	5:1:10; 70 °C; 4 h	2.17	9% TBAF/DMSO	SEC, HPLC, <sup>1</sup> H-NMR	[Ramos et al. 2005]
15	MCC; 117	TDMSCl, Imidazole	4.1:1; 24 h; 100 °C	2.06	7.8% LiCl/DMAC	FTIR, <sup>1</sup> H- NMR	[Heinze et al. 2012]
<i>Miscellaneous</i>							
16	Cellulose	Phenyl isocyanate, pyridine	2.7:1; 12 h; RT	2.6	9% LiCl/DMAC	FTIR	[Williamson et al. 1998]
17	Cotton linter; 640	Graphene	85 °C; 0.5 h		9% LiCl/DMAC	SEM, TGA	[Zhang et al. 2012]

The data of Table 1.5 show the multitude of experimental conditions that have been employed for cellulose derivatization. For the same cellulose, the effects of reaction time, temperature, and the molar ratio [derivatizing agent]/ [AGU] on the DS of the product have been evaluated. For the reaction of celluloses with different DP, Ic, porosity, and  $\alpha$ -cellulose content, the interest has been on understanding the effects of these structural characteristics on the DS of the products. (Ramos et al. 2005; Ramos, et al. 2011; Gruber and Gruber 1981; El Seoud et al. 2000; Heinze et al. 2005; Shen 2009; Bansal et al. 2010; Wada and Nishiyama 2011).

### 1.8. Ionic liquids

Ionic liquids, ILs, are composed only of ions and, by operational definition, have melting points < 100 °C. ILs have been intensively studied in the last decade as new solvents for various applications in electrochemistry, analytical chemistry, and organic synthesis (Olivier-Bourbigou et al. 2010; Koel et al. 2009). Various ionic liquids have been used for the dissolution of cellulose (Swatloski et al., 2002). There are several reasons for the explosive interest in the use of ILs as solvents for cellulose dissolution, regeneration, and derivatization as shown in Figure 1.28.

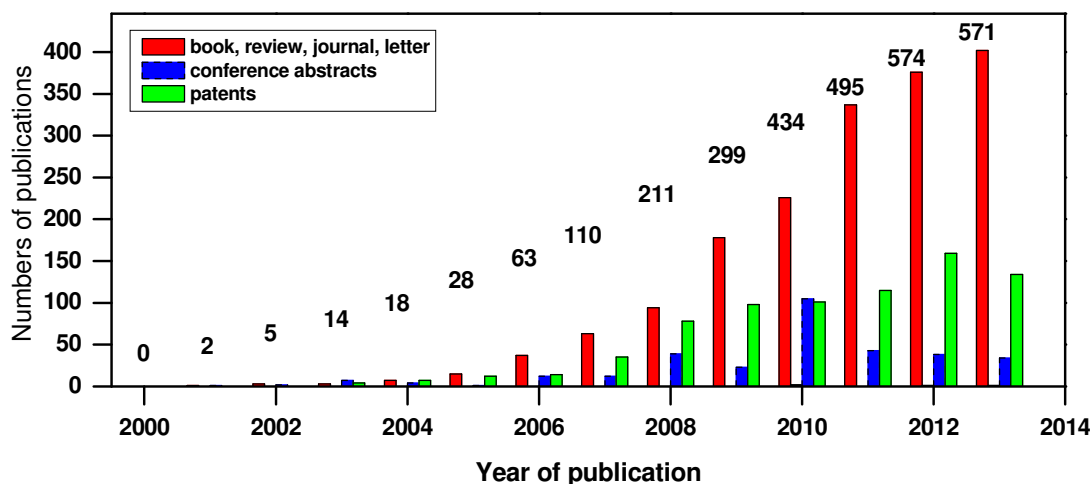


**Figure 1.28:** Publications between 2000 to 2013, found in the SciFinder® database for the term “cellulose and ionic liquid”, presented in columns (red correspond to articles, book, letter, published in English/other languages, black for dissertations, blue for conference abstracts and green for patents. Total numbers of publications/year are given in numbers above. We have also found 12 dissertations by searching the SciFinder database for the term “cellulose and ionic liquids, biomass and ionic liquids”.

Being ionic in nature, there is no need for an additional electrolyte, e.g., LiCl, for cellulose dissolution; no pretreatment, e.g., thermal, is required for biopolymer activation. The most important advantage, however, is their structural versatility because combinations of different cations and anions can generate an unlimited number of molecular structures. Some of these cations and anions have been shown in Figure 1.29 (El Seoud et al. 2007; Gericke et al. 2012).

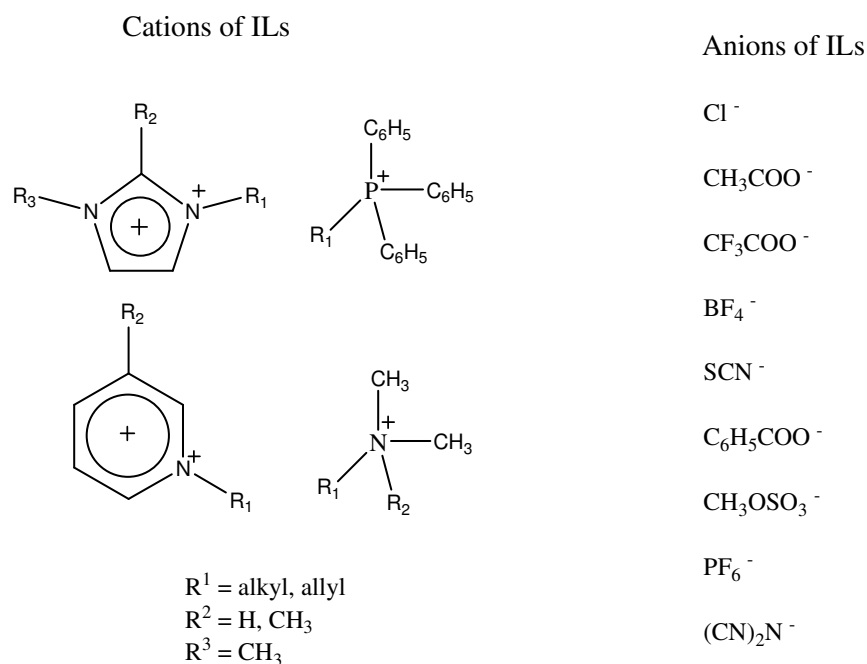


**Figure 1.29:** Common structures of cations and anions of ILs (El Seoud et al. 2007)

Ionic liquids dissolve cellulose because the interactions between the electrolyte ions and the hydroxyl groups of the anhydroglucose glucose unit, AGU, disrupt the strong intra- and intermolecular hydrogen bonds present in cellulose. Of these, the interactions (anion $\cdots$ H-O-AGU) are most important, although the nature of the cation plays a role (El Seoud et al. 2013).

The use of ILs, however, is associated with some limitations. Based on the current catalog of a reagent supplier, the cost of one mole of 1-allyl-3-methylimidazolium chloride, AlMelmCl is ca. ten times greater than one mole of a LiCl solution in DMAC. Relative to the SE/DAS employed with cellulose, the viscosities of many ILs are high. For example, at 80 °C the zero-shear viscosity of the structurally related IL (1-allyl-3(1-butyl) imidazolium chloride; AlBulmCl), is 36.4 times that of 8% LiCl/DMAC. Dissolution of 5 wt% of MCC in AlBulmCl increases the viscosity, relative to that of pure IL, by factors between 6.3 and 11.6, depending on the temperature, T. At 25 °C, the viscosity of 5 wt% of MCC, in AlBulmCl is ca. 6.7 times that of 5 wt% MCC/LiCl-DMAC (Possidonio et al. 2010). These differences in viscosity are relevant to cellulose derivatization in *any* solvent because lower viscosity favors the reaction due to the concomitant increase in reagent diffusion rate, as given by the Einstein-Stokes equation (Berry

et al. 2000). In view of the documented favorable effects of lower viscosity on the accessibility of amino acid residues of some enzymes ((a) Somogyi et al. 1988; (b) Punyiczki and Rosenberg 1992), and on the rate constants of enzymatic reactions (Sitnitsky AE 2008), it is clear that lower medium viscosity should lead to enhanced cellulose accessibility/reactivity. Finally, some reagents for synthesis of cellulose carboxylic esters (e.g., long-chain acid anhydrides) are immiscible in certain ionic liquids.

In principle, many of these limitations can be attenuated/eliminated by using mixtures of IL and DAS that are efficient in cellulose swelling, e.g., DMSO and DMAC (Gericke et al. 2011). This use is still incipient, calling for extensive studies in order to determine the binary mixture compositions that are best for a given class of reactions, e.g., esterification. An important impetus for these studies is the fact that many of the properties of binary solvent mixtures that are relevant to cellulose dissolution/derivatization, e.g., empirical polarity, acidity, basicity, and viscosity do not vary linearly as a function of mixture composition (Sato et al. 2010; Hauru et al. 2012; Le et al. 2012). Therefore, more research is necessary to understand the properties of the IL-molecular solvent binary mixtures and how their interactions with cellulose affect accessibility of the latter, hence its reactivity. There is also need to assess the efficiencies of these solvent mixtures with those of the “classical” and extensively employed SE/DAS.

### **1.8.1. Some physical properties of ionic liquids**

Some of the properties of ionic liquids that are relevant to their use as solvents for cellulose are discussed in the following section:

#### **1.8.1.1. Thermal stability**

Most ionic liquids are thermally stable. Their decomposition temperature ranges from 300 to 400 °C (Pinkert et al. 2009). It has been suggested that the stability of ionic liquids depends upon the anions; however it can be affected by other factors as well. Decomposition of anion takes place via dealkylation reaction whereas the cation undergoes alkyl migration and elimination reactions (Baranyai et al. 2004). In comparison with tetraalkylammonium salts, imidazolium salts are most stable (Ngo et al. 2000).



### 1.8.1.2. Polarity

Polarity is another important factor, which determines the dissolution ability of these solvents to various extents. There are several properties involved to determine the polarity such as columbic forces, inductive effect, hydrogen bonding, and electron pair donor and acceptor ability. Because of such forces, the precise solvent polarity has remains the major issue (Chiappe et al. 2005). The most common methods to determine the polarity of ionic liquids is to measure the solvatochromic parameters. The polarity of ionic liquids can also be determined empirically by means of solvatochromic pyridinium N-phenolate betaine dyes as shown below in Figure 1.30 (Reichardt, C. 2005).

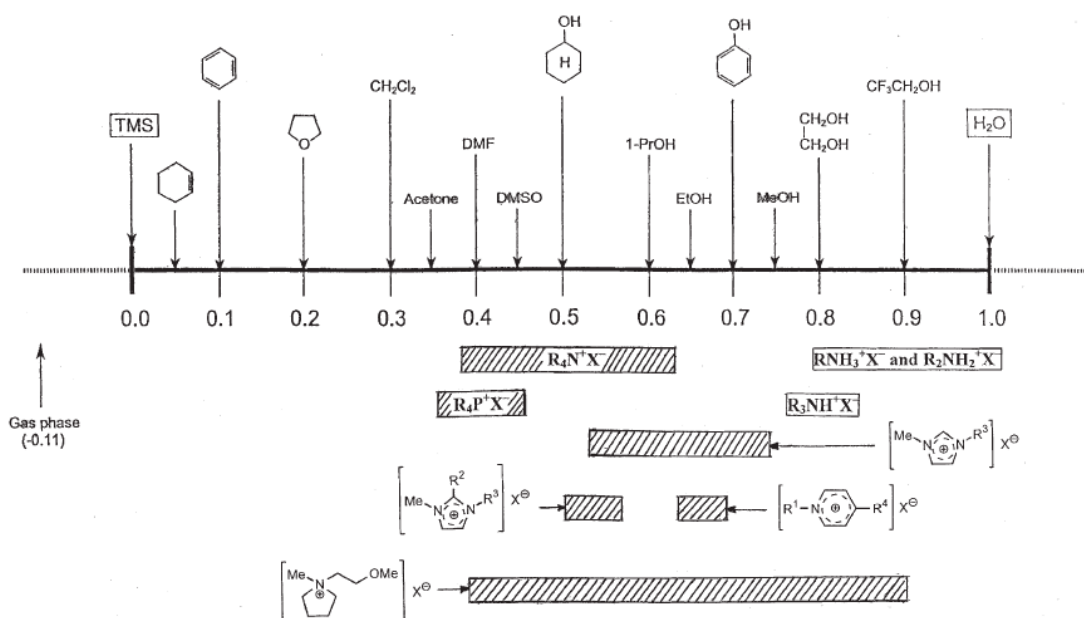


**Figure 1.30:** Normalized solvent polarity scale with  $E_T(30) = 0.00$  for tetramethylsilane (TMS) and  $E_T(30) = 1.00$  for water as arbitrarily fixed points, with ordering of fourteen selected solvents and the inclusion of eight groups of ILs. The experimentally inaccessible gas-phase  $E_T(30)$  value is calculated by extrapolation.

In this procedure, fourteen common solvents have been employed shown above the scale line starting from nonpolar (tetramethylsilane, TMS) to polar ( $H_2O$ ) and eight groups of ionic liquids have been shown below the scale line. The range of  $E_T(30)$  values ( $E_T(30)$ ) is an

empirical solvent polarity scale of Reichardt betaine (RB); it is a dye which changes color according to polarity of the solvent under study) obtained for eight groups of ionic liquids have been determined directly or indirectly by means of the standard betaine dye and these are comparable to those of dipolar non-hydrogen bonding and dipolar hydrogen bonding solvents; depending on the inherent molecular structure of the ionic liquids studied. On the other hand,  $E_T(33)$  is a solvent polarity scale of Wolfbeiss betaine, (WB); a solvatochromic dye that is structurally similar to RB, with lower pKa.

### **1.8.1.3. Viscosity**

The viscosity of ionic liquids is the major factor which restricts its use in the commercial applications. The viscosity is higher than water and common organic solvents and similar to oils and it decrease with increasing temperature (Okoturo et al. 2004; Harris et al. 2008; Nawaz et al. 2014; in press). It is suggested that ILs with high surface tension must possess low viscosity, ions must be relatively small and liquid should contain large free spaces. Ionic liquids with such properties are imidazolium salts with C4-C6 alkyl chains (Abbott 2004). ILs with polyfluorinated anions has low viscosity (Chiappe et al. 2005). Similarly, 1-alkyl-3-methylimidazolium salts with branched alkyl chains reduce the viscosity.

### **1.8.1.4. Hydrogen bonding**

Intra and intermolecular hydrogen bonds have an important effect on the dissolution behaviour of the ionic liquids. The presence of hydrogen bonding was first reported in imidazolium ILs in 1986 (Abdul-Sada et al. 1986). This columbic force (the C-H $\cdots$ X (X) Cl, Br interaction) is not very strong and has a little effect but it become very strong in imidazolium halides ILs with some covalent character as well (Wang et al. 2006). All aromatic protons in the cation ring involve in the hydrogen bonding but most acidic proton (C2-H) has the largest effect (Zhang et al. 2010). Hydrogen bonding interaction has been shown in imidazolium based ILs halide in Figure 1.31.

### 1.8.2. Cellulose dissolution and dissolution mechanism in ILs

The first cellulose solvent was organic salt with low melting points which was used in early 1930s (Graenacher, C. 1934). Pyridinium salts have been reported to use with DMSO and DMF as a co-solvent for cellulose dissolution and further modification into spherical beads (Linko et al. 1977). In 2002, research group of Swatloski (Swatloski et al. 2002) reported the use of 1-(1-butyl)-3-methylimidazolium chloride (BuMeImCl) as a cellulose solvent. He explored the effects of ILs on the dissolution properties of cellulose with changing the structure of cation and anion. They further revealed that ILs cannot dissolve cellulose at room temperature but at high temperature of 100-110 °C. Cellulose solubility was further explored by (Wu et al. 2004) in 1-allyl-3-methylimidazole chloride (AlMeImCl). They showed that this ionic liquid is much better solvent for cellulose solubility. The solubility of cellulose in ionic liquids depends upon the degree of polymerization of cellulose (Zhai et al. 2007). They further confirmed that there is no side reaction during cellulose solubility in ionic liquids. The purity of ionic liquid is an important factor for cellulose solubility. Presence of small amount of water has a large effect on the aggregation state, hence the reactivity of dissolved cellulose (El Seoud et al. 2005). The most frequently used among IL anions are chloride and acetate. There is a strong intermolecular hydrogen bonding between cations and anions. Such strong hydrogen bonding interaction has been shown in 1-ethyl-3-methylimidazolium chloride (interaction of imidazolium cation and chloride anions (Novoselov et al. 2007) as shown in Figure 1.31.

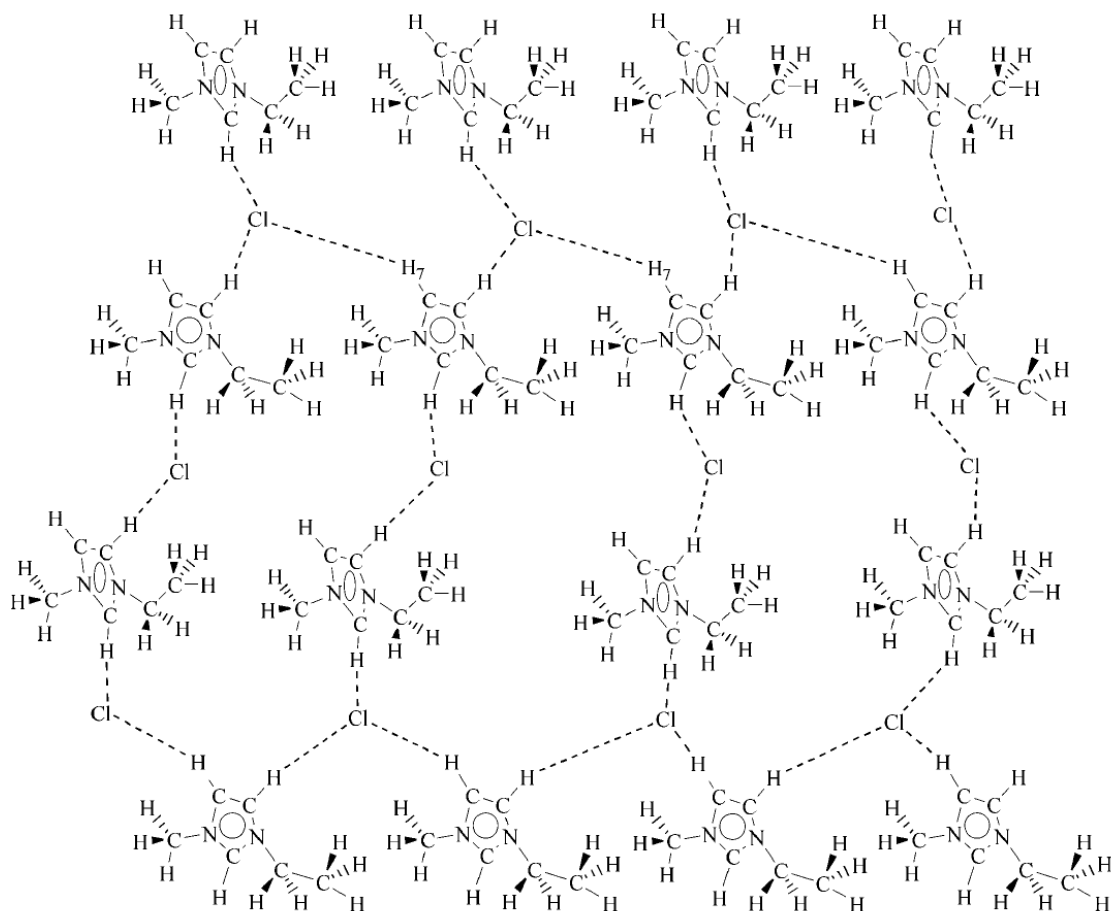


**Figure 1.31:** Hydrogen bonding interaction between imidazolium cation and chloride anion (reproduced from [Novoselov et al. 2007] with permission).

Recently, it has been reported that ILs acetates are more efficient in dissolving the fibrous cellulose (eucalyptus) than their halides counterpart (El Seoud et al. 2011).

The mechanism of cellulose dissolution in low viscous 1-ethyl-3-methylimidazolium acetate has been recently reported using cellobiose (model for cellulose). The solvation process has been investigated using  $^1\text{H-NMR}$  spectroscopic technique (Zhang et al. 2010). There is a strong interaction between imidazolium cation and acetate anion themselves as reported in several computer simulation studies and experimental work (Avent et al. 1994; Headley et al. 2002; Dong et al. 2006). When cellobiose is added in ionic liquid; the results show that with increasing concentration of IL there is a marked decrease in chemical shift value of imidazolium ring

proton especially more acidic C2-H and smaller effect on less acidic C4-H and C5-H. Acetate ion prefers to form hydrogen bond with hydroxyl protons in cellobiose. As a result, interaction of acetate ion with imidazolium ring proton especially C2-H decreases as shown below in Figure 1.32.

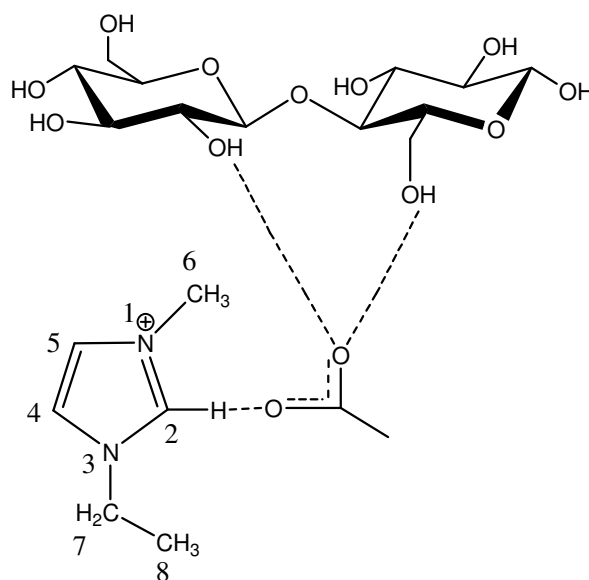


**Figure 1.32:** Hydrogen bonding interaction between 1-ethyl-3-methylimidazolium acetate (EtMelmAc) and cellobiose (model for cellulose).

### 1.8.3. Cellulose derivatization in ionic liquids with mixtures of DAS

Various derivatives of cellulose have been synthesized such as acylates, carbamate and benzoylate using ILs such as AlMelmCl; BuMelmCl; BnMelmCl; EtMelmCl, and EtMelmAc (Nawaz et al. 2014, in press; Zhang et al. 2005; Bagheri et al. 2008; Koehler et al. 2007). The degree of substitution (DS) depends on the various factors such as acylating reagent mole ratio to AGU, acylation time, use of catalyst and temperature but also on the dissolution state of cellulose (Koehler et al. 2007; Feng et al. 2008). When cellulose is protected with 4-methoxytrityl in AlMelmCl, its reactivity is increased for further modification (Granstrom et al. 2009). The synthetic procedure for different derivatives of cellulose such as ester, ethers, sulfonates, carbanilates, azides, hemiacetals, amines and deoxyderivatives has been shown below in Figure 1.33 (Pinkert et al. 2009).

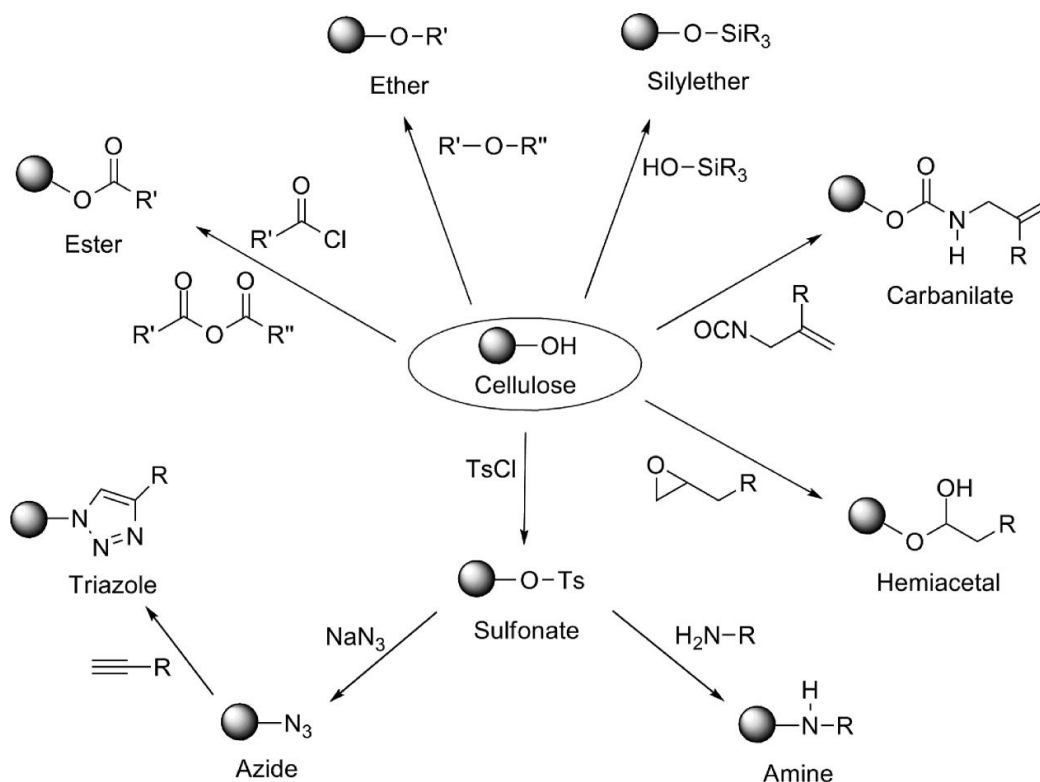


**Figure 1.33:** Different routes for cellulose modification in ILs (reproduced from [Pinkert et al. 2009] with permission).

In addition to this, cellulose sulfates have been successfully prepared in BuMelmCl, AlMelmCl, and AlMelmAc using different sulfating agents (Gericke et al. 2009). Sulfation of biopolymer has been achieved under homogeneous reaction conditions in nonderivatizing cellulose solvent reported first time. The radiation-induced and ring opening graft polymerization of cellulose has been done using BuMelmCl (Hao et al. 2009). Cellulose-based macroinitiator, cellulose 2-bromoisobutyrylate was synthesized for atom transfer radical polymerization in homogeneous reaction condition using AlMelmCl. This reaction was monitored without using any catalyst and protecting group (Meng et al. 2009).

Microwave assisted acetylation of cellulose in AlBuImCl has been reported to yield a higher DS of 2.8 compared to the derivatization under conventional heating (DS = 2.2; reaction conditions in both cases: 8 h, 80 °C, 4.5 equivalents acetic anhydride) (Possidonio et al. 2010; El Seoud et al. 2011). The use of ILs with fluoride anion (IL-F) is challenging because of side reactions. Neat

1-allyl-3-methylimidazolium fluoride (AlMelmF) is used as a solvent in microwave-assisted acylation of cellulose. The results are disappointing due to side reactions in the IL proper and F<sup>-</sup>-mediated hydrolysis of the produced ester. A dramatic improvement is observed, when AlMelmF/DMSO mixture is employed (Casarano and El Seoud 2013). This mechanism is shown below in Figure 1.34. Finally, the formation of acyl fluoride (RCOF) by the reaction between TAAF and acetic- or hexanoic anhydride  $(\text{CH}_2=\text{CH}-\text{CH}_2)_4\text{N}^+ \text{F}^- + (\text{RCO})_2\text{O} \rightarrow \text{RCOF} + (\text{CH}_2=\text{CH}-\text{CH}_2)_4\text{N}^+ \text{OCR}$  has been demonstrated by FTIR. That is, a part of cellulose derivatization probably proceeds by the reaction of cellulose and acyl fluoride [Casarano et al. 2011].

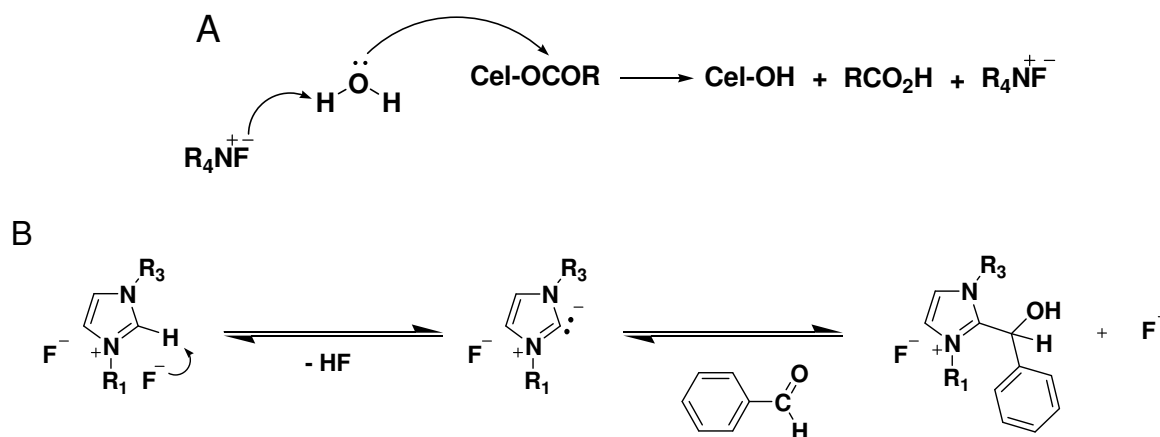


**Figure 1.34:** Part A) Suggested mechanism for the fluoride ion-mediated cellulose ethanoate hydrolysis through a general base catalyzed attack of water on the ester acyl group. Part B) Suggested mechanism for the reactions occurring in the IL-F/aldehyde mixture. The initial step is F<sup>-</sup>-mediated abstraction of C2-H of the imidazolium ring, followed by nucleophilic addition of the ylide formed to the carbonyl group of benzaldehyde.

Thus ILs are far from being “spectator” solvents. The new approach (use of IL-F/DMSO) is attractive because of its efficiency, low cost, and applicability to the derivatization of any polymer.

## 1.9. Solvatochromism

Solvatochromism is the ability of a chemical substance to change color due to a change in solvent polarity. The increasing solvent polarity cause hypsochromic shift (or blue shift) which corresponds to negative solvatochromism (Christian et al. 2010). The sign of the solvatochromism depends on the difference in dipole moment between the ground and excited states of the chromophore. The continuous interest in understanding the solvation is that most reactions are carried out in solution, including pure solvents and their mixtures (El Seoud 2007). The careful selection of the solvent is an important factor, e.g., use of aromatic and halogenated solvents has noticeably decreased in organic synthesis and industrial chemical processes. Understanding the solute/solvent interactions has become important by the introduction of “green” solvents such as supercritical CO<sub>2</sub> (Leinter W. 2002) and room-temperature ionic liquids (Welton T. 1999; Wasserscheid, P. 2000; Dupont, J. 2002).

### 1.9.1. Understanding solvation process

The effects of solvents on chemical phenomena cannot be rationalized by a single, macroscopic solvent property because it contain several type of interactions such as; solute-solvent, hydrogen-bonding, ion-dipole, London dispersion, solvophobic and dipole-induced dipole forces (El Seoud 2009). These effects are the combination of several solvent properties as given by the Taft–Kamlet–Abboud (TKA) equation (Laurence, C. et al. 1994).

$$\text{SDP} = \text{constant} + a (\text{SA}) + b (\text{SB}) + dp (\text{SdP}) + h(\delta^2\text{H}) \quad (1.4)$$

Where (SDP) is solvent-dependent phenomenon such as rate constant, equilibrium constant, spectroscopic shift and is modeled as a linear combination of two hydrogen-bonding terms, in which the solvent is the hydrogen bond donor ( $a (\text{SA})$ ), or the hydrogen bond acceptor ( $b (\text{SB})$ ), a dipolarity/polarizability term ( $dp (\text{SdP})$ ) and a cavity term ( $h(\delta^2\text{H})$ ) related to Hildebrand solubility parameter. The parameters, ( $\text{SA}$ ) ( $\text{SB}$ ) and ( $\text{SdP}$ ) are known as solvatochromic parameters because they are determined by using solvatochromic probes (vide infra; hereafter designated as “probes”); the subscript (S, for solvent) is employed.



The fact that the UV–vis spectra, absorption or emission, of some compounds are particularly sensitive to the medium (solvent, solvent mixtures, etc.) has been exploited in order to calculate (SA) (SB) and (SdP) of eq. 1 (Reichardt C. 2003; 2004; 2008). Figure 1.35 shows the structures of some of these probes, along with their acronyms, pKa in water, and log *P* (Silva, P. L. et al. 2008).

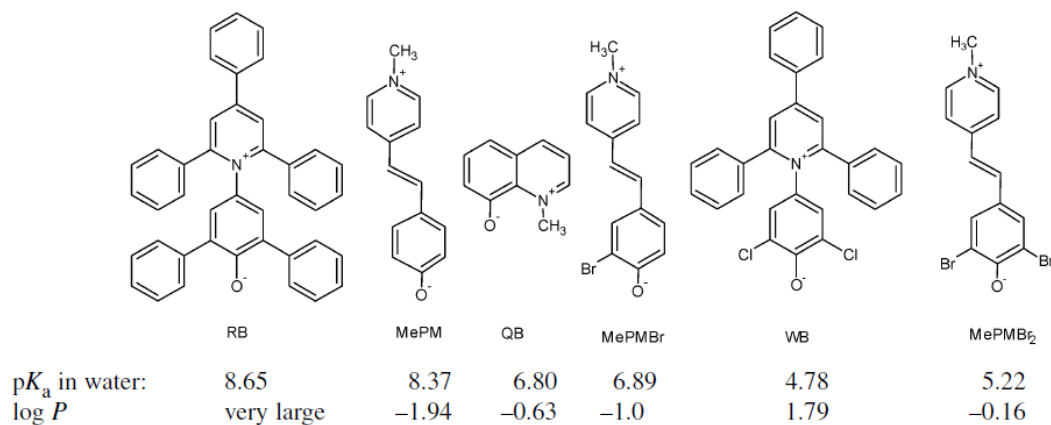


**Figure 1.35:** Molecular structures of selected solvatochromic probes, along with their pKa values in water and log *P*.

In summary solvatochromic studies are important because  $E_T$  (probe) quantifies the relative importance to solvation of the physicochemical properties such as polarity, acidity, basicity and polarizability of both substrate and solvent, or mixtures of solvents.

## 2. OBJECTIVES

This thesis is concerned with the factors that affect cellulose derivatization under homogeneous reaction conditions. Of these, we were interested in the molecular structure of the derivatizing agent; the effect of catalyst; and the reaction medium. We intended to analyze the effect of these variables quantitatively by employing kinetic data, namely, rate constants and activation parameters. Specifically, we were interested in:

- 1- Study of the relationship between the molecular structure of carboxylic acid anhydrides (ethanoic, propanoic, butanoic, pentanoic, and hexanoic) and their efficiency in the uncatalyzed acylating of MCC in SE/DAS,
- 2- Effect of catalysis on acylation by the above-mentioned anhydrides and comparison with the uncatalyzed reaction in the same solvent system;
- 3- Study of the relationship between the efficiency of acetylation of MCC by acetic anhydride in mixtures of an IL and DAS: Dependence on the nature of DAS;
- 4- Study of the relationship between the efficiency of acetylation of MCC by acetic anhydride in mixtures of an IL and DAS.

### 3. Experimental Part

#### 3.1. Material

##### 3.1.1. Cellulose

Microcrystalline cellulose (MCC; Avicel PH 101) was obtained from FMC, Philadelphia [DP<sub>v</sub>, by viscosity = 150 (ASTM 2001), I<sub>c</sub>, by X-ray diffraction = 0.82 (Buschle-Diller and Zeronian 1992)].

##### 3.1.2. Solvents and reagents

All solvents and reagents were purchased from Alfa Aesar or Merck and were purified as recommended elsewhere (Armagero & Chai, 2003). Cyclohexylmethanol (CHM) and DMAC were distilled from CaH<sub>2</sub> under reduced pressure. The pH of 20% solution of DMAC in water was equal to that of water. The expanded scale pH paper employed is able to detect  $1.4 \times 10^{-4}$  mol L<sup>-1</sup> of diethylamine (model for dimethylamine, a typical impurity in DMAC). Traces of water were removed from *trans*-1,2-cyclohexanediol (CHD) by azeotropic distillation with n-heptane. Ethanoic-, propanoic-, and butanoic-anhydride were distilled from P<sub>4</sub>O<sub>10</sub>. Distillation of pentanoic and hexanoic anhydrides from the same reagent led to the production of the corresponding carboxylic acids; they were purified by fractional distillation under reduced pressure. p-toluenesulfonyl chloride (TsCl) was purified by dissolving 10 g in 25 ml of dry chloroform. The solution was filtered, 125 mL of dry hexane was added, the solution filtered, and the solvent evaporated to give a white solid, m.p. 67–68 °C; literature m.p. 67–69 °C (Hacon et al, 2007). The purity of the molecular solvents was established from their density (DMA 4500M resonating-tube densimeter; Anton Paar, Graz) (Lide 2004) and empirical polarity, E<sub>T</sub>(33) in kcal/mol, as determined by the solvatochromic indicator 2,6-dichloro-4-(2,4,6-triphenyl-1 pyridinio)phenolate, WB (Tada et al. 2000). Allyl chloride was purified by washing with HCl, and then with dilute Na<sub>2</sub>CO<sub>3</sub> solution, water, followed by drying on anhydrous MgSO<sub>4</sub> and distillation. N-Methylimidazole; dimethylsulfoxide (DMSO); acetonitrile (MeCN) and sulfolane were distilled from CaH<sub>2</sub>.

## **3.2. Material characterization: cellulose; cellulose derivatives of model compounds for cellulose**

### **3.2.1. Determination of index of crystallinity by X-ray diffraction**

Cellulose (MCC) was dissolved in 6% LiCl/DMAC and was precipitated in water and then regenerated cellulose was filtered and air dried. Degree of crystallinity of cellulose was determined using X-ray diffraction method. Zeiss URD-6 universal diffractometer was used in the reflection geometry in the angular range 10–50° (2 $\theta$ ). The CuK radiation from the anode operating at 40 kV and 20 mA was monochromatized by using a 15 mm Nickel (Ni) foil. The data were recorded with a Rigaku Miniflex diffractometer (Tokyo) operating at 30 kV, 15 mA and  $\lambda(\text{CuK}\alpha) = 0.154 \text{ nm}$ , 0.02 ° /minute.  $I_c$  was calculated from Eqn. (3.1) (Buschlediller and Zeronian 1992):

$$I_c = 1 - I_{\min}/I_{\max} \quad (3.1)$$

Where,  $I_{\min}$  is the intensity minimum, between  $2\theta = 18^\circ$  and  $19^\circ$  (amorphous region of native cellulose) or between  $2\theta = 14^\circ$  and  $15^\circ$  (amorphous region of mercerized cellulose), and  $I_{\max}$  is the intensity maximum, between  $2\theta = 22^\circ$  and  $23^\circ$  (attributed to the crystalline region of the sample).

### **3.2.2. Degree of polymerization of cellulose by viscosity**

The apparatus used for the measurement of degree polymerization of cellulose by viscosity method was Schott model AVS 360 automatic viscometer following a normal ASTM D1795-96. The solution of CUEN (solution of cupric ethylenediamine) was used (ASTM D1795-96, 2001).

All the samples were saturated with nitrogen to prevent oxidation reaction. All the measurements were taken at 25 °C in triplicates. One solution of CUEN: H<sub>2</sub>O (1:1) was prepared and flow time of this mother solution was obtained. Then cellulose which was dried under reduced pressure at 60 °C for 5 h was dissolved in this mother solution with proportion of 1 g in

2 mL solution. The dilution of this solution was made and flow time was determined for each concentration, and then relative viscosity ( $\eta_{rel}$ ) was determined from these flow time data using the following equation 3.2 (Ludmila thesis 2010).

$$(\eta_{rel}) = \left\{ t_{solution} / t_o \right\} \quad (3.2)$$

where

$\eta_{rel}$  = relative viscosity

$t_{solution}$  = flow time of the solution of cellulose in CUEN-H<sub>2</sub>O

$t_o$  = flow time for the solvent CUEN-H<sub>2</sub>O (1:1)

Graph between Ln ( $\eta_{rel}$  /concentration of solution of CUEN-cellulose) versus concentration of solution of cellulose/CUEN showed the linear relationship and concentration of this linear relation corresponds to the values of intrinsic viscosity of the solution. The degree of polymerization was calculated from the intrinsic viscosity  $[\eta]$  using the following equation 3.3.

$$DP_v^{0.905} = 0.75 \times [\eta] \quad (3.3)$$

A similar procedure was employed for the determination of  $DP_v$  for the cellulose triacetate but in a different solvent; DMAC (Kamide et al., 1979).

### 3.2.3. Ester characterization of model compounds by FTIR and <sup>1</sup>H NMR

The acetates of CHM and CHD synthesized; were in liquid state and gave IR- (Vector-22 FTIR spectrophotometer; neat sample, 32 scans at 0.5 cm<sup>-1</sup> digital resolution), and <sup>1</sup>H NMR spectra (Bruker DPX 300 NMR spectrometer; CDCl<sub>3</sub>) that agreed with the results reported elsewhere for cyclohexylmethanol acetate and *trans*-1,2-cyclohexanediol acetate (AIST 2001; Das et al. 2006; Khaja and Xue 2006; Zeynizadeh and Sadighnia 2010; Zeynizadeh and Sadighnia 2011). The molecular structures of the products obtained are shown below in Figure 3.1.

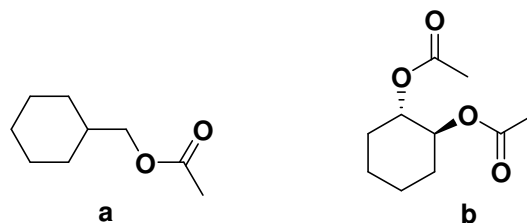


**Figure 3.1:** Chemical structures of (a) cyclohexymethyl acetate and (b) *trans*-cyclohexane-1,2- diacetate.

### 3.2.4 Determination of the degree of substitution of cellulose esters

Cellulose acetate, butyrate and hexanoate products (0.1925g) synthesized in LiCl/DMAC, IL/DMAC, IL/MeCN, IL/DMSO and IL/Sulfolane; were taken in 100mL round bottom flask with small magnetic stirrer. Flask was gently rotated by hand to spread the sample in a thin layer on the bottom of flask. Then 7mL of acetone was added drop wise along the walls of the flask without disturbing the thin layer of sample and wait for 30 minutes. Then 4mL of DMSO was added along the sides of flask without stirring. Flask was closed loosely with stopper and system was left until the formation of complete solution. More DMSO can be added if complete solution does not form. To the sample was added 3mL, 1 N NaOH solution drop wise to form finely divided precipitate and to avoid lump formation. The flask was closed and the mixture was left to react for 2 hours (30minutes for acetate). After that 10mL of hot water (60-70 °C) was added along the sides of flask and wait for 2 minutes under stirring. Then was added 2-3 drops of indicator phenolphthalein and excess NaOH was titrated with 1N H<sub>2</sub>SO<sub>4</sub> solution. Then was added 0.2mL extra H<sub>2</sub>SO<sub>4</sub> solution to check the completion of reaction. Again 2-3drops of indicator phenolphthalein was added and titrated with 1N NaOH solution. Same process was used for a blank run (without cellulose ester). Using these readings, DS of cellulose esters was calculated by using the following formula (ASTM D871-96, 2002)

$$(D - C) N_{H_2SO_4} + (A - B) N_{NaOH} \times (F/W) \quad (3.4)$$

Where;

A = NaOH required for titration of sample.

B = NaOH required for titration of blank.

D = H<sub>2</sub>SO<sub>4</sub> required for titration of blank.

C = H<sub>2</sub>SO<sub>4</sub> required for titration of sample.

N<sub>H<sub>2</sub>SO<sub>4</sub></sub> = Normality of H<sub>2</sub>SO<sub>4</sub> solution.

N<sub>NaOH</sub> = Normality of NaOH solution.

F = 4.305 for acetyl and 6.005 for acetic acid

W = Weight of sample used.

### 3.3. Syntheses

#### 3.3.1. Syntheses of CHM and CHD acetates

The kinetic experiments were repeated on a larger scale (three times) in three-necked round-bottom flasks. In order to simplify the separation of the acetates of CHM and CHD we used LiCl suspension in acetonitrile as a solvent instead of LiCl/DMAC. The required amount of ROH; 2.14 mL, 17 mmol CHM, or 1.07 mL, 8.6 mmol of CHD was added to LiCl acetonitrile suspension. Ethanoic anhydride 8 mL (84 mmol) was added and the reaction was carried out for 4 h at 80 °C under nitrogen.

In case of imidazole catalyzed reaction; the above mentioned procedure was modified, as follows: MeCN, 25 mL was introduced into 100 mL three-necked round bottom flask, equipped with a condenser and a drying tube. The bath temperature was adjusted to ca. 60 °C, and 8 mL (84 mmol) of ethanoic anhydride was added, followed by addition of, 1 g LiCl and 11.76 g (0.172 mol) of Im; the mixture was stirred for 5 min. The required amount of ROH; 2.14 mL, 17 mmol CHM, or 1.07 mL, 8.6 mmol of CHD was added, and the reaction mixture was stirred for 30 min, at 60 °C.

In both of the above mentioned procedures; after evaporation of the solvent, the residue was carefully neutralized with a cold aqueous solution of NaHCO<sub>3</sub>, and then extracted with 30 mL of CH<sub>2</sub>Cl<sub>2</sub>. The organic layer was washed with cold dilute HCl (in order to extract Im), with water, dried with anhydrous MgSO<sub>4</sub>, and then the solvent was evaporated. The liquid products (pure liquids between NaCl plates) cyclohexymethyl acetate (79% yield) or *trans*-1,2-

cyclohexane diacetate (75% yield) gave IR- (Bruker Vector-22 FTIR spectrophotometer; neat sample, 32 scans at  $0.5\text{ cm}^{-1}$  digital resolution), and  $^1\text{H}$  NMR spectra (Bruker DPX 300 NMR spectrometer;  $\text{CDCl}_3$ ) identical to those published elsewhere;(AIST 2001; Das, Reddy & Tehseen, 2006; Khaja & Xue, 2006; Zeynizadeh & Sadighnia, 2010; Zeynizadeh & Sadighnia, 2011).

### 3.3.2. Syntheses of cellulose esters in LiCl/DMAC

The kinetic experiments were repeated on a larger scale (three times) in three-necked round-bottom flasks. A 2% solution of MCC in 6% LiCl/DMAC was obtained as discussed in section 3.4.2. To 25 mL of this solution were added the appropriate volumes of ethanoic-, butanoic-, or hexanoic anhydride, so that the molar ratio of the corresponding anhydride/AGU was 4.5. The solution was stirred under nitrogen for 4 h at  $80\text{ }^\circ\text{C}$ . Cellulose esters were precipitated in ethanol; repeatedly suspended in the same solvent (3 x 200 mL), then filtered, and dried for 48 h under reduced pressure, over  $\text{P}_4\text{O}_{10}$ , at  $60\text{ }^\circ\text{C}$ . The ester DS was determined by titration (ASTM 2002); DS = 2.1, 1.7, 2.5, for ethanoate, butanoate, and hexanoate, respectively.

### 3.3.3. Syntheses of cellulose acetate in IL/DAS

Cellulose esters were synthesized on a larger scale (thrice) in a three-necked round-bottom flask. After MCC dissolution, cellulose was reacted with ethanoic anhydride ( $\text{Ac}_2\text{O}/\text{AGU} = 4.5$ ), under the following conditions: 1.887mol/L IL/DMAC, 30 min at  $40\text{ }^\circ\text{C}$ ; 2.647mol/L IL/MeCN, 2 h at  $40\text{ }^\circ\text{C}$  and 1.258mol/L IL/DMSO, 30 min at  $40\text{ }^\circ\text{C}$  and 1.258mol/L IL/sulfolane 3 h at  $60\text{ }^\circ\text{C}$ . The resulting solutions were added to hot ethanol; the solid precipitated was repeatedly suspended in the same solvent (3 x 200 mL;  $60\text{ }^\circ\text{C}$ ), then filtered, washed with water, and dried at  $60\text{ }^\circ\text{C}$  for 24 h, under reduced pressure, over  $\text{P}_4\text{O}_{10}$ . The products gave IR spectra (Vector 22 FTIR spectrophotometer; KBr pellet) similar to authentic cellulose acetate. The degrees of substitution, DS, of the esters were determined by titration (ASTM 2002). DS = 2.39, 2.47, 1.80 and 2.64 for IL-DMAC, IL-MeCN, IL-DMSO and IL-sulfolane respectively.



### 3.3.4. Microwave-assisted synthesis of 1-allyl-3-methylimidazolium chloride (AlMelmCl)

*N*-Methylimidazole (40 mL; 0.501 mol) was introduced into a flask provided with magnetic stirrer and a reflux condenser through which cold water (ca. 10 °C) was circulated (in order to prevent loss, on heating, of allyl chloride). Allyl chloride (43 mL; 0.527 mol) was slowly added (15 min), with efficient stirring at room temperature. The flask was then introduced into the cavity of a microwave reactor (CEM Discover model DU-8316) and heated at 70 °C, 50 W irradiation potential, for 90 min. The product was cooled, and then vigorously stirred with cold ethyl acetate (ca. 0 °C) for 15 minutes; the upper layer (ethyl acetate) was separated. A small aliquot of the latter was agitated with water, and the pH of the aqueous phase measured. This process was repeated until the aqueous phase was neutral (expanded pH-scale paper; 3 x 160 mL ethyl acetate). The IL was dissolved in 150 mL methanol, and stirred overnight with heat-activated charcoal (3h, 150 °C, under reduced pressure). The suspension was filtered, and the alcohol removed to give slightly amber IL; this was further dried at 60 °C under reduced pressure for 4 h. The product gave the expected <sup>1</sup>H NMR spectrum (Varian Innova-300 NMR spectrometer) (Sato et al. 2010) and its solution in water showed the absence of acid or base impurity (expanded- scale pH paper). Pure AlMelmCl was stored in tightly-stoppered bottles.

## 3.4. Kinetic studies

### 3.4.1. Equipment

The progress of the acylating reaction was monitored by following the increase in solution conductivity ( $\lambda$ ) as a function of time, by employing Fisher Accumet AR-50 ion meter, equipped with a Metrohm 6.0910.120 conductivity electrode, inserted in a home-built double-walled conductivity cell through which water is circulated from a thermostat, see Figure 3.2 below. Data acquisition and the solution temperature were controlled with a PC. Precise temperature control within the reaction solution was achieved by using a PT-100 temperature sensor attached to the computer via RS-232 serial port, the CPU controlled the thermostat.

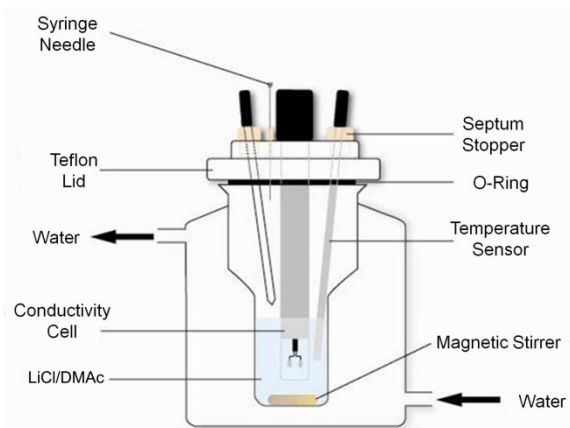


**Figure 3.2:** Schematic representation of the apparatus used to monitor the kinetic of acylation of model compounds and cellulose through the variation of the solution conductivity. Conductivity data acquisition and temperature control of the reaction solution are controlled by a computer.

### 3.4.2. Preparation of solutions for kinetic studies: cellulose solutions in LiCl/DMAC and in IL/DAS

#### *LiCl/DMAC*

LiCl (8 g) was dried at 300 °C for two hours, and then cooled to room temperature under reduced pressure. The electrolyte was quickly weighed (6.0 g) in 100 mL volumetric flask; 80 mL of dry DMAC were added, the flask was stoppered and sonicated (Laborrette 17, Fritsch, Berlin) until a clear solution was obtained, *ca.* 6.5 h. The solution volume was completed to the mark with fresh solvent.

MCC (2.0 g; 12.3 mmol AGU) and LiCl (6.0 g) were weighed into a 250 mL three-neck round-bottom flask. The latter was equipped with a stopcock, 100 mL graduated addition funnel (no equilibration side arm) and a magnetic stirring bar. The flask was immersed into an oil bath, and then connected to a vacuum pump. The pressure was reduced to 2 mmHg, the system was heated to 110 °C in *ca.* 40 min, and then kept under these conditions for 30 additional minutes. The vacuum pump was turned off, the stopcock closed, the heating bath removed, and 60 mL of pure DMAC were added dropwise. The system was then brought to atmospheric pressure with dry, oxygen-free nitrogen. The addition funnel was substituted by a

condenser with a drying tube, and the flask was quickly equipped with an efficient mechanical stirrer. The temperature was raised to 150 °C in *ca.* 35 min, and the cellulose slurry was vigorously stirred for 90 min (IKA Labortechnik, model RW 20, 500 rpm) at this (bath) temperature. The latter was decreased to 50 ± 5 °C in 2 h, and the slurry was left under these conditions with magnetic stirring overnight; a clear cellulose solution was obtained. The cellulose solution was transferred to 100 mL volumetric flask, whose volume was completed by adding DMAC that has been employed in washing the walls of the round-bottom flask.

### ***IL/DAS***

MCC (0.7 g, 43.2 mmol) was weighed into a three-necked round-bottom flask fitted with magnetic stirrer and 100 mL graduated addition funnel (no equilibration side arm) containing the appropriate mass of IL (from 42(36.7mL) to 84 (73.6mL) g for IL-DMAC and 58.8-to 84 g for IL-MeCN) and from 21.59 (19.63mL) to 33.6 (30.6mL) g for IL-DMSO and 30.90 (24.53mL) to 53.97 (42.84mL) g for IL-Sulfolane. The flask was connected to a vacuum pump (2 mmHg) and heated to 110 °C in *ca.* 30 min, and then kept under these conditions for additional 45 min. While maintaining the reduced pressure, the IL was slowly introduced, with continuous stirring. The mixture (MCC plus IL) was kept under these conditions for additional 20 min, and then the pressure was brought to atmospheric with dry, oxygen-free nitrogen. The temperature was decreased to 80 °C in one hour, and the mixture was stirred at this temperature for additional 3 h. The DAS, 50 (lowest IL content) to 10mL (highest IL content) of DMAC, or 30 to 10 mL of MeCN, and 70 (lowest IL content) to 50mL (highest IL content) of DMSO, or 60 to 40 mL of Sulfolane, was slowly added with continuous stirring. The resulting clear solution was transferred into 100 mL volumetric flask and the volume was completed up to the mark by molecular solvent (*ca.* 10mL) that has been employed to wash the addition funnel and the round-bottom flask. All solutions of MCC/IL-DAS were clear and isotropic, as indicated by examination between two Polaroid plates against light.

### 3.4.3. Kinetics of acylation of model compounds of cellulose in LiCl/DMAC, and IL/DAS

The experiments were carried out as follows: 10 mL of a solution of the model compounds studied (CHM or CHD) in 6% LiCl/DMAC or in 1.887mol/L, IL/DMAC; 1.258mol/L, IL/DMSO; or 1.258mol/L, IL/Sulfolane was introduced into the conductivity cell, the latter was quickly closed, and heated to the desired temperature. After thermal equilibration, 4 mL of DAS containing the appropriate anhydride were added;

The following modifications were done for Imidazole-catalyzed (hereafter written as Im) reactions in LiCl/DMAC: 5 mL of DMAC containing the appropriate anhydride were introduced into the conductivity cell followed by the addition of required mass of solid Im. After thermal equilibration, the solution of the compound studied (CHM and CHD) in 10 mL of 6% LiCl/DMAC was introduced into the conductivity cell.

The increase in ( $\lambda$ ) due to liberation of carboxylic acid was recorded as a function of (t). A home-developed non-linear regression analysis program was used for calculating the values of the observed rate constants ( $k_{obs}$ ), by minimizing the sum of the squares of the residuals (between experimental and calculated  $\lambda$ , Marquardt-Levenberg algorithm). The agreement between calculated and experimental "infinity" conductivity ( $\lambda_{\infty}$ ) was routinely checked. The relative standard deviation in  $k_{obs}$ , i.e., ((standard deviation/ $k_{obs}$ ) 100), was  $\leq 0.5$ , that between  $k_{obs}$  of triplicate runs was  $< 3\%$ . Figure 3.3 shows typical plot for the variation of solution conductivity of CHM as a function of (t) in 6% LiCl/DMAC.

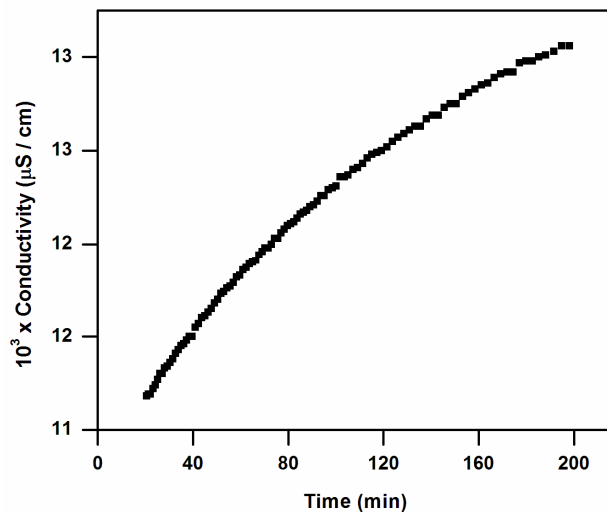


**Figure 3.3:** Variation of solution conductivity as a function of time (t) for uncatalyzed acylation of CHM with propionic anhydride ( $\text{Pr}_2\text{O}$ ) at  $65^\circ\text{C}$

Detail of the experimental conditions employed for the acylation of model compounds are shown below in Table 3.1 and 3.2.

**Table 3.1:** Experimental details of the kinetic experiments on the acylation of cyclohexylmethanol, CHM and *trans*-1,2-cyclohexanediol, CHD by carboxylic acid anhydrides<sup>a,b</sup>

Reagent	<i>Final</i> molarity of the hydroxyl compound and Final molar ratio of anhydride per <i>single</i> OH of CHM and CHD
CHM	CHM = $0.0308 \text{ mol L}^{-1}$
	Ethanoic 68.6
	Propanoic 50.6
	Butanoic 39.6
	Pentanoic. 32.1
	Hexanoic. 28.1
CHD	CHD = $0.0616 \text{ mol L}^{-1}$
	Ethanoic 34.3
	Propanoic 25.3
	Butanoic 19.8
	Pentanoic. 16.0
	Hexanoic. 14.0

a- The final LiCl concentration is 4.28%, or 1.007 mol L<sup>-1</sup>

b-The experiment was carried out by adding 4 mL of acid anhydride in DMAC to 10 mL of 6% LiCl/DMAC. The final molarities are calculated based on 14 mL solution, i.e., by considering no volume change on mixing of both solutions.

**Table 3.2:** Experimental conditions for the imidazole-catalyzed acylation of model compounds with acid anhydrides<sup>a,b</sup>

Model compounds	Concentration mol L <sup>-1</sup> (OH)	Anhydride concentration; mol L <sup>-1</sup>	Imidazole concentration; mol L <sup>-1</sup>
CHM	0.0288	0.288	0.576
CHD	0.0576	0.576	1.152

a- The final LiCl concentration was 4 %, or 0.943 mol L<sup>-1</sup>. The experiment was carried out by adding 10 mL of CHM or CHD in 6% LiCl/DMAC to 5 mL of a solution of acid anhydride plus imidazole in pure DMAC. The final molarities are calculated based on 15 mL solution, i.e., by considering no volume change on mixing of both solutions.

b- CHM and CHD carry one and two (OH) groups per molecule, respectively. Therefore the ROH concentrations are listed as moles of (OH)/liter. As shown in the second and third columns, the molar ratios [reagent]/[OH] are 10 and 20 for acid anhydride, and imidazole, respectively.

#### 3.4.4. Kinetics of acylation of cellulose in LiCl/DMAC, and IL/DAS

The conductivity experiments were performed for the acylation of cellulose (MCC) in different solvent systems as follows. The solution of cellulose to be studied (10mL) was introduced into the conductivity cell; the latter was quickly closed, and heated to the desired temperature (30 to 85 °C). The *final concentrations* employed were, in mol/L: MCC = 0.0924; LiCl/DMAC = 1.007; IL/DMAC = 1.887, 2.269, 2.647, 3.025, 3.404 and 3.782; IL/MeCN = 2.647, 3.025, 3.404, and 3.782; IL/DMSO = 1.007, 1.258 and 1.573 and IL/Sulfolane = 1.258, 1.573, 1.887 and 2.201. After thermal equilibration, 4 mL of DMAC, MeCN, DMSO or Sulfolane,

containing the appropriate amount of  $\text{Ac}_2\text{O}$  to give a *final anhydride concentration* of 1.057 mol/L was added and the increase in ( $\lambda$ ) was recorded as a function of (t).

Figure 3.4 shows typical plots of the variation conductivity as a function of (t) in IL-DAS media as shown below.

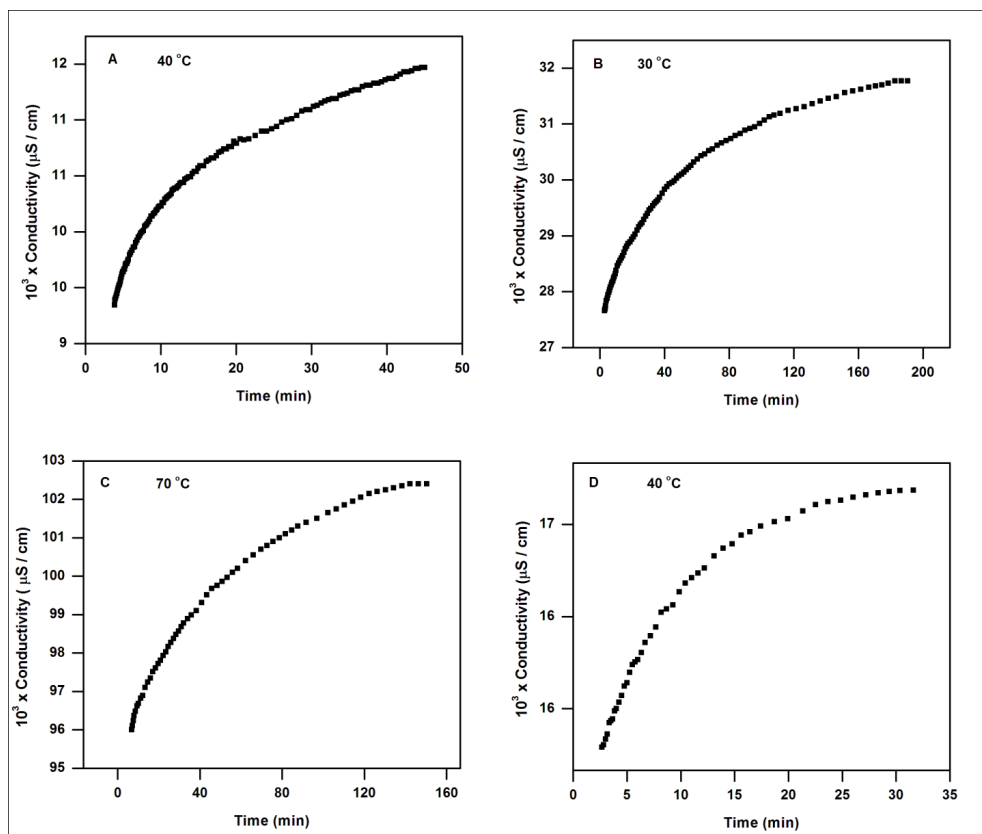


**Figure 3.4:** Typical plots showing the variation of solution conductivity in function of time obtained for reaction of MCC with  $\text{Ac}_2\text{O}$  in (A) 1.887mol/L, IL-DMAC at 40 °C; (B), 2.647mol/L, IL-MeCN at 30 °C; (C), 1.258mol/L, IL-Sulfolane at 70 °C and (D); 1.007mol/L, IL-DMSO at 40 °C until its value was practically constant.

The values of the third order rate constant ( $k_3$ ) were obtained by dividing the corresponding  $k_{\text{obs}}/[\text{anhydride}][\text{LiCl}]$ ;  $k_{\text{obs}}/[\text{anhydride}][\text{imidazole}]$  or  $k_{\text{obs}}/[\text{anhydride}][\text{AlMeImCl}]$ ; the activation parameters were obtained from the dependence of  $k_3$  on T, by using standard

equations (Anslyn and Dougherty 2006). Details of the experimental conditions employed for each compound are listed in Table 3.3 below.

**Table 3.3:** Concentration of IL/DAS used for the acetylation of MCC in IL/DAS at different temperatures, from 30 to 70 °C.

IL/DMAC, mol/L <sup>a</sup>	IL/MeCN, mol/L <sup>a</sup>	IL/DMSO, mol/L <sup>b</sup>	IL/Sulfolane, mol/L <sup>c</sup>
1.887	2.647	1.007	1.258
2.269	3.025	1.258	1.573
2.647	3.404	1.573	1.887
3.025	3.782	-----	2.201
3.404	-----	-----	-----
3.782	-----	-----	-----

a- reaction was carried out at 30, 40, 50 and 60 °C;

b- 40, 50 and 60 °C;

c- 50, 60 and 70 °C;

d- acetic anhydride concentration used, was constant in all cases; 1.057 mol/ L

### 3.5. Mechanistic studies

#### 3.5.1. Detection of the intermediate in imidazole-catalyzed acylation by

##### <sup>1</sup>H NMR and FTIR

<sup>1</sup>H NMR (Varian, Gemini-300) and FTIR (Bruker Victor-22) have been employed in order to detect the (possible) formation of reactive intermediates, formed by the reaction between the anhydride and the catalyst, as follows:

##### <sup>1</sup>H NMR

Equal volumes of solutions in DMSO-*d*<sub>6</sub> of acetic anhydride (0.05 mol L<sup>-1</sup>) and TsCl (0.05 mol L<sup>-1</sup>) were mixed in a glass tube, agitated (vortex) and quickly transferred to the NMR tube



(Wilmad 535pp). The spectrum of the resulting solution was recorded as a function of time. The same experiment was repeated with Im, by using  $\text{CDCl}_3$  as solvent.

## FTIR

Equal volumes of solutions in  $\text{CD}_3\text{CN}$  of acetic anhydride (0.42 mol/L) and Im (0.42 mol/L) were mixed in a glass tube, agitated (vortex) and quickly transferred to the IR cell ( $\text{CaF}_2$ , 0.015 mm). The spectrum of the resulting solution was recorded as a function of time.

## 3.6. Theoretical calculations

### 3.6.1. Molecular dynamics, MD, simulations in LiCl/DMAC

Gromacs 4.0.7 software package has been employed for all MD simulations (Van Der Spoel et al., 2005). Two systems were simulated, each containing the following number of molecules: 250, DMAC; 25, CHD, and either 100, ethanoic anhydride, or 100 of *N*-acetylimidazole. The simulation was performed at 300K, for 30ns by using OPLS force field, isothermal-isobaric (NPT) ensemble, periodic boundaries and the smooth particle-mesh Ewald (PME) algorithm for long-range electrostatic interactions (Jorgensen, Maxwell & Tirado-Rives, 1996). Equilibration of the ensemble was checked by monitoring the potential energy and density. The optimized geometry of CHD; ethanoic anhydride; and *N*-acetylimidazole were calculated as previously described in 5.2.1. OPLS-optimized DMAC geometry and topology was that reported elsewhere (Jorgensen, & Tirado-Rives, 2005; Carl et al., 2012). The partial charges on the atoms were calculated by using the AM1 wave function via the CM1A approach (Storer, Giesen, Cramer & Truhlar, 1995), as implemented in the AMSOL 7.1 program (Jorgensen 1986; Kaminski & Jorgensen, 1998). A sub-routine implemented in the Gromacs program has been employed for calculating the number of molecules that remain in contact as a function of time (in ps). This refers to molecules that remain within 0.56nm; the distance from (highly energy) zero separation to the end of the first solvation shell, i.e., the end of the first peak in the radial distribution function between the (O) of CHD and the acyl carbonyl carbon of either  $(\text{CH}_3\text{CO})_2\text{O}$ , or *N*- $\text{CH}_3\text{COIm}$ .

### 3.6.2. MD, simulations in IL-DAS

The approach employed is the same as in 3.6.1. Two systems were simulated, each containing 1 molecule of AGU oligomer, composed of 12 AGUs (dodecaose; hereafter designated as “oligomer”), 301 molecules of the IL, and 1143 molecules of the molecular solvent, either DMAC or MeCN and 1 molecule of AGU oligomer, 252 molecules of the IL, and 1143 molecules of the molecular solvent, either DMSO or Sulfolane. The simulation was performed at 300 K, for 75 ns by using GAFF (General Amber Force Field) force field (Wang et al. 2004), isothermal-isobaric (NPT) ensemble, periodic boundaries and the smooth particle-mesh Ewald (PME) algorithm for long-range electrostatic interactions (Jorgensen et al. 1996). The IL has its geometry optimized (gas phase) by using DFT calculation, by employing “good-opt” parameter using the program Orca 2.9 (Neese et al. 2011). The oligomer chain was drawn using Cellulose-Builder script (Gomes and Skaf 2012). Partial charges on the atoms were calculated by using the RESP (Restrained ElectroStatic Potential fit) approach (Bayly et al. 1993) as calculated by the RED (RESP ESP charge Derive) on-line server (Vanqualef et al. 2011). The topologies files for GAFF force field were generated by using the Acypye (Silva and Vranken 2012) and Antechamber 12 programs (Wang et al. 2006). GAFF-optimized geometries and topologies of DMAC and MeCN were taken from literature (Wang et al. 2004; Caleman et al. 2012) and the simulation boxes were generated using Packmol program (Martínez et al. 2009). We have checked the equilibration of the ensemble by monitoring the potential energy and density (in g/mL) as a function of simulation time. We have found that the potential energy versus simulation time curves reach equilibrium, i.e., remain essentially constant, after ca. 15 ns until the end of simulation (75 ns). Analysis of the results of MD simulations was done through the use of radial distribution functions (RDF) or by H-bond calculations made by using VMD (Visual Molecular Dynamics) software (Humphrey et al. 1996).

## 3.7- Additional experiments

### 3.7.1. Probing hydrogen bonding of ILs with CHM or cellobiose by FTIR

We have employed the following conditions to determine the effect of the AlMeImCl on ( $\nu_{OH}$ ), the stretching frequency of the hydroxyl group of CHM, or cellobiose: CaF<sub>2</sub> cell, 0.025 mm

path width; 32 spectra accumulated at  $0.5\text{ cm}^{-1}$  resolution. The *final* concentrations, in the IR cell, mol/L, were: CHM = 0.3 and IL = 0.086, in DMAC or MeCN and IL = 0.172 to 0.860 for DMSO and 0.344 to 0.860 for Sulfolane keeping the cellobiose concentration constant (0.086 mol/L).

### 3.7.2. Determination of the microscopic properties of reaction media by solvatochromic dyes

The molecular structures of the solvatochromic dyes employed (probes) are shown in Figure 3.5. The solvent descriptors that we have calculated from their Uv-vis spectra (Shimadzu UV 2550 spectrophotometer, at  $40\text{ }^{\circ}\text{C}$ ) are: WB (1), empirical polarity,  $E_T(33)$  in kcal/mol; *o*-*tert*-butylstilbazolium betaine (2) and *o,o'*-di-*tert*-butylstilbazolium betaine (3) solvent acidity (SA); 5-nitroindoline (4) and 1-methyl-5-nitroindoline (5), solvent basicity (SB). Aliquots of each probe solution in methanol (2 mL) were pipetted into 10 mL glass vials. The alcohol was evaporated under reduced pressure in the presence of  $\text{P}_4\text{O}_{10}$ . Aliquots of the solution to be tested (1 mL) were pipetted into the vials containing the solid, dry probe; the latter was dissolved (final probe concentration =  $0.75\text{-}1.5 \times 10^{-3}$  mol/L), the solution transferred into 1 cm path cell, and its absorbance was recorded. We have calculated the values of  $E_T(33)$ , SA, and SB from the values of  $\lambda_{\text{max}}$ , calculated from the first derivative of the spectra, as outlined elsewhere (Tada et al. 2000; Catalán 2009).

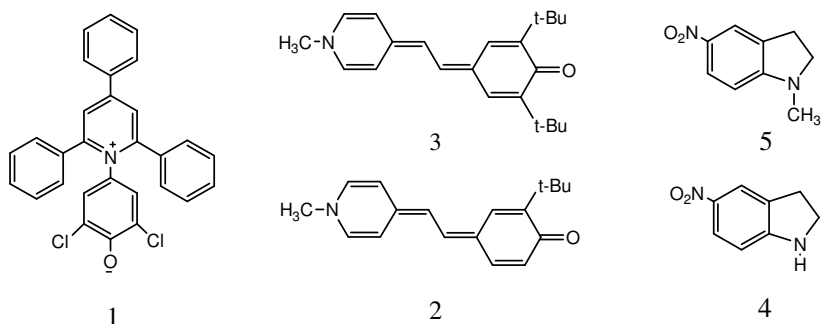


**Figure 3.5:** Molecular structures of the probes employed for the determination of the solvatochromic properties of the solvents. These include: 2,6-dichloro-4-(2,4,6-triphenyl-1-pyridinio)phenolate, WB (1); *o*-*tert*-butylstilbazolium betaine (2), and *o,o'*-di-*tert*-butylstilbazolium betaine (3); 5-nitroindoline (4), and 1-methyl-5-nitroindoline (5).

The solvent descriptors determined by these probes are: microscopic polarity; solvent acidity, and solvent basicity, respectively.

### **3.7.3. Rheology of mixtures of IL and DAS**

Viscosity data were obtained by using MCR 300 Physica Paar rheometer. The geometry employed in the measurements was a cone and plate fixture (50 mm diameter,  $1^\circ$ ). Temperature was adjusted by a Peltier plate, within a  $\pm 0.05$  °C maximum interval variation, for all experiments. Initially, we measured the stress response of a sample at 40 °C as a function of shear rate, in a range spanning from 10 to 200  $s^{-1}$ . For this experiment, a set of a hundred points were collected in a linear ramp. As the resulting flow curve profile proved to be Newtonian (linear dependence of shear stress on shear rate, implying a constant viscosity), a constant value of shear rate equal to 40 $s^{-1}$  was arbitrarily chosen and applied for the subsequent tests at 50, 60 and 70 °C respectively.

## 4. RESULTS AND DISCUSSIONS

### 4.1. Relevance of kinetic data to cellulose chemistry

There is little information on the kinetics and activation parameters of cellulose derivatization. This information is important *per se*, and because it allows calculation of the reaction time under a given set of experimental conditions, an important aspect in green chemistry. Additionally, kinetic data are required in order to compare: (1) The efficiency of different catalysts and solvent systems, where the same derivatizing agent is employed; (2) The reactivity of distinct derivatizing agents, for the same catalyst; (3) The reactivity of celluloses with different structural characteristics, under given set of reaction conditions.

The reason for the small amount of published kinetic data is that the experiment is either difficult to carry out, or is laborious. One has to determine the consumption of the derivatizing agent, this may not be feasible, e.g., because of the strong absorption of-, or light scattering by the reaction mixture. Another possibility is the (laborious) determination of the DS of the product as a function of time (t). Therefore, we decided to find out an instrumental method that renders determination of ( $k_{obs}$ ) feasible, and to carry out the reaction, where possible, under pseudo first-order conditions. Uv-Vis and IR spectroscopy were discarded because of the interference of solution background, and possible light scattering. We selected conductivity because acylation liberates a carboxylic acid that dissociates, leading to solution conductivity ( $\lambda$ ) increases as a function of (t). Because there is no guarantee that the observed increase in ( $\lambda$ ) is due to the reaction of interest we have experimentally demonstrated, *in every case*, that ester of high DS is produced under the conditions of the kinetic experiment. The advantage of carrying out chemical kinetic under first-order conditions is known, namely the concentration of the species that is being followed, reactant or product, need not be known; any property that change proportionally to the progress of the reaction (conductivity, light absorption, pH etc.) can be employed in order to calculate the value of  $k_{obs}$ . We have used conductivity to follow the rate of uncatalyzed and Im-catalyzed acylation of MCC in LiCl/DMAC. Additionally, we have studied the uncatalyzed acetylation of MCC in IL/DAS (where DAS refers to DMAC, DMSO, MeCN and Sulfolane).

## 4.2. Uncatalyzed acylation of cellulose in LiCl/DMAC

### 4.2.1. Setup of the kinetic experiment and calculation of the individual rate constants

The biopolymer was reacted with a series of carboxylic acid anhydrides,  $N_c = 2, 3, 4, 5, 6$  in the temperature (T) range of 65 to 85 °C as shown in the first column of Table 4.1; the other two columns refer to model compounds for cellulose whose use is discussed below. Only acetic anhydride was used in the case of IL-DAS as solvent system. The (large) ratios of anhydride/OH used mean that the acylation reactions have been carried out under pseudo-first order conditions. This is corroborated by the straight lines of  $\ln(\lambda_\infty - \lambda_t)$  versus (t), as shown in Figure 4.1.

**Table 4.1:** Ratio of the acid anhydrides employed and the hydroxyl groups of model compounds and cellulose

Anhydrides used	Ratio Anhydride/OH of AGU <sup>a</sup>	Ratio Anhydride/OH of CHM	Ratio Anhydride/OH of CHD
Acetic	11.4	68.6	34.3
Propanoic	11.4	50.6	25.3
Butanoic	11.4	39.6	19.8
Pentanoic	11.4	32.8	16.4
Hexanoic	10.0	28.1	14.0

a- AGU = anhydroglucose unit

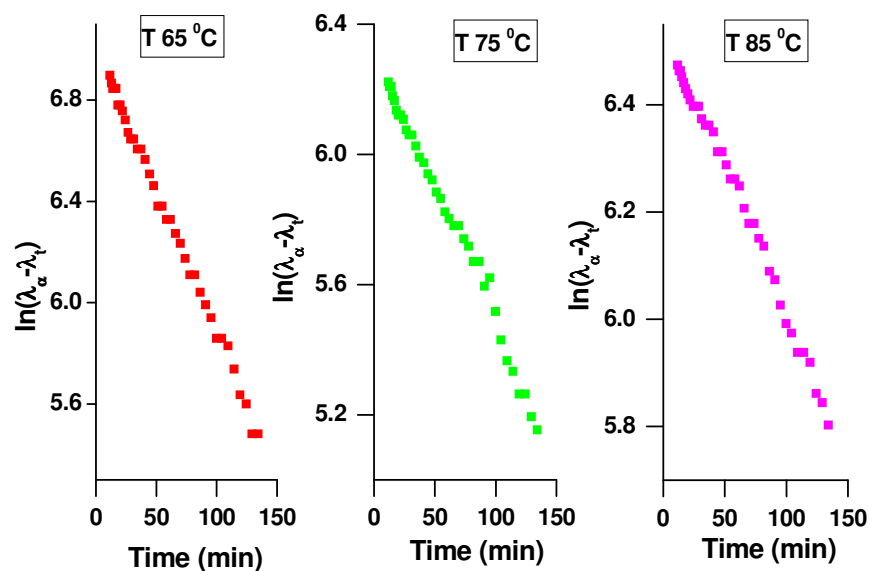


**Figure 4.1:** Typical plots showing the variation of solution conductivity as function of time obtained for CHM, CHD, and MCC. The symbols  $\lambda_\infty$  and  $\lambda_t$  refer to solution conductivity at the end of the reaction and at time (t), respectively.

Values of  $k_3$  were calculated from  $k_{\text{obs}}$  as given in Experimental. These values, however, refer to the sum of the rate constants of the reaction with the primary OH at C6,  $k_{3,\text{Prim(OH)}}$ , and the two secondary OH groups at C2 and C3 of the AGU,  $k_{3,\text{Sec(OH)}}$ . In order to split these rate constants into their components, we have employed cyclohexylmethanol (CHM, one Prim(OH)) and *trans*-1,2-cyclohexanediol (CHD, two Sec(OH)) as models for the C6-OH, and the C2-OH plus C3-OH groups of the AGU, respectively. Because CHM, CHD, and MCC carry one, two, and three OH groups, respectively, *all results listed refer to a single OH group*.

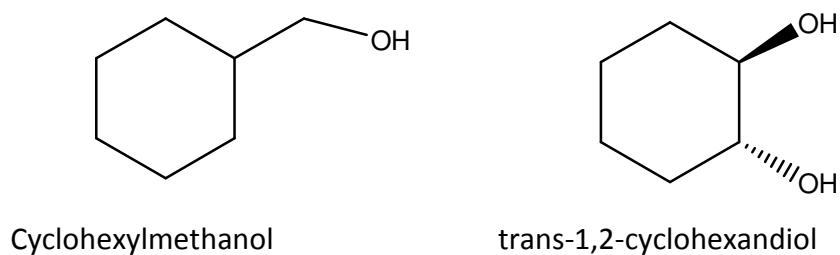


**Figure 4.2:** Model compounds for cellulose

The splitting of  $k_3$  into individual rate constants was carried out as follows: the two Sec(OH) are considered equal in reactivity (Malm et al. 1953; Kwatra et al. 1992; Tosh et al. 2000a), so that:

$$k_3 = k_{3,\text{Prim(OH)}} + 2 k_{3,\text{Sec(OH)}} \quad (4.1)$$

If the ratio  $(k_{3,\text{Prim(OH)}} / k_{3,\text{Sec(OH)}}) = \chi$ , then Eqn. 4.1 becomes:

$$k_3 = (2 + \chi) k_{3,\text{Sec(OH)}} \quad (4.2)$$

which can be solved for  $k_{3,\text{Sec(OH)}}$  if  $\chi$  is known; we considered  $\chi = (k_{3,\text{Prim(OH);CHM}} / k_{3,\text{Sec(OH); CHD}})$ . With this proviso, the rate constants and the activation parameters of the two types of hydroxyl groups of MCC have been calculated as a function of the experimental variable,  $N_c$ , and T.

Table 4.2 shows the values of  $k_3$ /OH group of the model compounds, the overall- and partial  $k_3$  for MCC, along with the corresponding activation parameters. We used  $\chi = 3.15$  as explained in detail below.

**Table 4.2:** Third order rate constants and activation parameters calculated for the acylation of cyclohexylmethanol, CHM; *trans*-1,2-cyclohexanediol, CHD, and microcrystalline cellulose, MCC, in 4.28% LiCl/DMAC<sup>a,b</sup>

Anhydride/Temperature	65 °C	75 °C	85 °C	$\Delta H^\ddagger$ , Kcal mol <sup>-1</sup>	$T\Delta S^\ddagger$ , kcal mol <sup>-1</sup>	$\Delta G^\ddagger$ , kcal mol <sup>-1</sup>
<b>CHM; <math>10^4 \times k_{3,\text{Prim(OH)}}</math>, L<sup>2</sup> mol<sup>-2</sup> s<sup>-1</sup></b>						
Ethanoic	1.137	1.471	1.871	5.30	-21.28	26.58
Propanoic	0.985	1.298	1.689	5.79	-20.87	26.66
Butanoic	0.933	1.245	1.641	6.10	-20.59	26.69
Pentanoic	1.174	1.568	2.052	6.02	-20.51	26.53
Hexanoic	1.335	1.768	2.295	5.82	-20.62	26.44
<b>CHD; <math>10^4 \times k_{3,\text{Sec(OH)}}</math>, L<sup>2</sup> mol<sup>-2</sup> s<sup>-1</sup></b>						



Anhydride/Temperature	65 °C	75 °C	85 °C	$\Delta H^\ddagger$ , Kcal mol <sup>-1</sup>	$T\Delta S^\ddagger$ , kcal mol <sup>-1</sup>	$\Delta G^\ddagger$ , kcal mol <sup>-1</sup>
Ethanoic		1.130				
Propanoic		0.917				
Butanoic		0.867				
Pentanoic		0.915				
Hexanoic		0.932				
<b>MCC, 10<sup>4</sup> x (overall k<sub>3</sub>), L<sup>2</sup> mol<sup>-2</sup> s<sup>-1</sup></b>						
Ethanoic	1.442	1.889	2.449	5.77	-20.56	26.33
Propanoic	1.278	1.731	2.314	6.54	-19.85	26.39
Butanoic	1.201	1.668	2.267	7.05	-19.44	26.49
Pentanoic	1.433	1.928	2.540	6.09	-20.10	26.19
Hexanoic	1.630	2.170	2.826	6.02	-20.28	26.30
<b>MCC; 10<sup>4</sup> x k<sub>3,prim(OH)</sub>, L<sup>2</sup> mol<sup>-2</sup> s<sup>-1</sup></b>						
Ethanoic	0.882	1.155	1.497	5.77	-20.08	25.85
Propanoic	0.781	1.058	1.415	6.54	-19.40	25.94
Butanoic	0.734	1.020	1.387	7.05	-18.93	25.98
Pentanoic	0.876	1.179	1.553	6.09	-19.77	25.86
Hexanoic	0.996	1.327	1.728	6.02	-19.71	25.77
<b>MCC, 10<sup>4</sup> x k<sub>3,sec(OH)</sub>, L<sup>2</sup> mol<sup>-2</sup> s<sup>-1</sup></b>						
Ethanoic	0.280	0.366	0.475	5.77	-20.83	26.60
Propanoic	0.248	0.336	0.449	6.54	-20.16	26.70
Butanoic	0.233	0.323	0.440	7.05	-19.69	26.74
Pentanoic	0.278	0.374	0.493	6.09	-20.53	26.62
Hexanoic	0.316	0.421	0.548	6.02	-20.51	26.53

<sup>a</sup> Except for the (overall k<sub>3</sub>) of MCC, the remaining rate constants refer to a *single* OH group.

They were calculated as follows: CHM; k<sub>3,Prim(OH)</sub> = k<sub>obs</sub>/[anhydride][LiCl]; CHD; k<sub>3,Sec(OH)</sub> =

$k_{\text{obs}}/(2x[\text{anhydride}][\text{LiCl}])$ . The values of  $k_3$  for the discrete (OH) groups of the AGU of MCC were calculated as indicated below.

<sup>b</sup> All activation parameters were calculated at 60 °C. The uncertainties in the activation parameters are  $\pm 0.1$  kcal mol<sup>-1</sup> ( $\Delta H^\ddagger$ , and  $\Delta G^\ddagger$ ) and 0.5 cal K<sup>-1</sup> mol<sup>-1</sup> ( $\Delta S^\ddagger$ ).

Considering these data, the following is relevant:

(i)- At the outset, discussion of the above data rests on the assumption that the increase in ( $\lambda$ ) as a function of (t) is due to acylation of the model compounds or cellulose proper. In order to secure this information, the kinetic experiments were repeated on a threefold scale, the produced esters were separated and their DS determined. As Table 4.3 shows, the reaction of CHM or CHD with acetic anhydride, under the conditions of the kinetic experiment produced the corresponding acetate.

**Table 4.3:** IR and <sup>1</sup>H NMR data of the reaction products of CHM and CHD under the conditions of the kinetic experiments.<sup>a</sup>

CHM				CHD			
$\tilde{\nu}$ , cm <sup>-1</sup>	Peak attribution	$\delta$ , ppm	Proton <sup>b</sup>	$\tilde{\nu}$ , cm <sup>-1</sup>	Peak attribution	$\delta$ , ppm	Proton <sup>b</sup>
2925; 2857	C-H	3.88	d, 2H	2944; 2867	C-H	4.85-4.75	m, 2H
1739	C=O, ester	2.06	s, 3H	1738	C=O, ester	2.09-2.01	m, 8H
1240	C(O)-O	1.75-1.57	m, 6H	1229	C(O)-O	1.74-1.64	m, 2H
		1.32-1.10	m, 3H			1.48-1.29	m, 4H
		1.02-0.91	m, 2H				

a- These spectral attribution agree with those published elsewhere (AIST 2001; Das et al. 2006; Khaja and Xue 2006; Zeynizadeh and Sadighnia 2010; Zeynizadeh and Sadighnia 2011).

b-The symbols (s, d, and m) refer to singlet, doublet, and multiplet, respectively

Likewise, as shown in item 3.2.4. of Experimental, acylation of MCC under the conditions of the kinetic run produced cellulose esters with DS = 2.1, 1.7, 2.5, for ethanoate, butanoate, and hexanoate, respectively. In summary, the reaction that is being followed by conductivity is the acylation of the model compounds, or MCC.

(ii)- The value of using the model compounds lies in eliminating the labor that would have been required in order to synthesize cellulose molecules specifically protected at positions C6, or C2 and C3. Even when labor is not the issue, some of these derivatives may not be suitable for the purpose. For example, the transformation (C6-OH → C6-tosylate) may be problematic because the tosylate group is labile and has been shown to be easily substituted by the acetate anion of an ionic liquid solvent (Koehler et al. 2007). The transformation (C6-OH → C6-C(C6-C(C<sub>6</sub>H<sub>5</sub>)<sub>3</sub>)) introduces steric crowding in the molecule (Kondo 1993). This may affect the reactivities at C2- and C3. The reaction of the model compounds *with each anhydride* shows that the ratio  $k_{3,\text{Prim(OH),CHM}}/k_{3,\text{Sec(OH),CHD}} > 1$ . To our knowledge, this is the first time that these ratios have been experimentally determined for an acylation reaction in SE/DAS. In LiCl/DMAC the reactivity ratios increase as a function of increasing  $N_c$ , according to the following second-degree polynomial ( $r^2$  = correlation coefficient), given in Eq. 4.3:

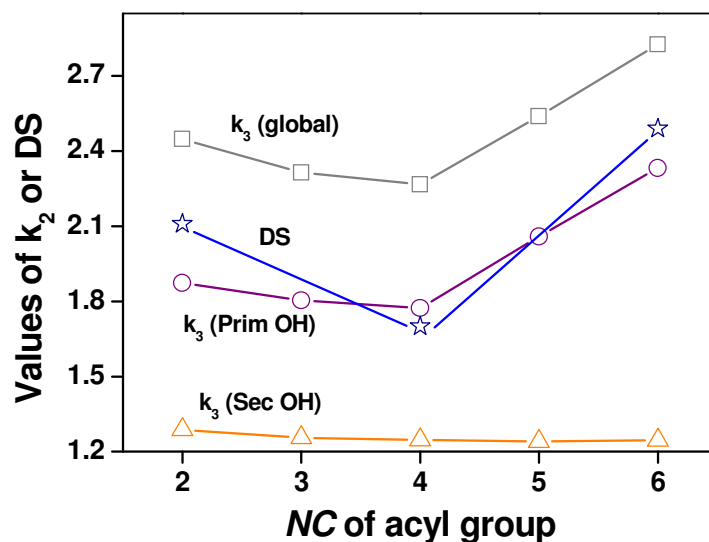
$$k_{3,\text{Prim(OH),CHM}}/k_{3,\text{Sec(OH),CHD}} = 1.354 - 0.078 N_c + 0.028 (N_c)^2; \quad r^2 = 0.971; \quad \text{sd} = 0.059 \quad (4.3)$$

Therefore, the outcome of the reaction, in terms of the substitution degree at C6- and C2 plus C3 depends on the derivatizing agent; *the preference for the C6 position increases as a function of increasing the molecular volume of the reagent*. This agrees with the known fact that it is possible to functionalize cellulose almost exclusively at the C6 position by voluminous reagents, e.g., the trityl group (Kondo 1993);

(iii) We now address the value of ( $\chi$ ). At the outset, we stress that the best ratio to be used is that based on the reaction of *cellulose* protected at C6 (to determine the reactivity at C2 and C3 of the AGU), and at (C2 + C3) to determine the reactivity at C6. As the synthesis of these cellulose derivatives is laborious, we decided to use model compounds and literature data. Depending on the solvent system employed in our study, the values of ( $\chi$ ) ranged from 1.3 to

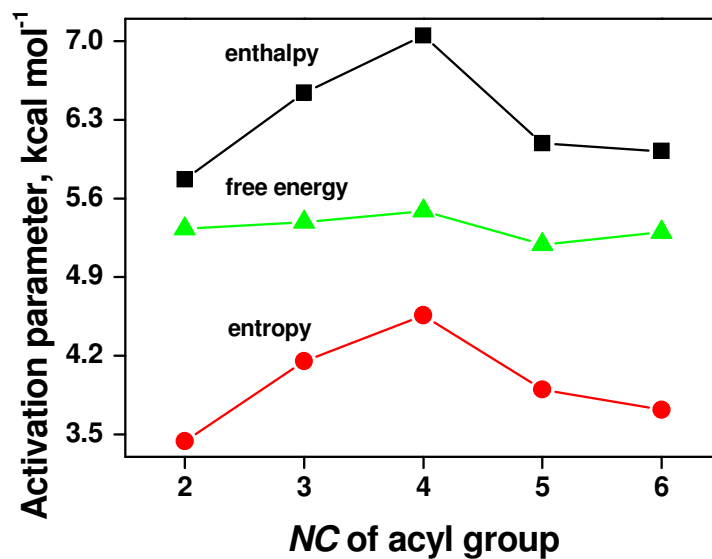
1.8. On the other hand, published data on the *heterogeneous* reactions of cellulose indicate larger difference in reactivity, e.g.,  $4 \pm 1$  for acetylation (Malm et al. 1953); 5 for acylation by palmitoyl chloride under reduced pressure (Kwatra et al. 1992); 5.8 for tosylation by tosyl chloride in pyridine (Heuser et al. 1950), and 4.3 for etherification by the sterically crowded tris(*p*-tolyl)chloromethane (Jain et al. 1985). A possible reason for the difference is that the acylation of CHM and CHD has been carried out under homogenous conditions, where the hydroxyl groups are readily accessible. This is not the case for the OH groups of cellulose under heterogeneous conditions. Additionally, cellulose solutions in LiCl/DMAC in the concentration employed in the kinetic study are not molecularly dispersed, but present as aggregates (Ramos et al. 2011), whose hydroxyl groups are less accessible than those of the model compounds. This difference in accessibility should result in larger  $k_{3,Prim(OH),MCC}/k_{3,Sec(OH),MCC}$ , as compared with  $k_{3,Prim(OH),CHM}/k_{3,Sec(OH),CHD}$ . Therefore, the lower limit of ( $\chi$ ) is 1.30, the upper is 5, we used the arithmetic mean 3.15 to split the results, resulting in the values reported in Table 4.2. This ratio is arbitrary, its value will affect the individual rate constants but not  $\Delta H^\ddagger$ . Its effect on  $T\Delta S^\ddagger$  and  $\Delta G^\ddagger$  is small  $\leq 0.3$  kcal/mol. That is, the ratio employed will not affect the validity of our conclusions (based on activation parameters) about the reason of differences of reactivity in the different solvent systems.

(iv)- The results obtained show a clear parallelism between the dependence on  $N_c$  of both the rate constants and DS of the synthesized esters as shown in Figure 4.3 . Figures 4.3 and 4.26 show the important fact that the *same dependence of DS on  $N_c$  is observed, independent of the medium, strong electrolyte/dipolar aprotic solvent or ionic liquid, or the method of heating, conventional (thermal) or by using microwaves.*



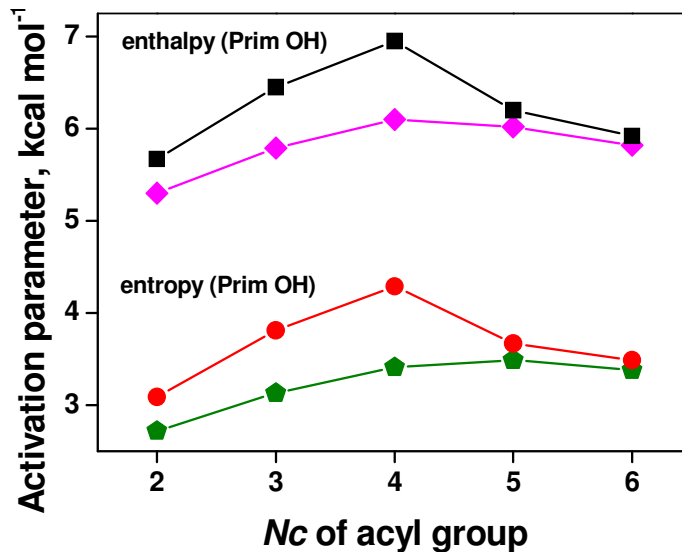
**Figure 4.3:** Dependence on the number of carbon atoms of the acyl group,  $N_c$  of the discrete rate constants at 85 °C or DS. Figure legend:  $\square$ ,  $\star$ ,  $\circ$ , and  $\triangle$  refer to overall  $k_3$ , DS,  $k_3$  Prim, and  $k_3$  Sec, respectively. For ease of visualization, we have plotted  $(k_2 \text{ Sec} + 1)$ ; all  $(T\Delta S^\ddagger + 24)$  and  $(\Delta G^\ddagger - 21)$ , in Figure 4.3, 4.4 and 4.5 respectively.

Figure 4.4 below shows the dependence on  $N_c$  of the activation parameters. The variations are admittedly small, but point out to a trend. Thus  $\Delta G^\ddagger$  slightly increases then decreases, due to a complex dependence of  $\Delta H^\ddagger$  and  $T\Delta S^\ddagger$  on this structural variable. The increase in  $\Delta H^\ddagger$  on going from ethanoic- to butanoic anhydride may be related to the decrease in the electrophilicity of the acyl group, due to the slight increase in the pKa of the corresponding carboxylic acid. The subsequent decrease in  $\Delta H^\ddagger$  on going from butanoic- to hexanoic anhydride may be related to favorable hydrophobic interactions between the carbon chains of the anhydride and cellulosic surface, whose lipophilicity has increased, due to its partial acylation. Surprisingly, the  $T\Delta S^\ddagger$  term increases on going from ethanoic- to butanoic anhydride, and then decreases. These cancellation effects lead to the subtle, but persistent variations of  $\Delta G^\ddagger$  as a function of increasing  $N_c$ .



**Figure 4.4:** Dependence on the number of carbon atoms of the acyl group and the activation parameters calculated for the overall  $k_3$ ; Figure legend:  $\blacksquare$ ,  $\blacktriangle$ , and  $\bullet$  stand for  $\Delta H^\ddagger$ ,  $\Delta G^\ddagger$ , and  $T\Delta S^\ddagger$ , respectively.

Finally, Figure 4.5 shows the parallelism between the activation parameters of the model compound and the C6-OH group of the biopolymer. This parallelism is satisfying because it can be taken to indicate that CHM, and most certainly CHD are representative models for the reactivities of the discrete OH groups of cellulose.



**Figure 4.5:** Dependence on the number of carbon atoms of the acyl group and the enthalpies ( $\Delta H^\ddagger$ , CHM), ( $\Delta H^\ddagger$ , MCC, Prim(OH)), and entropy terms ( $T\Delta S^\ddagger$ , CHM), ( $T\Delta S^\ddagger$ , MCC, Prim(OH)) for the model compound and the C6-OH group of cellulose, respectively, Figure legend: ■, ◆, ●, and ▽ apply to  $\Delta H^\ddagger$ , MCC, Prim(OH);  $\Delta H^\ddagger$ , CHM;  $T\Delta S^\ddagger$ , MCC, Prim(OH); and  $T\Delta S^\ddagger$ , CHM, respectively.

In summary, conductivity is a convenient technique to study the kinetics of cellulose derivatization, especially when the reaction is carried out under pseudo-first-order conditions. Model compounds (CHM, CHD) has been successfully applied to compare the reactivity and selectivity of prim (OH) and sec (OH) for cellulose. The selectivity for C6-OH increases as a function of increasing  $N_c$ . The kinetic results are satisfying because they show a parallelism between the effect of  $N_c$  on either the rate constants or the DS of esters synthesized.

### 4.3. Cellulose acetylation in IL-DAS

#### 4.3.1: Reaction order and product isolation

Depending on the concentration of IL, it is possible to consider cellulose acylation in IL/DAS as a variety of acylation in SE/DAS; IL is the “strong electrolyte”. The acylation reaction has been studied in IL mixed with four molecular solvents, namely, DMAC, MeCN, DMSO and Sulfolane. As given in Experimental section 3.4.5, we have carried out the kinetic runs under pseudo-first-order conditions, with the following molar concentration ratios:  $(\text{Ac}_2\text{O}/\text{cellulose}) = 11.44$ ;  $(\text{IL}/\text{cellulose}) = 20.41$  to  $40.93$  (DMAC),  $28.6$  to  $40.9$  (MeCN),  $10.89$  to  $17.02$  (DMSO) and  $13.61$  to  $23.82$  (sulfolane). Additionally, as shown in experimental, the reaction under study in the kinetic runs is acylation of cellulose. Excellent linear plots were observed for  $\ln(\lambda_\infty - \lambda_t)$  versus  $(t)$  in all cases, showing that the reaction is first order in cellulose, see Figures 4.6 and in appendix Table 7.1. Values of  $k_3$  were then calculated from  $k_3 = k_{\text{obs}}/[\text{Ac}_2\text{O}][\text{IL}]$ .

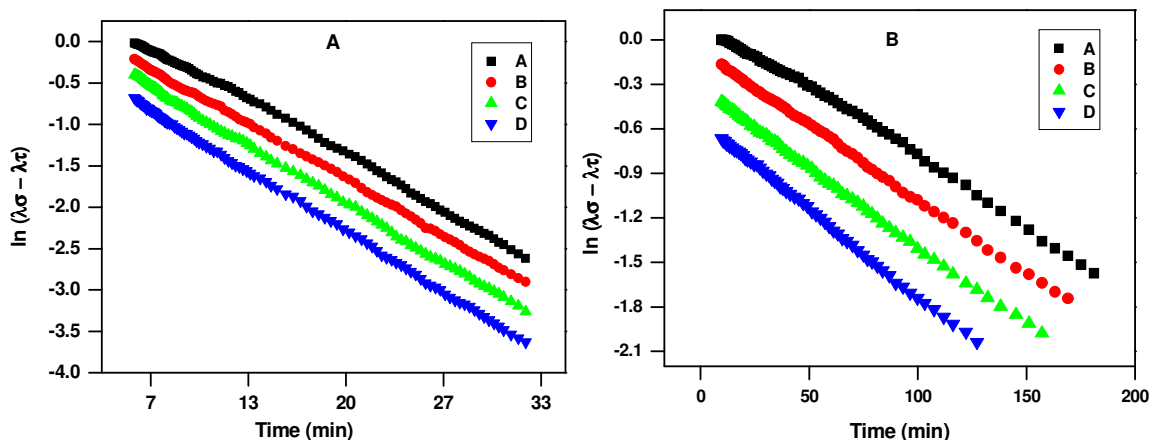


**Figure 4.6:** Plots for calculation of the pseudo first-order rate constant ( $k_{\text{obs}}$ ) for the reaction in mixtures IL-DAS. The symbols ( $\lambda_\infty$ ) and ( $\lambda_t$ ) refer to the conductivity at “infinity”- and any time ( $t$ ), respectively. Part (A) is for AIMeImCl-DMAC at  $[\text{IL}] = 1.887$  mol/L, and  $T$  (from bottom up) =  $30, 40, 50,$  and  $60$  °C, respectively. Part (B) is for AIMeImCl-MeCN at  $[\text{IL}] = 3.025$  mol/L, and  $T$  (from bottom up) =  $30, 40, 50,$  and  $60$  °C, respectively.

Surprisingly, for mixtures of the IL with each DAS, the values of ( $k_3$ ) were found to increase linearly as a function of  $[\text{IL}]$  as shown in Figure 4.7 below, and in appendix Tables 7.1,



7.2, 7.3 and 7.4. This dependence is not restricted to MCC, it has also been observed for CHM and CHD, as shown in Figure 4.8 below, and in appendix Figure 7.2.

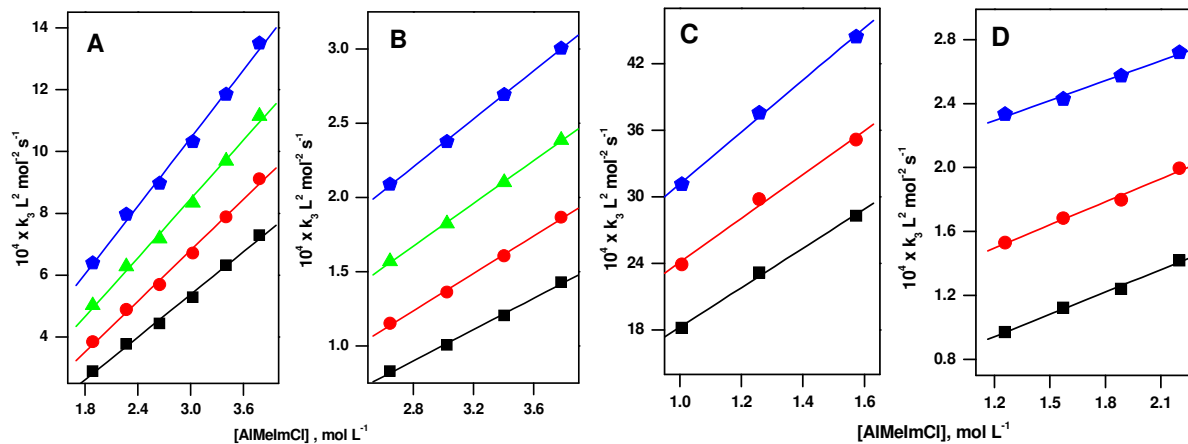


**Figure 4.7:** Dependence of overall  $k_3$  on [IL] in the systems IL-DMAC (part A); IL-MeCN (part B); IL-DMSO (part C), and IL-sulfolane (part D). Symbols  $\blacksquare$ ,  $\bullet$ ,  $\blacktriangle$ , and  $\blacklozenge$ , are for  $k_3$  at 30, 40, 50, 60 °C, for (part A and B), 40, 50, 60 °C (part C) and 50, 60, 70 °C (part D), respectively.

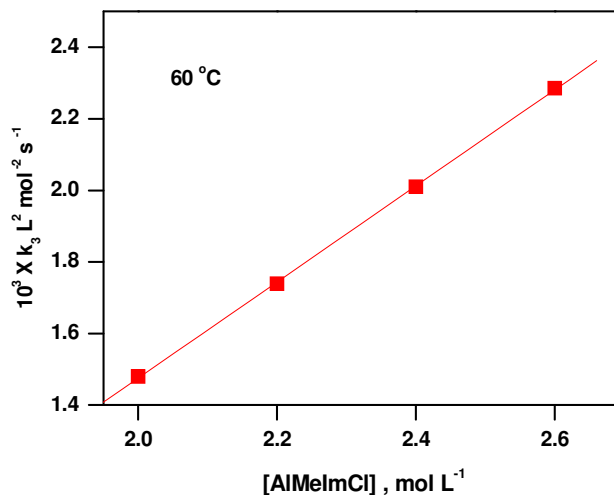


**Figure 4.8:** Relationship between  $k_3$  and molar concentration of ionic liquid for the acetylation of CHM in binary mixtures of AlMelmCl with DMAC at 60 °C.

We advance several reasons to explain this result:

- The IL is present as aggregate in the binary solvent mixture.

The results of several experimental techniques, including FTIR, (Jiang et al. 2011) conductivity (Bester-Rogac et al. 2011) and NMR spectroscopy (Hesse-Ertelt et al. 2010; Ananikov 2011) have indicated the association of ILs in several DAS. Thus, higher kinetic order in [IL] is not unexpected;

- The biopolymer is solvated by the IL, via hydrogen bonding and dipolar interactions.

The above-mentioned techniques, as well as cellulose solubility measurements and theoretical calculations have clearly indicated the strong interactions of cellulose-IL/DAS (El Seoud et al. 2007; Sashina et al. 2008; Pinkert et al. 2009; Arvela et al. 2010; Gericke et al. 2012). It is more likely, therefore, that cellulose is reacting as (cellulose-IL) hydrogen-bonded species, akin to the alcohol-IL complexes (Crosthwaite et al. 2005; Makowska et al. 2010) and water-IL complexes (Sato et al. 2012); this leads to the dependence of ( $k_3$ ) on [IL]. This explanation is similar to that advanced to explain a similar kinetic behavior in nucleophilic aromatic substitution reactions (aminolysis) in aprotic solvents; Figure 4.9. The formation of the zwitterionic ( $\sigma$ -complex) is third order because the 2,4-dinitrohalobenzene reacts with amine dimer. The decomposition of this complex is rate-limiting, and is catalyzed by amine, so that  $k_3$  is first order in [amine]. (Alvaro et al. 2010).

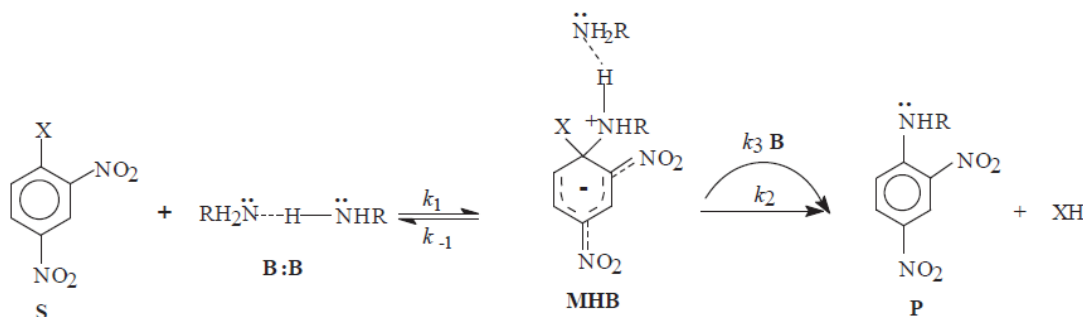


**Figure 4.9:** The “dimer nucleophilic mechanism” employed to explain the dependence of  $k_3$  on [amine] for the  $\text{Nu}_{\text{Ar}}\text{S}$  reaction of 2,4-dinitrohalo(chloro or fluoro)benzene in aprotic solvents. (Alvaro et al. 2010).

In order to corroborate the formation of (IL⋯AGU) hydrogen bonding, we have examined the systems by FTIR. Due to solubility problems, we used CHM (DMAC and MeCN) or cellobiose (DMSO and sulfolane) as models for the AGU. The stretching frequency of the hydroxyl group,  $\nu_{\text{OH}}$ , of 0.3 mol/L solution of CHM decreased from 3433 to 3416  $\text{cm}^{-1}$  in the presence of 0.086 mol/L IL; the corresponding figures for MeCN are 3538 and 3535  $\text{cm}^{-1}$ , respectively. For IL/DMSO and IL/Sulfolane the solution compositions employed are listed in appendix Table 7.5. As Figure 4.10 shows, there is a linear decrease of  $\nu_{\text{OH}}$  as a function of increasing [IL]. This can be attributed to the formation of hydrogen bonding, e.g., of the type (Cl-.....HO-Cell).

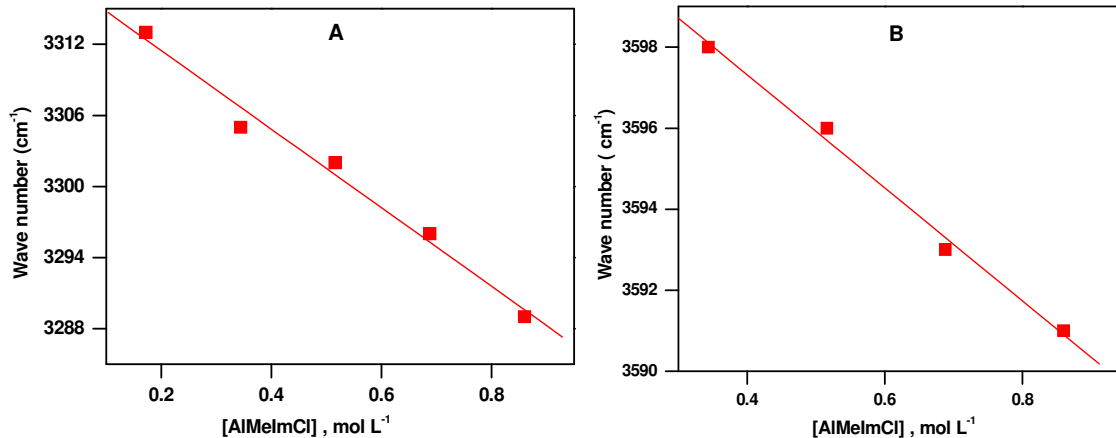


**Figure 4.10:** Graph between [IL] and wave number of Cellobiose ( $\text{cm}^{-1}$ ): A) in IL-DMSO, B) in IL/Sulfolane.

We have also used conductivity in order to probe the IL-cellulose hydrogen bonding. As shown in Figures 4.11 and 4.12; in most cases, the dependence of ( $\lambda$ ) on [IL] is linear; for the same IL concentration, the value of  $\lambda_{(\text{IL}/\text{DAS})} > \lambda_{(\text{MCC-IL}/\text{DAS})}$ , probably because the mobility of the free chloride ion of the IL is larger than that of the Cl<sup>-</sup>⋯H-O-AGU. Therefore, both FTIR and conductivity indicate that cellulose is reacting as a hydrogen-bonded species to the IL, i.e., the kinetic equation is given by:

$$k_{\text{obs}} = k_3 [\text{Cellulose-IL}][\text{IL}][\text{Anhydride}] \quad (4.4)$$

in agreement with Figure 4.7.

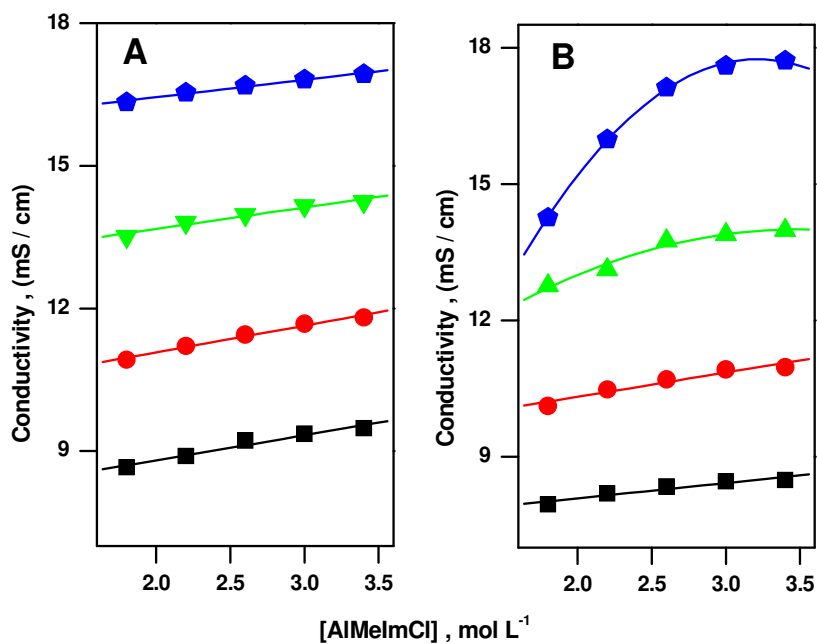


**Figure 4.11:** Dependence of solution conductivity on [IL] in the systems IL-DMAC (part A) and MCC-IL-DMAC (part B) in the presence of a fixed concentration of MCC, 0.0924 mol/L. Symbols ■, ●, ▲ and ◆ shows conductivity at 30, 40, 50 and 60 °C respectively.

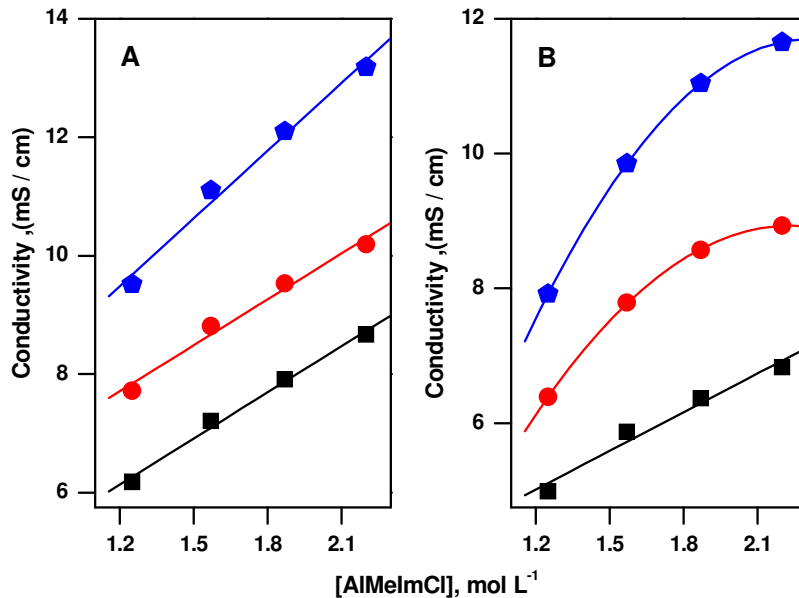


**Figure 4.12:** Dependence of solution conductivity on [IL] in the systems IL-Sulfolane (part A) and MCC-IL-Sulfolane (part B) in the presence of a fixed concentration of MCC, 0.0924 mol/L. Symbols ■, ●, and ◆ shows conductivity at 50, 60 and 70 °C respectively.

#### 4.3.2. Dependence of the kinetic data on the nature of the molecular solvents

Table 4.4 shows the dependence of ( $k_3$ ) on (T) for the reaction in IL-DAS. For comparison, we have also calculated (by extrapolation where needed) the values  $k_3$  and activation parameters at the same electrolyte concentration, LiCl or IL, and report the data in Table 4.5. From the former Table it is clear that the molecular liquid affects the rates of the reaction, the order is IL-DMSO > IL-DMAC > IL-sulfolane > IL-MeCN.

**Table 4.4:** Overall and partial third order rate constants  $k_3$ , and activation parameters calculated for the acetylation of microcrystalline cellulose in binary mixtures of AlMelmCl with: DMAC, MeCN, DMSO and sulfolane.<sup>a,b,c,d,e,f</sup>

(IL), mol/L/ Temperature	30 °C	40 °C	50 °C	60 °C	$\Delta H^\ddagger$ , kcal mol <sup>-1</sup>	$T\Delta S^\ddagger$ , kcal mol <sup>-1</sup>	$\Delta G^\ddagger$ , kcal mol <sup>-1</sup>
<i>Acetylation in IL-DMAC</i>							
$10^4 \times (\text{overall } k_3), \text{ L}^2 \text{ mol}^{-2} \text{ s}^{-1}$							
1.887	2.897	3.847	5.024	6.392	4.64	-19.79	24.44
2.269	3.775	4.891	6.283	7.968	4.33	-19.95	24.30
2.647	4.436	5.696	7.185	8.973	4.04	-20.16	24.22
	(5.36) <sup>c</sup>	(4.95) <sup>c</sup>	(4.58) <sup>c</sup>	(4.30) <sup>c</sup>			
3.025	5.286	6.712	8.337	10.32	3.80	-20.31	24.12
	(5.25) <sup>c</sup>	(4.93) <sup>c</sup>	(4.58) <sup>c</sup>	(4.34) <sup>c</sup>			
3.404	6.320	7.882	9.695	11.85	3.53	-20.48	24.03
	(5.25) <sup>c</sup>	(4.91) <sup>c</sup>	(4.61) <sup>c</sup>	(4.40) <sup>c</sup>			
3.782	7.293	9.114	11.15	13.50	3.45	-20.53	23.94
	(5.10) <sup>c</sup>	(4.89) <sup>c</sup>	(4.68) <sup>c</sup>	(4.49) <sup>c</sup>			
$10^4 \times k_{3, \text{Prim(OH)}}, \text{ L}^2 \text{ mol}^{-2} \text{ s}^{-1}$							
1.887	1.772	2.353	3.072	3.909	4.64	-20.13	24.77
2.269	2.309	2.991	3.843	4.873	4.34	-20.29	24.62
2.647	2.713	3.484	4.394	5.488	4.04	-20.51	24.55
3.025	3.233	4.105	5.099	6.312	3.80	-20.65	24.45
3.404	3.865	4.821	5.930	7.248	3.54	-20.82	24.36
3.782	4.460	5.574	6.819	8.257	3.45	-20.82	24.27
$10^4 \times k_{3, \text{Sec(OH)}}, \text{ L}^2 \text{ mol}^{-2} \text{ s}^{-1}$							
1.887	0.562	0.746	0.975	1.241	4.64	-20.89	25.53
2.269	0.733	0.949	1.220	1.547	4.34	-21.05	25.38
2.647	0.861	1.106	1.395	1.742	4.05	-21.26	25.30
3.025	1.026	1.303	1.618	2.003	3.80	-21.41	25.21

3.404	1.227	1.530	1.882	2.301	3.54	-21.58	25.12
3.782	1.416	1.769	2.165	2.621	3.45	-21.58	25.03
<b>Acetylation in IL-MeCN</b>							
<b><math>10^4 \times (\text{overall } k_3), \text{ L}^2 \text{ mol}^{-2} \text{ s}^{-1}</math></b>							
(IL), M/ Temperature	30 °C	40 °C	50 °C	60 °C	$\Delta H^\ddagger,$ kcal mol <sup>-1</sup>	$T\Delta S^\ddagger,$ kcal mol <sup>-1</sup>	$\Delta G^\ddagger,$ kcal mol <sup>-1</sup>
2.647	0.828	1.151	1.569	2.088	5.53 (1.49) <sup>e</sup>	-19.64 (0.52)	25.18 (0.96)
3.025	1.006	1.362	1.822	2.375	5.09 (1.29) <sup>e</sup>	-19.99 (0.32)	25.09 (0.97)
3.404	1.204	1.606	2.101	2.692	4.72 (1.19) <sup>e</sup>	-20.27 (0.21)	25.01 (0.98)
3.782	1.428	1.865	2.385	3.004	4.31 (0.86) <sup>e</sup>	-20.42 (0.11)	24.94 (1.00)
<b><math>10^4 \times k_{3, \text{Prim(OH)}}, \text{ L}^2 \text{ mol}^{-2} \text{ s}^{-1}</math></b>							
2.647	0.506	0.704	0.959	1.27	5.53	-19.98	25.51
3.025	0.615	0.833	1.11	1.45	5.10	-20.33	25.42
3.404	0.736	0.982	1.28	1.64	4.72	-20.62	25.34
3.782	0.873	1.14	1.45	1.83	4.31	-20.96	25.27
<b><math>10^4 \times k_{3, \text{Sec(OH)}}, \text{ L}^2 \text{ mol}^{-2} \text{ s}^{-1}</math></b>							
2.647	0.160	0.223	0.304	0.405	5.53	-20.74	26.27
3.025	0.195	0.264	0.353	0.461	5.10	-21.09	26.18
3.404	0.233	0.311	0.407	0.522	4.72	-21.38	26.10
3.782	0.277	0.362	0.463	0.583	4.31	-21.72	26.03

(IL), mol/L/ Temperature	40 °C	50 °C	60 °C	$\Delta H^\ddagger,$ kcal mol <sup>-1</sup>	$T\Delta S^\ddagger,$ kcal mol <sup>-1</sup>	$\Delta G^\ddagger,$ kcal mol <sup>-1</sup>
<b>Acetylation in IL-DMSO</b>						
<b><math>10^3 \times (\text{overall } k_3), \text{ L}^2 \text{ mol}^{-2} \text{ s}^{-1}</math></b>						
1.007	1.820	2.392	3.113	4.95	-18.44	23.39
1.258	2.317	2.980	3.758	4.36	-18.91	23.27
	(23.8) <sup>d</sup>	(19.4) <sup>d</sup>	(16.1) <sup>d</sup>			
1.573	2.829	3.516	4.443	4.01	-19.14	23.15
	(25.2) <sup>d</sup>	(20.9) <sup>d</sup>	(18.3) <sup>d</sup>			

$10^3 \times k_{3, \text{Prim(OH)}}, \text{L}^2 \text{mol}^{-2} \text{s}^{-1}$						
1.007	1.113	1.463	1.904	4.95	-18.81	23.76
1.258	1.417	1.822	2.298	4.36	-19.23	23.59
1.573	1.730	2.150	2.717	4.01	-19.49	23.50
$10^3 \times k_{3, \text{Sec(OH)}}, \text{L}^2 \text{mol}^{-2} \text{s}^{-1}$						
1.007	0.353	0.464	0.604	4.95	-19.56	24.51
1.258	0.449	0.578	0.729	4.36	-19.98	24.34
1.573	0.549	0.682	0.862	4.01	-20.22	24.23
<i>Acetylation in IL-Sulfolane</i>						
$10^4 \times (\text{overall } k_3), \text{L}^2 \text{mol}^{-2} \text{s}^{-1}$						
(IL), M/ Temperature	50 °C	60 °C	70 °C	$\Delta H^\ddagger,$ kcal mol <sup>-1</sup>	$T\Delta S^\ddagger,$ kcal mol <sup>-1</sup>	$\Delta G^\ddagger,$ kcal mol <sup>-1</sup>
1.258	0.971	1.530	2.334	9.01 (4.65) <sup>f</sup>	-16.49 (2.42) <sup>f</sup>	25.50 (2.23) <sup>f</sup>
1.573	1.123	1.683	2.429	7.84 ( 3.83)	-17.26 (1.88) <sup>f</sup>	25.10 (1.60) <sup>f</sup>
1.887	1.240	1.798	2.573	6.94	-17.90	24.84
2.201	1.420	1.995	2.721	6.50	-18.71	24.21
$10^4 \times k_{3, \text{Prim(OH)}}, \text{L}^2 \text{mol}^{-2} \text{s}^{-1}$						
1.258	0.593	0.935	1.427	9.01	-16.69	25.70
1.573	0.686	1.029	1.485	7.84	-17.79	25.63
1.887	0.758	1.099	1.573	6.94	-18.64	25.58
2.201	0.868	1.220	1.664	6.50	-19.02	25.52
$10^5 \times k_{3, \text{Sec(OH)}}, \text{L}^2 \text{mol}^{-2} \text{s}^{-1}$						
1.258	0.188	0.297	0.453	9.01	-17.43	26.44
1.573	0.218	0.326	0.471	7.84	-18.58	26.42
1.887	0.240	0.349	0.499	6.94	-18.95	25.89
2.201	0.275	0.387	0.528	6.50	-19.76	26.26

a-Except for the overall  $k_3$  of MCC, the remaining rate constants refer to a *single* OH group. The values of  $k_3$  for the discrete (OH) groups of the AGU of MCC were calculated as indicated in the text, i.e.,  $k_3 = k_{3, \text{Prim(OH)}} + 2 k_{3, \text{Sec(OH)}}$  and  $k_{3, \text{Prim(OH)}} / k_{3, \text{Sec(OH)}} = 3.15$



b- All activation parameters were calculated at 60 °C. The uncertainties in the activation parameters are  $\pm 0.1$  kcal mol<sup>-1</sup> ( $\Delta H^\ddagger$ , and  $\Delta G^\ddagger$ ) and 0.5 cal K<sup>-1</sup> mol<sup>-1</sup> ( $\Delta S^\ddagger$ ).

c- The numbers within parenthesis refer to: (overall  $k_3$  IL-DMAC/overall  $k_3$  IL-MeCN), at the same [IL].

d- The numbers within parenthesis refer to: (overall  $k_3$  IL-DMSO/overall  $k_3$  IL-Sulfolane), at the same [IL].

e- The numbers within parenthesis refer to: ( $\Delta\Delta H^\ddagger = \Delta H^\ddagger$  IL-MeCN -  $\Delta H^\ddagger$  IL-DMAC); ( $\Delta T\Delta S^\ddagger = T\Delta S^\ddagger$  IL-MeCN -  $T\Delta S^\ddagger$  IL-DMAC), and ( $\Delta\Delta G^\ddagger = \Delta G^\ddagger$  IL-MeCN -  $\Delta G^\ddagger$  IL-DMAC), at the same [IL].

f- The numbers within parenthesis refer to: ( $\Delta\Delta H^\ddagger = \Delta H^\ddagger$  IL-Sulfolane -  $\Delta H^\ddagger$  IL-DMSO); ( $\Delta T\Delta S^\ddagger = T\Delta S^\ddagger$  IL-Sulfolane -  $T\Delta S^\ddagger$  IL-DMSO), and ( $\Delta\Delta G^\ddagger = \Delta G^\ddagger$  IL-Sulfolane -  $\Delta G^\ddagger$  IL-DMSO), at the same [IL].

**Table 4.5:** Rate Constants (overall  $k_3$ ) and activation parameters for the acetylation of MCC in LiCl-DMAC; IL-DMAC, IL-MeCN, IL-DMSO and IL-Sulfolane <sup>a,b,c</sup>

Reaction medium; $k_3$ , L <sup>2</sup> mol <sup>-2</sup> s <sup>-1</sup> / T	40 °C	50 °C	60 °C	$\Delta H^\ddagger$ , <sup>d</sup> kcal mol <sup>-1</sup>	$T\Delta S^\ddagger$ , <sup>d</sup> kcal mol <sup>-1</sup>	$\Delta G^\ddagger$ , <sup>d</sup> kcal mol <sup>-1</sup>
LiCl/DMAC	0.675	0.928	1.250	5.72	-19.80	25.52
IL/DMAC	1.346	2.150	3.139	5.41	-19.39	24.80
IL/MeCN	0.104	0.378	0.751	7.26	-18.55	25.82
IL/DMSO	18.20	23.92	31.13	4.95	-18.44	23.39
IL/Sulfolane	0.270	0.851	1.404	9.53	-15.90	25.43

a- At a constant electrolyte concentration of 1.007 mol/L.

b- All rate constants should be multiplied by 10<sup>-4</sup>.

c- The values in this table are extrapolated from dependence of the activation parameter on [IL] using data from Table 4.2 and 4.4 shown above.

d- Activation parameters were calculated for the reaction at 60 °C. The uncertainties in the activation parameters are  $\pm 0.05$  kcal mol<sup>-1</sup> ( $\Delta H^\ddagger$ , and  $\Delta G^\ddagger$ ) and 0.2 cal K<sup>-1</sup> mol<sup>-1</sup> ( $T\Delta S^\ddagger$ ).

A rationale for effect of the DAS can be reached by examining the differences between the activation parameters, e.g., for the pair IL-DMAC and IL-MeCN. These are listed in Table 4.4, as the difference ( $\Delta\Delta$  activation parameter = activation parameter for IL/MeCN – that for IL-DMAC). Consider first  $\Delta\Delta H^\ddagger$ ; all differences are positive, i.e., the reaction in IL-DMAC has a lower enthalpy of activation, ranging from 0.86 to 1.49 kcal/mol. As usual for associative reactions (cellulose-IL/DAS-acid anhydride) there is a decrease in the degrees of freedom in going from reagent- to the transition state, i.e., the  $T\Delta S^\ddagger$  term is negative (Bruice 2006). Although all  $\Delta T\Delta S^\ddagger$  are positive (the entropy term for the reaction in IL-MeCN is more favorable) their *absolute* values are smaller than those of  $\Delta\Delta H^\ddagger$ . That is, the reaction in IL-DMAC is faster due to gain in activation enthalpy, not compensated by loss in the  $T\Delta S^\ddagger$  term. As an example, consider the reaction in the presence of 2.647 mol/L IL. It is faster in IL-DMAC because  $\Delta G^\ddagger$  is lower by 0.96 kcal/mol, due to gain in  $\Delta H^\ddagger$  (1.49 kcal/mol) and loss in  $T\Delta S^\ddagger$  (0.52 kcal/mol). The same trend in activation parameters have been observed for IL/DMSO and IL/Sulfolane solvent mixture. Figure 4.13 summarizes the *differences* between the activation parameters, calculated at 60 °C as a function of [IL].

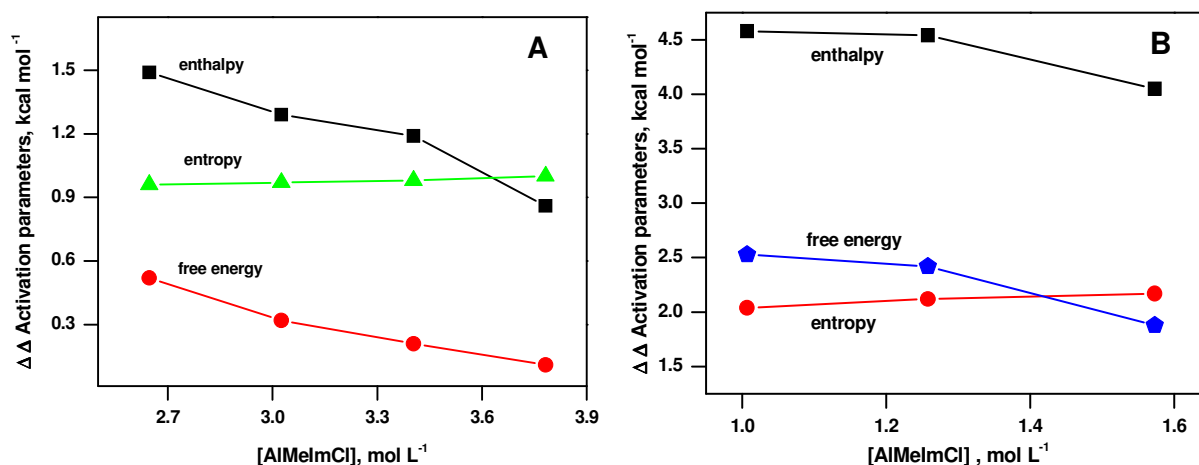


**Figure 4.13:** part A): Dependence of the difference in activation parameters on [IL]. The symbols are: ■ ( $\Delta H^\ddagger$  IL/MeCN -  $\Delta H^\ddagger$  IL/DMAC), ▲ ( $\Delta G^\ddagger$  IL/MeCN -  $\Delta G^\ddagger$  IL/DMAC) and ● ( $T\Delta S^\ddagger$  IL/MeCN -  $T\Delta S^\ddagger$  IL/DMAC). part B): ■ ( $\Delta H^\ddagger$  IL/Sulfolane -  $\Delta H^\ddagger$  IL/DMSO), ◆ ( $\Delta G^\ddagger$  IL/Sulfolane -  $\Delta G^\ddagger$  IL/DMSO) and ● ( $T\Delta S^\ddagger$  IL/Sulfolane -  $T\Delta S^\ddagger$  IL/DMSO).

The above discussion explains the difference in reactivity in terms of activation parameters, but does not explain the reason for the difference in activation parameters. In order to address this point we have to look into the macroscopic and microscopic parameters of the molecular solvents, since the IL is constant. We also have to consider the interactions between IL-molecular solvent, and cellulose-IL-molecular solvent. We start with the macroscopic parameters shown in Table 4.6 (dipole moment,  $\mu$ , relative permittivity (or dielectric constant,  $\epsilon$ ), and viscosity,  $\eta$ ).

**Table 4.6:** Physical properties of various dipolar aprotic solvents used in kinetic study at 25 °C.

solvent	dipole moment, $\mu$	dielectric constant, $\epsilon$	viscosity, cP
DMAC	3.72	37.8	2.14
DMSO	3.96	46.7	2.0
MeCN	3.84	37.5	0.34
Sulfolane	4.69	43.4	10.35

The reasons for the importance of these parameters are: the transition state of the reaction is more polar than the reagents, so that solvents that are themselves dipolar, and that can separate charges (i.e., with high  $\mu$  and  $\epsilon$ ), favor the reaction by stabilizing the transition state. On the other hand, the diffusion coefficients of the reactants in solution depends inversely on  $\eta$ , according to the Einstein-Stokes equation ((Berry et al. 2000). Therefore, less viscous solvents favor the reaction. As shown in Table 4.6 the only macroscopic property that is in agreement with the above-shown order of reactivity is viscosity; this is probably contributing to the slow reaction in sulfolane.

Table 4.6 is for pure molecular solvents. We have determined the rheology of the pure IL as well as solutions of MCC in these mixtures. Figure 4.14 shows representative rheology plot (shear stress as a function of shear rate) of IL-DMSO. The plot is linear which means that it is showing a Newtonian behavior.

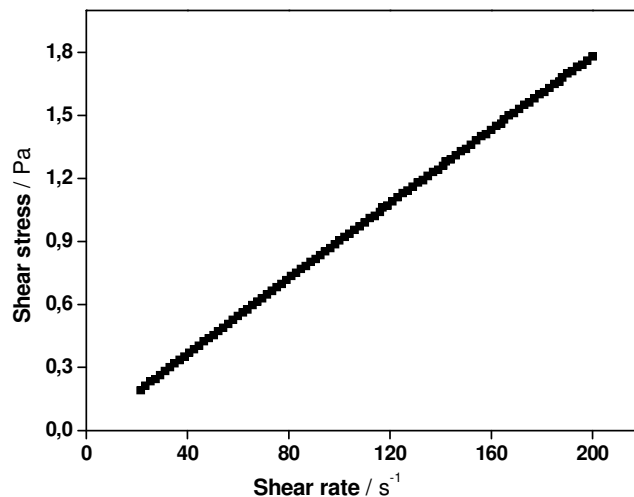


**Figure 4.14:** Representative rheology plot (shear stress as a function of shear rate) in 1.573 mol/L IL-DMSO at 40 °C.

All further experiments were carried out at a constant shear rate of 40 s<sup>-1</sup>. Figure 4.15 show a typical Arrhenius plot ( $\ln \eta$  at 40 s<sup>-1</sup> versus 1/T) whose slope is the activation energy (E) divided by gas constant (R) for viscous flow; values of these energies are shown in Table 4.7. Energies of flow, i.e., the energy necessary to make the layers of the liquid flow past each other, viscous liquids are associated with large  $E_{\text{flow}}$ . Table 7.6 in appendix lists the values of  $\eta$  as a function of T for all systems investigated. Table 4.7 shows that  $E_{\text{flow}}$  for the *pure* IL is more than double the  $E_{\text{flow}}$  of MCC solutions in IL/DAS. Among the latter solutions,  $E_{\text{flow}}$  is largest for MCC-IL-sulfolane. Therefore, pure sulfolane is more viscous than other molecular solvents. Likewise, MCC-IL-sulfolane is more viscous than MCC in the remaining IL-DAS, in agreement with our previous conclusion that higher viscosity of this system affects adversely the reactivity of the biopolymer.

Table 4.6, however, shows that other macroscopic properties cannot be employed for explaining the differences in reactivity. For example,  $\mu$  and  $\epsilon$  of sulfolane are highest among the solvents employed;  $\epsilon$  of DMAC and MeCN are practically the same. The fact that the effect of solvent on reactivity is not correlated with macroscopic properties is not surprising. This is because solute-solvent interactions are much more influenced by specific interactions,

including dipolar interactions, dispersion forces (van der Waals interactions) and hydrogen bonding, these are better represented by microscopic, i.e., solvatochromic, solvent parameters.

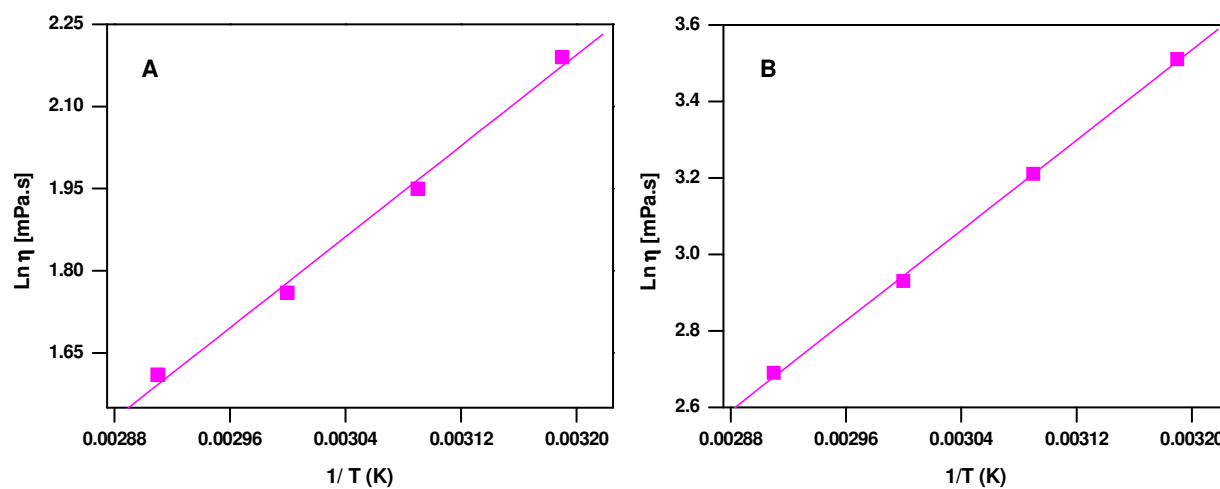


**Figure 4.15:** Typical Arrhenius plot ( $\ln \eta$  versus  $1/T$  at  $40 \text{ s}^{-1}$ ); (A) in 1.573 mol/L, MCC-IL-DMSO (B) in 1.573 mol/L, MCC-IL-Sulfolane, at 40-70 °C respectively.

**Table 4.7:** Energies of flow of pure IL and its solution with MCC and various DAS.

Solvent system (mol/L)	Activation energy (kJ/mol)
AlMelmCl (pure)	49.95
1.573 MCC-LiCl/DMAC	13.36
1.887 MCC-IL/DMAC	20.83
1.573 MCC-IL/DMSO	17.28
1.573 MCC-IL/Sulfolane	24.50

The effect of adding IL on the microscopic solvent properties of the medium can be accessed from the solvatochromic parameters shown in Figure 4.16 for the systems IL/DMAC, MCC-IL/DMAC and in Figure 4.17 for the system MCC-IL-DMSO, MCC-IL-Sulfolane. As given in Table 7.7 and 7.8 in appendix, the solvatochromic properties of the DAS are different. Whereas MeCN is more polar than DMAC ( $E_T(33)$ ), the latter solvent is much more basic (SB), i.e., is more efficient in hydrogen bonding to the hydroxyl groups of the AGU; this leads to more accessible biopolymer. The importance of medium basicity to cellulose dissolution/regeneration and, presumably, accessibility is well-documented (Lauri et al. 2012). The initial addition of IL causes

a huge increase in the empirical polarity of DMAC, followed by small, but persistent increase as a function of increasing [IL]. Both changes in polarity may be due to the preferential solvation of the polarity probe by IL, or (IL...DMAC), as explained elsewhere (El Seoud et al. 2007; El Seoud et al. 2009). Solvent acidity, SA, of pure DMAC is close to zero because this DAS carries no acidic hydrogen (Catalán 2009). Addition of the IL, however, leads to initial large increase in SA, because of the presence of the relatively acidic C2-H in the imidazolium heterocycle. Again, the subsequent increase in (SA) is much smaller as a function of [IL]. Introduction of the IL, with its acidic C2-H leads to a decrease in SB. As can be seen from Figure 4.16, there is a linear increase in the empirical polarity of the mixture as a function of increasing [IL].

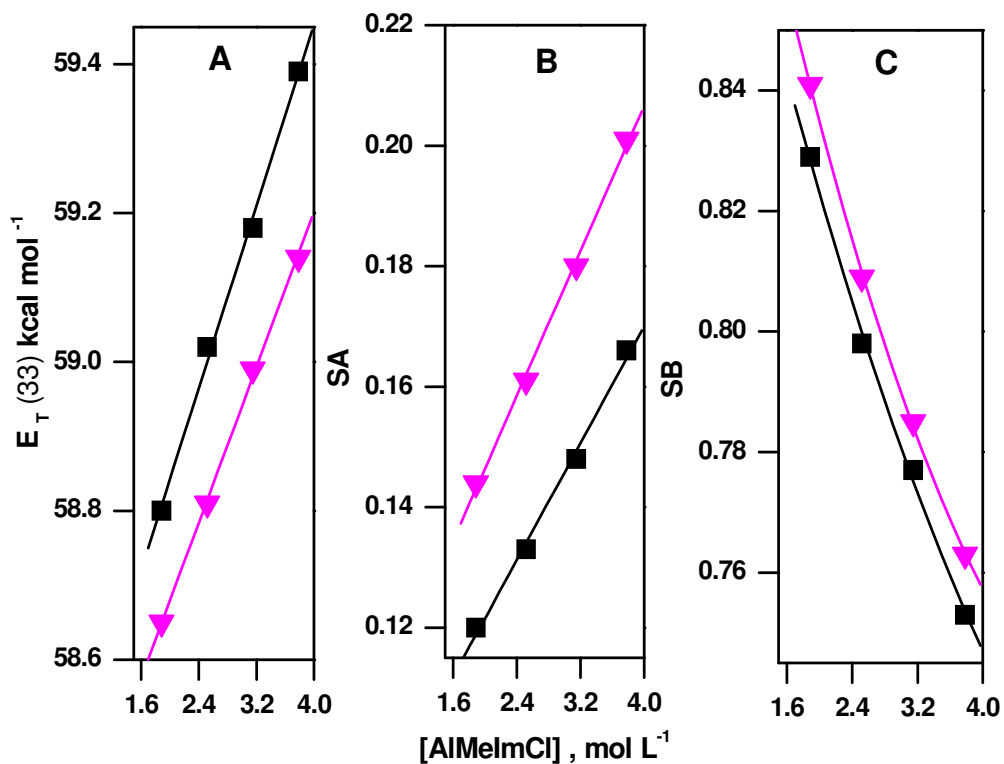


**Figure 4.16:** Dependence of solvent properties on [IL]: polarity,  $E_T(33)$ , (part A), acidity (part B) and basicity (part C); in IL-DMAC (■) and in MCC-IL-DMAC (▲) mixtures. All parameters are calculated from data at 40 °C.

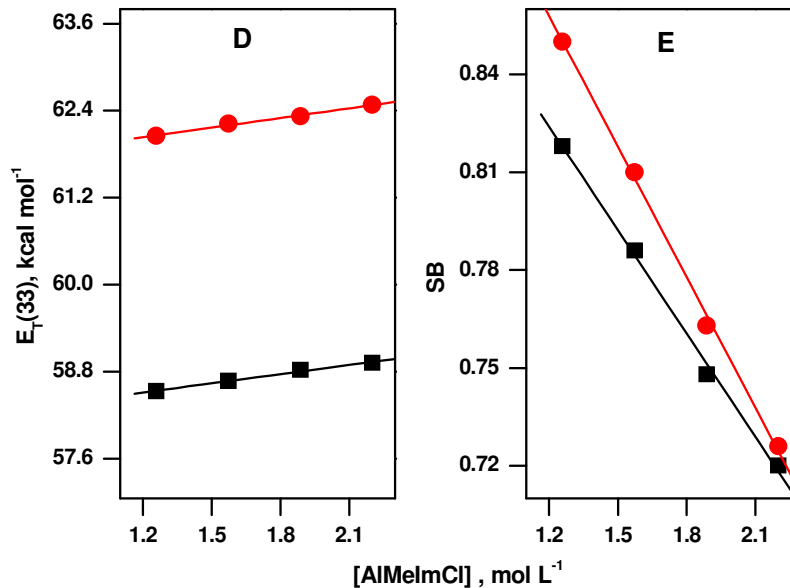


**Figure 4.17:** Dependence of solvent properties on [IL]: polarity,  $E_T(33)$ , (part A), and basicity (part B); in MCC-IL-DMSO (●) and in MCC-IL-Sulfolane (■) mixtures. All parameters are calculated from data at 40 °C.

The effect of co-dissolution of MCC on the solvatochromic parameters is small, indicating that solvation of the solvatochromic probes employed is dominated by its hydrogen-bonding and dipolar interactions with the IL or IL-DAS. Therefore, the initial large variations in the solvatochromic parameters on dissolving the IL clearly show that the microscopic properties of the medium, that are relevant to cellulose dissolution and accessibility, have been perturbed.

In summary, the complex effect of [IL] on ( $k_3$ ) may be due to two factors: (a) the formation of (MCC⋯IL) or (CHM⋯IL) hydrogen bonds, and (b) the change in the microscopic properties of binary solvent mixture, because of the large volume fractions of IL. Of the solvatochromic parameters investigated (SB) is important because a more basic solvent, in particular DMSO binds efficiently to the hydroxyl groups of the biopolymer and, presumably increases its accessibility. Therefore, solvent macroscopic properties are important when they differ largely; differences in microscopic properties maybe relatively small but are important to accessibility, hence reactivity. This discussion can be completed if information is available on the interactions that occur on molecular level, in particular in the solvation layer of the

biopolymer. This information has been secured from molecular simulations, MD calculations, as shown in the following section 4.4.

#### **4.4. MD simulations in IL-DAS**

We have carried out MD simulations in order to compare the interactions of cellulose with IL and DMAC, MeCN, DMSO or sulfolane. To our knowledge, this is the first time that MD simulations have been employed to probe the interactions of cellulose with these binary solvent mixtures. As a model for cellulose, we have employed glucose dodecamer (hereafter designated as “oligomer”); the systems studied included one oligomer, 301 molecules of IL and 1143 molecules of DMAC or MeCN, and one oligomer, 252 molecules of IL and 1143 molecules of DMSO or Sulfolane respectively. These compositions correspond to solutions 6.9-, 9.7-, 8.9- and  $7.2 \times 10^{-3}$  mol/L MCC in DMAC, MeCN, DMSO and Sulfolane respectively. Figure 4.18 and Table 4.8 summarizes the main results of these calculations.



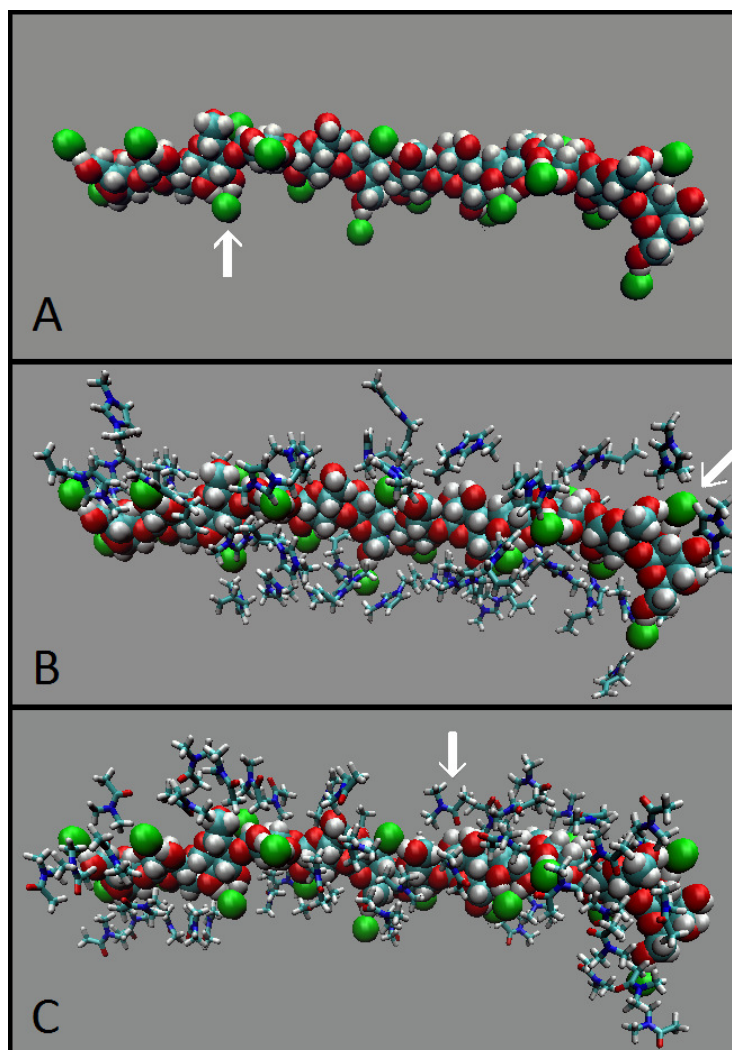


**Figure 4.18:** Snapshot of an MD simulation frame showing the oligomer and its first solvation shell (0.5 nm) for the system IL/DMAC. Part (A) shows the oligomer plus ( $\text{Cl}^-$ ). The arrow shows that this anion forms *simultaneous* hydrogen-bonds to two OH groups of the AGU. Part (B) shows the oligomer plus ( $\text{Cl}^-$ ) and  $\text{Im}^+$ . The arrow shows two  $\text{Im}^+$  hydrogen-bonded to a single ( $\text{Cl}^-$ ) via their C2-H. Part (C) shows the oligomer plus ( $\text{Cl}^-$ ) and DMAC. The arrow indicates the hydrogen bonding between C=O of DMAC and the OH of the AGU.

**Table 4.8:** Results of molecular dynamics simulations of the system oligomer/IL-DAS

Entry	Observed pair <sup>a</sup>	IL/DMAC		IL/MeCN		IL/DMSO		IL/Sulfolane	
		Solvation shell extension, nm <sup>a</sup>	Number of interacting species <sup>a</sup>	Solvation shell extension, nm <sup>a</sup>	Number of interacting species <sup>a</sup>	First solvation shell extension, nm	Number of species/(unit name)	First solvation shell extension, nm	Number of species/(unit name)
1	DAS COM <sup>b</sup> and oligomer surface	from 0.224 to 0.564, maximum at 0.444	<b>48.48</b> DMAC/oligomer 3.79 DMAC/AGU	from 0.216 to 0.476, maximum at 0.398	<b>35.17</b> MeCN/oligomer 2.93 MeCN/AGU	from 0.216 to 0.528, maximum at 0.408	<b>60.75</b> DMSO/oligomer 5.06 DMSO/AGU	from 0.234 to 0.536, maximum at 0.348	<b>63.87</b> Sulfolanes/oligomer 5.32 Sulfolanes/AGU
2	Cl <sup>-</sup> and oligomer surface	from 0.156 to 0.238, maximum at 0.182	<b>18.64</b> Cl <sup>-</sup> /oligomer 1.55 Cl <sup>-</sup> /AGU	from 0.156 to 0.236, maximum at 0.184	<b>20.87</b> Cl <sup>-</sup> /oligomer 1.74 Cl <sup>-</sup> /AGU	from 0.158 to 0.238, maximum at 0.184	<b>18.99</b> Cl <sup>-</sup> /oligomer 1.58 Cl <sup>-</sup> /AGU	from 0.158 to 0.244, maximum at 0.184	<b>5.57</b> Cl <sup>-</sup> /oligomer 0.46 Cl <sup>-</sup> /AGU
3	IM <sup>+</sup> COM and oligomer surface	from 0.184 to 0.748, maximum at 0.396	<b>45.35</b> IM <sup>+</sup> /oligomer 3.78 IM <sup>+</sup> /AGU	from 0.204 to 0.734, maximum at 0.380	<b>49.89</b> IM <sup>+</sup> /oligomer 4.16 IM <sup>+</sup> /AGU	from 0.194 to 0.742, maximum at 0.520	<b>39.46</b> IM <sup>+</sup> /oligomer 3.29 IM <sup>+</sup> /AGU	from 0.202 to 0.624, maximum at 0.398	<b>17.27</b> IM <sup>+</sup> /oligomer 1.44 IM <sup>+</sup> /AGU

<sup>a</sup> The numbers and distances of the species are average values, calculated for the simulation time interval 15 to 70 ns.

<sup>b</sup> COM = center of mass.

Regarding these data, the following is relevant

- Calculation of the radial distribution function, RDF, of all atoms present around the oligomer surface has indicated that the extension of its solvation layer can be taken as equal to 0.47 nm; this value has been employed throughout. In what follows, *all values given are average*, taken within the solvation layer;

- We dwell on the interactions between HO-AGU and the binary mixture components, because these are the interactions relevant to cellulose accessibility, hence reactivity. For ease of reading, we divide the discussion into two-part DMAC and MeCN;

- The arrows inserted in Figure 4.18 clearly indicate the formation of hydrogen-bonds in the system. Part (A) shows this bonding between ( $\text{Cl}^-$ ) and two hydroxyl groups of the AGU. This *simultaneous* bonding may explain the reason for the efficiency of ILs as solvents for cellulose and other biopolymers. It agrees with parts (I) and (II) of Figure 4.19 and red lines of Figure 4.20 where the very sharp peak of the RDF curves clearly indicates strong ( $\text{Cl}^- \cdots \text{HO-AGU}$ ) interactions in all studied DAS. The arrow in part (B) of Figure 4.18 shows the importance of C2-H to bonding of the ions of the IL proper. This agrees with the interpretation of the results of MD simulations by other authors (Dong et al. 2006; Hanbin et al. 2010). Part (C) shows the participation of DMAC in further hydrogen bonding to the hydroxyl of AGU.

- When comparing DMAC and MeCN, the importance of SB of the DAS is apparent from two pieces of evidence: Entry 1 of Table 4.8 shows that the number of DMAC molecules at the surface of the oligomer exceeds that of MeCN by 37.8%, although volume of the former is 90.6% larger than that of MeCN (0.1308 and 0.0686 nm<sup>3</sup>/molecule, for DMAC and MeCN, respectively). Additionally, in Figure 4.19 the sharp RDF peak in (III) indicates the presence of strong interactions between the C=O of DMAC and HO-AGU. On the other hand, this peak is absent in the RDF curve of (IV), indicating much weaker interactions between HO-AGU and MeCN; Continuing the analysis of entry 1 of Table 4.8, there are a larger number of molecules

of sulfolane than DMSO in the oligomer solvation shell and both are present in larger number than DMAC and MeCN. Sulfolane has a more structured peak in its RDF curve than DMSO (see blue lines in Figure 4.20) and, considering that the interactions with the oligomer occur in its (partially) positive H of OH groups, this is a reflex of the more negative charge present in its SO<sub>2</sub> group in relation to the one of SO group of DMSO, fact that gives to sulfolane a larger dipole moment than for DMSO (4.69D and 3.96D, respectively (Tilstam, U. 2012)). The sulfolane molecule is larger than DMSO (0.140 and 0.097 nm<sup>3</sup>/molecule, respectively) so it occupies a larger area on the oligomer surface than DMSO (or any other studied DAS, as it is present in larger number);

- Entries 2 and 3 of Table 4.8 show that the number of ions of the IL at the surface of the oligomer follows these orders: for (Cl<sup>-</sup>): MeCN > DMSO > DMAC >> sulfolane and for (Im<sup>+</sup>): MeCN > DMAC > DMSO >> sulfolane. This reflects the finite volume of the oligomer solvation shell, and the fact that it contains a smaller number of MeCN molecules than others DAS. In other words, this should not be taken to indicate weaker interactions between the IL and the oligomer.

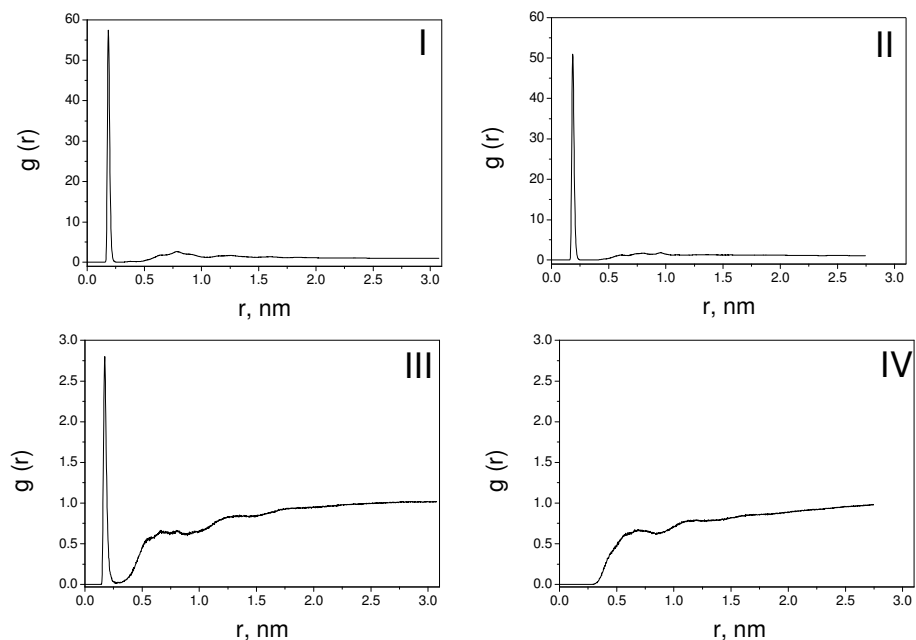


**Figure 4.19:** Parts (I) and (II) show the radial distribution function, RDF ( $g(r)$ ) of  $\text{Cl}^-$  around the HO-AGU of the oligomer, in DMAC, and MeCN, respectively. Parts (III) and (IV) show the RDF of the DAS around the HO-AGU of the oligomer, in DMAC, and MeCN, respectively.

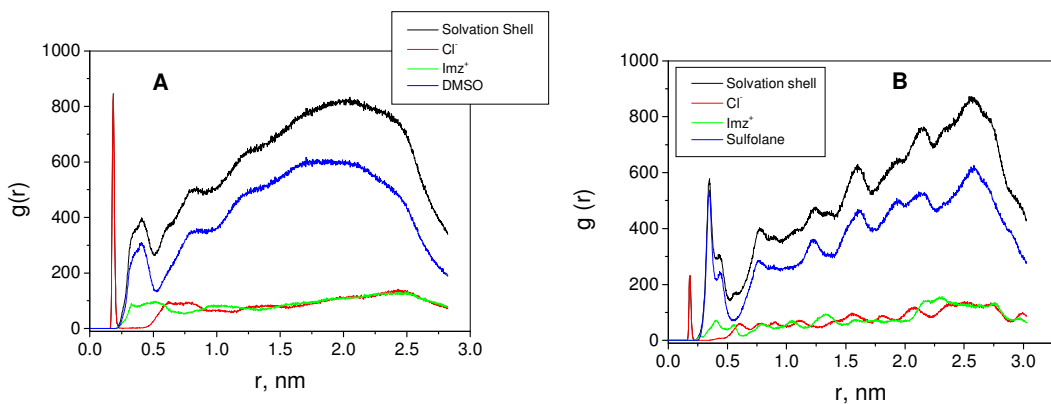


**Figure 4.20:** Parts (A) and (B) show the radial distribution function, RDF ( $g(r)$ ) of  $\text{Cl}^-$ ,  $\text{Im}^+$ , DAS and all them together (the solvation shell) around the HO-AGU of the oligomer, in DMSO, and Sulfolane, respectively.

In summary, our MD simulations show the oligomer interactions with both solvent components produces different solvation shell compositions. How this influence oligomer reactivity does remains to be determined by further studies.

## 4.5. Imidazole-catalyzed acylation of cellulose in LiCl/DMAC

We have extended the uncatalyzed study to MCC-catalyzed acylation in the same solvent system by carboxylic acid anhydrides; ethanoic-, propanoic-, butanoic-, pentanoic-, and hexanoic anhydride (all *normal-chain* compounds). It has been claimed that this reaction is catalyzed by tosyl chloride, TsCl (Tosh, Saikia & Dass, 2000a,b). The latter reaction, however, is not faster than its uncatalyzed counterpart! By using  $^1\text{H}$  NMR, we have shown that the acetylation reaction is not subject to catalysis due to the (claimed) formation of a reactive intermediate (mixed carboxylic-sulfonic anhydride, *vide infra*) which then (presumably) reacts with cellulose. (Tosh, Saikia & Dass, 2000a,b) We have then studied the imidazole (Im)-catalyzed acylation. Use of  $^1\text{H}$  NMR and FTIR has confirmed the intermediate formation of *N*-acylimidazole; a combination of kinetic data and theoretical calculations has shown that this is the actual acylating agent, in agreement with previous publications. (El Seoud et al. 1994; Hussain, Liebert & Heinze, 2004).

### 4.5.1. Acylation by acid anhydrides in the presence of tosyl chloride or imidazole

The observation that the acetylation of cellulose (DP = 900,  $0.0864 \text{ mol L}^{-1}$ ) in the presence of TsCl ( $0.308 \text{ mol L}^{-1}$ ) in DMAC (Tosh et al. 2000a,b) is not faster than the uncatalyzed acetylation of MCC, (Nawaz et al. 2012) begs for an explanation, even when the difference in DP is taken into account. Note that the difference in *Ic* of the two celluloses has no bearing on the kinetic results because cellulose is decrystallized on dissolution in LiCl/DMAC (Ramos et al. 2005). The reaction mechanism proposed is shown below: (Tosh et al. 2000a,b).

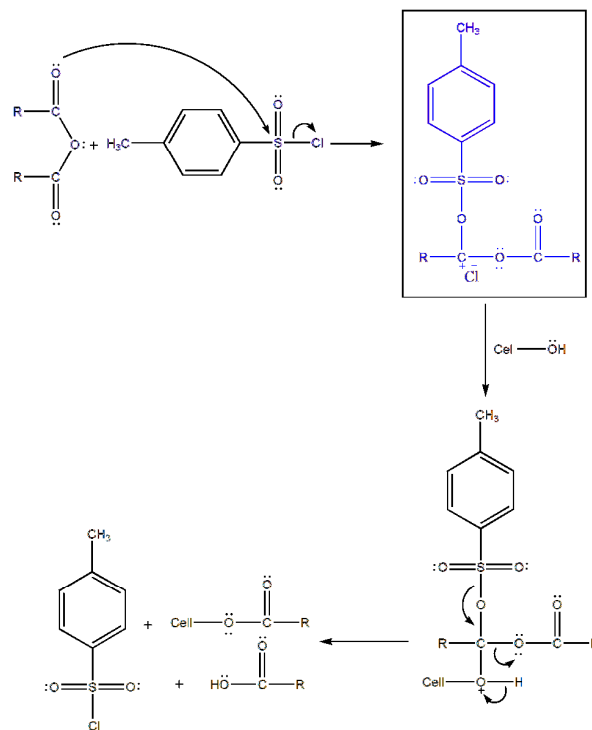


**Figure 4.21:** Suggested mechanism for the catalytic effect of TsCl on the acylation by acid anhydrides. The structure inside the frame is that of the expected intermediate. (Tosh et al. 2000a,b).

This catalysis, if it occurs, rests on the intermediate formation of the mixed carboxylic-sulfonic anhydride (structure depicted inside the frame) that is expected to be more reactive than the carboxylic anhydride. The formation of the latter intermediate has not been documented, (Tosh et al. 2000a,b) therefore, we employed  $^1\text{H}$  NMR in an attempt to detect its formation; the results are shown in Figure 4.22. Parts (A) and (B) of this Figure do not indicate a reaction between the two reagents, i.e., the spectrum of the mixture is the sum of the spectra of the two reagents. In other words, there is no detectable formation of the expected mixed anhydride. Therefore, the acetylation is, in fact, not subject to catalysis by TsCl. Note that the mixed anhydride, if it is formed, is stable (Kenichi, 2003a,b); its formation has been detected by NMR (Liu et al. 2008)

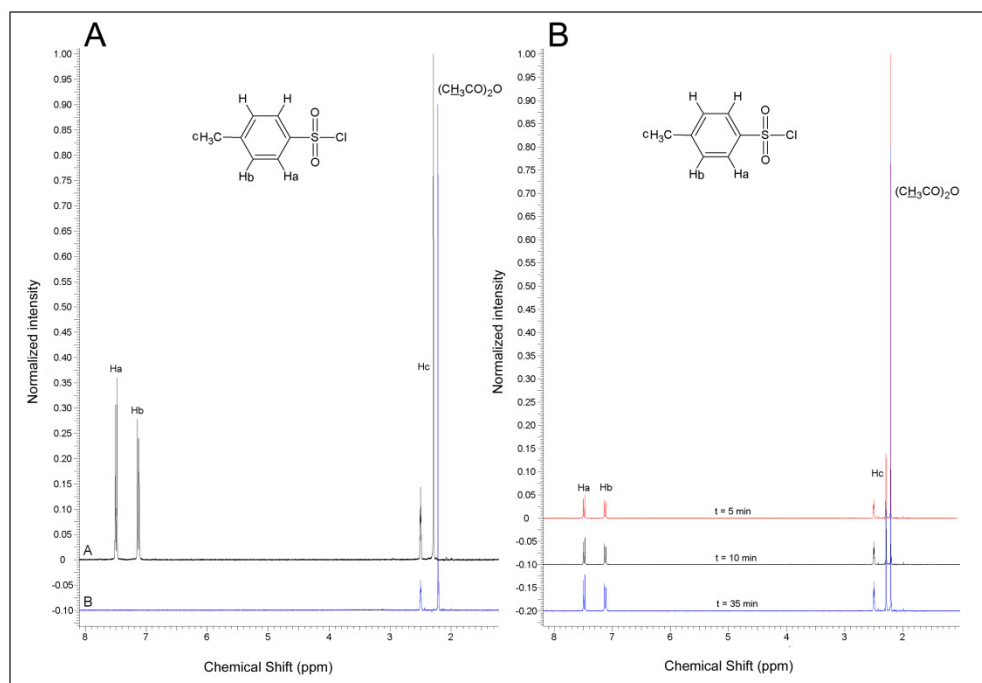


**Figure 4.22:** Part (A) shows superimposed  $^1\text{H}$  NMR spectra of authentic samples of acetic anhydride (lower curve) and tosyl chloride (upper curve) in DMSO- $d_6$  with the discrete hydrogens indicated. Part (B) shows the spectra of a mixture (in the same solvent) of acetic anhydride (0.05 mol/L) and tosyl chloride (0.05 mol/L) as a function of time.

We decided to investigate the use of Im. As shown in Figure 4.23, this catalysis, if it occurs, involves the intermediate formation of *N*-acyldiazole, RCOIm, and its subsequent reaction with cellulose. The products are cellulose carboxylate; carboxylic acid, and (regenerated) Im. The latter two products react to form imidazolium carboxylate.



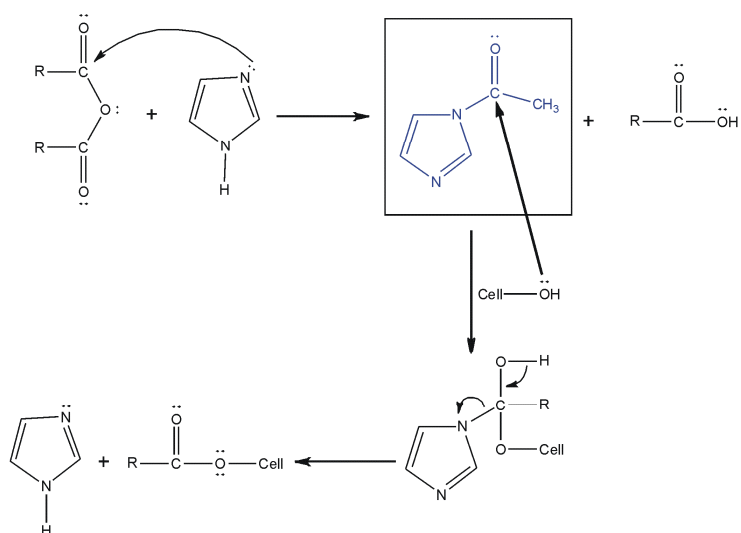


**Figure 4.23:** A complete reaction mechanism for the imidazole-catalyzed acylation of cellulose. The reaction sequence involves the intermediate formation of *N*-acylimidazole, followed by its reaction with cellulose to produce cellulose ester, plus imidazolium carboxylate.

#### 4.5.2. Detection of the intermediate in imidazole-catalyzed acylation, by $^1\text{H}$ NMR and FTIR

We have demonstrated by NMR study the formation of *N*-acylimidazole as the intermediate for the imidazole-catalyzed acylation of model compounds and cellulose. Figure 4.24 shows the  $^1\text{H}$  NMR spectra of the two authentic reactants, acetic anhydride and Im, as well as their mixture in  $\text{CDCl}_3$ , after 5 minutes of mixing. The formation of  $\text{CH}_3\text{COIm}$  and  $\text{CH}_3\text{CO}_2\text{H}$  is clearly evidenced by the appearance of new singlets at 2.60 and 2.09 ppm, respectively, and by the changes of the chemical shifts of the heterocyclic ring protons, namely: The hydrogen at positions 4 and 5 of Im are no more equivalent; the large shift ( $\text{Ha} \rightarrow \text{Ha}'$ ).

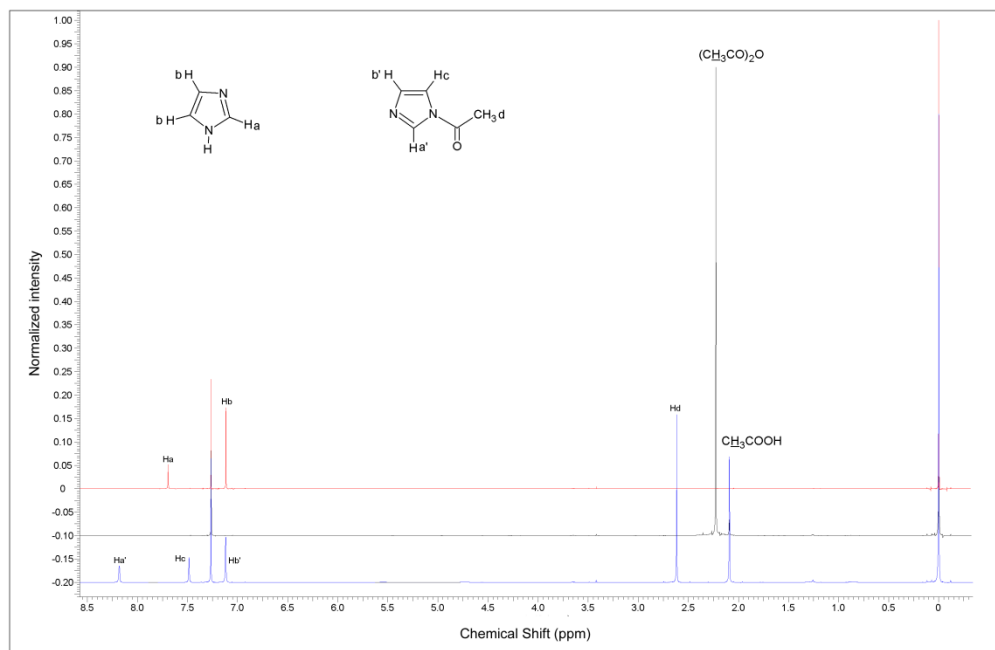


**Figure 4.24:**  $^1\text{H}$  NMR spectra in  $\text{CDCl}_3$  of authentic samples of imidazole (0.05 mol/L; upper plot); acetic anhydride (0.05 mol/L; middle plot) and an equimolar mixture of both reactants after five minutes of mixing, lower plot. The discrete hydrogens are labeled.

FTIR is a powerful technique in order to show the intermediate formation of  $\text{RCOIm}$ . The characteristic anhydride  $\nu_{\text{C=O}}$  “doublet” (due to asymmetric and symmetric stretching vibrations, respectively) at 1821- and 1751  $\text{cm}^{-1}$ , are replaced by peaks at 1737 and 1716  $\text{cm}^{-1}$ , due to the formation of *N*-acetylimidazole and acetic acid, respectively as shown in Figure 4.25.

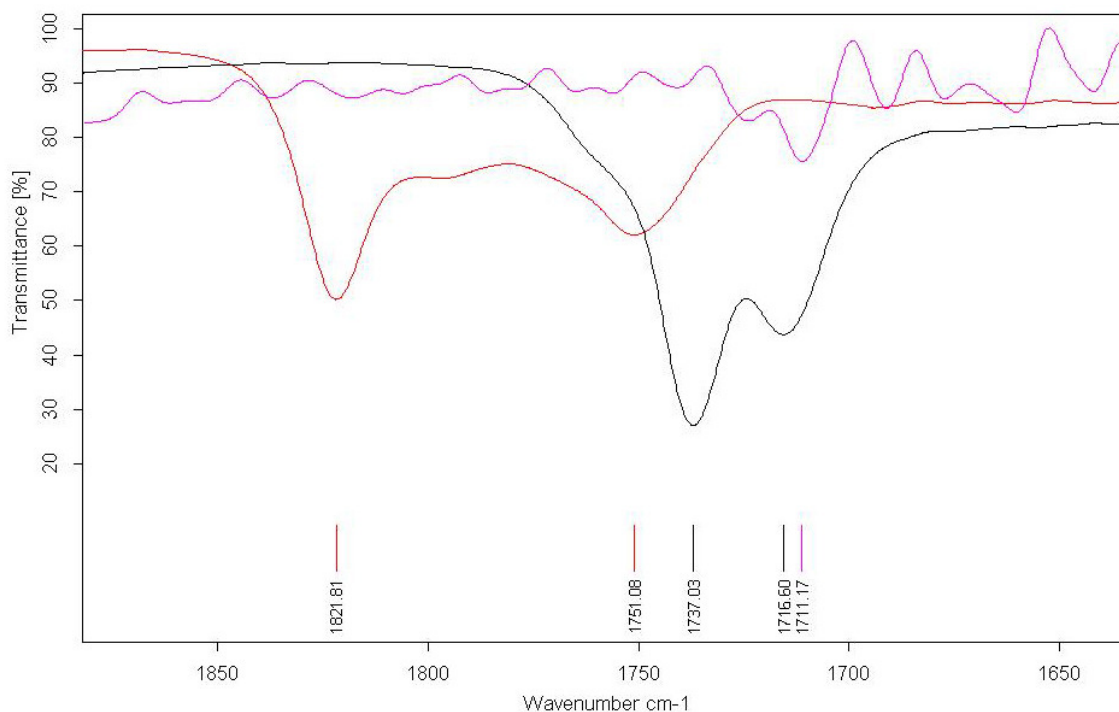


**Figure 4.25:** The IR 1850-1650  $\text{cm}^{-1}$  spectral region for the reaction of acetic anhydride and Im. Part (A) shows the spectra of authentic samples of Im (magenta line), ethanoic anhydride (black line) and the reaction products after the mixture of them: acetyl imidazole and acetic acid (red line).

#### 4.5.3. Proof that *N*-acylimidazole is the actual acylating agent

As shown in Table 7.9, one mol of acetic anhydride reacts with two mols of Im to produce one mol of *N*-CH<sub>3</sub>COIm plus one mol of imidazolium acetate. That *N*-acylimidazole is the actual acylating agent, which can be shown by several pieces of evidence:

(a)- Values of  $k_3$  have been calculated for the reaction of CHM (50 °C) with: A mixture of 20 mmol acetic anhydride plus 40 mmol Im; 20 mmol authentic *N*-acetyl imidazole; 20 mmol authentic *N*-CH<sub>3</sub>COIm in the presence of 20 mmol authentic imidazolium acetate. All rate constants were found to be *practically the same*, 2.170-; 2.015-; and  $1.997 \times 10^{-2} \text{ L}^2 \text{ mol}^{-2} \text{ s}^{-1}$ , respectively. This result also shows that the imidazolium acetate formed in the reaction has no (acid-base) catalytic effect.

(b)- Our theoretical calculations have shown that the reaction with RCOIm is more favorable than that with the precursor (RCO)<sub>2</sub>O. Thus the partial positive charge on the acyl-carbon of CH<sub>3</sub>COIm (0.293 a. u.) is larger than that on the corresponding group of acetic anhydride (0.235 a. u.).

**Table 4.9:** Mulliken atomic charges of ethanoic anhydride and *N*-acetylimidazole heavy atoms.

Ethanoic anhydride		<i>N</i> -acetylimidazole	
Atom	Partial atomic charges, a.u.	Atom	Partial atomic charges, a.u.
C1	-0.373202	N1	0.023269
C2	0.235411	C2	-0.053077
O3	-0.099726	N3	-0.269601
C4	0.184780	C4	-0.193651
C5	-0.462220	C5	-0.017994
O6	-0.299385	C6	0.292821
O7	-0.313378	C7	-0.497957
		O8	-0.358342

(c)- Additionally, molecular dynamics simulations were performed on mixtures containing DMAC; CHM; and acetic anhydride or *N*-CH<sub>3</sub>COIm; see Figure 4.26. The relevant information obtained is that the complex CHD/CH<sub>3</sub>COIm remains longer in contact. According to the “spatio-temporal” postulate, molecules will react if they stay at a critical distance for a certain length of time (Menger, 1985). As Figure 4.26 shows, these criteria apply more efficiently to the Im-catalyzed reaction. In summary, it is clear from the above discussion that *N*-acetylimidazole is the actual acylating agent.

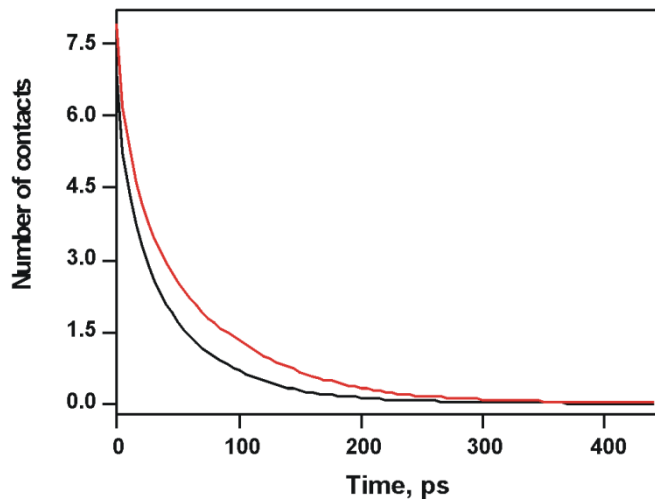


**Figure 4.26:** Number of molecules that remain in contact (i.e., inside a distance of 0.56nm) after collisions as function of time (in ps). Black line: contacts between ethanoic anhydride and CHD. Red line: contacts between *N*-acetylimidazole and CHD.

#### 4.5.4. Reaction order and activation parameters

We then proceeded to determine the rate constants and activation parameters of the Im-catalyzed acylation of cellulose by carboxylic acid anhydrides, from ethanoic- to hexanoic anhydride in LiCl/DMAC as shown in Table 4.10. We have carried out specific experiments; see Experimental section 3.3.1 and 3.3.2 in order to show that the expected reaction products (esters) of CHM, CHD, and MCC are obtained under the conditions of the kinetic runs. That is, *the reaction that is being followed by conductivity is Im-catalyzed acylation*. Excellent linear plots were observed for  $\ln(\lambda_{\infty}-\lambda_t)$  as a function of time (t) as shown in Figure 4.27.

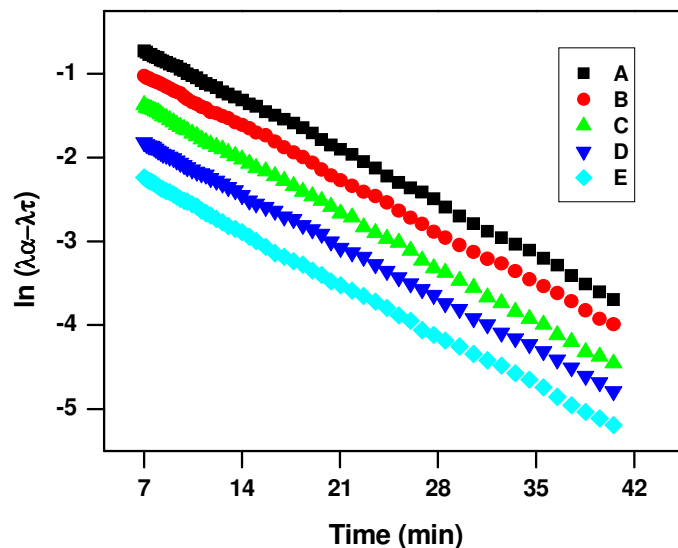


**Figure 4.27:** Typical plots showing the variation of solution conductivity in function of time obtained for MCC with different anhydrides (A, B, C, D, E,) for the ethanoic-, propanoic-, butanoic-, pentanoic-, and hexanoic anhydride at 40-, 40-, 60-, 60- and 40 °C respectively. The symbols  $\lambda_{\infty}$  and  $\lambda_t$  refer to solution conductivity at the end of the reaction and at time (t), respectively.

The reactivity ratio  $k_{3,\text{Prim(OH),CHM}}/k_{3,\text{Sec(OH),CHD}}$  was found to be 1.8. As we have argued previously, this ratio is smaller than that observed for the derivatization of cellulose under *heterogeneous* reaction conditions ( $4 \pm 1$ ) (Malm et al. 1953; Kwatra et al. 1992; Jain et al. 1985), most probably due to difference in accessibility of hydroxyl groups of the model compounds (totally accessible) and cellulose (primary hydroxyls more accessible than secondary ones). The reactivity ratio lies, therefore between 1.3 and 5; we have used the arithmetic means of the both (3.15) to split  $k_3$ .

Note that use of the lower limit, i.e.,  $k_{\text{obs,Prim(OH)}} / k_{\text{obs,Sec(OH)}} = 1.3$  affects the individual rate constants, but not the activation enthalpy,  $\Delta H^\ddagger$ . At 60 °C, the effect of changing the ratio (from 5 to 1.3) on the activation entropy term,  $T\Delta S^\ddagger$ , and activation free energy,  $\Delta G^\ddagger$  are negligibly small, 0.25 and 0.25 kcal/mol, respectively.

**Table 4.10:** Third order rate constants and activation parameters calculated for the imidazole-catalyzed acylation of microcrystalline cellulose, MCC in 4% LiCl/DMAC, at 75 °C.<sup>a,b</sup>

Anhydride/ Temperature	40 °C	50 °C	60 °C	70 °C	$\Delta H^\ddagger$ , kcal mol <sup>-1</sup> ; <sup>c</sup>	$T\Delta S^\ddagger$ , kcal mol <sup>-1</sup> ; <sup>c</sup>	$\Delta G^\ddagger$ , kcal mol <sup>-1</sup> ; <sup>c</sup>
<b>MCC, 10<sup>3</sup> x (overall k<sub>3</sub>), L<sup>2</sup> mol<sup>-2</sup> s<sup>-1</sup></b>							
Ethanoic	3.395	4.560	5.934	7.510	4.97 (-0.8)	-18.53 (2.03)	24.49 (-1.84)
Propanoic	2.466	3.365	4.570	5.740	5.39 (-1.15)	-18.28 (1.57)	24.68 (-1.71)
Butanoic	1.865	2.530	3.540	4.620	5.84 (-1.21)	-17.98 (1.46)	24.84 (-1.65)
Pentanoic	3.105	4.125	5.290	6.465	4.55 (-1.54)	-19.04 (1.06)	24.57 (-1.62)
Hexanoic	3.650	4.645	5.710	6.870	3.81 (-2.21)	-19.74 (0.54)	24.52 (-1.78)
<b>MCC; 10<sup>3</sup> x k<sub>3; Prim(OH)</sub>, L<sup>2</sup> mol<sup>-2</sup> s<sup>-1</sup>,<sup>d</sup></b>							
Ethanoic	2.076	2.789	3.629	4.593	4.97 (-0.8)	-19.85 (0.23)	24.82 (-1.03)
Propanoic	1.508	2.058	2.795	3.510	5.39 (-1.15)	-19.61 (0.21)	25.00 (-0.94)
Butanoic	1.140	1.547	2.165	2.825	5.84 (-1.21)	-19.33 (-0.40)	25.17 (-0.81)
Pentanoic	1.899	2.523	3.235	3.954	4.55 (-1.54)	-20.35 (-0.58)	24.90 (-0.96)
Hexanoic	2.232	2.841	3.492	4.202	3.81 (-2.21)	-21.03 (-1.30)	24.84 (-0.93)
<b>MCC, 10<sup>3</sup> x k<sub>3; Sec(OH)</sub>, L<sup>2</sup> mol<sup>-2</sup> s<sup>-1</sup>,<sup>d</sup></b>							
Ethanoic	0.659	0.885	1.152	1.458	4.97 (-0.8)	-19.26 (1.57)	25.58 (1.02)

Anhydride/ Temperature	40 °C	50 °C	60 °C	70 °C	$\Delta H^\ddagger$ , kcal mol <sup>-1</sup> ; c	$T\Delta S^\ddagger$ , kcal mol <sup>-1</sup> ; c	$\Delta G^\ddagger$ , kcal mol <sup>-1</sup> ; c
Propanoic	0.478	0.653	0.887	1.114	5.39 (-1.15)	-19.01 (1.15)	25.76 (-0.94)
Butanoic	0.362	0.491	0.687	0.897	5.84 (-1.21)	-18.72 (0.97)	25.93 (-0.81)
Pentanoic	0.602	0.801	1.027	1.255	4.55 (-1.54)	-19.75 (0.78)	25.66 (-0.96)
Hexanoic	0.708	0.901	1.108	1.333	3.81 (-2.21)	-20.43 (0.08)	25.60 (-0.93)

a- All rate constants and activation parameters were calculated/one hydroxyl group.

b- The activation parameters were calculated for the reaction at 60 °C. The uncertainties in the activation parameters are  $\pm 0.05$  kcal mol<sup>-1</sup> ( $\Delta H^\ddagger$ , and  $\Delta G^\ddagger$ ) and 0.2 cal K<sup>-1</sup> mol<sup>-1</sup> ( $\Delta S^\ddagger$ ).

c- The numbers within parenthesis refer to (activation parameter Im-catalyzed reaction – uncatalyzed reaction).

The values within parenthesis in the last three columns of Table 4.10 show the reason for the observed catalysis. *For all anhydrides studied, as compared with the uncatalyzed reaction, imidazole catalysis results in smaller enthalpy, and higher entropy of activation.* The reason of the smaller enthalpy may be traced to the above-mentioned higher electrophilic character of the acyl-carbon of RCOIm. The higher entropy of activation maybe attributed to the smaller volume of the acylating agent, RCOIm, as compared with the bulky anhydride, see Eqn. 4.5

$$V_{R(\text{CO})\text{Im}} = 1.142 + 0.324 V_{(\text{RCO})_2\text{O}} \quad r = 0.994 \quad \text{sd} = 0.0626 \quad (4.5)$$

(v) An important objective of this study was to compare the rate constants and activation parameters between uncatalyzed and catalyzed acylation of model compounds and cellulose. Consider first the values of DS shown in Figure 4.28. This contains data of the Im-catalyzed reaction and of the corresponding uncatalyzed acylation by carboxylic acid anhydrides, by using



conventional- (i.e., by convection) (Nawaz et al. 2012; Nawaz et al. 2013) or microwave heating (Possidonio et al. 2009). In all cases, the values of DS decrease on going from ethanoic- to butanoic-, then increase on going to hexanoic anhydride. Therefore, this behavior seems to be general, at least for acylation, independent of nature of acylating agent ((RCO)<sub>2</sub>O or RCOIm), the method of heating; the solvent (electrolyte/dipolar aprotic or IL), or the type of cellulose (MCC or fibrous).

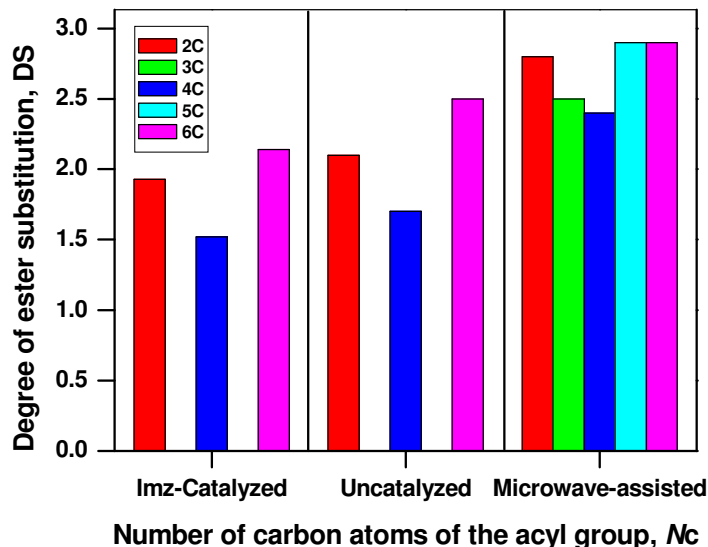


**Figure 4.28:** Dependence of the degree of substitution of cellulose esters, DS, on the number of carbon atoms of the acyl group of RCOIm or (RCO)<sub>2</sub>O, *N<sub>c</sub>*, whose value is shown in the insert. The results, from left to right refer to: Acylation by RCOIm in LiCl/DMAC; uncatalyzed acylation by (RCO)<sub>2</sub>O, conventional heating in LiCl/DMAC; acylation by (RCO)<sub>2</sub>O, microwave heating in the ionic liquid in 3-allyl-1-methylimidazolium chloride.

The reason for this dependence is shown in Figure 4.29. Parts (A) and (B) show that there is a clear parallelism between the dependence on *N<sub>c</sub>* of either DS, the overall, or individual rate constants. This is due to the enthalpy/entropy compensations that are clear in part (C). As an example, consider the results for *k<sub>3</sub>*. On going from ethanoic- to butanoic anhydride the (*unfavorable*) change in  $|\Delta H^\ddagger|$  is 0.87 kcal/mol, whereas the (*favorable*) change in the  $|T\Delta S^\ddagger|$  term is 0.55 kcal/mol. The corresponding changes on going from butanoic- to hexanoic anhydride are 2.03 and 1.76 kcal/mol for (*favorable*)  $|\Delta H^\ddagger|$  and (*unfavorable*)

$|\Delta S^\ddagger|$ , respectively. Therefore, the dependence of the rate constants, hence DS on  $N_c$  is complex due to subtle changes in the activation parameters, with the change in enthalpy dominating.

Although the variations in the activation parameters are admittedly small, they point out to a trend. The increase in  $\Delta H^\ddagger$  on going from *N*-acetyl- to *N*-butanoylimidazole may be related to the decrease in the electrophilicity of the acyl group. The subsequent decrease in  $\Delta H^\ddagger$  (*N*-butanoyl- to *N*-hexanoylimidazole) may be related to favorable hydrophobic interactions between the carbon chains of the *N*-acylimidazole and cellulosic surface, whose lipophilicity has increased, due to its partial acylation. The importance of hydrophobic interactions in cellulose chemistry has been recently advanced in order to explain some aspects of cellulose dissolution (Lindman et al. 2010; Medronho et al. 2012), as well as its interactions with ionic liquids. (Liu et al. 2010). These cancellation effects lead to the subtle, but persistent variations of  $\Delta G^\ddagger$  as a function of increasing  $N_c$ .

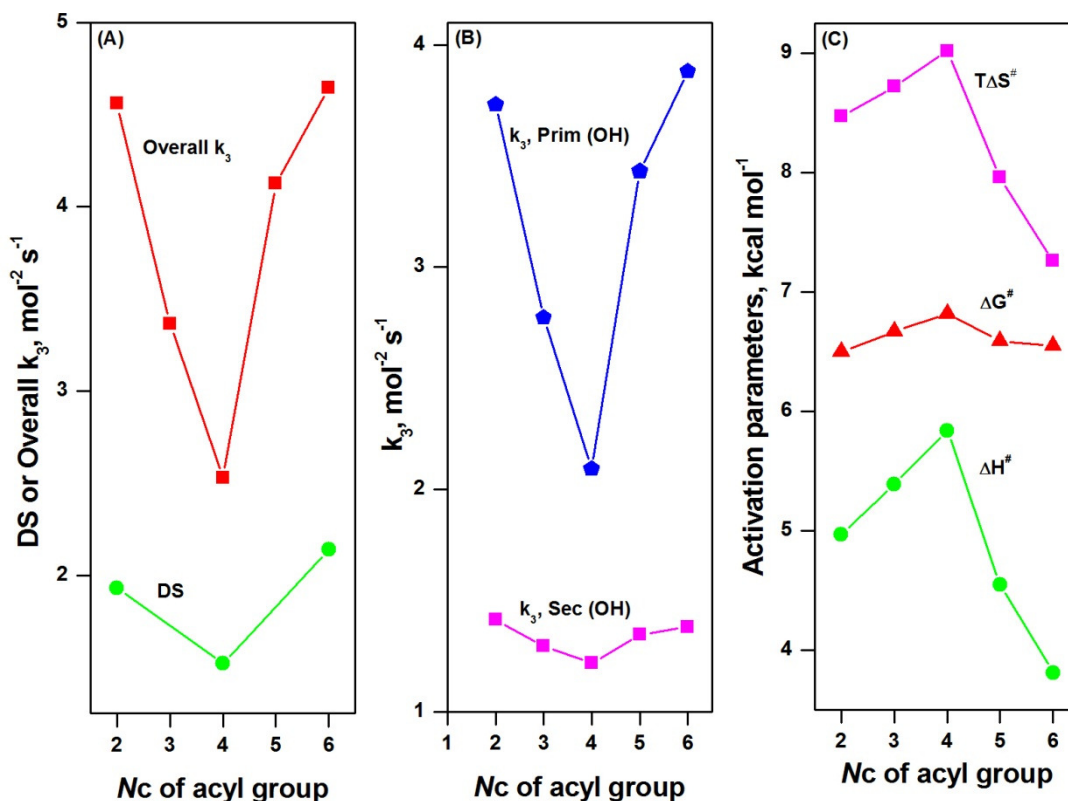


**Figure 4.29:** Im-catalyzed acylation of MCC; all plots are for the dependence on the number of carbon atoms of the acyl group of RCOIm,  $N_c$ : Part (A), DS and  $k_3$ ; Part (B),  $k_{3;\text{Prim(OH)}}$  and  $k_{3;\text{Sec(OH)}}$ ; part (C) the activation parameters. For ease of visualization, the data have been plotted by employing the following modifications: (A) ( $10^3 \times k_3$ ); (B) ( $10^3 \times k_{3;\text{Prim (OH)}}$ ), ( $(10^3 \times k_{3;\text{Sec(OH)}}) + 1$ ); (C), ( $T\Delta S^\ddagger + 27$ ) and ( $\Delta G^\ddagger - 17$ ).

In summary, esterification of cellulose by carboxylic acid anhydrides is efficiently catalyzed by imidazole. Spectroscopic data ( $^1\text{H NMR}$ ; FTIR) and the results of theoretical calculations clearly show that the acylating agent is *N*-acylimizale. The esterification reaction, however, is not subject to catalysis by TsCl. Catalyzed reaction is faster than uncatalyzed reaction due to lower enthalpy and higher entropy of activation.

## 5. CONCLUSION

Conductivity is a convenient technique to study the kinetics of cellulose derivatization. The use of the model compounds CHM and CHD permits dividing the overall rate constants of cellulose acylation into individual contributions from the primary and secondary hydroxyl groups of MCC. The former is more reactive for all anhydrides; the selectivity for C6-OH increases as a function of increasing  $N_c$ . The kinetic results show a parallelism between the effect of  $N_c$  on either the rate constants or the DS of esters synthesized. The nonlinear dependence of DS on  $N_c$  appears to be general, independent of the solvent employed or the method of heating (convection or microwave). In case of uncatalyzed acylation of MCC in LiCl/DMAC, it is attributed to subtle, complex variations in the reactions enthalpy and entropy.

MCC has been successfully acetylated in ionic liquid/dipolar aprotic solvents (IL/DAS). The reactivity order was found; IL/DMSO>IL/DMAC>IL/Sulfolane>IL/MeCN. The reactant in the acetylation reaction is most probably cellulose hydrogen-bonded to the IL. This conclusion is supported by the dependence of ( $k_3$ ) on [IL]; FTIR spectroscopy; conductivity measurements, and MD simulations; The basicity and dipolar character of DAS is important for cellulose reactivity; MD simulations have indicated stronger interactions of cellulose with both components of the IL/DMAC and IL/DMSO solvent, as compared with IL/MeCN and IL/Sulfolane. The IL/DAS offers the advantage that no cellulose pre-treatment is required; cellulose dissolution is much faster. Additionally, recovery of the IL is feasible, either by removing the volatiles under reduced pressure, or by salting-out.

It has been observed that using different ratios of ( $k_{\text{obs,Prim(OH)}}/k_{\text{obs,Sec(OH)}}$ ) affects the individual rate constants, but not the activation enthalpy,  $\Delta H^\ddagger$ . At 60 °C, the effect of changing the ratio to the upper limit, i.e., from 3.15 to 5 on  $T\Delta S^\ddagger$  and  $\Delta G^\ddagger$  are negligibly small, 0.15 and 0.15 kcal/mol, respectively. Likewise, the change to the lower limit, i.e., from 3.15 to 1.30, does not affect  $\Delta H^\ddagger$ , but leads to differences of 0.25 and 0.25, kcal/mol, for  $T\Delta S^\ddagger$  and  $\Delta G^\ddagger$ , respectively. That is, the ratio employed for splitting  $k_3$  does not affect the validity of any of the conclusions made, *vide infra*, on the origin of the reactivity difference between the reactions in IL-DMAC, IL-MeCN, IL/DMSO and IL/sulfolane.

Esterification of cellulose by carboxylic acid anhydrides is efficiently catalyzed by imidazole. Spectroscopic data ( $^1\text{H}$  NMR; FTIR) and the results of theoretical calculations clearly show that the acylating agent is *N*-acylimidazole. The esterification reaction, however, is not subject to catalysis by TsCl. As for the uncatalyzed reaction, C6-OH is more reactive for all *N*-acylimidazoles; the selectivity for C6-OH increases as a function of increasing *Nc*. The kinetic results are important because they show a parallelism between the effect of *Nc* on either the rate constants or the DS of esters synthesized. The nonlinear dependence of DS on *Nc* appears to be general, independent of the nature of the acylating agent; the solvent employed; the type of cellulose, or the method of heating (conventional or microwave). Relative to the uncatalyzed reaction, the diazole-mediated one is faster and is associated with smaller enthalpy- and larger entropy of activation, due to difference of the acylating agent.

## 6. REFERENCES

- Abbott, A. P. Application of hole theory to the viscosity of ionic and molecular liquids. **ChemPhysChem**. vol. 5, p. 1242-1246, 2004.
- Abdul-Sada, A. K., Greenway, A. M., Hitchcock, P. B., Mohammed, T. J., Seddon, K. R., Zora, J. A. Upon the structure of room temperature halogenoaluminate ionic liquids. **J. Chem. Soc., Chem. Commun.** p. 1753-1754, 1986.
- Acid Sulfite Pulping**, EPA-450/3-77-005, U. S. Environmental Protection Agency, Research Triangle Park, NC, January 1977.
- AIST (Copyright(C) 2001). Spectral database for organic compounds SDDBS. [http://riodb01.ibase.aist.go.jp/sdbs/cgi-bin/direct\\_frame\\_top.cgi](http://riodb01.ibase.aist.go.jp/sdbs/cgi-bin/direct_frame_top.cgi). (The SDDBS No of the product CHM is 52821.) Accessed 23 July 2011.
- Albanese, D., Landini, D., Penso, M. Hydrated tetrabutylammonium fluoride as a powerful nucleophilic fluorinating agent. **J. Org. Chem.** vol. 63, p. 9558–9589, 1998.
- Alvarez, O. M., Patel, M., Booker, J., Markowitz, L. Effectiveness of a biocellulose wound dressing for the treatment of chronic venous leg ulcers: Results of a single center randomized study involving 24 patients. **Wounds**. vol. 16, p. 224–233, 2004.
- Alvaro, C. S., Nudelman, N. S. The “dimer nucleophilic mechanism” for reactions with rate-limiting first step: derivation of the whole kinetic law and further kinetic results. **Int. J. chem. Kinet**, vol. 42, p. 735-742, 2010.
- Ananikov, V. P. Characterization of molecular systems and monitoring of chemical reactions in ionic liquids by nuclear magnetic resonance spectroscopy. **Chem. Rev.** vol. 111, p. 418–454, 2011.
- Anastas, P. T., Warner, J. C. Green chemistry: theory and practice, **Oxford University Press**: New York, p. 30, 1998.
- Anastas, P. T., Kirchhoff, M. M. Origins, current status, and future challenges of Green chemistry. **Acc. Chem. Res.** vol. 35, p. 689-694, 2002.
- Anastas, P. T., Wood-Black, F. Masciangioli, T. Exploring opportunities in green chemistry and engineering education. A workshop summary to the chemical sciences roundtable. National Research Council (US). **National Academies Press, Washington DC**, 2007.

- Anastas, P. T., Levy, I. J., Parent, K. E. *Green chemistry education. Changing the course of chemistry*, **ACS Publications, Washington DC**, 2009.
- Anastas, P. Twenty years of green chemistry, **Chem. Eng. News**. vol. 89, p. 62–65, 2011.
- Anslyn, E. V., Dougherty, D. A., **Modern physical organic chemistry**. University Science Books, Sausalito, p. 382, 2006.
- Antonious, M. S., Tada, E. B., El Seoud, O. A., Thermo-solvatochromism in aqueous alcohols: effects of the molecular structures of the alcohol and the solvatochromic probe. **J. Phys. Org. Chem.** vol. 15, p. 403-412, 2002.
- Armagero, W. L. F., & Chai, C. L. L. **Purification of Laboratory Chemicals**. (5th ed.). New York: Elsevier, 2003.
- Arvela, P. M., Anugwom, I., Virtanen, P., Sjöholma, R., Mikkola, J. P. Dissolution of lignocellulosic materials and its constituents using ionic liquids-A review. **Ind. Crops Products**, vol. 32, p. 175–201, 2010.
- Ass, B. A. P., Frollini, E., Heinze, T. Studies on the homogeneous acetylation of linters cellulose in the novel solvent system tetrabutylammonium fluoride trihydrate/ dimethylsulfoxide. **Macromol. Biosci.** vol. 4, p. 1008 –1013, 2004.
- Ass, B. A. P., Belgacem, M. N., Frollini, E. Mercerized linters cellulose: characterization and acetylation in *N,N*-dimethylacetamide/lithium chloride. **Carbohydr. Polym.** vol. 63, 1, p. 19-29, 2006.
- ASTM, D1795-94. Standard test methods for intrinsic viscosity of cellulose. 2001.
- ASTM D871-96. Standard test methods of testing cellulose acetate (solution method; procedure A), 2002.
- ASTM D1795-96. Standard test methods for intrinsic viscosity of cellulose, 2007.
- Atalla, R. H. Vanderhart, D. L. Studies on the structure of cellulose using Raman spectroscopy and solid state <sup>13</sup>C NMR. In cellulose and wood: chemistry and technology, **Proceedings of the 10<sup>th</sup> Cellulose Conference** (C. Schuerch, ed.). New York: John Wiley and Sons, p. 169-187, 1989.
- Austin, P. R. Chitin solutions, **US Patent No. 4**, DE 2707164 A1 19770825, 1977.

- Avent, A. G. Chaloner, P. A. Day, M. P. Seddon K. R. Welton, T. Evidence for hydrogen bonding in solutions of 1-ethyl-3-methylimidazolium halides, and its implications for room-temperature halogenoaluminate(III) ionic liquids. **J. Chem. Soc., Dalton Trans.** vol. 3405–3413, 1994.
- Azizi Samir, M. A. S., Alloin, F., Dufresne A. Review of recent research into cellulosic whiskers, their properties and their applications in nanocomposite field. **Biomacromolecules.** vol. 6, p. 612-626, 2005.
- Bäckdahl, H., Helenius, G., Bodin, A., Nannmark, U., Johansson, B. R., Risberg, B., et al. Mechanical properties of bacterial cellulose and interactions with smooth muscle cells. **Biomaterials.** Vol. 27, p. 2141–2149, 2006.
- Bagheri, M., Rodriguez, H., Swatloski, R. P., Spear, S. K., Daly, D. T., Rogers, R. D. Ionic liquid-based preparation of cellulose–dendrimer films as solid supports for enzyme immobilization. **Biomacromolecules.** vol. 9, p. 381-387, 2008.
- Bansal, P., Hall, M., Realff, M. J., Lee, J. H., Bommarius, A. S. Multivariate statistical analysis of X-Ray data from cellulose: A new method to determine degree of crystallinity and predict hydrolysis rates. **Bioresour. Technol.** vol. 101, p. 4461–4471, 2010.
- Baranyai, K. J., Deacon, G. B., MacFarlane, D. R., Pringle, J. M., Scott, J. L. Thermal degradation of ionic liquids at elevated temperatures. **Aust. J. Chem.** vol. 57, p. 145-147, 2004.
- Barthel, S. Heinze, T. Acylation and carbanilation of cellulose in ionic liquids. **Green Chem.** 301-306, 2006.
- Basnett, P., Knowles, C. J., Pishbin, F., Smith, C., Keshavarz, T., Boccaccini, R. A., Roy, I. Novel Biodegradable and Biocompatible Poly(3-hydroxyoctanoate)/Bacterial Cellulose Composites. **Adv. Eng. Mater.** DOI: 10.1002/adem.201180076, 2012.
- Bayly, C. I., Cieplak, P., Cornell, W. D., Kollman, P. A., A well-behaved electrostatic potential based method using charge restraints for deriving atomic charges: the RESP model. **J. Phys. Chem.** vol. 97, p. 10269-10280, 1993.
- Beatriz, A. P., Ass, B. A. P., Frollini, E., Heinze, T. Studies on the homogeneous acetylation of cellulose in the novel solvent dimethyl sulfoxide/tetrabutylammonium fluoride trihydrate. **Macromol. Biosci.** vol. 4, p. 1008–1013, 2004.



- Benjamin, M. A general description of commercial wood pulping and bleaching *processes*. ***J. Air Pollution Control Assoc.***, vol. 19, p. 155-161, 1969.
- BeMiller, J., Whistler, R. *Starch chemistry and technology*, 3rd ed.; ***Academic Press: Amsterdam***, . p. 879, 2009.
- Berger, W., Keck, M., Phillip, B., Schleicher, H. Nature of interactions in the dissolution of cellulose in nonaqueous solvent systems. ***Lenzinger Ber.*** vol. 59, p. 88–95, 1985.
- Bester-Rogac, M., Stopp, A., Johannes, H. J., Hefter, G., Buchner, R. Association of ionic liquids in solution: a combined dielectric and conductivity study of [bmim][Cl] in water and in acetonitrile. ***Phys. Chem. Chem. Phys.*** vol. 13, p. 17588–17598, 2011.
- Bielecki, S., Krystynowicz, A., Turkiewick, M., Kalinowska, H. Bacterial cellulose. ***Polysaccharides and Polyamides in the Food Industry. Properties, Productin and Patents.*** vol. 1, steinbuschel A, Rhee, S, K., Wiley-VCH, Weinheim, 2005.
- Biomass Energy Center. Biomassenergycentre.org.uk. (Accessed on 10 December 2013)
- Bishop, C. A. ***Vacuum deposition onto webs, films, and foils.*** Elsevier publisher, 225, Wyman street, Waltham, ISBN 0-8155-1535-9, p. 165, 2007.
- Bogan, R. T., Brewer, R. J. Cellulose esters, organic. In encyclopedia of polymer science and engineering; Kroschwitz, J.I., Bickford, M., Klingsberg, A., Muldoon, J., Salvatore, A., ***Eds.;*** ***Wiley-Interscience:*** New York, NY, USA, p. 158–181, 1985.
- Bobleter, O. Hydrothermal degradation and fractionation of saccharides and polysaccharides. ***Polysaccharides: Structural Diversity and Functional Versatility*** Dimitriu S, New York: Marcel Dekker, 1998.
- Borysiak, S., Doczekalska, B. X-ray diffraction study of pine wood treated with NaOH. ***Fibres and Textiles in Eastern Europe.*** January/December, vol. 13, p. 87-89, 2005.
- Bracelpa, ***Bracelpa association of Brazilian pulp and paper***, 2009, available online <http://www.bracelpa.org.br> (accessed on December 2013).
- Bracelpa, ***Bracelpa association of Brazilian pulp and paper***, 2011, available online <http://www.bracelpa.org.br> (accessed on December 2013).
- Browning, B. L. ***Methods of Wood Chemistry***, New York: John Wiley, 1967.

- Bruice, T. C. Computational approaches: reaction trajectories, structures, and atomic motions. Enzyme reactions and proficiency. **Chem. Rev.** vol. 106, p. 3119–3139, 2006.
- Buschle-diller, G., & Zeronian, S. H. Enhancing the reactivity and strength of cotton fibres. **J. Appl. Polym. Sci.** vol. 45, p. 967–979, 1992.
- Cai, Z., Hou, C., & Yang, G. Preparation and characterization of a bacterial cellulose/chitosan composite for potential biomedical application. **J. Appl. Polym. Sci.** vol. 121, p. 1488–1494, 2011.
- Caleano S. F., Dillard, B. M. Process Modifications For air pollution control In neutral sulfite semi-chemical mills. **J Air Pollut Control Assoc.** vol. 22, p. 195-199, March 1972.
- Caleman, C., van Maaren, P. J., Hong, M., Hub, J. S., Costa, L. T., van der, S. D., Force field benchmark of organic liquids: density, enthalpy of vaporization, heat capacities, surface tension, isothermal compressibility, volumetric expansion coefficient, and dielectric constant. **J. Chem. Theory. Comput.** vol. 8, p. 61-74, 2012.
- Callais, P. A. Derivatization and characterization of cellulose in lithium chloride and *N,N*-dimethylacetamide solutions. **Ph.D. Thesis, University of Southern Mississippi, Hattiesburg, MS, USA, 1986.**
- Cannetieri, E. V., Silva, J. B. A. E., Felipe, M. G. A. Application of factorial design to the study of xylitol production from eucalyptus hemicellulosic hydrolysate. **Appl. Biochem. Biotech.** vol. 94, p. 159-168, 2001.
- Cao, X., Sessa, J. D., Wolf, J. W., Willett, L. J. Static and dynamic solution properties of corn amylose in *N,N*-dimethylacetamide with 3% LiCl. **Macromolecules.** Vol. 33, p. 3314–3323, 2000.
- Carl, Caleman., Paul, J., van, Maaren., Minyan, Hong., Jochen, S., Hub, Luciano., T. Costa, & David, van der. Spoel. Force field benchmark of organic liquids: density, enthalpy of vaporization, heat capacities, surface tension, isothermal compressibility, volumetric expansion coefficient, and dielectric constant. **J. Chem. Theory Comput.** vol. 8, p. 61-74, 2012.
- Casarano, R., Nawaz, H., Possidonio, S., da Silva, V. C., El Seoud, O. A. A convenient solvent system for cellulose dissolution and derivatization: Mechanistic aspects of the acylation of

- the biopolymer in tetraallylammonium fluoride/dimethyl sulfoxide. *Carbohydr. Polym.* vol. 86, p. 1395–1402, 2011.
- Casarano, R., Fidale, L. C., Lucheti, M. C., Heinze, T., El Seoud, O. A. Expedient, accurate methods for the determination of the degree of substitution of cellulose carboxylic esters: Application of UV–vis spectroscopy (dye solvatochromism) and FTIR. *Carbohydr. Polym.* vol. 83, p. 1285–1292, 2011.
- Casarano, R. El Seoud. O. A. Successful application of an ionic liquid carrying the fluoride counter-ion in biomacromolecular chemistry: microwave-assisted acylation of cellulose in the presence of 1-allyl-3-methylimidazolium fluoride/DMSO mixtures. *Macromol. Biosci.* vol. 13, p. 191–202, 2013.
- Casarano, R., Pires, P. A. R., El Seoud. O. A. Acylation of cellulose in a novel solvent system: Solution of dibenzyltrimethylammonium fluoride in DMSO. *Carbohydr. Polym.* vol. 101 p. 444-450, 2014.
- Catalán, J., Toward a generalized treatment of the solvent effect based on four empirical scales: dipolarity (SdP, a new scale), polarizability (SP), acidity (SA), and basicity (SB) of the medium. *J. Phys. Chem. B.* vol. 113, p. 5951–5960, 2009.
- Ciacco, G. T., Liebert, T. F., Frollini, E., Heinze, T. Application of the solvent dimethylsulfoxide /tetrabutylammonium fluoride trihydrate as reaction medium for the homogeneous acylation of sisal cellulose. *Cellulose.* vol. 10, p. 125 –132, 2003.
- Chiappe, C.; Pieraccini, D. Ionic liquids: solvent properties and organic reactivity. *J. Phys. Org. Chem.* vol. 18, p. 275-297, 2005.
- Chaudemanche, C., Navard, P. Swelling and dissolution mechanisms of regenerated Lyocell cellulose fibers. *Cellulose.* vol. 18, p. 1–15, 2011.
- Chempath, S., Boncella, J. M., Pratt, L. R., Henson, N., Pivovar, B. S. Density functional theory study of degradation of tetraalkylammonium hydroxides. *J. Phys. Chem. C,* vol. 114, p. 11977–11983, 2010.
- Chrapava, S., Touraud, D., Rosenau, T., Potthast, A., Kunz, W. The investigation of the influence of water and temperature on the LiCl/DMAC/cellulose system. *Phys. Chem. Chem. Phys.* vol. 5, p. 1842–1847, 2003.

- Christian, R., Welton, T. Solvents and solvent effects in organic chemistry. (4th, updated and enl. ed. ed.). **Wiley-VCH. Weinheim.** p. 360, 2010.
- Crawford, R. L. *Lignin biodegradation and transformation.* **John Wiley. New York:** ISBN 0-471-05743-6, 1981.
- Crosthwaite, J. M., Aki, S. N. V. K., Maginn, E. J., Brennecke, J. F. Liquid phase behavior of imidazolium-based ionic liquids with alcohols: effects of hydrogen bonding and non-polar interactions. **Fluid Phase Equilib.** vol. 228-229, p. 303-309, 2005.
- Crowhurst, L., Mawdsley, P. R., Perez-Arlandis, J. M., Salter, P. A., Welton, T. Solvent-solute interactions in ionic liquids. **Phys. Chem. Chem. Phys.** vol. 5, p. 2790-2794, 2003.
- Cuissinat, C., Navard, P. Swelling and dissolution of cellulose part II: free floating cotton and wood fibres in NaOH-water-additives systems. **Macromol. Symp.** vol. 244, p. 19-30, 2006.
- Dalmeida, M. L. O. Chemical composition of lignocellulosic material. **Pulp and paper technology for manufacture of pulp.** IPT: São Paulo. vol. 1, p. 45-106, 1988.
- Das, B., Reddy, V. S., Tehseen, F. A mild, rapid and highly regioselective ring-opening of epoxides and aziridines with acetic anhydride under solvent-free conditions using ammonium-12-molybdophosphate. **Tetrahedron Lett.** vol. 47, p. 6865-6868, 2006.
- Dawsey, T. R., McCormick, C. L. The lithium chloride/*N,N*-dimethylacetamide solvent for cellulose: A literature review. **J. Macromol. Sci. Rev. Macromol. Chem. Phys.** vol. C30, p. 405-440, 1990.
- Diamantoglou, M., Vienken, J. Strategies for the development of hemocompatible dialysis membranes. **Macromol. Symp.** vol. 103, p. 31-42, 1996.
- Deguchi, S., Tsujii, K., Horikoshi, K. Cooking cellulose in hot and compressed water. **Chem. Commun.** vol. 31, p. 3293-3295, 2006.
- Diddens, I., Murphy, B., Krisch, M., Mueller, M. Anisotropic Elastic Properties of Cellulose Measured Using Inelastic X-ray Scattering. **Macromolecules.** vol. 41, p. 9755-9759, 2008.
- Diniz, J. M. B. F., Gil, M. H. Castro. J. A. A. M. Hornification—its origin and interpretation in wood pulps. **Wood Sci. Technol.** vol. 37, p. 489-494, 2004.
- Docherty, K. M., Kulpa, J., Charles, F. Toxicity and antimicrobial activity of imidazolium and pyridinium ionic liquids. **Green Chem.** vol. 7, p. 185-189, 2005.

- Dong, K.S. Zhang, J. Wang D. Yao, X. Q. Hydrogen bonds in imidazolium ionic liquids. *J. Phys. Chem. A*, vol. 110, p. 9775–9782, 2006.
- Duchemin, B. J. C., Staiger, M. P., Tucker, N. Newman, R.H. Aerocellulose based on all-cellulose composites. *J. Appl. Polym. Sci.* vol. 115, p. 216–221, 2010.
- Dupont, J., de Souza, R. F., Suarez, P. A. Z. Ionic liquids (molten salts) phase organometallic catalysis. *Chem. Rev.* vol. 102, p. 3667–3692, 2002.
- Eastmond, G. C., Ledwith, A., Russo, S., Sigwalt, P. *In Comprehensive polymer science; Eds; Pergamon Press: New York*, vol. 6, p. 135, 1989.
- Edgar, K. J., Arnold, K. M., Blount, W. W., Lawniczak, J. E., Lowman, D. W. Synthesis and properties of cellulose acetoacetate. *Macromolecules.* vol. 28, p. 4122–4128, 1995.
- Ekmanis, J. L., Turbak, A. F. Lab Highlights 251, *Waters Chromatography Division, Millipore, Milford*; 1986.
- Ekmanis, J. L. Gel permeation chromatographic analysis of cellulose. *Am. Lab. News*, vol. 19, p. 10–11, 1987.
- El-Kafrawy, A. Investigation of the Cellulose/LiCl/dimethylacetamide and cellulose/LiCl/N-methyl-2-pyrrolidinone solutions by <sup>13</sup>C-NMR spectroscopy. *J. Appl. Polym. Sci.* vol. 27, p. 2435–2443, 1982.
- El Seoud, O. A., Menegheli, P., Pires, P. A. R., & Kiyam, N. Kinetics and mechanism of the imidazole-catalyzed hydrolysis of substituted N-benzoylimidazoles. *J. Phys. Org. Chem.* vol. 7, p. 431–436, 1994.
- El Seoud, O. A., Marson, G. A., Ciacco, G. T., Frollini, E. An efficient, one-pot acylation of cellulose under homogeneous reaction conditions. *Macromol. Chem. Phys.* vol. 201, p. 882–889, 2000.
- El Seoud, O. A., Heinze, T. Organic esters of cellulose: New perspectives for old polymers. *Adv. Polym. Sci.* vol. 186, p. 103–149, 2005.
- El Seoud, O. A. Solvation in pure and mixed solvents: Some recent developments. *Pure Appl. Chem.* vol. 79, p. 1135–1151, 2007.

- El Seoud, O. A., Koschella, A., Fidale, L. C., Dorn, S., Heinze, T. Applications of ionic liquids in carbohydrate chemistry: a window of opportunities. *Biomacromolecules*. vol. 8, p. 2629–2647, 2007.
- El Seoud, O. A. Understanding solvation. *Pure Appl. Chem*. vol. 81, p. 697-707, 2009.
- El Seoud, O. A., da Silva, V. C., Possidonio, S., Casarano, R., Arêas, E. P. G., Gimenes, P. Microwave-assisted derivatization of cellulose, 2—The surprising effect of the structure of ionic liquids on the dissolution and acylation of the biopolymer. *Macromol. Chem. Phys*. vol. 212, p. 2541–2550, 2011.
- El Seoud, O. A., Nawaz, H., Arêas, E. P. G. Chemistry and applications of polysaccharide solutions in strong electrolytes/dipolar aprotic solvents: an overview. *Molecules*. Vol. 18, p. 1270-1313, 2013.
- Fidale, L. C., Heinze, T. El Seoud, O.A. Perichromism: A powerful tool for probing the properties of cellulose and its derivatives. *Carbohydr. Polym*. vol. 93, p. 129-134, 2013.
- Feng, L., Chen, Z.-I. Research progress on dissolution and functional modification of cellulose in ionic liquids, *J. Mol. Liq*. vol. 142, p. 1-5, 2008.
- Fengel, D., Wegener, G., *Wood, de Gruyter & Co., Berlin*: 1989.
- Fengel, D. Stoll, M. Crystals of cellulose grown from TFA solution. *Wood Sci. Technol*. vol. 23, p. 85-94, 1989.
- Fenn, D., Pohl, M., Heinze, T. Novel 3-*O*-propargyl cellulose as a precursor for regioselective functionalization of cellulose. *React. Funct. Polym*. vol. 69, p. 347–352, 2009.
- Fernandes Diniz, J.M.B., Gil, M.H. Castro, J.A.A.M. Hornification—its origin and interpretation in wood pulps. *Wood Sci. Technol*. vol. 37, p. 489-494, 2004.
- Fidale, L. C., Possidonio, S., El Seoud, O. A. Application of 1-allyl-3-(1-butyl)imidazolium chloride in the synthesis of cellulose esters: properties of the ionic liquid, and comparison with other solvents. *Macromol. Biosci*. vol. 9, p. 813–821, 2009.
- Fidale, L., C. G. Biopolymer modification. Aspects of cellulose derivatization under homogeneous reaction conditions. *Ph.D. Thesis, University of São Paulo, São Paulo, Brazil*. 2010

- Fink, H-P., Hofmann, D., Purz, H. Zur fibrillarstruktur nativer cellulose. *Acta Polym.* vol. 41, p. 131-137, 1990.
- French, A, D., Bertoniere, N. R. Cellulose. In: Kirk-Othmer *Encyclopedia of Chemical Technology*. Interscience, New York, vol 5. p. 476-496, 1993.
- Frisch, M. J., Trucks, G. W., Schlegel, H. B., Scuseria, G. E., Robb, M. A., Cheeseman, J. R., Scalmani, G., Barone, V., Mennucci, B., Petersson, G. A., Nakatsuji, H., Caricato, M., Li, X., Hratchian, H. P., Izmaylov, A. F., Bloino, J., Zheng, G., Sonnenberg, J. L., Hada, M., Ehara, M., Toyota, K., Fukuda, R., Hasegawa, J., Ishida, M., Nakajima, T., Honda, Y., Kitao, O., Nakai, H., Vreven, T., Montgomery, Jr., J. A., Peralta, J. E., Ogliaro, F., Bearpark, M., Heyd, J. J., Brothers, E., Kudin, K. N., Staroverov, V. N., Kobayashi, R., Normand, J., Raghavachari, K., Rendell, A., Burant, J. C., Iyengar, S. S., Tomasi, J., Cossi, M., Rega, N., Millam, J. M., Klene, M., Knox, J. E., Cross, J. B., Bakken, V., Adamo, C., Jaramillo, J., Gomperts, R., Stratmann, R. E., Yazyev, O., Austin, A. J., Cammi, R., Pomelli, C., Ochterski, J. W., Martin, R. L., Morokuma, K., Zakrzewski, V. G., Voth, G. A., Salvador, P., Dannenberg, J. J., Dapprich, S., Daniels, A. D., Farkas, Ö., Foresman, J. B., Ortiz, J. V., Cioslowski, J., Fox, D. J., Gaussian 09, Revision A.02. *Gaussian, Inc., Wallingford*. 2009.
- Frommer, J. Scanning tunnelling microscopy and atomic force microscopy in organic chemistry. *Angew. Chem.* vol. 31, p. 1298-1328, 1992.
- Gagnaire, D., Saint-Germain, J., Vincendon, M. NMR evidence of hydrogen bonds in cellulose solutions. *J. Appl. Polym. Sci. Appl. Polym. Symp.* vol. 37, p. 261–275, 1983.
- Gardner, K. H., Blackwell, J. The structure of native cellulose. *Biopolymers*. vol. 13, p. 1975-2001, 1974.
- Gericke, M., Liebert, T., Heinze, T. Interaction of ionic liquids with polysaccharides, 8 - synthesis of cellulose sulfates suitable for polyelectrolyte complex formation. *Macromol. Biosci.* vol. 9, p. 343-353, 2009.
- Gericke, M., Fardim, P., Heinze, T. Ionic liquids-promising but challenging solvents for homogeneous derivatization of cellulose. *Molecules*, vol. 17, p. 7458-7502, 2012.

- Glasser, W. G., Becker, U., Todd, G. J. Novel cellulose derivatives: Part VI. preparation and thermal analysis of two novel cellulose esters with fluorine-containing substituents. **Carbohydr. Polym.** vol. 42, p. 393–400, 2000.
- Gomes, T. C. F., Skaf, M. S., Cellulose-builder: A toolkit for building crystalline structures of cellulose. **J. Comput. Chem.** vol. 33, p. 1338-1346, 2012.
- Graenacher, C. Cellulose Solution. US Patent 1, 943,176, 1934.
- Granstrom, M., Olszewska, A., Makela, V., Heikkinen, S., Kilpelainen, I. A new protection group strategy for cellulose in an ionic liquid: simultaneous protection of two sites to yield 2,6-di-O-substituted mono-*p*-methoxytrityl cellulose. **Tetrahedron Lett.** vol. 50. p. 1744-1747, 2009.
- Gruber, E., Gruber, R. Viscosimetric determination of the degree of polymerization of cellulose. **Papier.** vol. 35, p. 133–141, 1981.
- Guo, Y., Wang, X., Li, D., Du, H., Wang, X., Sun, R. Synthesis and characterization of hydrophobic long-chain fatty acylated cellulose and its self-assembled nanoparticles. **Polym. Bull.** vol. 69, p. 389–403, 2012.
- Habibi, Y., Lucia, L. A., Rojas, O., J. Cellulose nanocrystals: chemistry, self-assembly and applications. **Chem. Rev.** vol. 110, p. 3479-3500, 2010.
- Hacon, J., Morris, A., Johnston, M. J., Shanahan, S. E., Barker, M. D., Inglis, G. G. A., Macdonald, S. J. F. Carbon-carbon bond forming reactions with substrates absorbed non-covalently on a cellulose chromatography paper support. **Chem. Commun.** vol. 6, p. 625-627, 2007.
- Hanbin, L., Kenneth, L., Holmes, B. M., Simmons, B. A., Singh, S. Understanding the interactions of cellulose with ionic liquids: a molecular dynamics study. **J. Phys. Chem. B.** vol. 114, p. 4293–4301, 2010.
- Hanley, S. J., Giasson, J., Revol, J-F. Gray, D. G. Atomic force microscopy of cellulose microfibrils - comparison with transmission electron-microscopy. **Polymer.** vol. 33, p. 4639-4642, 1992.
- Hao, Y., Peng, J., Li, J., Zhai, M., Wei, G. An ionic liquid as reaction media for radiation-induced grafting of thermosensitive poly (*N*-isopropylacrylamide) onto microcrystalline cellulose. **Carbohydr. Polym.** vol. 77, p. 779-784, 2009.



- Harris, K. R., Kanakubo, M., Woolf, L. A. Temperature and pressure dependence of the viscosity of the ionic liquid 1-butyl-3-methylimidazolium tetrafluoroborate: viscosity and density relationships in ionic liquids. *J. Chem. Eng. Data.* vol. 53, p. 1230, 2008.
- Hauru, L. K. J., Hummel, M., King, A. W. T., Kilpeläinen, I., Sixta, H. Role of solvent parameters in the regeneration of cellulose from ionic liquid solutions. *Biomacromolecules.* vol. 13, p. 2896–2905, 2012.
- Headley A. D. and N. M. Jackson, The effect of the anion on the chemical shifts of the aromatic hydrogens of liquid 1-butyl-3-methylimidazolium salts. *J. Phys. Org. Chem.* vol. 15, p. 52–55, 2002.
- Heinze, T., Rahn, K. Cellulose *p*-toluenesulfonate: a valuable intermediate in cellulose chemistry. *Macromol. Symp.* vol. 120, p. 103–113, 1997.
- Heinze, T. New ionic polymers by cellulose functionalization. *Macromol. Chem. Phys.* vol. 199, p. 2341–2364, 1998.
- Heinze, T., Dicke, R., Koschella, A., Kull, A. H., Klohr, E-A., Koch, W. Effective preparation of cellulose derivatives in a new simple cellulose solvent. *Macromol. Chem. Phys.* vol. 201, p. 627–631, 2000.
- Heinze, T., Koschella, A., Magdaleno-Maiza, L., Ulrich, A. S. Nucleophilic displacement reactions on tosyl cellulose by chiral amines. *Polym. Bull.* vol. 46, p. 7–13, 2001.
- Heinze, T., Liebert, T. Unconventional methods in cellulose fictionalization. *Prog. Polym. Sci.* vol. 26, p. 1689-1762, 2001.
- Heinze, T., Liebert, T. F., Pfeiffer, K. S., Hussain, M. A. Unconventional cellulose esters: synthesis, characterization *Cellulose.* vol. 10, p. 283–296, 2003.
- Heinze, T. Carboxymethyl ethers of cellulose and starch—A review. *Khimiya Rastitel'nogo Syr'ya* vol. 3, p. 13–29, 2005.
- Heinze, T. Schwikal, K. Barthel, S. Ionic liquids as reaction medium in cellulose functionalization. *Macromol. Biosci.* vol. 5, p. 520-525, 2005.
- Heinze, T., Koschella, A., Brackhagen, M., Engelhardt, J., Nachtkamp, K. Studies on non-natural deoxyammonium cellulose. *Macromol. Symp.* vol. 244, p. 74–82, 2006.

- Heinze, T., Pohl, M., Schaller, J., Meister, F. Novel bulky esters of cellulose. *Macromol. Biosci.* vol. 7, p. 1225–1231, 2007.
- Heinze, T., Lincke, T., Fenn, D., Koschella, A. Efficient allylation of cellulose in Dimethyl sulfoxide/tetrabutylammonium fluoride trihydrate. *Polym. Bull.* vol. 61, p. 1–9, 2008.
- Heinze, T. Hot topics in polysaccharide chemistry—selected examples. *Macromol. Symp.* vol. 280, p. 15–27, 2009.
- Heinze, T., Koehler, S. Dimethyl sulfoxide and ammonium fluorides novel cellulose solvents. *ACS Symp. Series.* vol. 1033, p. 103–118, 2010.
- Heinze, T., Sarbova, V., Nagel, V. C. M. Simple synthesis of mixed cellulose acylate phosphonates applying n-propyl phosphonic acid anhydride. *Cellulose.* vol. 19, p. 523–531, 2012.
- Heinze, T., Wang, Y., Koschella, A., Sullo, A., Foster, J. T. Mixed 3-mono, *O*-alkyl cellulose: synthesis, structure characterization and thermal properties. *Carbohydr. Polym.* vol. 90, p. 380–386, 2012.
- Hendrickson, E. R. Control Of Atmospheric Emissions In The Wood Pulping Industry, vol. I, HEW Contract Number CPA-22-69-18, *U. S. Environmental Protection Agency, Washington, DC*, March 15, 1970.
- Henniges, U., Kostic, M., Borgards, A., Rosenau, T., Potthast, A. Dissolution behavior of different celluloses. *Biomacromolecules.* vol. 12, p. 871–879, 2011.
- Herlinger, H., Hengstberger, M. Behavior of cellulose in unconventional solvents. *Lenzinger Ber.* vol. 59, p. 96–104, 1985.
- Hesse-Ertelt, S., Heinze, T., Kosan, B., Schwikal, K., Meister, F. Solvent effects on the NMR chemical shifts of imidazolium-based ionic liquids and cellulose therein. *Macromol. Symp.* vol. 294-II, p. 75–89, 2010.
- Heuser, E., Heath, M., Shockley, W. H. The rate of esterification of primary and secondary hydroxyls of cellulose with *p*-toluenesulfonyl (tosyl) chloride. *J. Am. Chem. Soc.* vol. 72, p. 670–674, 1950.
- Heyn, A. N. J., The microcrystalline structure of cellulose in cell walls of cotton, Ramie, and Jute Fibers As revealed By Negative Staining of Reactins. *J. Cell. Biol.* vol. 29, p. 181–197, 1966.

- Honjo, G. Watanabe, M. Examination of cellulose fiber by the low-temperature specimen method of electron diffraction and electron microscopy. **Nature**. vol. 181, p. 326-328, 1958.
- Huddleston, J. G., Broker, G. A., Willauer, H. D., Rogers, R. D. Free-energy relationships and solvatochromatic properties of 1-alkyl- 3-methylimidazolium ionic liquids. In *Ionic Liquids Industrial Applications for Green Chemistry*; **American Chemical Society: Washington, DC**, vol. 818, p. 270-288, 2002.
- Huglin, M. *Light scattering from polymer solutions*; **Academic Press: New York, NY, USA**, 1972.
- Humphrey, W., Dalke, A., Schulten, K., VMD - Visual Molecular Dynamics. **J. Mol. Graphics**. vol. 14, p. 33-38, 1996.
- Hussain, M. A., Liebert, T., Heinze, T. Acylation of cellulose with *N,N'*-carbonyldiimidazole-activated acids in the novel solvent dimethyl sulfoxide/tetrabutylammonium fluoride. **Macromol. Rapid Commun**. vol. 25, p. 916–920, 2004.
- Ishii, D., Tatsumi, D., Matsumoto, T. Effect of solvent exchange on the solid structure and dissolution behavior of cellulose. **Biomacromolecules**. vol. 4, p. 1238–1243, 2003.
- Isogai, A., Ishizu, A., Nakano, J. Preparation of tri-*O*-alkylcelluloses by the use of a nonaqueous cellulose solvent and their physical characteristics. **J. Appl. Polym. Sci**. vol. 31, p. 341–352, 1986.
- Isogai, A., Ishizu, A., Nakano, J. Dissolution mechanism of cellulose in sulfur dioxide-amine-dimethyl sulfoxide. **J. Appl. Polym. Sci**. vol. 33, p. 1283–1290, 1987.
- Izatt, R. M., Rytting, J. H., Hansen, L. D., Christensen, J. J. Thermodynamics of proton dissociation in dilute aqueous solution. V. An entropy titration study of adenosine, pentoses, hexoses, and related compounds. **J. Am. Chem. Soc**. vol, 88, p. 2641–2645, 1966.
- Jain, R. K., Agnish, S. L., Lal, K., Bhatnagar, H. L. Reactivity of hydroxyl groups in cellulose towards chloro(*p*-tolyl)methane. **Makromol Chem**. vol. 186 p. 2501–2512, 1985.
- Jiang, J. C., Lin, K. H., Li, S. C., Pao-Ming, S. P. M., Hung, K. C., Lin, S. H., Chang, H. C., Association structures of ionic liquid/DMSO mixtures studied by high-pressure infrared spectroscopy. **J. Chem. Phys**. vol. 134, 044506, 2011.

- Jorgensen, W. L., Optimized intermolecular potential functions for liquid alcohols. *J. Phys. Chem.* vol. 90, p. 1276-1284, 1986.
- Jorgensen, W. L., Maxwell, D. S., & Tirado-Rives, J. Development and testing of the OPLS all-atom force field on conformational energetics and properties of organic liquids. *J. Am. Chem. Soc.* vol. 118, p. 11225-11236, 1996.
- Jorgensen, W. L.; & Tirado-Rives, *J. Proc. Natl. Acad. Sci. U.S.A.* vol. 102, p. 6665, 2005.
- Kamide, K.; Miyazaki, Y.; Abe, T.; Mark-Houwink-Sakurada equations of cellulose triacetate in various solvents. *Makromol. Chem.* vol, 180, p. 2801, 1979.
- Kaminski, G. A., & Jorgensen, W. L. A quantum mechanical and molecular mechanical method based on CM1A charges: applications to solvent effects on organic equilibria and reactions. *J. Phys. Chem. B*, vol. 102, p. 1787-1796, 1998.
- Kenichi, T. Preparation of sulfonic acid anhydrides. *Jpn. Kokai Tokkyo Koho*, (JP 2003277345 A 20031002, 2003a.
- Kenichi, T. Purification of sulfonic acid anhydrides. *Jpn. Kokai Tokkyo Koho*, (JP 2003238522 A 20030827, 2003b.
- Kennedy, G. L., Jr. Biological effects of acetamide, formamide, and their monomethyl and dimethyl derivatives: Critical review. *Toxicology*. vol. 17, p. 129–182, 1986.
- Khaja, S. D., Xue, J., Ceric ammonium nitrate: novel and robust acetylating catalyst. *Lett. Org. Chem.* vol. 3, p. 554–557, 2006.
- Klemm, D., Phillip, B., Heinze, T., Heinze, U., Wagenknecht, W. *Comprehensive Cellulose Chemistry; Wiley-VCH: Weinheim*, vol. 1, p. 133, 1998.
- Klemm, D., Schumann, D., Udhardt, U., & Marsch, S. Bacterial synthesized cellulose – Artificial blood vessels for microsurgery. *Prog. Polym. Sci.* vol. 26, p. 1561–1603, 2001.
- Klemm, D. Heublein, B. Fink, H. P. Bohn, A. Fascinating biopolymer and sustainable raw material. *Angew. Chem. Int. Ed.*, vol. 44, p. 3358–3393, 2005.
- Klock, U., Muniz, G. I. B., Hernandez, J. A., Andrade, A. S. Quimica de Madeira, Curitiba: Universidade federal do parana, vol. 3, 2005.
- Kluge, S., Weston, J. Can a hydroxide ligand trigger a change in the coordination number of magnesium ions in biological systems? *Biochemistry*, vol. 44, p. 4877–4885, 2005.

- Koel, M., Ed. *Ionic liquids in chemical analysis*; **CRC Press: Boca Raton**, FL, USA, 2009.
- Köhler, S., Heinze, T. New solvents for cellulose: dimethyl sulfoxide/ammonium fluorides. **Macromol. Biosci.** vol, 7, p. 307–314, 2007.
- Koehler, S., Liebert, T., Schoebitz, M., Schaller, J., Meister, F., Guenther, W., Heinze, T. Interactions of ionic liquids with polysaccharides 1. unexpected acetylation of cellulose with 1-ethyl-3-methylimidazolium acetate. **Macromol. Rapid Commun.** vol. 28, p. 2311-2317, 2007.
- Koehler, S., Heinze, T. Efficient synthesis of cellulose furoates in 1-*N*-butyl-3-methylimidazolium chloride. **Cellulose**, vol. 14, p. 489-495, 2007.
- Kolb, C. H., Finn, M. G. Sharpless, K. B. "Click Chemistry: Diverse Chemical Function from a Few Good Reactions". **Angew. Chem. Intl. Ed.**..vol. 40, p. 2004-2021, 2001.
- Koschella, A., Heinze, T., Klemm, D. First synthesis of 3-*O*-functionalized cellulose ethers via 2,6-di-*O*-protected silyl cellulose. **Macromol. Biosci.** vol. 1, p. 49–54, 2001.
- Kondo, T. Preparation of 6-*O*-alkylcelluloses. **Carbohydr Res.** vol. 238 p. 231–240, 1993.
- Krässig, H. *Ullman's Encyclopedia of Industrial Chemistry, Campbell FT*, 5th ed.; Pfeifferkorn, R., Rousaville, J. F., **Eds.; VCH: Weinheim, Germany**, vol. 5, p. 375, 1986.
- Krässig, H. A. Cellulose: structure, accessibility and reactivity. **Gordon and Breach Publishers. Philadelphia.** ISBN 2-88124- 798-9. vol. 11, p. 307-313, 1993.
- Kuutti, L., Peltonen, J., Pene, J. and Teleman, O. Identification and surface-structure of crystalline cellulose studied by atomic force microscope. **Journal of Microscopy – Oxford.** vol. 178, p. 1-6, 1995.
- Kwatra HS, Caruthers JM, Tao BY. Synthesis of long chain fatty acids esterified onto cellulose via the vacuum-acid chloride process. **Ind Eng Chem Res.** vol. 31, 2647–2651, 1992.
- Kwolek, S., Morgan, P. W., Schaeffgen, J. R., Gulrich, L. W. Synthesis, anisotropic solutions, and fibers of poly(1,4-benzamide). **Macromolecules.** vol. 10, p. 1390–1396, 1977.
- Laurence, C., Nicolet, P., Dalati, M.T., Abboud, J-L, M. Notario., R. The Empirical Treatment of Solvent-Solute Interactions: 15 Years of  $\pi^*$  **J. Phys. Chem.** vol. 98, p. 5807-5816, 1994.
- Lavoine, N., Desloges, I., Dufresne, A., Bras, J. Microfibrillated cellulose- its barrier properties and applications in cellulosic materials: A review. **Carbohydr. Polym.** vol. 90, p. 735-764, 2012.

- Law, R. C. Cellulose acetate in textile application. **Macromol. Symp.** vol, 208, p. 255–265, 2004.
- Legeza, V. I., Galenko-Yaroshevskii, V. P., Zinov'ev, E. V., Paramonov, B. A., Kreichman, G. S., Turkovskii, I. I., et al. Effects of new wound dressings on healing of thermal burns of the skin in acute radiation disease. **Bull. Exp. Biol. Med.** vol. 138, p. 311–315, 2004.
- Leinter, W. Supercritical carbon dioxide as a green reaction medium for catalysis. **Acc. Chem. Res.** vol. 35, p. 746-756, 2002.
- Li, J., Martin-Sampedro, R., Pedrazzi, C., Gellerstedt, G. Fractionation and characterization of lignin-carbohydrate complexes (LCCs) from eucalyptus fibers. **Holzforschung**, vol. 65, p. 43–50, 2011.
- Lide, D. R., *CRC Handbook of chemistry and physics*: In: Lide, D. R. ed., 85<sup>th</sup> edition., CRC Press: Boca Raton, Florida, 2004.
- Liebert, T., Haensch, C., Heinze, T. Click chemistry with polysaccharides. **Macromol. Rapid Commun.** vol. 27, p. 208–213, 2006.
- Liebert, T., Heinze, T. Interaction of ionic liquids with polysaccharides. 5. Solvents and reaction media for the modification of cellulose. **BioResources** vol. 3, p. 576–601, 2008.
- Liebert, T., Heinze, T., Edgar, K.J., Eds. *Cellulose solvents: for analysis, shaping and chemical modification*; **ACS Symposium Series; Washington, DC**, USA, 2010.
- Lindman, B., Karlstroem, G., Stigsson, L. On the mechanism of dissolution of cellulose. **J. Mol. Liq.** vol. 156, p. 76–81, 2010.
- Linko, Y-Y. Viskari, R., Pohjola, L., Linko, P. Preparation and performance of cellulose beadentrapped whole cell glucose isomerase. **J. Solid-Phase Biochem.** vol. 2, p. 203-212, 1977.
- Liu, Y., Liu, L., Lu, Y., Cai, Y. An imidazolium tosylate salt as efficient and recyclable catalyst for acetylation in an ionic liquid. **Monatshefte Chem.**, vol. 139, p. 633-638, 2008.
- Liu, H., Kar, N., Edgar, J. K. Direct synthesis of cellulose adipate derivatives using adipic anhydride. **Cellulose.** vol. 19, p. 1279–1293, 2012.
- Ma, C., Xu, X-L., Ai, P., Xie, S-M., Lv, Y-C., Shan, H-Q., Yuan, L-M. Chiral separation of D, L-mandelic acid through cellulose membranes. **Chirality**, vol. 23, p. 379–382, 2011.

- Makowska, A., Dyoniziak, E., Siporska, A., Szydłowski, J. Miscibility of ionic liquids with polyhydric alcohols. *J. Phys. Chem. B*, vol. 114, p. 2504-2508, 2010.
- Malm, C. J., Tanghe, L. O., Laird, B. C., Smith, G. D. Relative rates of acetylation of the hydroxyl groups in cellulose acetate. *J. Am. Chem. Soc.* vol. 75, p. 80–84, 1953.
- Maneerung, T., Tokura, S., & Rujiravanit, R. Impregnation of silver nanoparticles into bacterial cellulose for antimicrobial wound dressing. *Carbohydr. Polym.* vol. 72, p. 43–51, 2008.
- Manno, M., Ruge, M., Cocheo, V. Double fatal inhalation of dichloromethane. *Hum. Exp. Toxicol.* vol. 11, p. 540–545, 1992.
- Marsano, E., Canetti, M., Conio, G., Corsini, P., Freddi, G. Fibers based on cellulose-silk fibroin blend. *J. Appl. Polym. Sci.* vol. 104, p. 2187–2196, 2007.
- Marson, G. A., El Seoud, O. A. A novel, efficient procedure for acylation of cellulose under homogeneous solution conditions. *J. Appl. Polym. Sci.* vol. 74, p. 1355–1360, 1999.
- Marson, G. A., El Seoud, O. A. Cellulose dissolution in lithium chloride/*N,N*-dimethylacetamide solvent system: relevance of kinetics of decrystallization to cellulose derivatization under homogeneous solution conditions. *J. Polym. Sci. A Polym. Chem.* vol. 37, p. 3738–3744, 1999.
- Marson, G. Acylation of cellulose under homogeneous reaction conditions. *M.Sc. Thesis, University of Sao Paulo, São Paulo*, Brazil, 1999.
- Martin, A. R., Martins, M. A., Mattoso, L. H. C., Silva, O. R. R. F. Chemical and structural characterization of sisal fibers from *Agave sisalana* variety. *Polímeros: Ciência e Tecnologia*, vol. 19, p. 40-46, 2009.
- Martínez, L., Andrade, R., Birgin, E. G., Martínez, J. M., Packmol: A package for building initial configurations for molecular dynamics simulations. *J. Comput. Chem.* vol. 30, p. 2157-2164, 2009.
- McCormick, C. L., Lichatowich, D. K. Homogeneous solution reactions of cellulose, chitin, and other polysaccharides to produce controlled-activity pesticide systems. *J. Polym. Sci. Polym. Lett. Ed.* vol. 17, p. 479–484, 1979.
- McCormick, C. L. Cellulose solutions. **US 4278790 A**, 14 July 1981.
- McCormick, C. L., Callais, P. A., Hutchinson, B. H. Jr. Solution studies of cellulose in lithium chloride and *N,N*-dimethylacetamide. *Macromolecules*, vol. 18, p. 2394–2401, 1985.

- McCormick, C. L., Dawsey, T. R., Newman, J. K. Competitive formation of cellulose *p*-toluenesulfonate and chlorodeoxycellulose during homogeneous reaction of *p*-toluenesulfonyl chloride with cellulose in *N,N*-dimethylacetamide-lithium chloride. ***Carbohydr. Res.*** vol. 208, p. 183–191, 1990.
- Medronho, B., Romano, A., Miguel, M-G., Stigsson, L., Lindman, B. Rationalizing cellulose (in) solubility: reviewing basic physicochemical aspects and role of hydrophobic interactions. ***Cellulose.*** vol. 19, p. 581-587, 2012.
- Meng, T., Gao, X., Zhang, J., Yuan, J., Zhang, Y., He, J. Graft copolymers prepared by atom transfer radical polymerization (ATRP) from cellulose. ***Polymer,*** vol. 50, p. 447-454, 2009.
- Menger, F. M., On the source of intramolecular and enzymatic reactivity. ***Acc. Chem. Res.*** vol. 18, p. 128-134, 1985.
- Meyer, K. H. and Misch, L. Positions des atomes dans le nouveau modele spatial de la cellulose. ***Helv. Chim. Acta.*** vol. 20, p. 232-245, 1937.
- Moellmann, E., Heinze, T., Liebert, T., Sarah, K. Homogeneous synthesis of cellulose ethers in ionic liquids. ***US 20090221813,*** 3 September 2009.
- Morgenstern, B., Kammer, H. W., Berger, W., Skrabal, P. Lithium-7 NMR study on cellulose/lithium chloride/*N,N*-dimethylacetamide solutions. ***Acta Polym.*** vol. 43, p. 356–357, 1992.
- Mühlethaler, K., ***In Cellulose Ultrastructure of Woody Plants,*** Cote, W.A. (Ed.), Syracuse: Syracuse University Press, p. 191-198, 1965.
- Muthukumar, M. Kuzmina O., Sashina E., Wawro D., Troshenkowa S. ***Fibres & Textiles in Eastern Europe.*** vol. 18, p. 32-37, 2010.
- Mussato, I. S., Roberto, I. C. Biotechnological production of xylitol from rice straw. ***Sci. biotech. Development.*** vol. 28, p. 34-39, 2002.
- Nagel, M. C. V., Heinze, T. Esterification of cellulose with acyl-1*H*-benzotriazole. ***Polym. Bull.*** vol. 65, p. 873–881, 2010.
- Nawaz, H., Casarano, R., El Seoud, O. A. First report on the kinetics of the uncatalyzed esterification of cellulose under homogeneous reaction conditions: a rationale for the



effect of carboxylic acid anhydride chain-length on the degree of biopolymer substitution. **Cellulose**. vol. 19, p. 199–207, 2012.

Nawaz, H., Pires, P. A. R., El Seoud, O. A. Kinetics and mechanism of imidazole-catalyzed acylation of cellulose in LiCl/*N,N*-dimethylacetamide, **Carbohydr. Polym.** vol. 92, p. 997–1005, 2013.

Neese, F., Becker, U., Ganiouchine, D., Kobmann, S., Petrenko, T., Riplinger, C., Orca - an ab initio, **DFT and semiempirical SCF-MO package (Version 2.9)**. Germany: University of Bonn, 2011.

Nevell, T. P., Zeronian, S. H. Cellulose chemistry and its applications. **Ellis Horwood Limited, London**: 1985.

Nevell, T.P, and Zeronian, S. H. Cellulose chemistry and its applications, **Ellis Horwood Limited, Chichester, West Sussex, PO 19, 1EB**, p. 266-267, 1987.

Ngo, H. L., LeCompte, K., Hargens, L., McEwen, A. B. Thermal properties of imidazolium ionic liquids. **Thermochim. Acta**, vol. 357-358, p. 97-102, 2000.

Nishi, Y., Uryu, M., Yamanaka, S., Watanabe, K., Kitamura, N., Iguchi, M., et al. The structure and mechanical properties of sheets prepared from bacterial cellulose. Part 2: Improvement of the mechanical properties of sheets and their applicability to diaphragms of electroacoustic transducers. **J. Mater. Sci.** vol. 25 p. 2997–3001, 1990.

Nishimura, H., Donkai, N., Miyamoto, T. Preparation and properties of a new type of comb-shaped, amphiphilic cellulose derivative. **Cellulose**, vol. 4, p. 89–98, 1997.

Novoselov, N. P. Sashina, E. S. Kuz'mina, O. G. Troshenkova. S. V. Ionic liquids and their use for the dissolution of natural polymers. **Russian J. Gen. Chem.** vol. 77, p. 1395-1405, 2007.

Okoturo, O. O., VanderNoot, T. J. Temperature dependence of viscosity for room temperature ionic liquids. **J. Electroanal. Chem.** vol. 568, p. 167-181, 2004.

Olivier-Bourbigou, H., Magna, L., Morvan, D. Ionic liquids and catalysis: recent progress from knowledge to applications. **Appl. Catal. A Gen.** vol. 373, p. 1–56, 2010.

Opendenbosch, V. D., Maisch, P., Fritz-Popovski, G., Paris, O., Zollfrank, C. Transparent cellulose sheets as synthesis matrices for inorganic functional Particles. **Carbohydr. Polym.** vol. 87, p. 257–264, 2012.

- Ostlund, A., Lundberg, D., Nordstierna, L., Holmberg, K., Nyden, M. Dissolution and gelation of cellulose in TBAF/DMSO solutions: the roles of fluoride ions and water. *Biomacromolecules*. vol. 10, p. 2401–2407, 2009.
- O'sullivan, C. A. Cellulose: the structure slowly unravels. *Cellulose*. vol. 4 p, 173-207, 1997.
- Peydecastaing, P., Vaca-Garcia, C., Borredon, E. Consecutive reactions in an oleic acid and acetic anhydride reaction medium. *Eur. J. Lipid Sci. Technol.* vol. 111, p. 723–729, 2009.
- Pezold-Welcke, K., Michaelis, N., Heinze, T. Unconventional cellulose products through nucleophilic displacement reactions. *Macromol. Symp.* vol. 280, p. 72–85, 2009.
- Phisalaphong, M., Jatupaiboon, N. Biosynthesis and characterization of bacteria cellulose–chitosan film. *Carbohydr. Polym.* vol. 74, p. 482–488, 2008.
- Pinkert, A., Marsh, K. N., Pang, S. S., Staiger, M. P. Ionic liquids and their interaction with cellulose. *Chem. Rev.* vol. 109, p. 6712–6728, 2009.
- Pinkert, A., Marsh, K. N., Pang, S. Reflections on the solubility of cellulose. *Ind. Eng. Chem. Res.* vol. 49, p. 11121–11130, 2010.
- Pionteck, H., Berger, W., Morgenstern, B., Fengel, D. Changes in cellulose structure during dissolution in LiCl: *N,N*-dimethylacetamide and in the alkaline iron tartarate system EWNN. I. Electron microscopic studies on changes in cellulose morphology. *Cellulose*. vol. 3, p. 127–139, 1996.
- Pliego, J. R., Pilo'-Veloso, D. Effects of ion-pairing and hydration on the SNAr reaction of the F<sup>-</sup> with *p*-chlorobenzonitrile in aprotic solvents. *Phys. Chem. Chem. Phys.* vol. 10, p. 1118–1124, 2008.
- Possidonio, S., Fidale, L. C., El Seoud, O. A. Microwave-assisted derivatization of cellulose in an ionic liquid: an efficient, expedient synthesis of simple and mixed carboxylic esters. *J. Polym. Sci. A*. vol. 48, P. 134–143, 2009.
- Possidonio, S., Fidale, L. C., El Seoud, O. A. Microwave -assisted derivatization of cellulose in an ionic liquid: an efficient, expedient synthesis of simple and mixed carboxylic esters. *J. Polym. Sci. A*: vol. 48, p. 134–143, 2010.
- Preston, R. D. Natural celluloses. *In Cellulose: Structure, Modification and Hydrolysis* (R. A. Young and R. M. Rowell, eds). John Wiley and Sons: New York, p. 3-27, 1986.

- Pringle, J. M., Golding, J., Baranyai, K., Forsyth, C. M., Deacon, G. B., Scott, J. L., MacFarlane, D. R. The effect of anion fluorination in ionic liquids—physical properties of a range of bis(methanesulfonyl)amide salts. *New J. Chem.* vol. 27, p. 1504-1510, 2003.
- Purz, H. J., Graf, H. and Fink, H-P. Electron-microscopic investigations of fibrillar and coagulation structures of cellulose. *Papier.* vol. 49, p. 714, 1995.
- Ramos, L. A., Assaf, J. M., El Seoud, O. A. Frollini, E. Influence of the supra-molecular structure and physico-chemical properties of cellulose on its dissolution in the lithium chloride/*N,N*-dimethylacetamide solvent system. *Biomacromolecules.* vol, 6, p. 2638–2647, 2005.
- Ramos, L. A., Frollini, E., Koschella, A., Heinze, T. Benzoylation of cellulose in the solvent dimethylsulfoxide/tetrabutylammonium fluoride trihydrate. *Cellulose.* vol. 12, p. 607–619, 2005.
- Ramos, L. A., Frollini, E., Heinze, T. Carboxymethylation of cellulose in the new solvent dimethyl sulfoxide/tetrabutylammonium fluoride. *Carbohydr. Polym.* vol. 60, p. 259–267, 2005.
- Ramos, L. A., Morgado, D. L., El Seoud, O. A. da Silva, V. C. Frollini, E. Cellulose. vol. 18, p. 385–392, 2011. and in ionic liquids. (*ECS Transactions.* vol. 16, p. 111-117, 2009).
- Ramos, L. A., Morgado, D. L., El Seoud, O. A., da Silva, V. C., Frollini, E. Acetylation of cellulose in LiCl-*N,N*-dimethylacetamide: first report on the correlation between the reaction efficiency and the aggregation number of dissolved cellulose. *Cellulose.* vol. 18, p. 385 – 392, 2011.
- Ramos, L. A., Morgado, D. L., Gessner, F., Frollini, E., El Seoud, O. A. A physical organic chemistry approach to dissolution of cellulose: effects of cellulose mercerization on its properties and on the kinetics of its decrystallization. *ARKIVOC* vol. 7, p. 416–425, 2011.
- Regiani, A. M., Frollini, E., Marson, G. A., Arantes, G. M., El Seoud, O. A. Some aspects of acylation of cellulose under homogeneous solution conditions. *J. Polym. Sci. A Polym. Chem.* vol. 37, p. 1357–1363, 1999.
- (a) Reichardt, C. *Solvents and Solvent Effects in Organic Chemistry*, 3rd ed., p. 5, 329, 389, VCH, Weinheim (2003); (b) Reichardt, C. *Pure Appl. Chem.* vol. 76, p. 1903-1919, 2004 ; (c) Reichardt, C. Pyridinium-*N*-phenolate betaine dyes as empirical indicators of solvent polarity: Some new findings *Pure Appl. Chem.* vol. 80, p. 1415-1432, 2008.

- Reichardt, C. Polarity of ionic liquids determined empirically by means of solvatochromic pyridinium N-phenolate betaine dyes. *Green Chem.* vol. 7, p. 339-351, 2005.
- Reichardt, C., Welton, T. Solvents and Solvent Effects in Organic Chemistry. 4 ed. **Wiley: VCH, Weinheim**, 2011.
- Review Of New Source Performance Standards For Kraft Pulp Mills, EPA-450/3-83-017, **U. S. Environmental Protection Agency**, Research Triangle Park, NC, September 1983.
- Rosenau, T., Potthast, A., Kosma, P. Trapping of reactive intermediates to study reaction mechanisms in cellulose chemistry. *Adv. Polym. Sci.* vol. 205, p. 153–197, 2006.
- Sashina, E. S., Novoselov, N. P., Kuzmina, O. G., Troshenkova, S. V. Ionic liquids as new solvents of natural polymers. *Fibre Chem.* vol. 40, p. 270-277, 2008.
- Sato, B. M., Oliveira, C. G., Clarissa, T. M., El Seoud, O. A., Thermo-solvatochromism in binary mixtures of water and ionic liquids: on the relative importance of solvophobic interactions. *Phys. Chem. Chem. Phys.* vol. 12, p. 1764–1771, 2010.
- Sato, B. M., Martins, C. T., El-Seoud, O. A. Solvation in aqueous binary mixtures: consequences of the hydrophobic character of the ionic liquids and the solvatochromic probes. *New J. Chem.* p. 2353–2360, 2012.
- Schumann, K., Pfeifer, A., Heinze, T. Novel cellulose ethers: synthesis and structure characterization of 3-mono-O-(30-hydroxypropyl) cellulose. *Macromol. Symp.* vol. 280, p. 86–94, 2009.
- Sealey, J. E., Samaranayake, G., Todd, J. G., Glasser, W. G. Novel cellulose derivatives. IV. preparation and thermal analysis of waxy esters of cellulose. *J. Polym. Sci. B Polym. Phys.* vol. 34, p. 1613–1620, 1996.
- Sharma, R. K., Fry, J. L. Instability of anhydrous tetra-n-alkylammonium fluorides. *J. Org. Chem.* vol. 48, p. 2112–2114, 1983.
- Sharman P. and G. Harris, *“High Yield pulping” Mill product News*, September-October p. 31, 1994.
- Shen, Q. Surface properties of cellulose and cellulose derivatives: A review. *ACS Symp Ser.* vol. 1019, p. 259–289, 2009.

- Siegmund, G., Klemm, D. Cellulose—Cellulose sulfonates: preparation, properties, subsequent reactions. *Polymer News*. vol. 27, p. 84–90, 2002.
- Silva, A. A., Laver, M. L. Molecular weight characterization of wood pulp cellulose: dissolution and size exclusion chromatographic analysis. *Tappi J.* vol. 80, p. 173–180, 1997.
- Silva, P. L., Pires, P. A. R., Trassi, M. A. S., El Seoud. O. A. Solvation in pure liquids: what can be learned from the use of pairs of indicators? *J. Phys. Chem. B*, vol. 112, p. 14976-14984, 2008.
- Silva, A. W. S., Vranken, W. F., *ACPYPE - AnteChamber PYTHON Parser interface*. BMC Research Notes 5, p. 367, 2012.
- Sjostrom, E. *Wood Chemistry: Fundamentals and applications*. Academic Press: San Diego, p. 293, 1993.
- Song, X., Chen, F., Liu, F. Preparation and characterization of alkyl ketene dimer (AKD) modified cellulose composite membrane. *Carbohydr. Polym.* vol. 88, p. 417–421, 2012.
- Source Category Report For The Kraft Pulp Industry**, EPA Contract Number 68-02-3156, Acurex Corporation, Mountain View, CA, January 1983.
- Spange, S., Reuter, A., Vilsmeier, E., Heinze, T., Keutel, D., Linert, W. Determination of empirical polarity parameters of the cellulose solvent *N,N*-dimethylacetamide/LiCl by means of the solvatochromic technique. *J. Polym. Sci. A Polym. Chem.* vol. 36, p. 1945–1955, 1998.
- Sponsler, O. L. Dore, W. H. The structure of ramie cellulose as derived from X-ray data. **Fourth Colloid Symposium Monograph**. vol. 41, p. 174-202, 1926.
- Srinivasa, P. C., Tharanathan, R. N. Chitin/chitosan safe, ecofriendly packaging materials with multiple potential uses. *Food Rev. Int.* vol. 23, p. 53–72, 2007.
- Steinbach, A., Winkenbach, R., Ehmsen, H. Material efficiency and sustainable development in chemistry: where do we stand today? *Chem. Ing. Tech.* vol. 83, p. 295–305, 2011.
- Storer, J. W., Giesen, D. J., Cramer. C. J., & Truhlar, D. G. Class IV charge models: a new semiempirical approach in quantum chemistry. *J. Comput. Aided Mol. Des.* vol. 9, p. 87-110, 1995.
- Striegel, A. M., Timpa, J. D. Molecular characterization of polysaccharides dissolved in Me<sub>2</sub> NAc-LiCl by gel-permeation chromatography. *Carbohydr. Res.* vol. 267, p. 271–290, 1995.

- Striegel, A. M., Timpa, J. D. Size exclusion chromatography of polysaccharides in dimethylacetamide-lithium chloride. **ACS, Symp. Series.** vol. 635, p. 366–378, 1996.
- Striegel, A. M. Theory and applications of DMAC/LiCl in the analysis of Polysaccharides. **Carbohydr. Polym.** vol. 34, p. 267–274, 1997.
- Striegel, A. M. Advances in the understanding of the dissolution mechanism of cellulose in LiCl/DMAC. **J. Chil. Chem. Soc.** vol. 48, p. 73–77, 2003.
- Sun, Y., Cheng, J. Dilute acid pretreatment of Rye straw and Bermudagrass for ethanol production. **Bioresource Technology**, vol. 96, p. 1599-1606, 2005.
- Swatloski, R. P., Spear, S. K., Holbrey, J. D., Rogers, R. D. Dissolution of cellulose with ionic liquids. **J. Am. Chem. Soc.** vol. 124, p. 4974–4975, 2002.
- Swatloski, R. P., Holbrey, J. D., Rogers, R. D. Ionic liquids are not always green: hydrolysis of 1-butyl-3-methylimidazolium hexafluorophosphate. **Green Chem.** vol. 5, p. 361-363, 2003.
- Tada, E.B., Novaki, L. P., El Seoud, O. A., Solvatochromism in pure and binary solvent mixtures: effects of the molecular structure of the zwitterionic probe. **J. Phys. Org. Chem.** vol. 13, p. 679–687, 2000.
- Tammanini, C., Haully, M. C. O. Agroindustrial residues for biotechnological production of xylitol. **Agricultural Sciences, Londrina.** vol. 25, p. 315-330, 2004.
- Tessier, P. M., Savoie, M. Pudlas. Industrial implementation of an advanced bleach plant control system. **Tappi Journal.** vol. 83, 1, p. 139-143, 2000.
- Tilstam, U. Sulfolane: A Versatile Dipolar Aprotic Solvent. **Org. Process Res. Dev.**, vol. 16, p. 1273-1278, 2012.
- Timpa, J. D. Application of universal calibration in gel permeation chromatography for molecular weight determinations of plant cell wall polymers: Cotton fiber. **J. Agric. Food. Chem.** vol. 39, p. 270–275, 1991.
- Tosh, B., Saikia, C. N., Dass, N. N. Homogeneous esterification of cellulose in the lithium chloride-*N,N*-dimethylacetamide solvent system: effect of temperature and catalyst. **Carbohydr Res.** vol. 327, p. 345-352, 2000a.
- Tosh, B., Saikia, C. N. Preparation of cellulose pentanoate of different degree of substitution: A detailed kinetics study. **Trends Carbohydr Chem.** vol. 6, p. 143–153, 2000b.

- Turbak, A. F., El-Kafrawy, A., Snyder, F. W., Auerbach, A. B. Solvent system for cellulose. **US 4302252 A**, 24 November 1981.
- Vaca-Garcia, C., Thiebaud, S., Borredon, M. E. Gozzelino, G. Cellulose esterification with fatty acids, including oleic acid, and acetic anhydride in lithium chloride/*N,N*-dimethylacetamide medium. **JAOCS**, vol. 75, p. 315–319, 1998.
- Van Der, Spoel. D., Lindahl, E., Hess, B., Groenhof, G., Mark, A. E., & Berendsen, H. J. GROMACS: Fast, flexible, and free. **J. Comput. Chem.** vol. 26, p. 1701–1718, 2005.
- Van Zyl, W. H., Chimphango, A. F. A., den Haan, R. Goergens, J. F., Chirwa, P. W. C. Next generation cellulosic ethanol technologies and their contribution to a sustainable Africa. **Interface Focus**. vol. 1, p. 196–211, 2011.
- Vanquelef, E., Simon, S., Marquant, G., Garcia, E., Klimerak, G., Delepine, J. C., R.E.D. Server: a web service for deriving RESP and ESP charges and building force field libraries for new molecules and molecular fragments. **Nucleic Acids Res.** (Web server issue) 39: W511-W517, 2011.
- Vincendon, M. Proton NMR study of the chitin dissolution mechanism **Makromol. Chem.** vol. 186, p. 1787–1795, 1985.
- Wada, M., Nishiyama, Y. Crystallinity index of cellulose measured by X-ray diffraction. **Cellulose Commun.** vol. 18, 87–90, 2011.
- Wang, J., Wang, W., Kollman, P. A., Case, D. A., Development and testing of a general amber force field. **J. Comput. Chem.** vol. 25, p. 1157-1174, 2004.
- Wang, J., Wang, W., Kollman, P. A., Case, D. A., Automatic atom type and bond type perception in molecular mechanical calculations. **J. Mol. Graphics Model.** Vol. 25, p. 247-260, 2006.
- Wang, Y., Li, H., Han, S. The chemical nature of the C–H···X<sup>-</sup> (X=Cl or Br) interaction in imidazolium halide ionic liquids. **J. Chem. Phys.** vol. 124, p. 044504-1/8, 2006.
- Wang, Z., Liu, S., Matsumoto, Y., Kuga, S. Cellulose gel and aerogel from LiCl/DMSO solution. **Cellulose**. vol. 19, p. 393–399, 2012.
- Wangaard, F. F. Paper, **Wood: Its structure and properties.** (ed.) University Park, PA: Pennsylvania State University, p. 335, 1981.

- Wasserscheid, P., Keim, W. Ionic liquids - new "Solutions" for transition metal catalysis. **Angew. Chem., Int. Ed.** vol. 39, p. 3772-3789, 2000.
- Welton, T. Room temperature ionic liquids. Solvents for synthesis and catalysis. **Chem. Rev.** vol. 99, p. 2071-2084, 1999.
- Williamson, L. S., McCormick, L. C. Cellulose derivatives synthesized via isocyanate and activated ester pathways in homogeneous solutions of lithium chloride/*N,N*-dimethylacetamide. **J. Macromol. Sci. A Pure Appl. Chem.** vol. 12, p. 1915–1927, 1998.
- Willhite, C. C., Katz, P. I. Dimethyl sulfoxide. **J. Appl. Toxicol.** vol. 4, p. 155–160, 1984.
- Woodcock, C. Sarko, A. Packing analysis of carbohydrates and polysaccharides II. Molecular and crystal structure of native ramie cellulose. **Macromolecules.** vol. 13, p. 1183-1187, 1980.
- Wu, J. Zhang, J. Zhang, H. He, J. Ren, Q. Guo, M. Homogeneous acetylation of cellulose in a new ionic liquid. **Biomacromolecules.** vol. 5, p. 266-268, 2004.
- Xu, D., Edgar, J. K. TBAF and cellulose esters: unexpected deacylation with unexpected regioselectivity. **Biomacromolecules.** vol. 13, p. 299–303, 2012.
- Xu, A., Zhang, Y., Zhao, Y., Wang, J. Cellulose dissolution at ambient temperature: Role of preferential solvation of cations of ionic liquids by a cosolvent. **Carbohydr. Polym.** vol. 92, p. 540-544, 2013.
- Yoshida, Y., Isogai, A. Thermal and liquid crystalline properties of cellulose *b*-ketoesters prepared by homogeneous reaction with ketene dimmers. **Cellulose.** vol. 13, p. 637–645, 2006.
- Yoshida, Y., Isogai, A. Preparation and characterization of cellulose  $\beta$  -ketoesters prepared by homogeneous reaction with alkylketene dimers: Comparison with cellulose fatty esters. **Cellulose.** vol. 14, p. 481–488, 2007.
- Young, R. *Cellulose structure modification and hydrolysis.* **John Wiley.** New York: ISBN 0-471-82761-4, 1986.
- Yousefi, H., Faezipour, M., Nishino, T., Shakeri, A., Ebrahimi, G. All-cellulose composite and nanocomposite made from partially dissolved micro-and nanofibers of canola straw. **Polym. J.** vol. 43, p. 559–564, 2011.



- Zabivalova, N. M., Boчек, A. M., Vlasova, E. N., Volчек, B. Z. Preparation of mixed cellulose ethers by the reaction of short flax fibers and cotton linter with monochloroacetamide. **Russ. J. Appl. Chem.** vol. 80, p. 300–304, 2007.
- Zabivalova, N. M., Boчек, A. M., Vlasova, E. N., Volчек, B. Z. Preparation of mixed ethers by reaction of carboxymethyl cellulose with urea and their physicochemical properties. **Russ. J. Appl. Chem.** vol. 81, p. 1622–1629, 2008.
- Zarth, C. S. P., Koschella, A., Pfeifer, A., Dorn, S., Heinze, T. Synthesis and characterization of novel amino cellulose esters. **Cellulose.** vol. 18, p. 1315–1325, 2011.
- Zeynizadeh, B., Sadighnia, L., A green protocol for catalytic conversion of epoxides to 1,2-diacetoxy esters with phosphomolybdic acid alone or its supported on silica gel. **Bull. Korean. Chem. Soc.** vol. 31, p. 2644–2648, 2010.
- Zeynizadeh, B., Sadighnia, L., One-pot catalytic conversion of epoxides to 1,2-diacetates with hydride transferring agents in acetic anhydride. **Synth. Commun.** vol. 41, p. 637–644, 2011.
- Zhai, W. Chen H.Z., Ma, R.Y. Chin. Structural characteristics of cellulose after dissolution and regeneration from the ionic liquid [bmim]Cl. **J. Beijing Univ. Chem. Technol.** (Natural Science Edition; ISSN: 16714628), vol. 34, p. 138-141, 2007.
- Zhang, H., Wu, J., Zhang, J., He, J. 1-Allyl-3-methylimidazolium chloride room temperature ionic liquid: a new and powerful nonderivatizing solvent for cellulose. **Macromolecules.** vol. 38, p. 8272-8277, 2005.
- Zhang, J., Zhang, H., Wu, J., Zhang, J., He, J., Xiang, J. NMR spectroscopic studies of cellobiose solvation in EmimAc aimed to understand the dissolution mechanism of cellulose in ionic liquids. **Phys. Chem. Chem. Phys.** vol. 12, p. 1941-1947, 2010.
- Zhang, X., Liu, X., Zheng, W., Zhu, J. Regenerated cellulose/graphene nanocomposite films prepared in DMAC/LiCl solution. **Carbohydr. Polym.** vol. 88, p. 26–30, 2012.

## 7. APPENDIX

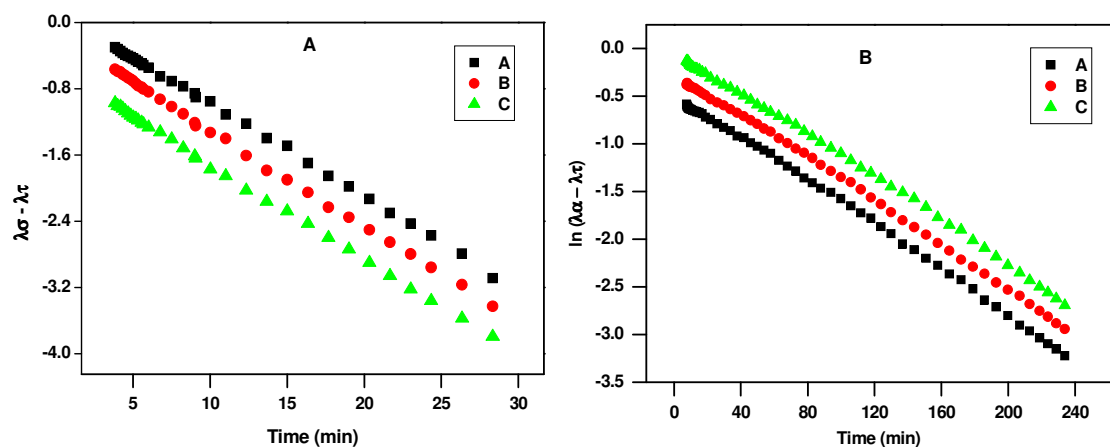


**Figure 7.1:** Plots for calculation of the pseudo first-order rate constant ( $k_{\text{obs}}$ ) for the reaction in mixtures IL-DAS. The symbols ( $\lambda_{\infty}$ ) and ( $\lambda_t$ ) refer to the conductivity at “infinity”- and any time (t), respectively. Part (A) is for AIMelmCl-DMSO at  $[\text{IL}] = 1.007 \text{ mol/L}$ , and T (from bottom up) = 40, 50, and 60 °C, respectively. Part (B) is for AIMelmCl-Sulfolane at  $[\text{IL}] = 1.573 \text{ mol/L}$ , and T (from bottom up) = 50, 60, and 70 °C, respectively.

**Table 7.1:** Observed rate constants of the reaction,  $k_{\text{obs}}$  in  $\text{s}^{-1}$ , and  $k_3$ ,  $\text{L}^2 \text{mol}^{-2} \text{s}^{-1}$ , at different temperatures and  $[\text{AIMelmCl}]$  for the acetylation of MCC in binary mixtures of AIMelmCl with DMAC.

$\text{Ac}_2\text{O}$ (1.057mol/L)	Temperature, °C	$k_{\text{obs}}$ , $\text{s}^{-1}$	$k_3 = k_{\text{obs}}/[\text{Ac}_2\text{O}][\text{IL}]$ ; $\text{L}^2 \text{mol}^{-2} \text{s}^{-1}$
<b>AIMelmCl</b>			
1.887 mol/L; 30 v % L	30	$5.776 \times 10^{-4}$	$2.897 \times 10^{-4}$
	40	$7.670 \times 10^{-4}$	$3.847 \times 10^{-4}$
	50	$1.001 \times 10^{-3}$	$5.024 \times 10^{-4}$
	60	$1.274 \times 10^{-3}$	$6.392 \times 10^{-4}$
2.269 mol/L; 36 v %	30	$9.052 \times 10^{-4}$	$3.775 \times 10^{-4}$
	40	$1.172 \times 10^{-3}$	$4.891 \times 10^{-4}$
	50	$1.506 \times 10^{-3}$	$6.283 \times 10^{-4}$

---

	60	$1.910 \times 10^{-3}$	$7.968 \times 10^{-4}$
2.647 mol/L; 42 v %	30	$1.240 \times 10^{-3}$	$4.436 \times 10^{-4}$
	40	$1.593 \times 10^{-3}$	$5.696 \times 10^{-4}$
	50	$2.009 \times 10^{-3}$	$7.185 \times 10^{-4}$
	60	$2.509 \times 10^{-3}$	$8.973 \times 10^{-4}$
3.025 mol/L; 48 v %	30	$1.599 \times 10^{-3}$	$5.286 \times 10^{-4}$
	40	$2.145 \times 10^{-3}$	$6.712 \times 10^{-4}$
	50	$2.665 \times 10^{-3}$	$8.337 \times 10^{-4}$
	60	$3.121 \times 10^{-3}$	$1.032 \times 10^{-3}$
3.404 mol/L; 54 v %	30	$2.273 \times 10^{-3}$	$6.320 \times 10^{-4}$
	40	$2.835 \times 10^{-3}$	$7.882 \times 10^{-4}$
	50	$3.488 \times 10^{-3}$	$9.695 \times 10^{-4}$
	60	$4.263 \times 10^{-3}$	$1.185 \times 10^{-3}$
3.782 mol/L; 60 v %	30	$2.758 \times 10^{-3}$	$7.293 \times 10^{-4}$
	40	$3.642 \times 10^{-3}$	$9.114 \times 10^{-4}$
	50	$4.456 \times 10^{-3}$	$1.115 \times 10^{-3}$
	60	$5.351 \times 10^{-3}$	$1.339 \times 10^{-3}$
CHM	60	$1.410 \times 10^{-3}$	$7.071 \times 10^{-4}$
CHD	60	$8.425 \times 10^{-4}$	$4.225 \times 10^{-4}$

---

**Table 7.2:** Observed rate constants of the reaction,  $k_{\text{obs}}$  in  $\text{s}^{-1}$ , and  $k_3$ ,  $\text{L}^2 \text{mol}^{-2} \text{s}^{-1}$ , at different temperatures and  $[\text{AlMeImCl}]$  for the acetylation of MCC in binary mixtures of AlMeImCl with MeCN.

<b>Ac<sub>2</sub>O (1.057mol/L)</b>	<b>Temperature, °C</b>	<b><math>k_{\text{obs}}</math>, s<sup>-1</sup></b>	<b><math>k_3 = k_{\text{obs}}/[\text{Ac}_2\text{O}]</math> [IL]; L<sup>2</sup> mol<sup>-2</sup> s<sup>-1</sup></b>
<b>AlMeImCl</b>			
2.647 mol/L; 42 v %	30	$2.316 \times 10^{-4}$	$0.828 \times 10^{-4}$
	40	$3.219 \times 10^{-4}$	$1.151 \times 10^{-4}$
	50	$4.388 \times 10^{-4}$	$1.569 \times 10^{-4}$
	60	$5.842 \times 10^{-4}$	$2.088 \times 10^{-4}$
3.025 mol/L; 48 v %	30	$3.218 \times 10^{-4}$	$1.006 \times 10^{-4}$
	40	$4.354 \times 10^{-4}$	$1.362 \times 10^{-4}$
	50	$5.824 \times 10^{-4}$	$1.822 \times 10^{-4}$
	60	$7.592 \times 10^{-4}$	$2.375 \times 10^{-4}$
3.404 mol/L; 54 v %	30	$4.332 \times 10^{-4}$	$1.204 \times 10^{-4}$
	40	$5.778 \times 10^{-4}$	$1.606 \times 10^{-4}$
	50	$7.559 \times 10^{-4}$	$2.101 \times 10^{-4}$
	60	$9.685 \times 10^{-4}$	$2.692 \times 10^{-4}$
3.782 mol/L; 60 v %	30	$5.710 \times 10^{-4}$	$1.428 \times 10^{-4}$
	40	$7.454 \times 10^{-4}$	$1.865 \times 10^{-4}$
	50	$9.532 \times 10^{-4}$	$2.385 \times 10^{-4}$
	60	$1.201 \times 10^{-3}$	$3.004 \times 10^{-4}$

**Table 7.3:** Observed rate constants of the reaction,  $k_{\text{obs}}$  in  $\text{s}^{-1}$ , and  $k_3$ ,  $\text{L}^2 \text{mol}^{-2} \text{s}^{-1}$ , at different temperatures and  $[\text{AlMeImCl}]$  for the acetylation of MCC in binary mixtures of AlMeImCl with DMSO.

<b>Ac<sub>2</sub>O (1.057mol/L)</b>	<b>Temperature, °C</b>	<b><math>k_{\text{obs}}</math>, <math>\text{s}^{-1}</math></b>	<b><math>k_3 = k_{\text{obs}}/[\text{Ac}_2\text{O}]</math> [IL]; <math>\text{L}^2 \text{mol}^{-2} \text{s}^{-1}</math></b>
<b>AlMeImCl</b>			
1.007 mol/L; 16 v %	40	$1.936 \times 10^{-3}$	$1.820 \times 10^{-3}$
	50	$2.545 \times 10^{-3}$	$2.392 \times 10^{-3}$
	60	$3.312 \times 10^{-3}$	$3.113 \times 10^{-3}$
1.258 mol/L; 20 v %	40	$3.079 \times 10^{-3}$	$2.317 \times 10^{-3}$
	50	$3.960 \times 10^{-3}$	$3.280 \times 10^{-3}$
	60	$4.994 \times 10^{-3}$	$4.158 \times 10^{-3}$
1.573 mol/L; 25 v %	40	$4.698 \times 10^{-3}$	$2.829 \times 10^{-3}$
	50	$5.840 \times 10^{-3}$	$3.516 \times 10^{-3}$
	60	$7.379 \times 10^{-3}$	$4.443 \times 10^{-3}$
CHM	50	$9.862 \times 10^{-3}$	$5.937 \times 10^{-3}$
CHD	50	$6.015 \times 10^{-3}$	$3.621 \times 10^{-3}$

**Table 7.4:** Observed rate constants of the reaction,  $k_{\text{obs}}$  in  $\text{s}^{-1}$ , and  $k_3$ ,  $\text{L}^2 \text{mol}^{-2} \text{s}^{-1}$ , at different temperatures and  $[\text{AlMeImCl}]$  for the acetylation of MCC in binary mixtures of AlMeImCl with Sulfolane.

<b>Ac<sub>2</sub>O (1.057mol/L)</b>	<b>Temperature, °C</b>	<b><math>k_{\text{obs}}</math>, <math>\text{s}^{-1}</math></b>	<b><math>k_3 = k_{\text{obs}}/[\text{Ac}_2\text{O}]</math> [IL]; <math>\text{L}^2 \text{mol}^{-2} \text{s}^{-1}</math></b>
<b>AlMeImCl</b>			
1.258 mol/L;20 v %	50	$1.290 \times 10^{-4}$	$9.71 \times 10^{-5}$
	60	$2.033 \times 10^{-4}$	$1.530 \times 10^{-4}$
	70	$3.075 \times 10^{-4}$	$2.314 \times 10^{-4}$
1.573 mol/L;25 v %	50	$1.876 \times 10^{-4}$	$1.130 \times 10^{-4}$
	60	$2.797 \times 10^{-4}$	$1.683 \times 10^{-4}$
	70	$4.117 \times 10^{-4}$	$2.479 \times 10^{-4}$
1.887 mol/L;30 v %	50	$2.472 \times 10^{-4}$	$1.240 \times 10^{-4}$
	60	$3.585 \times 10^{-4}$	$1.798 \times 10^{-4}$
	70	$5.131 \times 10^{-4}$	$2.573 \times 10^{-4}$
2.201 mol/L;35 v %	50	$3.302 \times 10^{-4}$	$1.420 \times 10^{-4}$
	60	$4.640 \times 10^{-4}$	$1.995 \times 10^{-4}$
	70	$6.329 \times 10^{-4}$	$2.721 \times 10^{-4}$

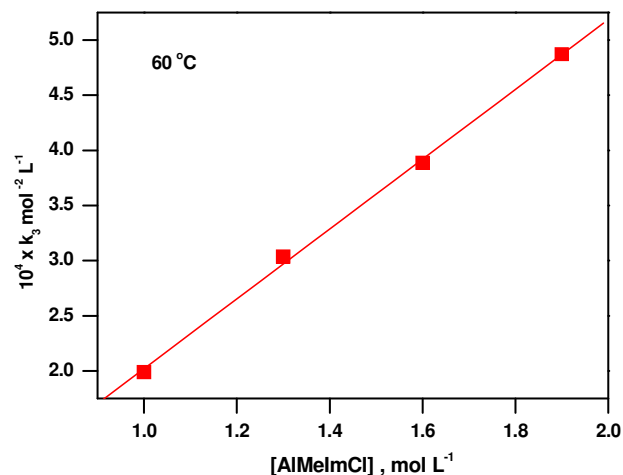


**Figure 7.2:** Relationship between  $k_3$  and molar concentration of ionic liquid for the acetylation of CHM in binary mixtures of AlMelmCl with Sulfolane at 60 °C.

**Table 7.5:** Determination of the effect of [IL] on the FTIR spectrum of cellobiose in IL/DMSO and IL/Sulfolane solvent mixture.

Molar conc. of Cellobiose	Molar conc. of IL (mol/L)	Ratio b/w IL : CellB	Wave number (cm <sup>-1</sup> ) N OH cellobiose
<b>Solvent DMSO</b>			
-----	Pure DMSO	----	3332
<b>0.086</b>	0.172	2:1	3313
---	0.344	4:1	3305
---	0.516	6:1	3302
---	0.688	8:1	3296
---	0.860	10:1	3289
<b>Solvent Sulfolane</b>			
<b>0.086</b>	0.344	4:1	3598
---	0.516	6:1	3596
---	0.688	8:1	3593
---	0.860	10:1	3591

**Table 7.6:** Viscosity of various solvent systems: IL/DMSO; IL/sulfolane; IL/DMAC; LiCl/DMAC and pure IL samples at 40 to 70 °C.

Temperature	1/T	Viscosity,[mPa·s]	Ln $\eta$	Viscosity,[mPa·s]	Ln $\eta$
		<b>1.573 mol/L, IL-DMSO</b>		<b>1.573 mol/L, IL-Sulfolane</b>	
40 °C ( 313 K)	0.00319	8.61	2.19	33.6	3.51
50°C (323 K)	0.00309	7.03	1.95	24.8	3.21
60°C (333 K)	0.00300	5.80	1.76	18.8	2.93
70°C (343 K)	0.00291	5.03	1.61	14.7	2.69
		<b>1.573 mol/L, LiCl-DMAC</b>		<b>1.88 mol/L, IL-DMAC</b>	
40 °C ( 313 K)	0.00319	8.15	2.09	11.69	2.46
50°C (323 K)	0.00309	6.37	1.85	9.02	2.20
60°C (333 K)	0.00300	5.35	1.67	7.41	2.00
70°C (343 K)	0.00291	4.27	1.45	5.73	1.74
		<b>Viscosity of pure AlMelmCl</b>			
40 °C ( 313 K)	0.00319	294.7	5.685		
50°C (323 K)	0.00309	152	5.023		
60°C (333 K)	0.00300	88.49	4.482		
70°C (343 K)	0.00291	56.17	4.028		



**Table 7.7:** Solvatochromic parameters for IL/DMAC and MCC-IL/DMAC, and their pure components.<sup>a</sup>

<b>IL/DMAC; 40 °C</b>			
<b>Solvent; Molarity of IL (mol/L) in DAS</b>	<b>E<sub>T</sub>(33), kcal mol<sup>-1</sup></b>	<b>SA</b>	<b>SB</b>
<b>Pure DMAC<sup>b</sup></b>	<b>51.50</b>	<b>0.024</b>	<b>0.804</b>
1.887	58.80	0.120	0.829
2.520	59.02	0.133	0.798
3.150	59.18	0.148	0.777
3.782	59.39	0.166	0.753
<b>Pure IL</b>	<b>59.85</b>	<b>0.131</b>	<b>0.651</b>
<b>MCC-IL/DMAC; 40 °C</b>			
1.887	58.65	0.144	0.841
2.520	58.81	0.161	0.809
3.150	58.99	0.180	0.785
3.782	59.14	0.201	0.763

a- E<sub>T</sub>33, SA, SB refer to the empirical polarity, acidity, and basicity, respectively, of the solvent or binary solvent mixture (Reichardt et al. 2011).

b- Solvatochromic parameters for pure DMAC were taken from literature (Antonious et al. 2002; Catalán 2009). The corresponding values for pure MeCN are: 55.4, 0.044, and 0.356, for E<sub>T</sub>(33), SA, and SB, respectively (Antonious et al. 2002; Catalán 2009). *All other solvatochromic parameters were determined in the present work.*

**Table 7.8:** Solvatochromic parameters for MCC-IL/DMSO, MCC-IL/Sulfolane, and their pure components.<sup>a</sup>

MCC-IL/DMSO; 40 °C		
Solvent; Molarity of IL (mol/L) in DAS	E <sub>T</sub> 33, kcal/mol,	SB
<i>Pure DMSO<sup>b</sup></i>	<b>55.1</b>	<b>0.647</b>
1.007	61.91	0.835
1.258	62.05	0.818
1.573	62.22	0.786
1.887	62.32	0.748
2.201	62.48	0.720
<i>Pure IL</i>	<b>59.85</b>	<b>0.651</b>
MCC-IL/Sulfolane; 40 °C		
<i>Pure Sulfolane<sup>b</sup></i>		0.365
1.258	58.53	0.850
1.573	58.67	0.810
1.887	58.82	0.763
2.201	58.92	0.726

**Table 7.9:** Experimental details for the imidazole-catalyzed acylation of hydroxyl-carrying compounds (ROH).<sup>a,b</sup>

ROH	[ROH]; listed as mol L <sup>-1</sup> (OH)	Anhydride concentration; mol L <sup>-1</sup>	Imidazole concentration; mol L <sup>-1</sup>
CHM	0.0288	0.288	0.576
CHD	0.0576	0.576	1.152
MCC	0.0864	0.864	1.728

a- The experiment was carried out by adding 10 mL of ROH in 6% LiCl/DMAC to 5 mL of a solution of acid anhydride plus imidazole in pure DMAC. The final LiCl concentration was 4 %, or  $0.943 \text{ mol L}^{-1}$ .

b- CHM, CHD, and the AGU of MCC carry one, two, and three (OH) groups per molecule, respectively. Therefore the ROH concentrations are listed as moles of (OH)/liter. As shown in the second and third columns, the molar ratios [reagent]/[OH] are 10 and 20 for acid anhydride, and imidazole, respectively.

## CURRICULUM VITAE

### Haq Nawaz

Place and date of birth: Muzaffar Garh, Punjab, Pakistan: 01 January 1984.

### Education:

School and college: Muzaffar Garh

University education: Master of Science in (Chemistry); The Islamia University of Bahawalpur, Bahawalpur (2003-2005), Punjab, Pakistan.

### Collaboration abroad:

Work as collaborator in the laboratory of Prof. Dr. Herbert Sixta, Aalto University, Espoo, Finland.

**Project title:** "Solvents for cellulose dissolution and derivatization: Mixtures of ionic liquids and DMSO". Period of project: 10/06/2013 to 23/08/2013

**Research funds:** TWAS-CNPq (The academy of sciences for the developing world; The Brazilian National Council for scientific & Technological development).

## PUBLICATIONS

- 1-Haq Nawaz; Paulo A. R. Pires; Thaís A. Bioni, Elizabeth P. G. Arêas, Omar A. El Seoud; Mixed solvents for cellulose derivatization under homogeneous conditions: Kinetic, spectroscopic, and theoretical studies on the acetylation of the biopolymer in binary mixtures of an ionic liquid and molecular solvents. *Cellulose*, (accepted) **2014**.
- 2-Haq Nawaz; Paulo A. R. Pires; Omar A. El Seoud; Kinetics and mechanism of imidazole-catalyzed acylation of cellulose in LiCl/*N,N*-dimethylacetamide. *Carbohydrate Polymers*, v. 92, p. 997–1005, **2013**.
- 3-Omar A. El Seoud; Haq Nawaz; Elizabeth P. G. Arêas. Chemistry and Applications of Polysaccharide Solutions in Strong Electrolytes/Dipolar Aprotic Solvents: An Overview. *Molecules*, v. 18, p. 1270-1313, **2013**.
- 4-Haq Nawaz; Romeu Casarano; Omar A. El Seoud; First report on the kinetics of the uncatalyzed esterification of cellulose under homogeneous reaction conditions: a rationale for the effect of

carboxylic acid anhydride chain-length on the degree of biopolymer substitution *Cellulose*, v. 19, p. 199-207, **2012**.

5-Romeu Casarano; Haq Nawaz; Shirley Possidonio; Valdineia C. da Silva; Omar A. El Seoud; A convenient solvent system for cellulose dissolution and derivatization: Mechanistic aspects of the acylation of the biopolymer in tetraallylammonium fluoride/dimethyl sulfoxide. *Carbohydrate Polymers*, v. 86, p. 1395-1402, **2011**.